Multimodal neurofeedback based on EEG/fMRI imaging techniques and visuo-haptic feedback for stroke rehabilitation

Mathis Fleury

UNIVERSITÉ DE RENNES 1

THESE DE DOCTORAT DE

L'UNIVERSITE DE RENNES 1

ECOLE DOCTORALE N° 601
Mathématiques et Sciences et Technologies de l'Information et de la Communication

Par
Mathis Fleury

Multimodal Neurofeedback based on EEG/fMRI Imaging Techniques and Visuo-Haptic Feedback for Stroke Rehabilitation

Thèse présentée et soutenue à Rennes, le 26/02/2021
Unité de recherche : IRISA UMR CNRS 6074 / Inria Rennes

Direction de la Thèse :

Co-dir de thèse :	Anatole LÉCUYER	Directeur de Recherche, Inria Rennes, France
Co-dir de thèse :	Christian BARILLOT†	Directeur de Recherche, Inria Rennes, France

Rapporteurs avant soutenance :

Fabien LOTTE	Directeur de Recherche, Inria Bordeaux, France
Ranganatha SITARAM	Professeur, St. Jude Children's Research Hospital, États-Unis

Composition du Jury :

Président :	Patrick BOUTHEMY	Directeur de Recherche, Inria Rennes, France
Rapporteurs :	Fabien LOTTE	Directeur de Recherche, Inria Bordeaux, France
Examinateurs :	Andrea KUBLER	Professeure, Université de Würzburg, Allemagne
	Michelle HAMPSON	Professeure Associée, Université de Yale, États-Unis
	Pierre MAUREL	Maitre de Conférence, Université de Rennes, France
	Patrick BOUTHEMY	Directeur de Recherche, Inria Rennes, France
Co-dir. de thèse :	Anatole LÉCUYER	Directeur de Recherche, Inria Rennes, France

A PhD Thesis

Multimodal Neurofeedback based on EEG/fMRI Imaging Techniques and Visuo-Haptic Feedback for Stroke Rehabilitation

by Mathis Fleury

April 28, 2021

University of Rennes

Contents

Aknowledgments

J'aimerais d'abord exprimer ma sincère gratitude envers mes directeurs de thèse Anatole et Christian. Je les remercie tout d'abord de m'avoir donné l'opportunité de travailler dans leur groupe et pour leur soutien constant et leur présence positive durant ces années. Ils ont toujours encouragé ma liberté intellectuelle, m'ont soutenu dans ma participation aux réunions et conférences et ont stimulé l'échange d'idées. Au-delà de l'aspect scientifique, je tiens surtout à remercier le soutien moral et tous les encouragements que j'ai reçu et qui m'ont très certainement donné la force d'accomplir cette thèse. Vous avez fait de mon doctorat un joyeux voyage et m'ont appris à être un meilleur scientifique et une meilleure personne.

Je remercie également tous les membres de mon jury : Fabien Lotte et Ranganatha Sitaram pour avoir tous les deux acceptés d'être rapporteurs de ce travail ainsi qu'à Andrea Kübler, Michelle Hampson et Pierre Maurel pour avoir examiné ce travail et Patrick Bouthemy d'avoir présidé le jury durant ma soutenance de thèse. Vos commentaires perspicaces et vos encouragements, ainsi que les questions et discussions passionnantes que nous avons eues, me permettront d'élargir mes recherches avec différentes perspectives. J'ai été honoré de soutenir ma thèse devant vous tous.

Je tiens aussi à remercier l'ensemble des personnes que j'ai cotoyé au travail lors de ces 3 dernières années, ces jours dans les équipes Empenn et Hybrid ont été joyeux, surtout grâce à mes collègues de laboratoire –> remerciement à l'ensemble du couloir ! Une petite pensée à Benoit, Pierre, Quentin, Mathieu et Cédric pour nos innombrables parties de baby-foot ou encore ces fameuses parties de pandemic legacy dont j'aimerais bien finir la dernière saison !

Merci aux médecins, Isabelle Bonan et Simon Butet pour les moments d'échanges lors du projet Hemisfer. Merci aussi à Salomé Lefranc avec qui la collaboration a été très fructueuse, je te souhaite bonne chance pour ta thèse ! Je tenais aussi à remercier Pauline Cloerec pour ton aide précieuse lors de cette dernière année.

Je voudrais adresser des remerciements spéciaux à Pierre Maurel, qui m'a accueillis au sein d'Empenn lors de mon master 2 et sans qui je ne serais (bien entendu) pas là aujourd'hui. Mais aussi à toi Giulia, ce fut un immense plaisir de travailler avec toi durant ces 3 dernières années. Rien qu'à penser à toutes les séances de NF que nous avons passé ensemble me rends nostalgique, et pourtant nous savons tous les deux à quel point c'était stressant mais compensé par des moments de joies !!

Merci à l'équipe des manips de Neurinfo ainsi qu'à Elise et Isabelle, pour leur soutien, et leurs encouragements dans les projets MR HANDS et HEMISFER, merci d'avoir partagé ces moments de joie (enfin seulement si tout fonctionne bien !).

Pour finir, au tour des amis/amies et famille. Merci à vous d'être là depuis tant d'années et surtout de m'avoir supporté pendant ces dernières années! Merci à Loulou, Malo, Elisa, Ronan, Titouan, Thibaut, Maxime, Cédric, Mayo, Juliette, Victoire, Léonardo avec qui j'ai tant partagé et qui continuent de m'apporter beaucoup. Enfin, Marie, merci pour tout. Merci de m'avoir aidé, écouté, soutenu et réussi à me faire rire lorsque j'en avais le plus besoin. Un infini merci à mes parents et mes soeurs pour votre confiance aveugle d'amour et votre soutien à nul autre pareil.

Résumé en Français

Contexte et Motivation

Il est dans la nature humaine d'explorer le monde qui nous entoure, de manifester de la curiosité pour ce que nous voyons, touchons ou entendons. Ces interactions avec notre environnement sont inhérentes à la multimodalité, car nous utilisons souvent non pas seulement un sens mais une combinaison de ceux-ci, et parfois simultanément. Que les sens soient utilisés activement ou passivement lors de l'exploration de notre environnement, ils confirment ou infirment les attentes de notre environnement, ce qui nous amène finalement à percevoir de nouvelles informations.

Imaginez maintenant la possibilité d'observer l'activité de votre cerveau dans le but de mieux la comprendre, voire de la moduler. Voici, en quelques mots, la définition du Neurofeedback (NF)[1, 205] : le processus consistant à renvoyer à un individu des informations en temps réel sur son activité cérébrale en cours, afin qu'il puisse s'entraîner à autoréguler les substrats neuronaux de fonctions comportementales spécifiques. Cette technique est devenue de plus en plus populaire en tant qu'outil d'entraînement à l'autorégulation du cerveau, que ce soit pour la rééducation cérébrale de patients souffrant de troubles psychiatriques et neurologiques. Cette technique constitue une alternative non invasive lorsque les médicaments et la rééducation conventionnelle ont peu ou pas d'effet. Par exemple, à la suite d'un accident vasculaire cérébral (AVC), où la récupération motrice devient limitée après un an [2], des changements peuvent se produire entraînant une réorganisation fonctionnelle étendue du réseau moteur, même dans des zones corticales éloignées d'une lésion focale [3]. Le NF devrait aider à induire une plasticité neuronale adaptative en choisissant des schémas spécifiques et contribuer ainsi à restaurer la fonction motrice perdue [4, 5].

L'autorégulation de l'activité cérébrale est possible grâce aux techniques d'imagerie cérébrale, telles que l'electroencéphalographie (EEG) qui mesure l'excitabilité électrique du cerveau, ou l'Imagerie par résonnance magnétique (IRMf) qui mesure l'activité cérébrale par l'effet l'effet du signal BOLD (blood oxygen-level dependent (BOLD)). Individuellement, ces techniques d'imagerie ont permis d'approfondir notre compréhension du traitement cognitif et d'améliorer le diagnostic clinique. Bien qu'elles soient technologiquement éloignées et qu'elles mesurent des signaux différents, l'EEG et l'IRMf sont à d'autres égards très complémentaires. En effet, l'EEG a une très haute résolution temporelle (millisecondes), ce qui lui permet de détecter des rythmes cérébraux allant du delta (0,5-4 Hz) au gamma (> 30 Hz) et de fournir ainsi une mesure directe de l'activité électrophysiologique du cerveau, mais sa résolution spatiale est très limitée (centimètres). En revanche, l'IRMf mesure indirectement l'activité cérébrale par le biais de la réponse BOLD, qui offre une grande résolution spatiale pour la localisation fonctionnelle, bien que la résolution temporelle soit

limitée à quelques secondes, voire à des centaines de millisecondes avec les approches récentes. Il convient également de noter que le signal BOLD ne reflète pas directement l'activité neuronale mais est davantage l'expression de mécanismes hémodynamiques et métaboliques : [6].

L'idée de fusionner ces deux modalités n'est pas tout à fait récente et remonte à 1993, lorsque Ives et al. [7] ont enregistré pour la première fois un EEG pendant une acquisition écho-planaire (ce qu'on appelle aujourd'hui IRM fonctionnelle ou IRMf) [8] (voir figure 1). A ce jour, de nombreuses études ont prouvé l'intérêt de combiner simultanément EEG-IRMf pour l'étude non invasive du fonctionnement du cerveau humain [9]. Mais cette technique a également des applications cliniques, puisque sa première application a été de localiser l'insurgence de décharges épileptiques chez des patients subissant une évaluation pré-chirurgicale [7, 10] et a également contribué de manière significative à faire progresser l'étude de l'état de repos, du sommeil et des fonctions cérébrales cognitives.

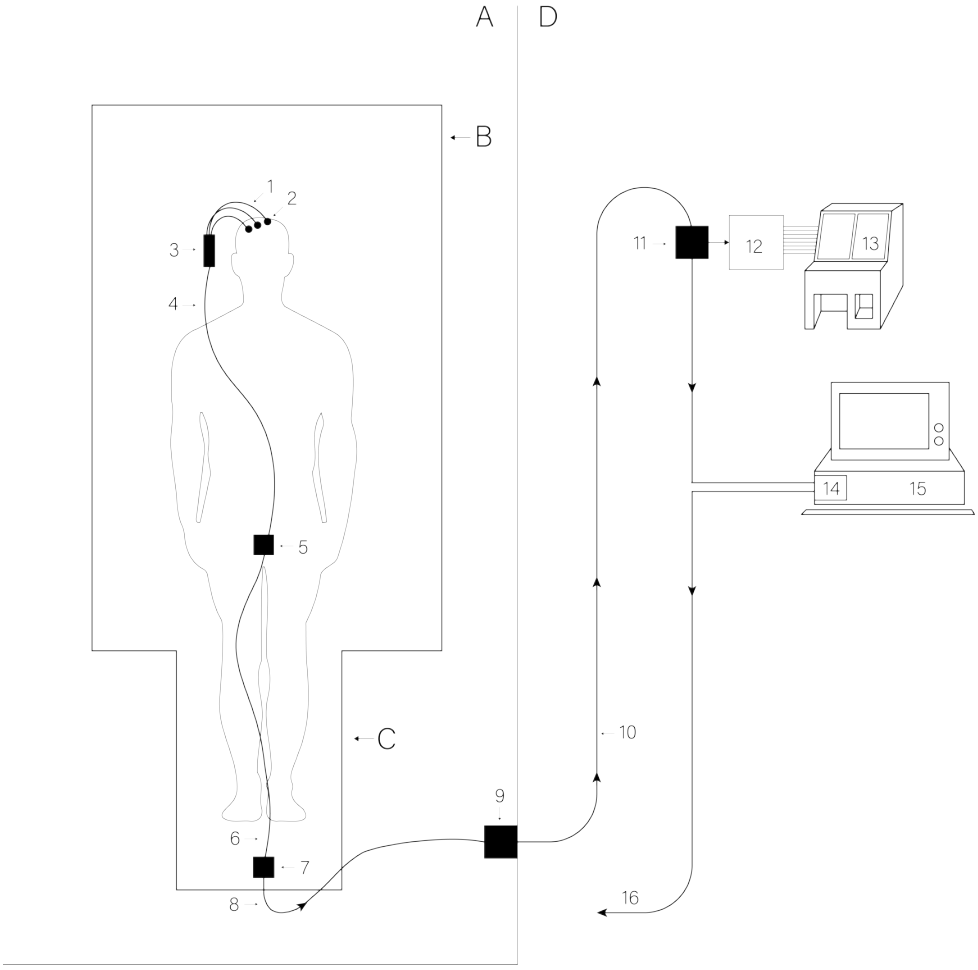

Figure 1: Diagramme en bloc du premier système permettant la combinaison de l'EEG et de l'IRMf, proventant des travaux de Ives et al. [7]. Ils ont permis l'introduction d'un casque compatible IRM dans un scanner de 1,5T.

Dans le contexte de le NF, l'association EEG-fMRI est encore assez récente et trois études marquantes peuvent être mentionnées. La première étude remonte à 2013, lorsque Meir-Hasson et al. ont introduit l'idée de l'EEG-fMRI-NF par le biais d'une méthode qui produit

une empreinte EEG permettant de dériver un prédicteur du signal BOLD associé dans une région profonde spécifique du cerveau [11]. La deuxième étude a été menée par Zotev et al., qui ont conçu le premier EEG-fMRI-NF en temps réel, dans lequel les caractéristiques de l'EEG et de l'IRMf sont renvoyées au sujet. Ces études révolutionnaires ont ouvert la voie à l'étude de la validation des paradigmes intermodaux et à la conception de nouveaux NF combinant les deux modalités. Enfin, Perronnet et al. [12] ont mené une étude sur la forme que pourrait prendre une rétroaction combinant les caractéristiques de l'EEG et de l'IRMf. Malgré tout, des défis subsistent concernant la physiologie de base, la conception de l'étude, la qualité des données, leur analyse/intégration et leur interprétation.

D'une manière générale, il convient d'établir une distinction entre le NF et les interfaces cerveau-ordinateur (ICO) dans lesquelles les individus visent à réguler directement des dispositifs externes plutôt que des substrats neuronaux. Cependant, les deux permettent la traduction directe de l'activité neuronale en un signal contrôlé d'un retour auditif, visuel ou haptique de cette activité en temps réel qui peut rendre compte de la performance du sujet. Ce feedback est, par définition, utilisé pour combler le fossé entre ce qui est appris et ce qui reste à apprendre. C'est pourquoi le choix du feedback est crucial dans la construction d'une étude NF, en donnant une importance égale à sa conception et à son contenu. Par exemple, dans l'interaction homme-homme, le fait de voir une personne parler facilite la compréhension, par rapport au fait de seulement entendre la personne parler [13]. Alors que la majorité des études NF utilisent des feedback visuels, nous en venons à nous demander si ce feedback unimodal est optimal et écologique pour un bon apprentissage. Dans notre vie quotidienne, nous sommes confrontés la plupart du temps à des stimuli multimodaux plutôt qu'unimodaux. En effet, nous utilisons plusieurs sens de manière séquentielle ou parallèle, pour explorer activement ou passivement notre environnement, pour confirmer des attentes sur le monde et pour percevoir de nouvelles informations. En outre, des études ont suggéré que le seuil d'activation neuronale est atteint plus rapidement avec l'apprentissage multimodal qu'avec l'apprentissage unimodal [14], car les stimuli multimodaux sont généralement perçus plus rapidement et plus précisément que les stimuli unimodaux [15]. Une autre considération théorique à prendre en compte est le fait que les utilisateurs préfèrent l'interaction multimodale à l'interaction unimodale lorsque la complexité d'une tâche est accrue [16]. Cette théorie a été motivée par la *Théorie des ressources multiples* de Wicken. [17], qui stipule que les tâches peuvent être mieux exécutées et avec moins de ressources cognitives lorsqu'elles sont réparties entre plusieurs modalités.

Lors de la création d'un feedback pour une étude NF, ces considérations doivent être prises en compte car l'autorégulation de sa propre activité cérébrale est une tâche complexe qui impose une charge cognitive élevée. Comme mentionné ci-dessus, l'unimodalité est la norme mais il existe des études utilisant plusieurs modalités. Par exemple, en 2008, Buch et al. ont fourni pour la première fois un retour visuo-haptique à des patients victimes d'un AVC chronique à partir d'une tâche d'imagerie motrice (IM) [18]. Ils ont démontré qu'ils étaient capables de contrôler volontairement le retour visuel et le retour haptique contingent. Plus tard, l'enquête de Brower [19] a montré que le retour visuo-tactile a de meilleures performances que la stimulation unisensorielle.

Comme l'illustre la figure 3, la multimodalité dans le NF peut être divisée en deux parties.

Figure 2: La première orthèse introduit dans le domain des interfaces cerveau-machine (ICM), de Pfurtscheller et al. [20]. Le sujet devait imaginer un mouvement de sa main pour faire fonctionner l'appareil, qui se base directement sur les signaux bioélectriques de son cerveau.

La première concerne l'entrée: l'utilisation de multiples techniques de neuro-imagerie différentes pour enrichir la qualité des informations données à l'utilisateur. La seconde concerne la sortie: rendre compte à l'utilisateur, non pas d'une modalité de rétroaction, mais d'une multisensorialité correspondant à la cohésion de multiples sens. Ce n'est pas une simple additivité mais une approche complémentaire qui est recherchée ici.

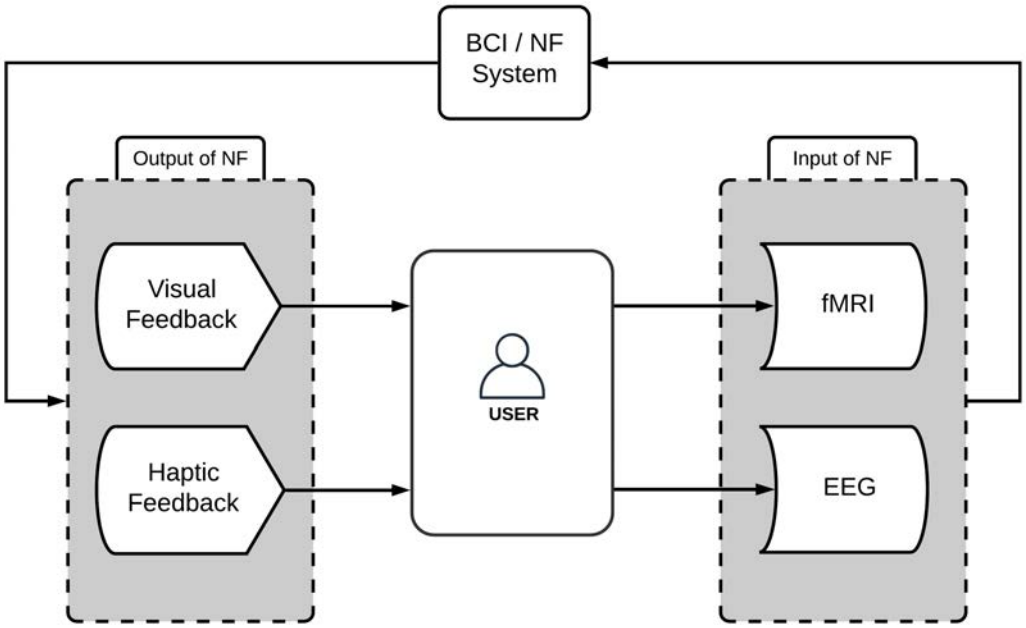

Figure 3: Cadre d'interaction multimodale pour le neurofeedback. L'utilisateur fournit l'entrée grâce à la régulation de son activité cérébrale mesurée par des modalités de neuroimagerie (EEG ou/et IRMf par exemple): l'entrée du NF. Tout en recevant un feedback de son activité cérébrale par le biais d'un retour uni- ou multi-sensoriel: la sortie du NF.

Objectives and Contributions

Dans ce contexte, l'objectif de cette thèse est de contribuer à la fois à l'entrée et à la sortie du NF multimodale.

En ce qui concerne la sortie du NF multimodale, notre objectif principal est de répondre à l'interrogation suivante : Comment concevoir un feedback multisensoriel efficace ? Plus précisément, comment pouvons-nous fusionner les informations visuelles et haptiques dans un feedback combiné ? Avec ces interrogations en tête, nous présenterons de nouvelles méthodes dans le but de combiner ces deux sens de manière optimale. Dans un deuxième temps, nous étudierons également l'utilisation du feedback visuo-haptique dans un contexte de NF, afin de déterminer si les performances sont améliorées par rapport au feedback unisensoriel.

En ce qui concerne **l'entrée du NF multimodale**, notre objectif est de savoir comment améliorer l'intégration des deux techniques : EEG et IRMf, et également d'étudier son apport dans un contexte de réhabilitation. Notre premier objectif est d'améliorer la fusion de l'EEG et de l'IRMf et notre second objectif est d'évaluer le NF multimodale basée sur l'EEG/IRMf dans un contexte de réhabilitation.

Vous trouverez ensuite les travaux réalisés, qui suivent l'ordre d'apparition des chapitres de cette thèse. Le manuscrit est divisé en trois parties : La partie 1 présente un état de l'art de l'EEG-fMRI pour le NF ainsi qu'une revue de l'utilisation du retour haptique pour les BCI/NF. La partie 2 décrit nos études et contributions concernant l'utilisation d'un feedback

multisensoriel pour le NF, enfin la partie 3 détaille nos contributions liées à la sortie de le NF multimodale et nous insisterons notamment sur l'utilisation de l'EEG-fMRI-NF pour la rééducation des accidents vasculaires cérébraux.

Partie 1 : Travaux connexes. Cette partie présente l'état de l'art sur l'utilisation des entrées et des sorties pour le neurofeedback multimodal.

- **Chapter 1 : L'apport du Neurofeedback multimodal : Combinaison de l'EEG et de l'IRMf**
  Chapter 1 présente un état des lieux de la combinaison de deux méthodes de neuro-imagerie différentes comme entrées pour le NF multimodale : EEG et IRMf. Tout d'abord, nous nous concentrons sur les propriétés générales de l'EEG et de l'IRMf, telles que leurs caractéristiques de résolution spatiale et temporelle. Ensuite, nous analysons les différentes approches pour l'intégration des données EEG-fMRI pour le NF : approches symétriques ou asymétriques et analyses d'activation ou de connectivité. Nous étudions les différents travaux utilisant l'EEG et l'IRMf pour le NF. Nous proposons ensuite une classification des études EEG-fMRI pour le NF. Nous insistons particulièrement sur l'utilisation simultanée de l'EEG-IRMf et de l'EEG-IRMf. Enfin, nous analysons les paradigmes les plus couramment utilisés dans ces études : le paradigme de l'imagerie motrice et le paradigme du réseau émotionnel.

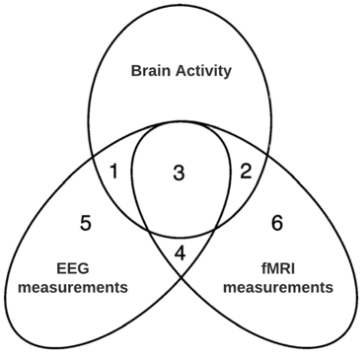

Figure 4: Chapter 1 décrit l'ensemble des études combinant l'EEG-fMRI pour NF.

- **Chapter 2 : Sortie du Neurofeedback multimodal : Ajout de l'haptique au retour visuel**
  Chapter 2 se concentre sur la sortie de le NF multimodale. Pour ce faire, nous passons en revue le retour haptique pour le NF. Nous nous concentrons d'abord sur la perception haptique humaine avant de décrire les différentes propriétés des interfaces haptiques, qu'elles soient tactiles ou kinesthésiques. Ensuite, nous analysons les différentes applications de l'haptique pour le NF et les interfaces cerveau-ordinateur. Deux familles de paradigmes sont étudiées : le paradigme d'imagerie motrice et les paradigmes de stimulation externe, tels que le P300 et le potentiel évoqué somatosensoriel à l'état stable. Enfin, nous discutons de la contribution et de l'utilité du retour haptique pour le NF.

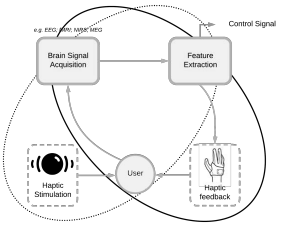

Figure 5: In Chapter 2, we describe the use haptic feedback for BCI/NF.

Partie 2 : Vers un Neurofeedback multimodal basé sur la stimulation visuelle et haptique. Dans cette partie, nous étudions l'interaction de deux feedbacks différents sous deux modalités différentes (EEG et IRMf). Plus précisément, le feedback haptique utilisé est un feedback proprioceptif basé sur l'illusion de mouvement. Nous menons une étude pour déterminer l'impact d'un feedback visuel congruent avec cette illusion de mouvement. Ensuite, nous

réalisons une étude pour évaluer l'impact d'une vibration sur le signal EEG. Enfin, nous introduisons ce nouveau feedback visuo-haptique dans une étude NF-IRMf.

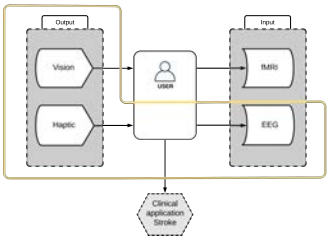

Figure 6: Chapter 3 présente des études dans lesquelles les participants étaient confrontés à un retour proprioceptif grâce à une stimulation haptique.

- **Chapter 3 : Étude d'une rétroaction visuo-haptique pour le neurofeedback basé sur l'EEG**
  Chapter 3 présente les résultats de nos deux études sur des sujets sains (N = 30/20) sur l'utilisation d'un retour visuo-haptique pour EEG-NF. Nous avons développé un nouveau feedback visuo-haptique pour le NF. Ce feedback multisensoriel consiste en une combinaison de feedback visuel (main virtuelle) et de feedback haptique délivré de manière vibro-tactile. La première étude examine comment le retour haptique est complémentaire au retour visuel et la seconde étude nous permet d'évaluer l'impact de ce retour haptique spécifique sur les signaux EEG. Ces deux études nous permettent de créer notre propre NF et de l'utiliser pour la rééducation post-AVC.
- **Chapter 4 : Étude du retour visuo-haptique pour le neurofeedback basé sur l'IRMf**
  Chapter 4 présente les résultats de la première étude IRMf-NF sur des sujets sains (N = 15) qui implique un feedback visuo-haptique. Dans cette étude, nous comparons le feedback multisensoriel et unisensoriel afin d'évaluer les avantages de la multisensorialité. Nous introduisons trois types de feedback (visuel, haptique et visuo-haptique) et étudions leurs effets sur une tâche de MI avec une conception intra-groupe.

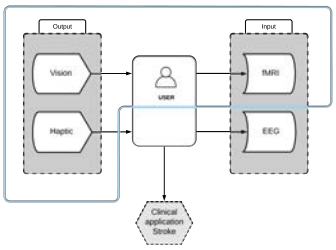

Figure 7: Dans Chapter 4, nous présentons une étude IRMf basée sur le NF dans laquelle les participants ont effectué le NF avec un feedback multisensoriel ou unisensoriel.

Partie 3 : Vers un Neurofeedback multimodal basé sur l'EEG-IRM pour la réadaptation après un accident vasculaire cérébral. Cette partie rassemble nos contributions concernant les études basées sur l'utilisation de l'EEG-fMRI-NF pour la réadaptation post-AVC. D'une part, nous présentons une première contribution à l'intégration de l'EEG et de l'IRMf grâce à une nouvelle méthode de détection automatisée des électrodes dans le scanner RM. D'autre part, nous étudions l'impact de le NF pour la neuroréhabilitation des patients victimes d'un AVC.

- **Chapter 5 : Détection automatisée des électrodes pour l'EEG-IRM multimodal**
  Chapter 5 présente une nouvelle technique de détection de la position des électrodes en IRMf. Nous utilisons une séquence RM spéciale pour obtenir la position des électrodes sur un

volume RM. Cette méthode n'a pour coût supplémentaire que le temps d'acquisition de la séquence dans le protocole RM. Nous démontrons que notre méthode permet une détection des électrodes beaucoup plus précise que la détection semi-automatique qui est plus couramment utilisée dans les protocoles EEG/IRM.

- **Chapter 6 : Neurofeedback EEG-fMRI multimodal pour la réadaptation après un accident vasculaire cérébral : Une étude clinique**
  Chapter **??** présente une étude de le NF sur des patients victimes d'un accident vasculaire cérébral (N = 4) avec EEG/IRMf. Dans le contexte de la neuroréhabilitation, nous étudions l'impact de le NF chez quatre patients victimes d'un AVC avec EEG-fMRI. L'objectif de ce travail pilote était de tester la faisabilité de l'entraînement à le NF par EEG-fMRI sur des patients victimes d'un AVC sur plusieurs sessions. Cette étude de faisabilité donne des indications utiles pour la conception de futures études cliniques avec le NF.

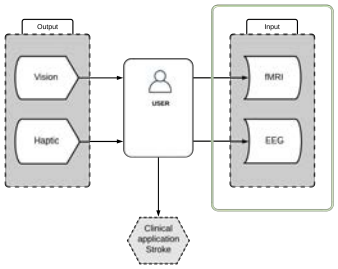

Figure 8: Dans cet article, nous présentons deux nouvelles techniques de détection de la position de l'EEG à l'intérieur du scanner RM.

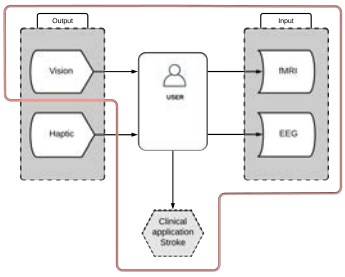

Figure 9: Chapter 6 décrit l'étude réalisée sur un patient victime d'un accident vasculaire cérébral avec une NF multimodale basée sur l'EEG-fMRI.

General Introduction

Context and Motivation

It is human nature to explore the world surrounding us, to manifest curiosity about what we see, touch or hear. These interactions with our environment are inherent to multimodality, as we often use not just one sense but a combination of them, and sometimes simultaneously. Whether senses are used actively or passively when exploring one's setting, they either confirm or deny the expectations of our environment, ultimately leading one to perceive new information.

Now imagine the possibility of observing your brain activity with the intent of gaining a better understanding of it, and even modulate it. This is, briefly, the definition of Neurofeedback (NF)[1, 205]: the process of feeding back real-time information to an individual about his/her ongoing brain activity, so that he/she can train to self-regulate neural substrates of specific behavioural functions. This technique has become increasingly popular as a training tool for brain self-regulation, either for brain rehabilitation of patients with psychiatric and neurological disorders, or for peak performance training of healthy subjects. This allows a non-invasive alternative when drugs and conventional rehabilitation have little or no effect. For instance, following a stroke, where motor recovery becomes limited after one year [2], changes may occur resulting in a widespread functional reorganisation of the motor network, even at cortical areas distant from a focal lesion [3]. NF should help to induce adaptive neural plasticity by electing specific patterns and thereby contribute to restoring lost motor function [4, 5].

Self-regulation of brain activity is possible thanks to brain imaging techniques, such as the Electroencephalography (EEG) which measures the electrical excitability of the brain, or the functional Magnetic Resonance Imaging (fMRI) which measures the brain activity through the blood oxygen-level dependent (BOLD) effect. Individually, these imaging techniques have helped to further our understanding of cognitive processing and to improve clinical diagnostics. Although they are technologically distant and measuring different signals, EEG and fMRI are in other aspects very complementary. Indeed, the EEG has a very high temporal resolution (milliseconds), allowing it to detect brain rhythms ranging from delta (0.5-4 Hz) to gamma (> 30 Hz) and thus providing a direct measurement of the brain electrophysiological activity, but its spatial resolution is very limited (centimetres). In contrast, fMRI indirectly measures brain activity through the BOLD response which provides a great spatial resolution for functional localisation, though temporal resolution is limited to a few seconds, or up to hundreds of millisecond with recent approaches. It should also be noted that the BOLD signal does not directly reflect neural activity but is more the expression of heamodynamic and metabolic mechanisms [6].

The idea of merging these two modalities is not quite recent and dates back to 1993, where Ives and colleagues [7] recorded for the first time EEG during echo-planar acquisition (what is now called Functional MRI or fMRI) [8] (See Figure 1). To date, numerous studies have proved the value of combining simultaneously EEG-fMRI for the non-invasive study of human brain function [9]. But this technique has also clinical applications, since its first application was to locate the insurgence of epileptic discharges in patients undergoing presurgical evaluation [7, 10] and has also significantly contributed in advancing the study of resting state, sleep and cognitive brain function.

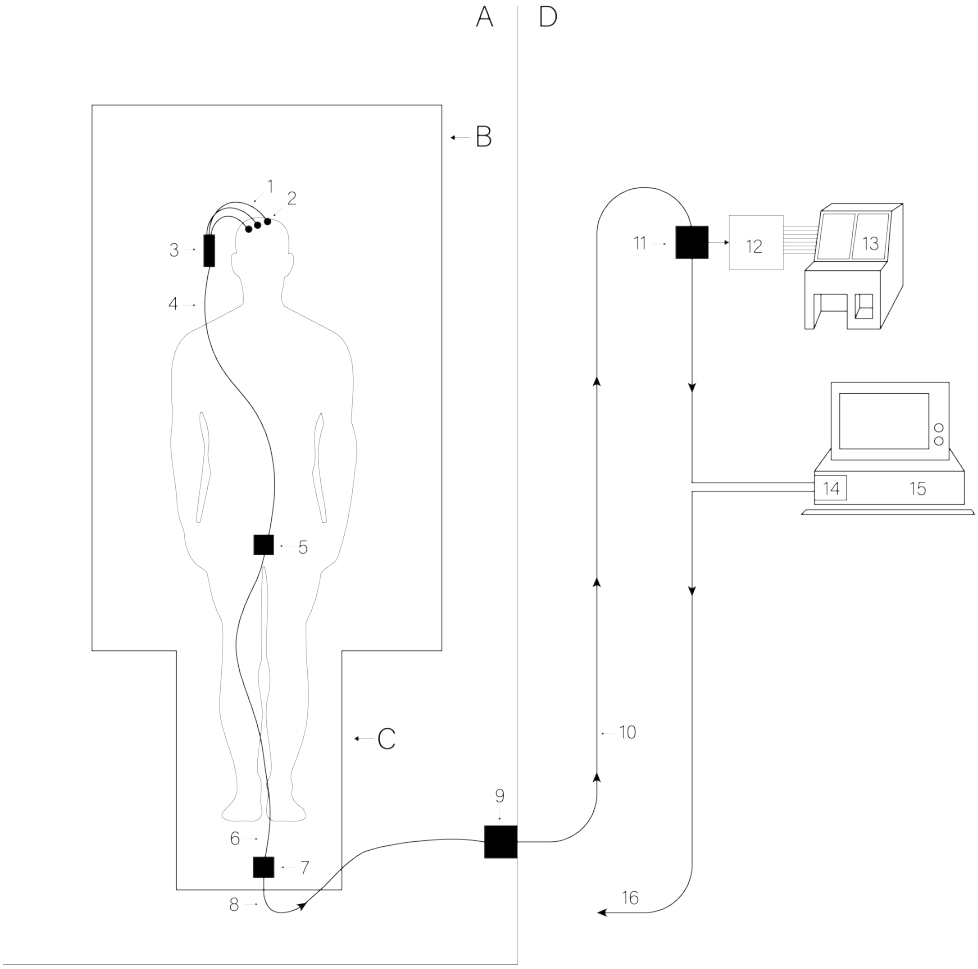

Figure 1: Block Diagram of the first system that enables to combine EEG and fMRI, from Ives and colleagues [7]. They made full use of MR-compatible electrodes within a 1.5 T whole body MR-scanner.

In the context of NF, the association of the EEG-fMRI is still rather recent and three milestone studies can be mentionned. The first study dates back to 2013, when Meir-Hasson and colleagues introduced the idea of fMRI informed EEG-NF through a method that produces an EEG fingerprint allowing to derive a predictor of the associated BOLD signal in a specific deep region in the brain [11]. The second study was conducted by Zotev and colleagues whom designed the first EEG-fMRI-NF in real time in which features from EEG and fMRI were fed back to the subject. These ground-breaking studies paved the way in enabling the study of cross-modal paradigm validation and new NF design that would combine both modalities. Last but not least, Perronnet and colleagues [12] conducted a study on the

form that feedback combining both EEG and fMRI features could take. Despite, challenges remain concerning basic physiology, study design, data quality, analysis/integration and interpretation.

Generally speaking, there is a distinction to be made between NF and brain-computer interfaces (BCI) in which individuals aim to directly regulate external devices instead of neural substrates. However, both allow direct translation of neural activity into a controlled signal of an auditory, a visual or a haptic feedback of this activity in real-time that can report the subject's performance. This kind of feedback is, by definition, used to bridge the gap between what is learned and what remains to be learned. This is why the choice of feeback is crucial in the construction of an NF study, by giving equal importance to its design and content. For instance, in human-human interaction, seeing a person talking makes it easier to understand, as compared with only hearing the person talking [13]. While the majority of NF studies use visual feedback, we come to question if this unimodal feedback is optimal and ecological for good learning. In our daily life, we face, most of the time, multimodal stimuli rather than unimodal. Indeed, we use many senses sequentially or in parallel, to actively or passively explore our surroundings, to confirm expectations about the world and to perceive new information. In addition, studies have suggested that the threshold of neuronal activation is reached more quickly with multimodal learning than with unimodal learning [14], as multimodal stimuli are typically perceived more quickly and accurately than unimodal stimuli [15]. Another theoretical consideration to take into account, is the fact that users prefer multimodal rather than unimodal interaction when the complexity of a task was increased [16]. This theory has been motivated by Wicken's *Multiple Resource Theory* [17], which stipulates that tasks can be performed better and with fewer cognitive resources when distributed across modalities.

When creating feedback for a NF study, these considerations should be taken into account because self-regulating its own brain activity is a complex task that imposes a high cognitive load. As mentioned above, unimodality is the norm but there are studies using several modalities. For instance, in 2008, Buch and colleagues deliver for the first time a visuo-haptic feedback to chronic stroke patients from a Motor Imagery (MI) task [18]. It was demonstrated that they were able to voluntarily control both visual and contingent haptic feedback. Later, the investigation from Brouwer [19] showed that visuo-tactile stimulation has better performance over unisensory stimulation.

As illustrated in Figure 3, the multimodality in NF can be divided into two parts. The first concerns the input: the use of multiple different neuroimaging techniques to enrich the quality of information given to the user. The second concerns the output: to report to the user, not a feedback modality, but a multisensoriality corresponding to the cohesion of multiple senses. It is not just an additivity but a complementary approach that is sought here.

Figure 2: The first hand orthosis introduced in BCI from Pfurtscheller and colleagues [20]. The subject had to imagine a movement of his hand to operate the device, which is directly based on his brain's bioelectric signals.

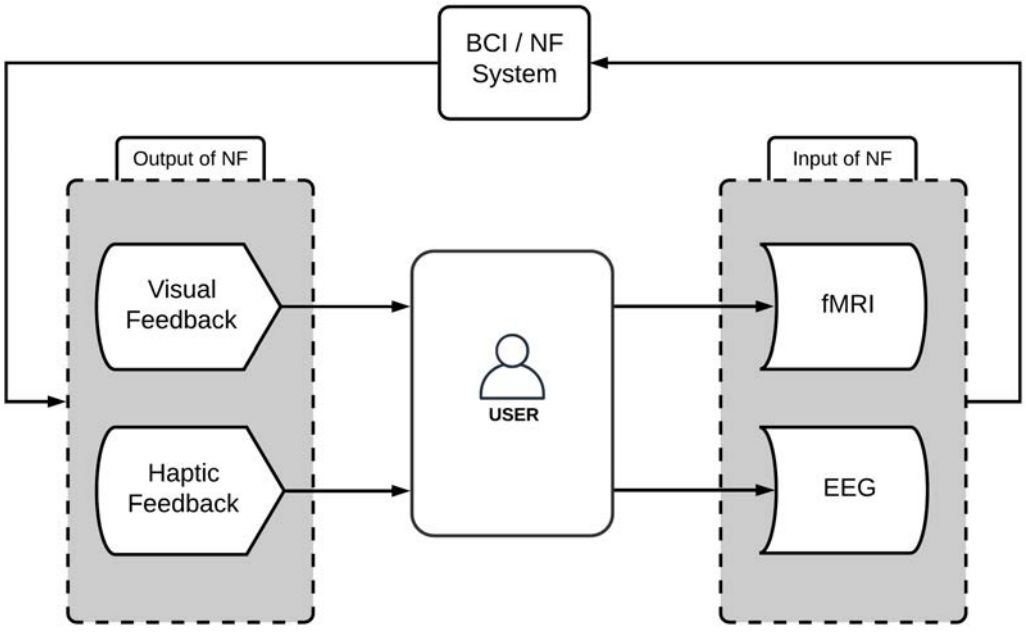

Figure 3: Multimodal interaction framework for neurofeedback. The user provides the input thanks to the regulation of his or her cerebral activity measured through neuroimaging modalities (EEG or/and fMRI for example): the input of NF. While receiving a feedback of his or her brain activity through uni- or multi-sensory feedback: the output of NF.

Objectives and Contributions

With this context in mind, the objective of this thesis is to contribute to both input and output of multimodal NF.

Regarding **the output of multimodal NF**, our primary aim is to answer the following interrogation: How to design an effective multisensory feedback? More specifically, how can we merge visual and haptic information into a combined feedback? With these interrogations in mind, we will present new methods with the intention of combining these two senses in an optimal way. In a second step, we will also study the use of visuo-haptic feedback in a NF context, in order to find out whether performance is improved compared to unisensory feedback.

Regarding **the input of multimodal NF**, our goal is to know how to improve the integration of the two techniques: EEG and fMRI, and also to study its contribution in a rehabilitation context. Our first objective is to improve the fusion of EEG and fMRI and our second objective is to assess mulitmodal NF based on EEG/fMRI into a rehabilitation context.

Here afterwards, you will find the work carried out, which follow the order of appearance of the chapters of this thesis. The manuscript is divided into three parts: Part 1 provides a state-of-the-art of EEG-fMRI for the NF as well as a review of the use of haptic feedback for BCI/NF. Part 2 describes our studies and contributions regarding the use of a multisensory feedback for NF, finaly part 3 details our contributions related to the output of multimodal NF and we will notably insist on the use of EEG-fMRI-NF for stroke rehabilitation.

Part 1 : Related Work. This part presents state-of-the-art on the use of both inputs and outputs for multimodal neurofeedback.

- **Chapter 1 : Input of Multimodal Neurofeedback: Combining EEG and fMRI**
  Chapter 1 provides a state-of-the-art of the combination of two different neuroimaging methods as inputs for multimodal NF: EEG and fMRI. Firstly, we focus on the general properties of the EEG and fMRI, such as their spatial and temporal resolution characteristics. Then we analyse the different approaches for the integration of EEG-fMRI data for NF: symmetric or asymmetric approaches and activation or connectivity analyses. We study the different works using EEG and fMRI for NF. Then, we propose a classification of EEG-fMRI based NF studies. We insist particularly on the simultaneous use of EEG-fMRI and EEG-informed fMRI. Finally, we analyse the most commonly used paradigms in these studies: the Motor Imagery Paradigm and the Emotion Network Paradigm.
- **Chapter 2 : Output of Multimodal Neurofeedback: Adding Haptics to Visual Feedback**
  Chapter 2 focuses on the output of multimodal NF. To do so, we provide a review of haptic feedback for NF. We first focus on human haptic perception before describing the different properties of haptic interfaces, whether tactile or kinaesthetic. Then, we analyse the different applications of haptic for NF and brain-computer interfaces. Two families of paradigms are studied: the motor imagery paradigm and external stimulation paradigms, such as the P300 and the steady-state somatosensory evoked potential. Finally, we discuss the contribution and utility of haptic feedback for NF.

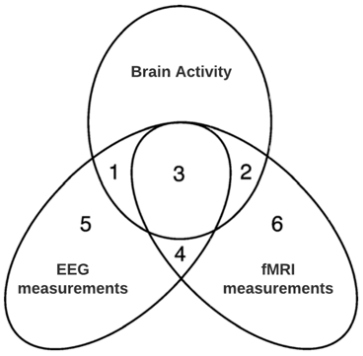

Figure 4: Chapter 1 describes the set of studies combining the EEG-fMRI for NF.

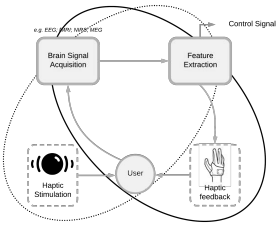

Figure 5: In Chapter 2, we describe the use haptic feedback for BCI/NF.

Part 2 : Towards Multimodal Neurofeedback based on Visual and Haptic Stimulation. In this part, we study the interaction of two different feedback under two different modalities (EEG and fMRI). More specifically, the haptic feedback used is a proprioceptive feedback based on the illusion of motion. We conduct a study to determine the impact of visual feedback congruent with this illusion of movement. Then we conduct a study to assess the impact of a vibration on the EEG signal. Finaly, we introduce this novel visuo-haptic feedback in a fMRI-NF study.

- **Chapter 3 : Study of a Visuo-Haptic Feedback for EEG-based Neurofeedback**
  Chapter 3 presents the results of our two studies on healthy subjects (N = 30/20) on the use of a visuo-haptic feedback for EEG-NF. We developed a new visuo-haptic feedback for NF purpose. This multisensory feedback consists of a combination of visual feedback (virtual hand) and haptic feedback delivered in a vibro-tactile way. The first study investigates how haptic feedback is complementary to visual feedback and the second study enable us to assess how this specific haptic feedback impacts EEG signals. These two studies allow us to create our own NF and to use it for stroke rehabilitation.
- **Chapter 4 : Study of Visuo-Haptic feedback for fMRI-based Neurofeedback**
  Chapter 4 presents the results of the first fMRI-NF study on healthy subjects (N = 15) that involves a visuo-haptic feedback. In this study we compare multisensory and unisensory feedback in order to assess the benefits of multisensoriality. We introduce three types of feedback (visual, haptic, and visuo-haptic) and study their effects on a MI task with a within-group design.

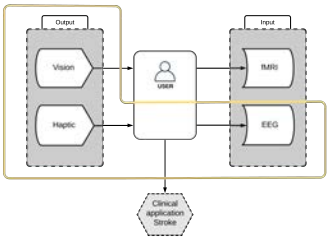

Figure 6: Chapter 3 presents studies in which participants were facing a proprioceptive feedback thanks to a haptic stimulation.

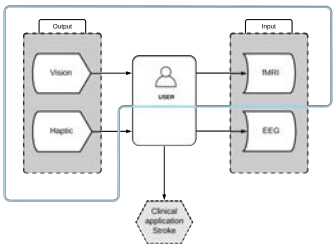

Figure 7: In Chapter 4, we present a NF based fMRI study in which participants performed NF with a multisensory or unisensory feedback.

Part 3 : Towards Multimodal Neurofeedback based on EEG-fMRI for Stroke Rehabilitation. This part gathers our contributions regarding studies based on the use of EEG-fMRI-NF for stroke rehabilitation. On one hand, we present a first contribution to integrate EEG and fMRI thanks to a new method of automated electrodes detection inside the MR scanner. On the other hand, we study the impact of NF for neurorehabilitation for stroke patients.

- **Chapter 5 : Automated Electrodes Detection for Multimodal EEG-fMRI**
  Chapter 5 presents a new technique for detecting the position of electrodes in fMRI. We use a special MR sequence to obtain electrodes positions on a MR-volume. This method only has for additional cost the acquisition time of the sequence in the MR protocol. We demonstrate that our method achieves a significantly more accurate electrode detection compared to a semi-automatic detection one that is more commonly used during EEG/fMRI protocols.
- **Chapter 6 : Multimodal EEG-fMRI Neurofeedback for Stroke Rehabilitation: A clinical study**

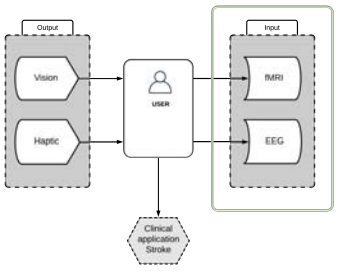

Figure 8: In Chapter 5, we present two novel techniques for detecting the EEG position inside the MR scanner.

Chapter 6 presents a NF study on stroke patients (N = 4) with EEG/ fMRI. In the context of neurorehabilitation, we investigate the impact of NF in four stroke patients with EEG/fMRI. The objective of this pilot work was to test the feasibility of the EEG-fMRI NF training on stroke patients over several sessions. These feasability study give useful indications for the design of future clinical studies with NF.

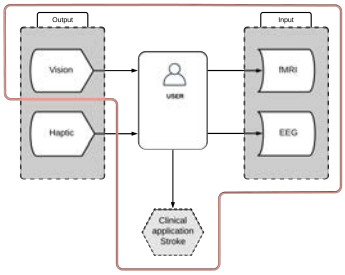

Figure 9: Chapter 6 describes the study performed with stroke patient on a multimodal EEG-fMRI based NF.

Related Work

Input of Multimodal Neurofeedback: Combining EEG and fMRI

1

Preamble: *This chapter presents an overview of the integration of the EEG and fMRI, two complementary modalities by nature, which can be exploited in a multimodal way for NF purposes.*

1.1 Introduction

How can we measure brain activity? This question has been around for many years and began to be answered by Berger (1929) who first acquired (or measured) human brain activity [21]. This first experiment was conducted using Electroencephalography (EEG), which allows the electrical activity of the brain to be measured using electrodes located on the scalp. Since this first experiment, other non-invasive imaging modalities have been used to study brain functionality, based in particuliar on the electrical, magnetic and haemodynamic responses of the brain. These techniques, also known as imaging modalities, can be used to study brain functionality in a non-invasive way. While unimodal techniques typically do not have both high temporal and high spatial resolution, multimodal techniques can combine the advantages of single modalities yielding a more complete view on brain activity with an unprecedented spatiotemporal resolution. This very high resolution could be useful to understand how the different elements of the brain take part in various perceptual and cognitive activities [22].

Behind these neuroimaging techniques lies the neuronal activity within the brain, which generates ionic currents that are often modelled as electric dipoles. These dipoles, which can be characterised by their electromagnetic field, can be measured respectively by EEG and Magnetoencephalography (MEG). Brain activity can also be measured indirectly thanks to the heamodynamic activity, in fact the cerebral activity induces changes in oxygen concentrations in order to supply energy to the neurons, known as the haemodynamic response (Hemodynamic Response Function (HRF)) [6]. This relationship between oxygen-rich and oxygen-poor blood, also called blood-oxygen-level-dependent (BOLD), generates changes that can be detected by functional magnetic resonance imaging (fMRI) or functional Near-Infrared Spectroscopy (fNIRS) [23].

However, these three modalities have different properties even if they register data at regular time intervals, and thus reflect temporal dynamics; their spatial and temporal resolution varies greatly. fMRI is characterised by a very high spatial resolution of the order of a millimetre but a low temporal resolution (1s) as opposed to EEG and MEG which have a high temporal resolution but have a low spatial resolution (a little less with MEG). This synergy, which already seems to be taking shape, goes even further because EEG and MEG measurements are surface-based while fMRI can detect deep areas of the brain.

Because of the complementarity (in time and space) of EEG and fMRI, advanced technologies focused on the integration and simultaneous recording of EEG and fMRI signals to provide bi-modal setting [22, 24]. This new technology opened a new research field increasing knowledge [25]. In order to better illustrate the problem linked to this multimodal integration, we relied on the Venn diagram by Biessman and colleagues that can show easily the benefits and pitfalls of the integration of EEG and fMRI (see Figure 1.1). Indeed, the integration of these two modalities also have their limits, their very heterogeneous nature and the fact that brain processes are very complex systems that depend on many latent phenomena mean that simultaneously extracting useful information from them is not an evident task. That is why the challenge of understanding the relationship between EEG and fMRI is not fully accomplished [26].

In this chapter, we will therefore focus on the contribution of the two most widely used non-invasive imaging methods in the field of neurosciences and more precisely for NF and BCI. Indeed, although fMRI answers the questions of *where* and EEG answers the question of *when*, then what is the real scientific question that implies the fusion of EEG/ fMRI? The very aim of NF answers this question, which is to find out what is the best feedback to give to report brain activity and lead to more efficient neuroadaptive changes and more effective clinical outcomes [27].

The remaining of this chapter is organised as follows: firstly, we provide an overview of existing EEG-fMRI combinations in Section 1.2. Secondly, we surveyed recent studies exploiting EEG-fMRI as neuroimaging modalities in NF in Section 1.3, showing the experimental and technical challenges. These articles are then discussed in Section 1.4, where we also identify some remaining challenges.

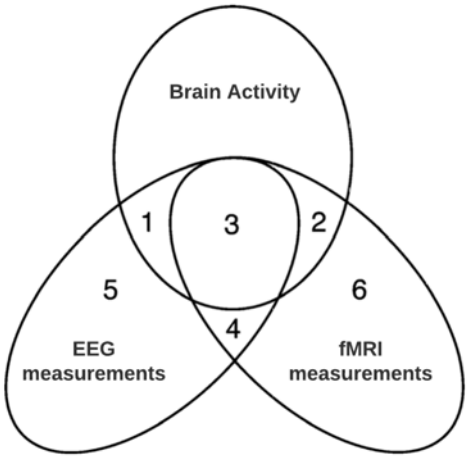

Figure 1.1: Venn diagram of EEG-fMRI neuroimaging analysis methods (adapted from [28]); certain aspects of the brain activity are reflected in electrophysiological recordings (EEG) and others in hemodynamic measurements (fMRI). While some aspects such as fast neuronal oscillations are only detectable in electrophysiological signals (area 1), other aspects (such as activity in deep brain structures) are easier to investigate using BOLD signal (area 2). Aspects that are reflected in both modalities can be subdivided into signals originating from neural activity (area 3) and non-neural physiological processes reflected in both modalities, such as muscle contractions that lead to head movement (area 4). Besides these common artefact sources, there are many artefacts that are reflected in one modality only (area 5 and 6).

1.2 Why and How should EEG and fMRI be combined ?

The study of the simultaneous combination of the EEG and fMRI is an expanding area of research, particularly under the impetus of studies on sleep or epilepsy [25]. Their integration into studies on NF is rather recent and was pioneered by Zotev et al. [29].

1.2.1 General Properties of EEG & fMRI Modalities for NF Purpose

This section describes the properties of EEG and fMRI, their advantages and disadvantages. The aim of this section is thus to shed light on the limitations of both modalities and advantages of their combined use.

EEG modality

EEG is one, if not the most widely used non-invasive brain imaging technique for studying brain activity (the most widely used for NF). EEG measures electrical brain activity caused by the flow of electric currents during synaptic excitations and inhibitions of neuronal dendrites, mainly in the superficial layers of the cortex. It is therefore a direct measure of electrical activity. The electrical signals are measured by electrodes located on the scalp (Figure 1.2) and each of them allows to measure a spatio temporally smoothed version of the local field potential [22], integrated over an area of 10 cm^2 or more [30].

Scalp EEG activity shows oscillations at a variety of frequencies and several of them show some characteristics in terms of frequency ranges, spatial distributions and are associated with different states of brain functioning (e.g., waking and the various sleep stages). In the literature, EEG is typically described in terms of activity types which are rhythmic activity and transients. These rhythmic activities can be divided into certain frequency bands which are proved to have certain biological significant or certain distribution over the scalp. Six types of frequency bands can be identified: Delta (0.5-4 Hz) which is associated with deep sleep and wake up states; Theta (4- 7 Hz) which is generated with idling, creative inspiration, unconscious material, drowsiness, and deep meditation; Alpha & Mu (8-13 Hz) which is associated with relaxation, concentration, and sometimes in attention and Mu is a centrally located alpha frequency that represents the sensorimotor cortex, it should be noted that while it resembles the alpha rhythm, it is not affected by eye opening; Beta (12-30 Hz) which is associated with motor behaviour and is generally attenuated during active movements; and Gamma (>30 Hz) which could be detected at somatosensory cortex and is also shown during short term memory matching of recognised objects, sounds, or tactile sensations [31].

Generally, neuroimaging modalities are considered to be divided into two categories: invasive and non-invasive. One way to record better signals is to use electrodes implanted in the brain. This invasive thechnique allows the exploration and recording of electrical events in deeper regions thanks to metal or glass electrodes (Electrocorticography). However,

the use of invasive electrodes implies significant drawbacks due to the risk of performing surgery and the apparent gradual degradation of the recorded signals.

EEG has been widely used in NF over the years to induce long-lasting behavioural changes thanks to its relatively low cost and portability, both in healthy volunteers and in patients [32].

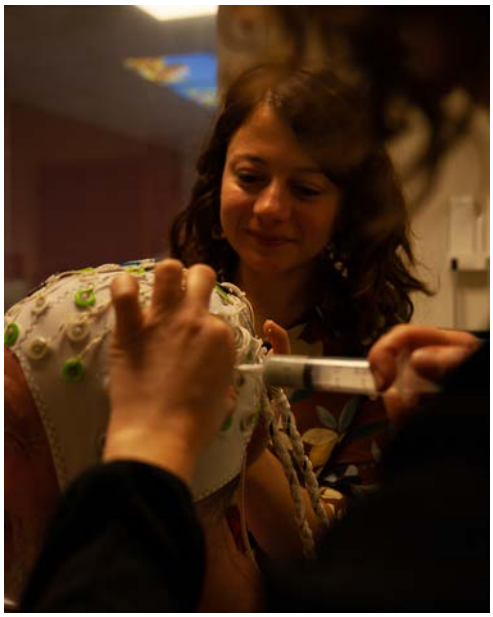

Figure 1.2: Photography of a 64-channel MR-compatible EEG (Brainproduct).

fMRI modality

In the field of cognitive neuroscience, fMRI has become the go-to mainstay as a non-invasive braining imaging method. Thanks to a much higher spatial resolution than EEG, fMRI provides unparalleled access to detailed patterns of activity in the human brain (both cortical and subcortical target regions). Here we will focus not on fMRI in general but rather on its real time aspect,real time functional Magnetic Resonance Imaging (rtfMRI), which permits a non-invasive view of brain function (thanks to BOLD contrast) in vivo and in *real time*. We talk about *real time*, but in reality it is rather the ability to capture the brain signal every 1-2 s. In addition, blood oxygenation level changes 2 to 6 seconds after the stimulus. HRF is used to model BOLD signal [33, 34].

Indeed, contrary to the EEG which directly measures neuronal activity, fMRI is an indirect measure of brain activity because it does not measure neuronal activity exactly but rather the consequences of neuronal activity. The pathway from neural activity to the fMRI activity map is schematised in Figure 1.3.

In general, it is common to consider that the spatial resolution of fMRI is high, but it is especially high compared to the EEG since its spatial resolution is typically of up to 2 mm^3 (for each voxel); a volume that would encompass approximately 187 134 neurons in

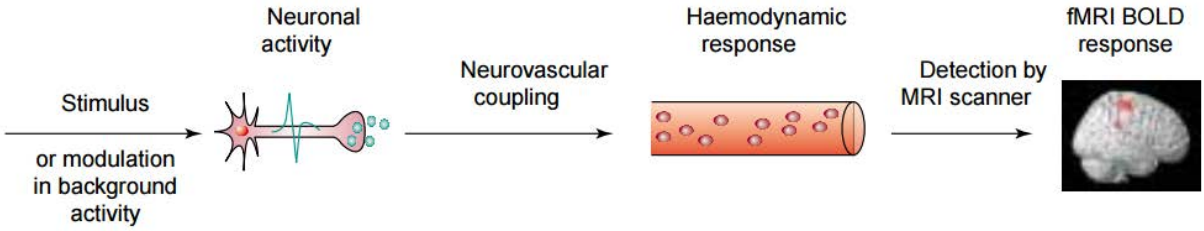

Figure 1.3: Schematic of the detection of neural response to a stimulus with fMRI BOLD signal. From [35]

cortex [36]. However, this value can be improved by suppressing macrovascular signals and contrasting different experimental conditions appropriately [1].

These properties can be valuable for NF applications [27]. Recent studies suggest that fMRI is a mature technology to use in the context of NF training [37, 38] NF-based fMRI (or fMRI-NF) works by providing a feedback representing HRF in a given ROI. The advantages of fMRI in terms of spatiality are substantial for NF because it makes it possible to reinforce engagement or regulation of these specific ROIs [39]. A review on the design of fMRI-NF studies can be found in [40].

1.2.2 EEG–fMRI multimodal Integration for NF

General properties of Fusion of EEG and fMRI features

In this section, we will discuss the different multimodal analysis methods for EEG-fMRI features. The studies mentioned below are therefore not all related to the NF but could underline the dearth of studies. A review on simultaneous EEG-fMRI can be found in [41]. This categorisation is based on the work of Biessman and colleagues [28], who have classified these methods according to the type of analysis used. Two main fusion features are reported: Asymmetric and symmetric fusions, that is dividing analysis methods in those that bias one modality towards features extracted from the other modality (asymmetric approaches) and methods that try to analyse both modalities at the same time (symmetric approaches); and activation and connectivity analysis, that is dividing single brain regions and network analysis.

Asymmetric and symmetric fusion : Multimodal data integrations are categorised as symmetrical and asymmetrical. Asymmetric approaches mainly use one of the modality information to bias the brain activity estimates of another modality (Figure 1.4). Most asymmetric methods can be seen as regression, a form of supervised learning [28]. The most influential asymmetric fusion methods include time prediction, that is: asymmetric EEG Based fMRI analyses where fMRI analysis is based on the temporal information of EEG where a specific EEG feature is convoluted with the HRF to model the fMRI waveform [9]; or spatial constraints, that is: asymmetric fMRI Based EEG Analyses where the EEG imaging is based on the spatial prior of fMRI: the EEG source reconstruction is constrained by the spatial activity information obtained from the fMRI [24, 42]. Symmetric approaches

try to analyse both modalities at the same time by establishing a common generative model or the use of interactive information to explain two modalities [43, 44]. The interest of this approach is to overcome the problems associated with asymmetrical approaches, since during the selection of the characteristics of the "primary" modality (the one used to bias the estimation of the other modality), characteristics may be selected that are not reflected at all in the other ("secondary") modality. For example, a large vessel might lead to highly active voxels in an fMRI time series, but the dipole source of interest does not necessarily coincide with this very location [28]. Different methods can be used in symmetric analyses to address this problem, such as model driven and mutual information [44–47].

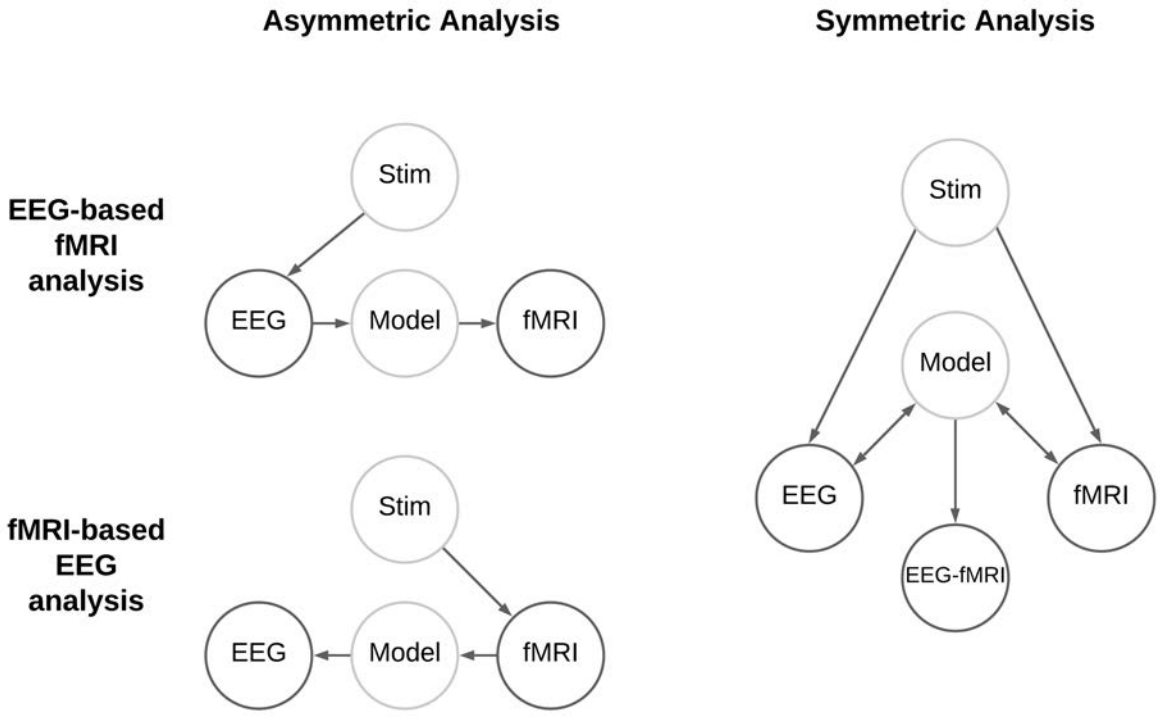

Figure 1.4: Multimodal methods as categorised into asymmetric or symmetric approaches (grey indicates optional nodes); in asymmetric analyses features from one modality are used to improve brain activity estimates of another modality, sometimes via a generative model of the latter modality (From [28]).

Activation and Connectivity Analyses : Another categorisation to be taken into account in the EEG-fMRI analyses is the distinction between studies that locate activation patterns and those that investigate functional connectivity between regions. Although the majority of the studies are activation based, it is also interesting to see how specific brain regions interact together. Indeed, many cognitive processes require more than one active brain area and if brain areas interact they will show correlated activity. In fact, most of the processes so far examined with fMRI studies (e.g.,emotion processing, motor response, language,pain perception, etc.) include the coordinated activity of several brain regions [37, 48]. Most functional connectivity studies in the context of fMRI are based on correlations between voxels (see, e.g., [49, 50]). In [49], univariate correlation coefficients are used to quantify functional connectivity. In [51], Principal Component Analysis (PCA) is used to

reveal connectivity patterns. Also Independent Component Analysis (ICA) is often used for functional connectivity [50].

Classification of NF-based EEG-fMRI studies

In the literature, we can find different ways of combining EEG and fMRI for NF, simultaneously or not. In order to classify these different combinations, we will base ourselves on the taxonomy elaborated by Perronnet et al. [52]. In this taxonomy, we can find two categories, the one that uses one modality as NF signal, such as Passive fMRI during EEG-NF (pfMRI) or Passive EEG during EEG-NF (pEEG), EEG-informed fMRI-NF (iEEG) and fMRI before/after EEG-NF (efMRI); and the one that uses both modalities as NF signals, such as EEG-fMRI-NF that refers to simultaneous EEG-fMRI for NF (EEG-fMRI). These combinations do not have the same technological implications and difficulties. But share sometimes similar objectives, such as overcoming the cost-intensive, cumbersome and tiring aspects of fMRI, while keeping a good specificity in EEG-NF training [53].

fMRI before/after EEG-NF (efMRI) : Using fMRI before and after EEG-NF can be used to evaluate functional outcomes of the EEG-NF training such as connectivity or change in cerebral plasticity. This can be done during the resting state [54].

Passive fMRI during EEG-NF (pfMRI) : Recording passive fMRI during EEG-NF allows to evaluate and validate the EEG-NF protocol and to find BOLD correlation of the EEG-NF training. The main disadvantage is that MR artefacts affect the EEG signal and therefore the quality of the online signal could be lower.

Passive EEG during fMRI-NF (pEEG) : Recording passive EEG during fMRI-NF allows to evaluate the fMRI-NF protocol and to identify electrophysiological correlates of the fMRI-NF training. In this configuration EEG artefact correction is performed offline. This approach can be used to explore EEG correlates of fMRI-NF that could be used as potential targets for EEG-NF or EEG-fMRI-NF

EEG-informed fMRI NF or EEG Finger-Print NF (iEEG) : In literature, two terms can be found: EEG-informed fMRI or EEG Finger-Print (EFP). The all-around term used in the literature is EEG-informed fMRI, but that sometimes one can find EFP what defines the same thing. The term EEG-informed fMRI refers to methods extracting features from EEG signals in order to derive a predictor of the associated BOLD signal in a specific ROI [55] (Figure 1.5). The interest is to be able to reproduce EEG-fMRI-NF in real time with EEG only in order to increase the quality of EEG-NF sessions. To export fMRI information outside the scanner, most of the methods intend to predict the fMRI BOLD signal activity in a specific ROI by learning from an EEG signal recorded simultaneously inside the fMRI scanner [11, 56]. For a comprehensive review on EEG-informed fMRI [57, 58].

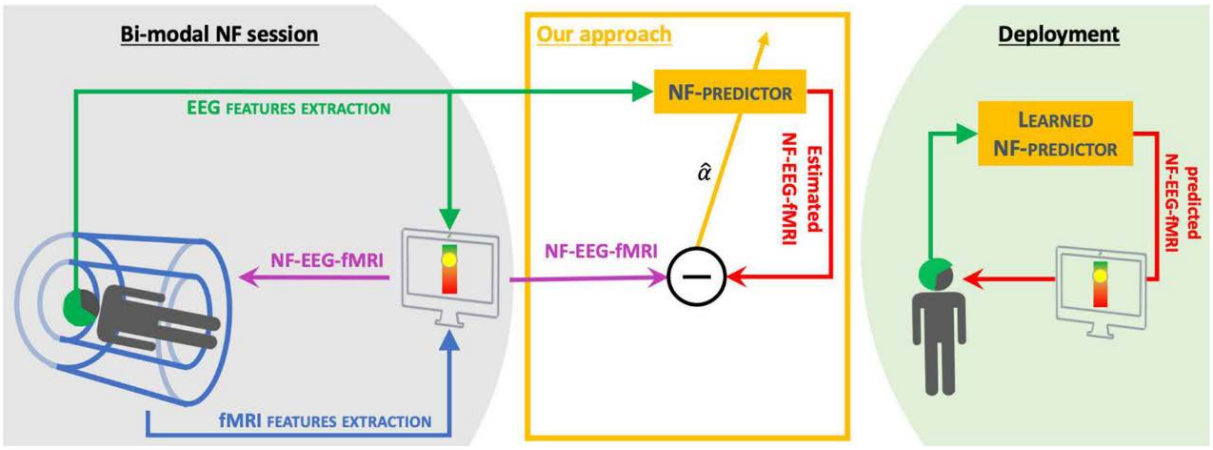

Figure 1.5: Schematic of EEG-informed fMRI from Cury et al [55]. The idea of this method is to use data from NF-based EEG-fMRI sessions to create an NF-fMRI or NF-EEG-fMRI predictor to add missing information during EEG sessions only.

EEG-fMRI-NF (EEG-fMRI) : EEG-fMRI-NF refers to the combined use of simultaneous EEG and fMRI features for NF. Here the EEG must be cleaned of all artefacts (Ballistocardiogram (BCG), gradient artefacts and electric signal caused by radio-frequency pulse (pulse artefacts) [59]) in real time and not offline [60, 61]. This type of protocol can be seen as the combination of EEG-NF and fMRI-NF protocol. From a technical point of view we refer to the work from Mano and colleagues [62] who describe how to build an NF based EEG-fMRI platform (See section 1.2.3 for more details). An open source hardware and software system for acquisition and real time processing can be found in [63]. In addition to the technical difficulty of implementing the EEG inside the MR system, these studies must also answer the question of the form that takes the feedback. How to represent two features corresponding to different neuromarkers so that the subject can regulate them optimally?

1.2.3 The Challenge of Integrating EEG and fMRI: A Focus on EEG-fMRI-NF at Neurinfo Plateform

This section insists on the technical aspects behind a real-time EEG-fMRI acquisition for NF. Although there are many theoretical advantages to the simultaneous acquisition of EEG and MRI, from a technical point of view this integration is complex. We will take the example of the Neurinfo platform located in Rennes (France), which we use for our EEG-fMRI-NF experiments (notably in Chapter 4 and Chapter 6). This plateform comprises:

- EEG Subsystem: As for technological issues, the entire EEG hardware must be MR-compatible and sufficiently comfortable for the subject. Improper use of the equipment may result in considerable risks. Regarding safety, a potential risk for the subjects comes from electrodes and the heating of conducting leads during MR radio frequency transmission, resulting in discomfort or even burns [65]. To address this issue we used the solution from Brain Products: A 64-channel EEG cap, equipped with a drop-down electrocardiogram electrode for heart pulse measurements. This cap is connected to an MR-compatible amplifier by a strip cable placed inside the

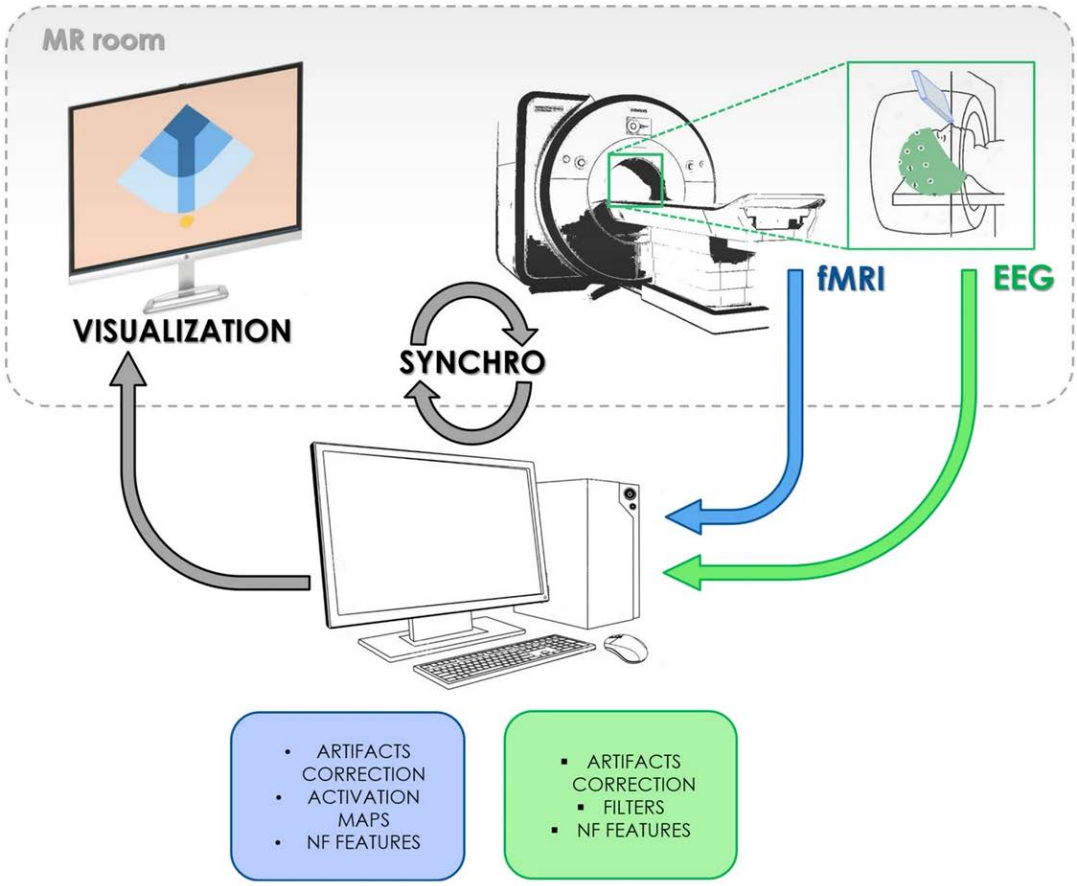

Figure 1.6: Schematic of the EEG-fMRI-NF Neurinfo plateform (from [64]). Features from EEG and fMRI are used as NF in a bi-dimensional form.

MR tube (powered by MR-compatible battery). One of the main concerns related to the simultaneous acquisition of MRI and EEG for NF is of course the MR gradient artefact, that must be corrected. This artefact that is caused by the scanner's alternating gradient magnetic field has a fixed pattern, and its amplitude is typically 100–1000 times of the amplitude of physiology signal. To address this issue, we rely on a TTL signal that is sent during MR acquisition and matches the scan time of MR (each Time of Repetition (TR)). This trigger allows to filter the EEG signals by subtracting the artefacts as a template.

- fMRI Subsystem : The MR imaging is performed on a Siemens 3T scanner (MAGNETOM Prisma, Siemens Healthineeers, Erlangen, Deutschland) with 64-channel head coil enabling a secure installation of the EEG cap and connection of the bundle to amplifiers. Based on Faraday law of electromagnetic induction, it is important to minimise the area of any loop formed by the EEG cap or wire, this leads to reduce artefacts induced by the changing magnetic fields.

The EEG and fMRI features are centralised and synchronised into a single unit, called *NF Unit*, which also allows us to calculate the NF score. Once the multimodal data are joint, the NF score can be returned thanks to a visual display at the end of the MR tube (See Figure 1.7 C).

Figure 1.7: Photography of the preparation of a simultaneous EEG-fMRI-NF session with a 3T MRI and a 64 EEG cap. (a) EEG subsystem installation and impedance check outside the MR environment, (b) Installation of the MR coil and EEG impedance recheck, (c) Placement of the amplifiers, battery and LCD display.

1.3 NF-based EEG-fMRI

The following section describes the state-of-the-art of NF applications based on EEG-fMRI neuroimaging modalities. This review of the literature was conducted in accordance with PRISMA guidelines [66]. We conducted a PubMed search using the following key-words: "EEG" AND "fMRI" AND "NF" resulted in 81 publications. We then screened out conference proceedings, articles only using EEG or fMRI modality, articles unavailable in english, and others that were falsely identified as NF studies by the search engine. Within the remaining publications, we identified articles reporting original research studies. This excluded reviews, opinion pieces, methods only papers, and the ones using other non-fMRI/EEG modalities. During the process of reviewing the articles (described below), several additional research studies missed in the initial literature search were identified and added to the review. Articles reporting secondary analysis or reusing participant data were not included so as not to over represent single studies (final number of unique studies $n = 15$). Two main families of paradigms were found: the network-based emotion paradigm with applications for Major Depressive Disorder (MDD) or for Post-Traumatic Stress Disorder (PTSD) patients; and the Motor Imagery (MI) paradigm with applications for stroke patients.

1.3.1 Emotion Network Paradigm

To date, the amygdala is highly represented as a feature in the EEG-fMRI-NF studies, with various combinations of EEG-fMRI such as simultaneous EEG-fMRI and passive EEG during fMRI-NF or EFP. Amygdala-based NF refers to the fact that the amygdala is the region of emotions and seems to be a very good neuromarker for rehabilitation. This feature is very suitable for the EEG-fMRI as it is a fairly deep region in the brain and difficult to reach with EEG only. The first study that reported amygdala as fMRI feature for EEG-fMRI-NF was designed by Zotev and colleagues [29] thanks to the anterior study from Johnston and colleagues [67], in which they claimed that after localising emotional

network using fMRI only, subjects could upregulate target areas, including the insula and amygdala. These studies used positive autobiographical memories as a task during NF trials.

An extensive body of research in both humans and experimental animals has established that the amygdala plays a central role in several aspects of emotion processing, such as recognition of both positively- and negatively-balanced emotional stimuli, reward learning, and appetitive or aversive conditioning. The involvement of the amygdala during mood self-induction has been reported in several studies [68, 69]. Therefore, the possibility of volitional modulation of left amygdala activity using fMRI-NF training provides a valuable tool to study neurophysiological regulation within neural networks involved in emotional processing [70]. Several fMRI-NF studies have also revealed the potential of emotion regulation for clinical utility to reduce symptoms associated with chronic pain [71], smoking cessation [72], anxiety [73], PTSD [74], and MDD [75].

In simultaneous EEG-fMRI-NF the frontal asymmetry is used as an EEG feature. For instance, [29] proposed a fMRI-EEG-NF based on the frontal EEG power asymmetry in the high-beta band (FBA; 21–30 Hz) and upregulation of BOLD fMRI activation in the left amygdala (9 healthy subjects) (See Figure 1.8). This EEG feature would seem to be an important and widely used feature for emotion and emotional reactivity [76]; indeed, many EEG studies have indicated that depression and anxiety are associated with reduced relative activation of the left frontal regions and increased relative activation of the right frontal regions (meta-analysis from [77]). They claimed that the combined protocol could be more efficient than either the EEG-NF or the fMRI-NF protocol performed separately. In a follow-up study with the same paradigm [78], the authors conducted a proof-of-concept study with MDD patients (experimental group $n = 16$, control group $n = 9$). Participants demonstrated significant upregulation of the left amygdala BOLD activity, FAA, and FBA during the EEG-fMRI-NF task. Their results also demonstrated that Frontal Alpha Asymmetry (FAA) and FBA showed temporal correlations with amygdala BOLD activity.

In EEG-informed fMRI NF the BOLD activity of the amygdala is predicted thanks to a time-frequency representation extracted from the EEG data [11], yielding an EEG model of weighted coefficients (Figure 1.5). It has also been shown that this prediction model can reliably probe amygdala BOLD activity and, that compared with sham-NF, EEG-informed fMRI (called amygdala EEG finger print in the paper) can lead to improved amygdala BOLD downregulation capacities via fMRI-NF [79]. In a recent study with a double-blind randomised controlled trial and a large sample ($n = 180$), Keynan and colleagues [80] demonstrated in a follow-up fMRI-NF (approximately 1 months after the training) greater amygdala BOLD downregulation and amygdala–ventromedial prefrontal cortex functional connectivity following EEG-informed fMRI NF relative to the no-NF. It is interesting to note that the control group who received an NF based on the alpha/theta ratio did not undergo this last fMRI-NF session.

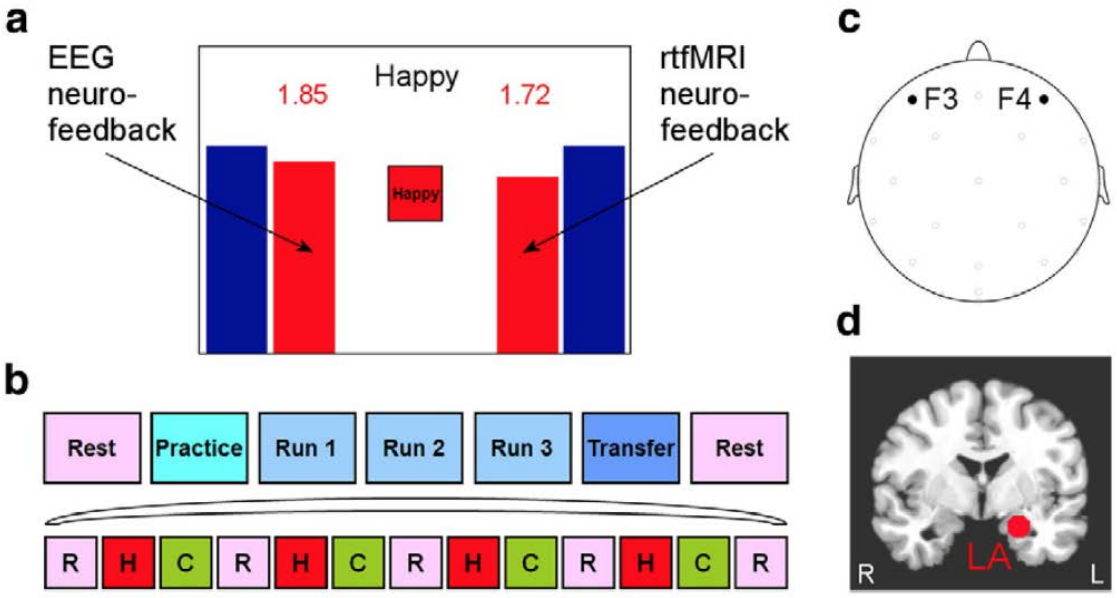

Figure 1.8: EEG-fMRI-NF experimental protocol for emotional self-regulation described (from Zotev, Phillips,et al. [29]).

1.3.2 Motor Imagery Paradigm

MI combined with EEG-NF or fMRI-NF is a very popular approach and is considered to be a promising approach for neurorehabilitation and in particularly for stroke patients [81]. In simultaneous EEG-fMRI, two neuromarkers need to be considered, one for the EEG, the other for the fMRI. Compared to the amygdala-based NF, the regions involved for the MI are cortical and are therefore easily detectable even for the EEG. When imagining movement (or executing movement), amplitude desynchronisations are detected in the alpha and beta bands (8-30 Hz) from the sensorimotor cortices: also known as Event-Related Desynchronisation (ERD) [82, 83]. On the fMRI-NF side, most MI paradigm involve primarily upregulation of Primary Motor Cortex (M1) or premotor/Supplementary Motor Cortex (SMA) [40, 84], but the choice of the ROI is still controversial [40]. Indeed, Berman and colleagues [84] found that M1 regulation was possible during finger tapping but not motor imagery, while Mehler and colleagues [85] found that neurofeedback was associated with a decrease in primary motor but an increase in SMA engagement activity during MI.

In simultaneous EEG-fMRI-NF studies, ERD over sensorimotor cortex and upregulation of BOLD motor areas have been used as features. These studies have been conducted by Perronnet and colleagues [12, 52], who performed the first EEG-fMRI-NF with healthy subjects ($n = 10$) with MI paradigm [52]. In this study, MI-based EEG-fMRI-NF was compared to unimodal MI-based EEG-NF and MI-based fMRI-NF. The authors reported that MI-related hemodynamic activity was higher during EEG-fMRI-NF than during EEG-NF, suggesting that EEG-fMRI-NF could indeed be more specific or more engaging than EEG-NF. It also highlighted that during bimodal EEG-fMRI-NF subjects could happen

to regulate one modality more than the other, hence supporting the hypothesis that different neural mechanisms are involved during regulation of fMRI or EEG activity with NF [29]. In a follow-up study, the same authors concentrated on the representation of the EEG-fMRI feature. A two-dimensional feedback (2D) (See Figure 1.6) in which each dimension depicted the information from one modality was compared to an uni-dimensional feedback (1D) that integrated both types of information. It was reported that 1D and 2D integrated feedback are both effective but online fMRI activations were significantly higher in the 1D group than in the 2D group.

In passive fMRI during EEG-NF, a study from Zich and colleagues [4], showed that MI-based EEG-NF allows subjects to generate enhanced cortical activation in EEG but also higher BOLD activity compared to MI with no feedback. Interestingly, the study revealed that the contralateral activity in EEG and fMRI were correlated while the laterality patterns were not. The revelation that EEG and fMRI signatures of MI are not redundant suggests a potential for bimodal EEG-fMRI-NF.

In EEG-informed fMRI NF, a recent study from Cury and colleagues proposed a new model able to exploit EEG only to predict fMRI-NF or EEG-fMRI-NF during MI tasks. They showed that predicting NF-fMRI scores from EEG signals adds information to NF-EEG scores and significantly improves the correlation with bi-modal NF sessions compared to classical NF-EEG scores.

Table 1.1: NF-based EEG-fMRI studies *Note.* S: Simultaneous EEG-fMRI; pfMRI: Passive fMRI during EEG-NF; pEEG: Passive EEG during fMRI-NF; iEEG: EEG-Informed fMRI-NF or EEG fingerprint; efMRI: fMRI before/after EEG-NF NP: Number of Patient; NS: Number of subject; SP: Stroke patients; PTSD: Post-traumatic stress disorder patients; MDD: Major depressive disorder patients; FAA: Frontal Asymmetry in alpha band; T/A: Theta/Alpha (4-7 Hz)/(8-13 Hz) Band; FBA: Frontal Asymmetry in high beta band; RA/LA: Right/Left Amygdala; rACC: left rostal anterior cingulate cortex; pSTS: right posterior Superior Temporal Sulcus; FEPN: Facial Expressions Processing Network; HEI: Happy Emotion Induction; MI: Motor imagery;

Combination	fMRI-NF feature	EEG-NF feature	Task	Paper purpose	NP/NS	Reference
EEG-fMRI	LA	Frontal Asymmetry in the high-beta band (21-30 Hz)	HEI	Research	-/9	[29]
EEG-fMRI	LA + rACC	FAA (7.5-12.5 Hz) + FBA (21-30 Hz)	HEI	Rehabilitation	16-8/-MDD	[78]
EEG-fMRI	M1	Laterality index between C1 and C2 in the alpha band (8-12 Hz) over sensori-motor cortex	MI	Research	-/10	[86]
pEEG	LA	N/A	HEI	Rehabilitation	13/-MDD	[87]
pEEG	LA	N/A	HEI	Rehabilitation	20-11/-PTSD	[88]
pEEG	pSTS	N/A	Mental imagery of facial expression	Research	-/13	[89] & [90]
pfMRI	N/A	SMR	MI	Research	-/24	[4]
pfMRI	N/A	SMR	N/A (control the ball)	Rehabilitation	9-8/- CP	[91]
pfMRI	N/A	T/A	Relaxation with eyes closed	Research	-/45	[92]
iEEG	Motor cortex	PSD alpha/beta band (8–30 Hz)	MI	Research	-/17	[55]
iEEG	pSTS	N/A	Mental imagery of facial expression	Research	-/10	[56]
iEEG	RA	T/A from occipital electrodes	Relaxation	Research	-/20	[93]
iEEG	RA	N/A	Lower the volume of an auditory stimulus	Research	-/15-9	[94]
iEEG	RA	T/A	Relaxation	Research	-/90-45-45	[80]
efMRI	N/A	Alpha band (8-12 Hz) over midline parietal cortex (Pz)	N/A	Research	-/34	[54]
efMRI	N/A	Alpha band (8-12 Hz) over midline parietal cortex (Pz)	N/A	Rehabilitation	21/-PTSD	[74]

1.4 Discussion

Integrating complementary sources of information about neural activity in a meaningful way can significantly increase the overall amount of information extracted. Data fusion techniques have been highly successful in neuroimaging in general and in NF / BCI in particular. This is why NF based EEG-fMRI studies have gained interest in recent years. These studies employed different ways of combining these modalities, the most used being simultaneous EEG-fMRI and EEG-informed fMRI but other combinations exist such as passive EEG during fMRI / passive fMRI during EEG or fMRI before / after EEG. In the literature, researchers using EEG-fMRI as a means to provide NF have focused on two main paradigms: MI paradigm and Emotion Network Paradigm. In each of these paradigms, clinical applications have been addressed with promising results. However, there are still limitations and challenges that must be addressed by the NF community. In this section, we will discuss some of these points regarding the study design or new NF applications and limitations of current solutions.

In this state-of-the art, we focused on the EEG-fMRI as NF modalities. Many studies have been focused on the contribution of this bimodality. Indeed, their complementarity is no longer justified as many studies and reviews have shown the potential behind the achievement of a very high spatiotemporal resolution. However, there are still limits that are intrinsic to the nature of this modality: the portability. Indeed, fMRI is both the brake and engine of this research, its high temporal resolution being counterbalanced by its high cost and stationary aspect. However, some studies have addressed this problem thanks to the EEG-informed fMRI, the aim is to approximate the BOLD signal of a specific ROI during EEG-fMRI sessions in order to be able to render it during EEG only sessions. With the limitation that this method is still individual and specific to each subject [55]. A recent study has used this learning method with subjects who were not involved in the construction of the model [80], but without taking into account the progression of the subject through the sessions because "a change in strategy for the task might impact the learned model, as the relation between the EEG and fMRI signals may change" [55]. A possible improvement of this method would be to predict the evolution of the score through the sessions.

In order to overcome this problem of portability while keeping the possibility of measuring the haemodynamic response would be to use the fNIRS, that measures infrared light absorption of haemodynamic signals in the brain by scalp optodes at a spatial resolution of 2–5 cm^2 [95]. Moreover, EEG can be used simultaneously with NIRS without major technical difficulties. There is no influence of these modalities on each other and a combined measurement can give useful information about electrical activity as well as hemodynamics at medium spatial resolution. Several NF studies have already made full use of fNIRS as brain imaging modalities as revealed by this review [95]. Some studies developed fully integrated wireless wearable EEG-NIRS bimodal acquisition system [96], that could be used for NF applications with multiple sessions [97] and even rehabilitation [98]. However, fNIRS cannot be used to measure cortical activity more than 4 cm deep due to limitations in light emitter power and has more limited spatial resolution. A review on the use of EEG-fNIRS for BCI can be found in [99].

A fusion of EEG-fMRI that has not be studied in NF is fMRI-informed EEG, where EEG electromagnetic source reconstruction benefits from the spatial information of fMRI signals; in this approach, the ill-posed problem of EEG source imaging (LORETA) can be moderated with fMRI spatial constraints [22, 42, 100]. This spatial information can therefore provide feedback related to the activity of a specific ROI rather than basing training on scalp activity. In 2017, Noorzadeh and colleagues [101] proposed to adapt a symmetrical approach based on EEG and fMRI for the estimation of the brain sources. They showed that their model provide better spatio-temporal resolution of the estimation of neuronal sources.

Comparing the progress between the two most commonly used EEG-fMRI paradigms for NF, it is interesting to note that there have been no MI-based EEG-fMRI studies in patients where, conversely, in the paradigm of emotion, many studies have been produced [74, 78, 87, 88]. Yet it would be interesting to study this paradigm for stroke patients, indeed, recent studies have revealed the potential of NF training for stroke rehabilitation [81] (for a review, see e.g. [5]). In addition to having the possibility of training the patient on two neuromarkers, MRI makes it possible to verify the effectiveness of NF training using structural magnetic resonance imaging and Diffusion Tensor Imaging (DTI), which could make it possible to study the integrity of the ipsilateral Corticospinal Tract (CST).

The question of the fusion of EEG-fMRI features is also fundamental and must be addressed in future studies. Indeed, when is the NF score, which relies on combinations of complementary analysis as well as recording techniques, is the most revealing of the subject's brain activity? That is why multimodal NF can benefit from a segment of machine learning that is called data fusion, because it subsumes techniques that combine information from multiple signal sources as well as associated databases [102, 103]. Nevertheless, as pointed out by Oviatt [16], the main advantage of multimodal interaction is not enhanced efficiency but decreased error rate, flexibility to choose between alternating input modes, and a wider range of users.

1.5 Conclusion

In this chapter, we summarised and discussed the state-of-the-art when combining EEG-fMRI for neurofeedback. We outlined the different studies implying this system such as fMRI informed EEG-NF or simultaneous EEG-fMRI-NF. This chapter also stressed the potential of EEG-fMRI for NF studies to improve their design by increasing the pertinence of feedback provided. Further studies are however required to test the use of EEG-fMRI for BCI and NF in order to complete our knowledge of EEG-fMRI fusion for NF.

Output of Multimodal Neurofeedback: Adding Haptics to Visual Feedback

2

Preamble: *This chapter surveys the use of haptic as feedback for neurofeedback or brain-computer interfaces by presenting a state-of-the-art based on the various haptic technologies and their applications to brain-computer interfaces and neurofeedback.*

2.1 Introduction

Since the past decade, advances in brain science and computer technology have led to a growth in the development in Neurofeedback (NF) and Brain-Computer Interfaces (BCI) applications. Recent technological advances such as machine learning analyses, wireless and real-time recordings have increased interest in NF and BCI approaches, especially EEG-based BCI/NF. One of the cornerstones of NF and BCI is the feedback given to the subject. The subject relies on the feedback to learn and improve his mental strategy. Traditionally, visual feedback has been mostly employed in BCI/NF applications and commonly represented in the form of activity meters or continuous line or graphs (See Figure Figure 2.1), but its use may seem questionable in some cases. For example, a visual feedback is not always suitable for individuals with an impaired visual system or during a mental motor imagery task, which requires a great abstraction from the subject. In this case, haptic feedback could seem more appropriate and more intuitive than visual feedback [104]. However, haptic feedback is more often used conjointly with visual feedback to provide enriched information to the user.

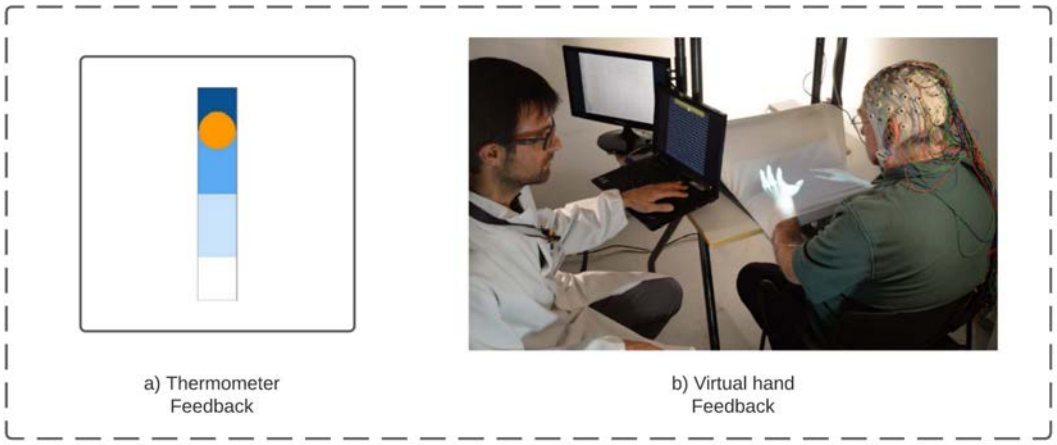

Figure 2.1: Visual feedback used in NF/BCI studies. (a) Activity meter feedback, the ball reflect the subject current level of activity [52]. (b) Virtual Hand that performs the imagined movement on successful trials [105].

Visual feedback has been shown to be the sensory input that produces the best learning processes [106]. However, still to this day, other existing feedback modalities have been less explored even though specific circumstances require differential feedback due to the pathology itself or requirements of the rehabilitation process, e.g. for Locked-In Syndrome (LIS) patients [107]. Moreover, it has been suggested that providing haptic feedback could improve the sense of agency, a technology acceptance-related factor, in Motor Imagery (MI) BCI's [108]. Preliminary studies report that BCI performance is not affected by the specific type of feedback [19], i.e whether visual, auditory or haptic. Nevertheless, the combination of multiple feedback, which can be called multisensory feedback, is expected to provide enriched information [109]. However, an efficient feedback should not be too complex, and should be provided in manageable pieces [110].

Haptic feedback is still scarcely used in the BCI/NF community although the haptic sense is the only one that allows us to interact with the world around us and, at the same time, to perceive these interactions [111]. However, applications related to haptic-based BCI are multiple: such as rehabilitation and entertainment. For example, the majority of the clinical papers included in this survey focus on stroke patients, because haptic-based BCI/NF seems to be a promising way for rehabilitation, as this non-invasive technique may contribute to close the loop between brain and effect [112]. Haptic-based BCI could also be used as a communication application to perform daily living activities independently, i.e. wheelchair driving system [113, 114]. Given that haptic feedback has evolved since the past decades, and that haptic displays are becoming more and more sophisticated, they become unobtrusive, and thus more effective and more acceptable by the user. In this paper, the term "haptic feedback" is used to categorise two different types of feedback: tactile and kinaesthetic (Figure 2.5).Tactile feedback refers to the sense of touch which allows to recognise texture, pressure or a vibration stimuli. On the other hand, kinaesthetic feedback represents proprioception which allows to perceive the force/torques felt in contact with the body as well as to know its position in the space, even with closed eyes [115].

Haptic interfaces also have different purposes whether in BCI or NF. Historically, NF has been used to develop internal control while BCI is primarily intended to instruct control over external objects (orthosis, computer, etc.) and by definition NF is a biofeedback from brain areas [1], with the purpose of self-modulation of brain activity, i.e. a personal control and not a redirection on an object. Following the given definitions of NF and BCI, this survey will distinguish the concepts of NF or BCI on the basis of the rationale of their implementation. For example, when a patient with a stroke uses an exoskeleton as a feedback, the goal is not to control that skeleton for controlling it, but to work the perilesional areas in order to activate the plasticity systems. In this case, as the purpose is to enhance neuronal activity, the term NF is appropriate. However, if the paradigm is to control the orthosis, then we will speak of BCI.

In their recent paper, Van Erp and Brouwer [116] provide an extensive state-of-the-art of touch-based BCI. Our survey aims to complement this review with an extension to all haptic modalities/cues and both BCI/NF applications. Our objective is to better understand the current possibilities of haptic feedback and further improve the design of future studies.

The remaining of this paper is organised as follows: first, we provide an overview of existing haptic technology Section 2.2. Secondly, we surveyed recent studies exploiting haptic feedback in BCI/NF Section 2.3, showing the experimental and technical challenges. These articles are then discussed Section 2.4, where we also propose guidelines on the use of haptic, and identify some remaining challenges. Finally, a conclusion is given Section 2.5.

2.2 Fondamentals of Haptic Interfaces

The study of haptic interfaces is an expanding research area focusing on human touch and interaction with the environment through touch. Its integration within BCI experiments is rather recent (2007) and was pioneered by Cincotti et al. and Chatterjee et al. [104, 117]. The term haptic can be defined as 'sensory and/or motor activity of the skin, muscles, joints and tendons' (ISO, 2011 244 :1). An information delivered through a haptic device is resolutely different from a visual display. The design of a haptic feedback depends on a in-depth knowledge of the human haptic sense, either of the tactile sense or the kinesthetic sense.

2.2.1 Haptic Perception

The purpose of a feedback in a standard BCI/NF protocol is to give a cue of a specific brain activity in order to have a beneficial impact on the learning of a task of BCI/NF [118]. Thus, the impact of a feedback is not only dependent on its content but on the way it is presented to the subject [119]. In this sense, the knowledge of the human haptic sense is a fundamental step in the elaboration of a haptic interface for BCI/NF. Haptic interfaces have possible interactions with many parts of the body which implies that our sense of touch has the potential to become a very useful tool for digital interaction. The human skin is capable of detecting mechanical stimulation, heat and pain [120]. When a haptic event arises, an emission of a sequence of voltage pulses is generated and transmitted through the nerves directly to the brain the information is processed. For example, picking up an object and feeling its properties (shape, texture, weight, etc.) requires integrating information from tactile and kinaesthetic senses. The primary motor cortex is the physiological location where haptic information is processed. A visualisation of a schematic coronal cut of the distribution of the parts of the body in the primary motor cortex shows an important proportion being used by the hands and the fingers (Figure 2.2).

The tactile sense is associated with receptors distributed under the surface of the skin. This sense is commonly called "sense of touch", since tactile receptors (high frequency sensors) discriminate very fine surface properties such as small shapes and fine textures and with a particularly high density under the palm and the fingers [121]. In the case of the hands, four types of physiological receptors can be found, as described in [122]: "our fingertips can sense a wide range of tactile stimuli, such as temperature, pressure, pain, or vibration".

The kinaesthetic sense or proprioception or force is associated with receptors in muscles, tendons and joints and provide information about movement, position and torque of limbs [123]. The term "proprioception" is also used for properties regarding the whole body whereas kinaesthetic refers to the perception of properties of limbs, however, this differentiation will be neglected in this survey.

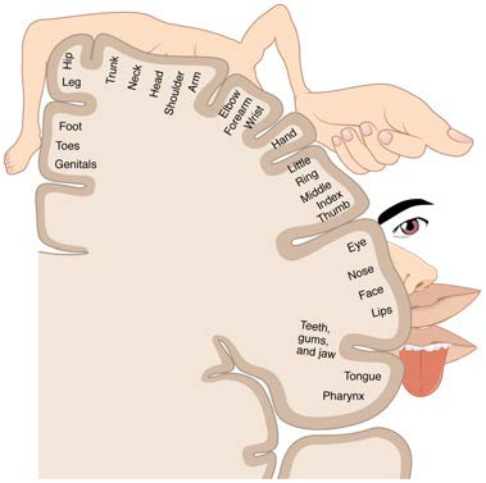

Figure 2.2: Functional brain areas in the motor cortex [124]

2.2.2 Haptic Interfaces and Actuators Technologies

This section presents the wide spectrum of existing haptic technologies. Haptic feedback can take different shapes, but two main categories can be distinguished: tactile-feedback or force-feedback. Before describing them in more details, several important properties of haptic interfaces will be provided.

General properties of haptic interfaces

Grounded vs. Wearable Interfaces This categorisation is based on whether the haptic interfaces are mobile or are anchored to the environment. The design of haptic interfaces recently started to take into account portability as a crucial parameter [125]. Furthermore, wearable devices should not limit the user's motion and enable to stimulate grasping-related sensations whereas grounded devices restrain the user's motion but enable to stop and block him. *Ground-based interfaces* are haptic interfaces anchored in the environment. Ground-based haptic interfaces can generally be classified as link-type, magnetic-levitation-type, and tension-based-type [126]. The PHANToM, a 6 Degree-Of-Freedom (DOF) force-feedback pen that provides a force-reflecting interface between a human user and a computer is an example of a performing link-type haptic interface [127]. *Wearable haptic interfaces* are grounded on the body of the user. Wearable devices are not limited to a constrained workspace, therefore they allow users to move freely and perceive haptic feedback in a much larger range. On the other hand, wearability introduces power limitations. Devices must be built with miniature technology and actuation is limited due to weight and power

consumption. Pacchierotti and colleagues [128] provide a list of guidelines for the design of wearable tactile devices that includes multiple factors such as the form factor, the weight, the impairment, and the comfort (Figure 2.3).

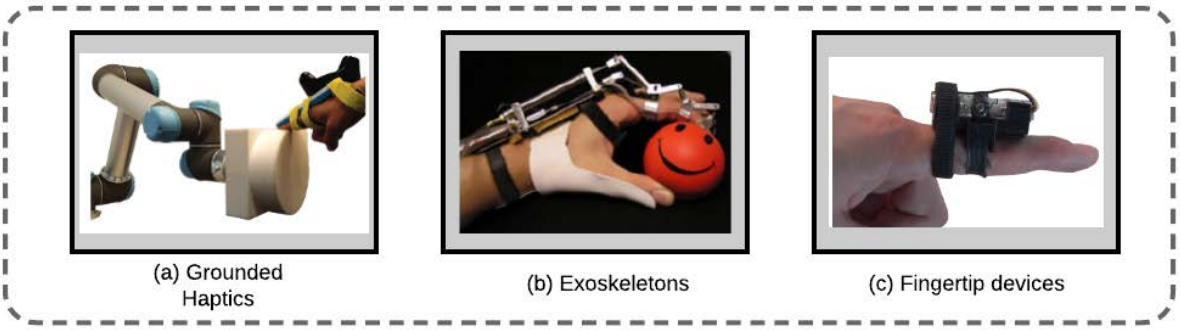

Figure 2.3: Wearability in haptic: from grounded haptic interfaces to more wearable and portable designs. (a) ENTROPiA: a cylindrical spinning prop attached to a robot to provide haptic virtual texture [129]; (b) Hand exoskeleton for natural pitching [130]; (c) Cutaneous display providing normal and shear stimuli [131]

Active vs Passive Touch Haptic feedback can be divided in two categories: active and passive. Usually active touch refers to the act of touching, while passive touch refers to being touched [132]. In the first case, the sensation is brought by the perceiver and in the other case by an external device. Hence, passive haptics refer to the haptic properties of physical objects, such as a keyboard or a cup of coffee, and active haptics refer to the haptic that are actively generated by the device, based on haptic actuators and software. In the haptic field most interfaces are active, which is not the case for haptic-based BCI/NF. Indeed, haptic-based BCI/NF interfaces use calculated feedback from the brain activity and not from the sense of touch. *Passive touch* refers to the fact that the haptic feedback is not calculated according to the user. For example, a standard vibrotactile alert from a mobile phone can be considered as a passive feedback.

Direct contact, intermittent contact and indirect contact interfaces In the design of a haptic interface, the nature of contact between the user and the interface can be of three types. *Direct contact interfaces* correspond to an attached haptic interface the user is always in contact with the device. *Intermittent contact interfaces* where the contact is limited with the device and only provided when required. For example, Frisoli and colleagues developed a grounded fingertip haptic interface a plate enters in contact with the user whenever the finger touches a virtual surface [133] (cf. Figure Figure 2.4). *Indirect/Mid-air interfaces* produce haptic feedback to the user without any contact with him and therefore does not constrained the wearing of gloves or the holding of a device [134]. UltraHaptics [135], a grounded ultrasonic device is an example of a mid-air device that provides multi-point haptic feedback on the user's skin. A state-of-the-art on mid-air devices can be found in [134].

Tactile interfaces

Tactile feedback stimulates the skin surface through a direct contact. Tactile interfaces can be separated depending on the sensations they provide: vibration, contact, pressure, temperature, curvature, texture, softness / hardness, friction [136]. Generally, tactile devices must be light weight and small, and if the tactile display is to be worn by mobile users, it must minimise power consumption [137]. This review will focus on vibration, contact, pressure interfaces as these are the most common tactile interfaces in the BCI/NF community. Only feedback related to vibration, contact, pressure, temperature and electrotactile will be described in this section. These are the most commonly used feedback in the BCI/NF community today.

Vibratory feedback Vibrotactile feedback is generated by mechanical vibration normal or transverse to the surface skin area. Mechanical vibration conveys tactile information modulating vibration frequency, amplitude, duration, timbre or spatial location. Vibrotactile feedback uses the same principle as audio headphones, i.e converting electrical signals to sound waves. The quality of vibrotactile stimulus perception is influenced by the frequency of the vibration ((50-300)Hz which corresponds to the bandwidth of the human tactile sense), by the body position and underlying tissues. The use of oscillating pressure (sinusoidal or square and amplitude modulations) also adds new DOF to the design of vibrotactile stimuli, such as waveform shape and amplitude modulations at different modulation frequencies of the carrier frequency [136]. Vibrotactile devices delivering variable pressure on the skin have been employed for instance as an alternative sensitive channel for blind or deaf individuals [138]. The sensitivity of vibrotactile stimulation depends on body position and age of the subjects [139].

Contact and pressure feedback Contact or pressure feedback can be used to simulate encounters with virtual object surfaces. Pneumatic systems can simulate this effect or surface encounter devices that follow and anticipate the operator's movements [140]. For example, Frisoli and colleagues proposed a grounded fingertip haptic interface a plate enters in contact with the user whenever the finger touches a virtual surface [133].

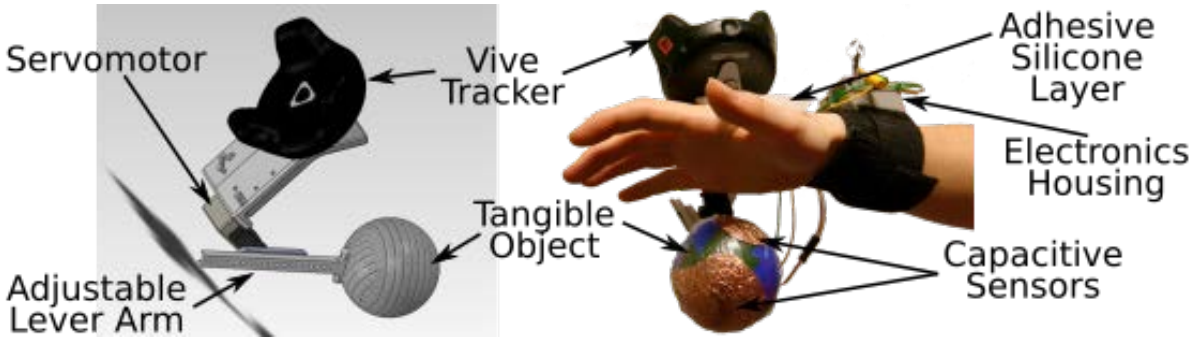

Figure 2.4: Conceptual schematic of a intermittent contact interface: the tangible object comes in contact with the hand when the finger grabs the virtual ball [141]

Thermal feedback Thermal interfaces provide thermal cues to the user that are usually experienced during interactions with objects. Following this principle, Guiatni and colleagues [142] created a haptic interface that provides thermal and force feedback for surgical operation (Figure 2.5.c). The thermal feedback was coordinated to the thermophysical properties and temperatures of living organs in order to help the surgeon's perception. Thermal feedback was also proposed to add thermal sensing system for prostheses [143]. For the prosthesis users, thermal stimulation improves the interaction with the surrounding environment and provides them with useful information for daily activities such as material discrimination, pain avoidance, and psychological comfort. A state-of-the-art on thermal displays can be found in [144].

Electrical feedback A light electrical stimulation, also known as electrotactile stimulation, can raise the user's awareness and can be used for tactile feedback. Several electrotactile displays have been developed as sensory aids for hearing [145], visual disabilities [146] or can be also used to create perceptual illusions of surface changes [147]. Variations in intensity and temporal parameters of stimulation and in the spatial sequence of electrodes activated can be used to convey information [137]. However, both the absolute threshold and subjective magnitude of electrotactile stimulation increase rapidly with changes in current amplitude [148]. Stimulation current must be controlled carefully to avoid painful sensations. The level of intensity is usually established during a practice session before the recordings. The electrotactile stimulation can also be used as a tongue display unit (Figure 2.5.d), consisting of a signal generator that controls the voltage output, a flexible connector cable and the electrode array. A survey on electrical feedback can be found in [149].

Kinaesthetic Interfaces

Contrary to tactile feedback, force-feedback addresses the kinaesthetic sense, involving positions, velocities, forces and constraints sensed through muscles and tendons. A kinaesthetic feedback can provide information about the limb position or strength applied. These devices are usually grounded since the display of the force or motion is deliver through a tool (i.e. PHANToM [127] or Omega). However, grasping haptic devices and exoskeletons include wearable devices (i.e. haptic gloves). Haptic clinical devices such as orthoses or robotic systems have notably been used to guide the movements of paralysed limbs of the patients [155].

Grounded force feedback Force-feedback devices serve usually two main purposes: to measure the positions and contact forces to the user's hand (and/or other body parts), and also to display contact forces and positions to the user. These haptic interfaces are usually composed of rotating joints that connect rigid links [127]. Force-feedback devices can be categorised according to the DOF provided by each device, from a simple 1 DOF device to a complex 7 DOF device. Other designs such as cable systems or stringed haptic interfaces also meet this definition, as tension-based systems (Figure 2.5.a). Cables are fixed

around the corners of a structure, such as a cube. Each cable includes a torque motor, cable, tensioning mechanism and force sensor. Tension-based haptic interfaces [156], have the advantages of fast reaction speed, simple structure, smooth manipulation, and scalable workspace[157].

Exoskeletons devices the anthropomorphism of the exoskeleton allows to provide forces on natural degrees of freedom on the body (Figure 2.5.b), they have to fit naturally the hand without impairing it or interfering with its actions. Exoskeletons can be heavier [158] and decrease the comfort of the user. The terms orthosis or exoskeleton are in general used to indicate the system effectors, often in an ambivalent way. This review will use the definition from Herr [159] stipulating that "generally exoskeleton augments the performance of an able-bodied wearer, whereas orthosis are used to assist a person with a limb pathology and help correct, rehabilitate or support parts of the body". A state-of-art on wearable kinaesthetic interfaces can be found in [128].

Functional Electrical Stimulation (FES) , also known as electrical muscle stimulation, is a more intensive stimulation (up to 150V [160]) than electrotactile stimulation [161]. This electrical stimulation actuates muscle contraction and thus provides a kinaesthetic sensation. FES has been efficiently used for motor rehabilitation after stroke in [154, 162, 163]. [164] (Figure 2.5.c), showing promising results for motor recovery. A state-of-art on FES can be found in [149].

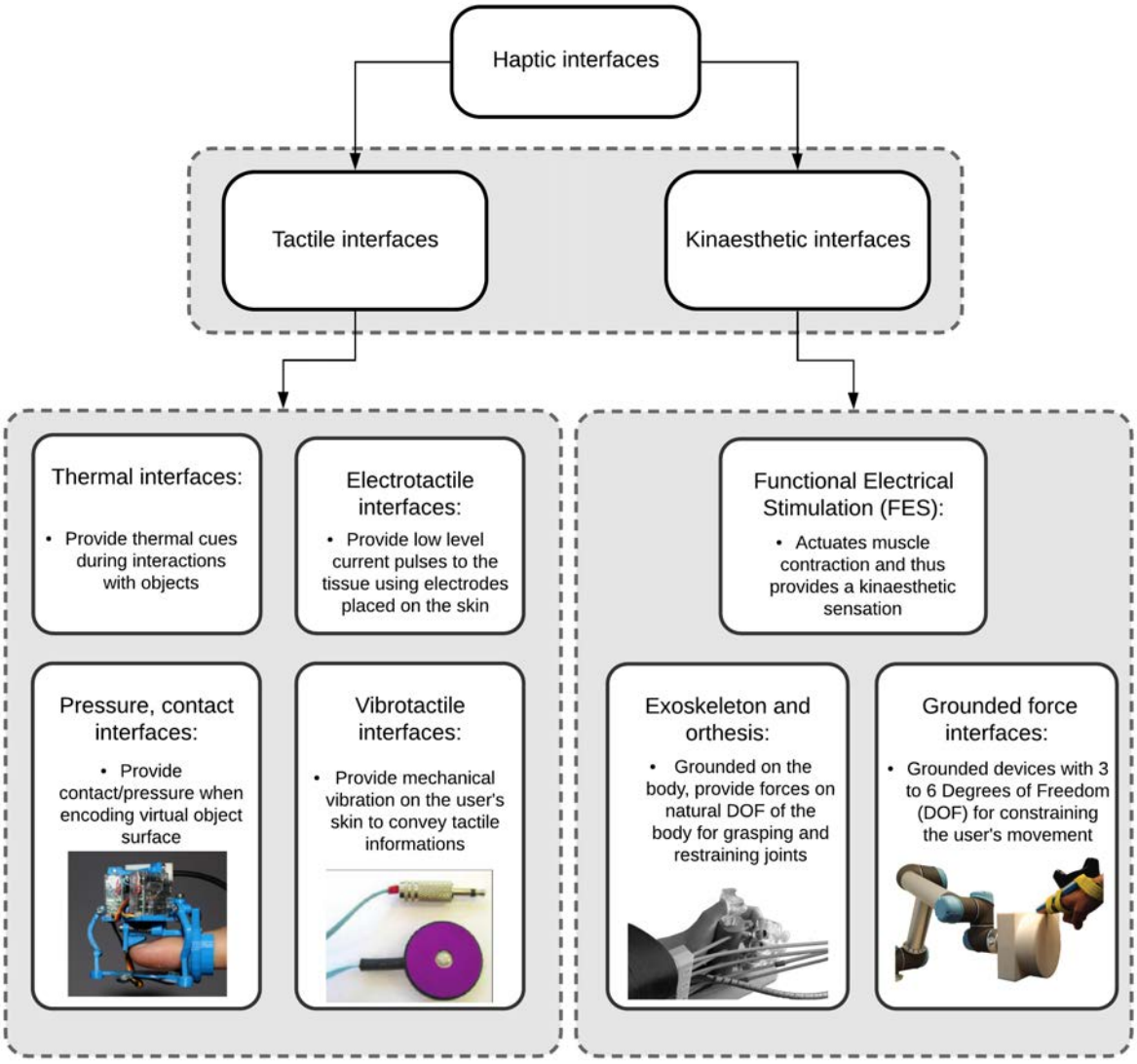

Figure 2.5: Haptic interface classification. Four representative tactile stimulation interfaces are presented (a) Vibrotactile Actuators (C2-tactors [150]); (b) Pressure and contact interfaces [151]; (c) Thermal display integration in a medical precision tool for invasive procedures simulation [142]; (d) Tongue stimulated with an array of electrodes [152]. Three representative kinaesthetic stimulation interfaces. (a) Cable system, basic Structure of SPIDAR-G [126]; (b) Orthosis developed by Ramos-Murguialday et al.[153]; (c) FES in a post-stroke rehabilitation application [154].

2.3 Haptic feedback in BCI/NF

The following section describes the state-of-the art haptic applications to different BCI and NF paradigms. To date, the MI paradigm is the most used paradigm for haptic feedback, its interest being in the possibility to close the sensory-motor loop: the user imagines a movement and the modulated signal can be employed to control haptic interfaces that in turn give the subject a sensory-motor stimulus. Other paradigms requiring less training , such as P300 and Steady-State Somatosensory Evoked Potential (SSSEP), have also be used in association with haptic interfaces. These haptic sensors are used to stimulate parts of the body (different frequencies) and the elicited EEG signals are processed to generate control commands. Haptic displays have therefore different purposes in these two kind of BCI: in sensory motor paradigms is to give a haptic feedback from the brain activity of the subject whereas for P300 and SSSEP haptic interfaces are used as stimulation and the evoked brain activity is further decoded for a command (Figure 2.6).

BCI can be divided into three classes: active, reactive, and passive [116]. Only BCI applications that are based on brain pattern and are actively or reactively generated by the user will be considered in this review: the active BCIs (aBCI) and reactive BCIs (rBCI). aBCI provide a non-muscular communication between the brain and the external environment without external stimuli, for instance in SensoriMotor Rhythms (SMR) paradigms [83, 165–167]. A rBCI use external stimuli to provide informations to the subject, for example, in somatosensory evoked potential (SSEP) or P300 paradigms. Passive BCIs pBCI, which measure the cognitive or emotional state of the subject from brain patterns without any need for specific user activity [168], will be disregarded, as it is out of the scope of the present work.

For an interactive system, our sense of touch is ideal because of its nature. For example, our haptic sense is bidirectional because human can perceive and actuate via touch [169]. In terms of interface design, this means that touch can be used as an input and output tool.

2.3.1 Motor Imagery Paradigms

Sensorimotor rhythms (SMR) remains the most popular motor imagery paradigm in haptic-based BCI/NF. SMR refers to localised brain rhythms desynchronization in the upper alpha band (10–12 Hz) usually accompanied by changes in synchronisation in the beta band (13–25 Hz) [83] occurring when performing a real or imagined motor task. This paradigm seems well adapted to haptic based-BCI where tactile and kinaesthetic feedback can potentially mimic the natural representation of limb state variables [184]. Most of the SMR-based haptic system use kinaesthetic sensation as feedback from MI performance. The first SMR-based orthosis (hand orthosis, 1 finger) was designed by Pfurtscheller and colleagues [20] for a tetraplegic patient: it was shown that after a period of training (5 months) the patient was able to efficiently control the orthosis with foot or hand MI. Kinaesthetic systems differ in their design that can for instance involve the whole hand or just a few fingers. In most of the studies examined (cf Table Table 2.1), since the input signal was uni-dimensional, these

Table 2.1: SMR based haptic *Note.* K: Kinaesthetic, H: Hand, F: Finger(s) P: Portable, G: Grounded, D: Discrete, C: Continuous, PP: Physical practice, *: MEG., T-Vib: Tactile vibrotactile, V: Visual, T: Thumbs, I, Index, M: Middle finger, NP: Number of Patient, NS: Number of Subjects, SP: Stroke patients, TP: Tetraplegic Patient, BP: Blindness patient, SCP: Spinal Cord injuries Patients, FC: Feedback Comparison, HI: Haptic Influence, HD: haptic design, DOF: Degree Of Freedom

Haptic sensation	Actuator technology	Portability	MI Task	Multimodality	Haptic Gain	C/D	Paper purpose	NP/NS	References
K	H orthosis (3 F)	G	Grasp H	V (grasping H), PP	N/A	C	Rehabilitation	4/- SP	[170]
K	H orthosis (H flexion)	G	Open H	V (bar)	Sup	D	Research HI	-/10	[171]
K	H orthosis (all F)	G	Open/close H	none	N/A	C	Research HD	-/23	[153]
K	H orthosis (all F)	G	Reach / grasp / bring H	none	N/A	C	Rehabilitation/ Clinical	16/16 SP	[172]
K*	H orthosis (4 F)	G	Open/grasp H	V (bar)	N/A	D	Rehabilitation/ Research SP/HD	8/- SP	[18]
K*	H orthosis (all F)	G	Moving H	none	N/A	C/D	Rehabilitation	4/20 SP	[173]
K*	H orthosis (all F)	G	Open H	none	N/A	C	Research HD	-/30	[174]
K	H orthosis (H flexion)	G	Open F	V (grasp H)	=	D	Rehabilitation/ Research FC	12/- SP	[175]
K	H orthosis (all F)	P	Open H	V (clue/color change)	N/A	C	Rehabilitation/ Clinical	55/19 SP	[163]
K	H orthosis (2 F)	P	Open H	V (clue)	N/A	C	Rehabilitation/ Research brain location	10/- SP	[176]
K	H orthosis (2 F)	P	Open/grasp H	V (bar)	N/A	D	Research HD	-/11	[177]
K	H orthosis (2 F)	P	none	none	N/A	D	Rehabilitation	6/- TP	[178]
K	H orthosis (1 F)	P	not specific	V (bar)	N/A	D	Rehabilitation	1/- TP	[20]
K	Arm orthosis	G	Flexion / extension forearm	V (arrow)	N/A	D	Rehabilitation/ Research HI	2/6 SP	[112]
K	Arm orthosis (2 DOF)	G	Arm direction	V (target)	N/A	D	Rehabilitation	54/- SP	[179]
K	H knob	G	Grasp H	V (cue)	N/A	D	Rehabilitation	21/- SP	[180]
T-Vib	Mechanical vibrators (on the biceps)	P	H R/L	V (bar)	N/A	C	Research HD	-/6	[117]
T-Vib	Mechanical vibrators (upper part of the trunk)	P	H R/L	V (bar)	=	D	Research/ Rehabilitation FC	30/3 SCP	[104]
T-Vib	Mechanical vibrators (neck)	P	H or foot	V (bar)	=	C	Research FC, HI	-/6	[181]
T-Vib	Eccentric rotating mass (neck)	P	Tapping with F	none	N/A	D	Research	-/11	[182]
T-Vib	Gloves with 5 eccentric rotating mass vibrator per H	P	H R/L	V	N/A	C	Research/ Entertainment FC	-/18	[183]
E-T	Tongue display unit array	P	H and foot	V (bar)	=	C	Rehabilitation/ Research HD & FC	1/10 BP	[152]
FES	ES of the forearm	P	open H	none	N/A	D	Rehabilitation	16/- SP	[154]
FES	ES of the forearm	P	H and foot	none	N/A	D	Rehabilitation	1/- TP	[160]

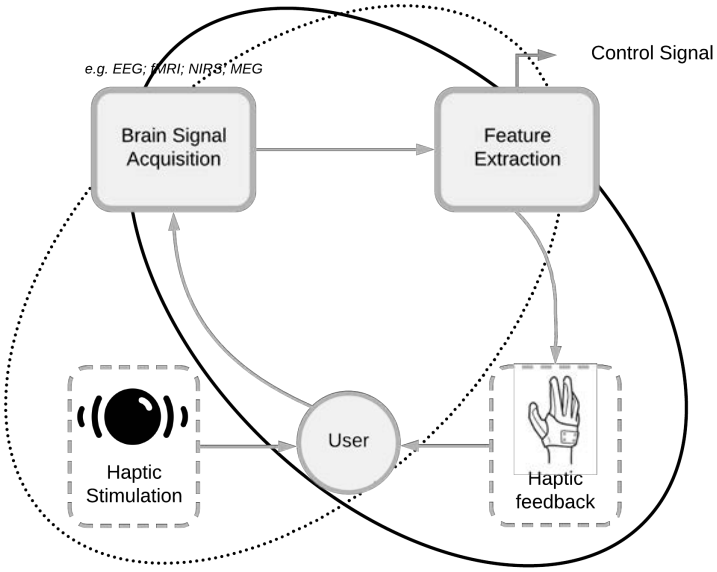

Figure 2.6: Implementation of haptic feedback in active BCIs (aBCI) and reactive BCIs (rBCI).In aBCI haptic interfaces provide the feedback from user's neural activity whereas in rBCI haptic interfaces provide a stimulation and the elicited brain activity is further decoded and transmitted as a command. aBCI loop (black circle) and rBCI (black doted circle).

systems used only one DOF, even if the system could deliver more (i.e. 7 DOF arm orthosis from [112]). Different types of movements can be then transmitted, such as grasping or opening the hand. Grounded systems are usually used for kinaesthetic feedback since orthosis are heavy [18, 153, 170, 171, 175, 179, 180]. However, the portability is an important factor for haptic interfaces, that should not limit the motion of the owner. Based on this, some studies investigated portable kinaesthetic feedback [163, 176, 177].

Haptic feedback can be delivered both continuously (where the feedback is given during the execution of the mental task and directly reports the neural activity) and discretely (where the feedback is given after a threshold). For example, [185] proposed a system composed of a mechanical hand orthosis attached to the upper limb to extend and close all fingers in order to investigate the effect of proprioception on BCI control. They showed that in healthy subjects SMR based BCI/NF training with contingent haptic feedback improves BCI performance and motor learning, enhancing SMR desynchronisation during MI. These results were also found by Soekadar and colleagues [173], who showed that a graded haptic feedback outperformed binary feedback for faster BCI learning and more accurate SMR-ERD modulation.

The use of tactile feedback for SMR based BCI/NF has also been developed in the past years, because of its higher portability, comfortably and affordability with respect to kinaesthetic

interfaces. Tactile interfaces have been firstly used to unload the visual channel [104, 181, 182], for individuals with impaired vision [152] or patients with spinal cord injury [104]. Chatterjee and colleagues [117] demonstrated that users can control a BCI system using only tactile feedback with vibrotactile stimulators placed on the right or left upper arm. They found out that vibrotactile feedback helped the subject to regulate contralateral imaginary tasks. In a lingual electrotactile study, Wilson et and colleagues [152] demonstrated that task performance with tactile feedback was comparable to visual feedback. In an extended experiment with 30 healthy and three spinal cord injured participants, Cincotti and colleagues [104] showed that the vibrotactile channel can function as a valuable feedback modality, especially when the visual channel is loaded by a secondary task.

Even if the first study implying haptic feedback for clinical applications was a case report with a tetraplegic patient [20], a large part of these studies focus on stroke rehabilitation [18, 112, 163, 170, 172, 173, 175, 179]. Haptic based MI-BCI is promising for functional rehabilitation for stroke patients, as this training can be also applied to patients with no residual movement. The aim of BCI/NF is to stimulate neural plasticity in perilesional brain motor areas and support upper limb functional improvement [186, 187]. Since haptic BCI/NF based SMR achieve motor imagery with concurrent motor learning via kinaesthetic feedback, it is natural to think of rehabilitation for stroke patients even in a chronic condition. In these applications the question of the cortical target is still open. Usually the control of the orthosis is modulated by the ipsilesional side of the brain [105], contralateral to the affected hand, however, the ability to modulate perilesional activity is decreased with increased cortical damage [188]. For example, Bundy and colleagues [176] studied the controlesional motor area for the control of a portable exoskeleton, the assumption being that the recovery is optimal in the contralesional side and that functional improvements may be elicited [189]. In 2008, Buch and colleagues [18] demonstrated that chronic stroke patients with upper limb hemiplegia were able to control a magnetoencephalography (MEG) BCI by voluntarily modulating the ipsilesional SMR amplitude while receiving contingent haptic feedback with a hand orthosis. The haptic system used was a grounded mechanical orthosis attached to the plegic hand, one on each fingers except the thumb. The feedback was given in a passive way, with a movement of the orthosis elicited only if the modulation had reached a certain threshold at the end of the trial. Kinaesthetic feedback is mostly employed for stroke rehabilitation in agreement with the fact that rehabilitation outcomes of motor functions is more efficient with proprioceptive feedback. Most studies for rehabilitation imply kinaesthetic feedback but FES based-MI was also performed for patients. In an early case report from Pfurtscheller and colleagues, they applied non-invasive techniques to restore grasp functionality in a tetraplegic patient through FES [160]. This same method was applied with chronic stroke patients in [181].The interested reader can find more information about BCI applications for stroke rehabilitation in the review that Lopez-Larraz and colleagues [155] presented in 2018.

2.3.2 External Stimulation Paradigms

Brain signals can be elicited using external stimulation. Frequently used paradigms include SSEP as well as Event-Related Potentials (ERPs). Most BCI using ERPs can be used without any prior training and are less affected by the phenomenon called "BCI-illiteracy" problem (i.e the BCI system fails to correctly detect the mental state of its user). The following paragraph will deal with external paradigms (P300 and SSSEP) and their relationship with haptic modality. To the best of our knowledge, contrary to SMR-based BCI/NF where haptic technologies are used to provide the feedback, in external stimulation paradigms haptic interfaces are mostly employed as a stimulus.

P300

P300 is a positive deflection of the EEG signal occurring around 300 ms after presentation of a given stimulus (visual, haptic or auditory). A major strength of this paradigm is its reproducibility and stability as a feature for rBCI [199]. The majority of P300-based BCI studies use the visual channel as stimulation (cf Table Table 2.2): one of the motivation of using haptic for P300 based-BCI is indeed to reduce the dependence of the gaze in rBCI. The interest here is less to imitate a kinaesthetic or tactile sensation but rather to give the haptic stimulation in the most efficient way. Indeed, most of haptic-based P300 studies use tactile sensation as stimulation rather than kinaesthetic sensation. The first appearance of this paradigm in a haptic-based BCI study is from Aloise and colleagues [190], they investigated the influence of a tactile stimulus on classification performance in eight subjects. Tactile stimulus was provided with 8 vibrotactile stimulators placed at different positions on hands and wrists. They reported that tactile stimulus increased the latency of the principal P300 component (600ms peak after haptic stimulus against 400ms with the visual stimulus) and that online classification performance was weaker than with visual stimulus (68% against 93%). Other studies using vibrotactile tactors in P300-based BCI followed, differing on the place where they vibrators were located: on the wrist, on the arm, on the palm [200], on the neck and even on the head [201].

The presence of other forms of haptic interfaces in P300-based BCI studies is still marginal and further studies are required to assess if they have potential to enhance BCI efficiency. Kinaesthetic stimulation with force feedback has been investigated in [198] where the kinaesthetic sensation was delivered through a joystick to the subject's dominant hand and provided 4 different movements corresponding to the different directions. Hamada and colleagues [196] tested the first non-contact method for producing tactile sensation for BCI (mid-air haptics) while in [197] tactile pressure sensation was tested.

P300 paradigm requires less training and may achieve higher accuracy than MI paradigm [202] and has the potential to be used for the control of communication system for patients with LIS. LIS is a condition where the patient cannot communicate or have control on his motor function except for vertical eye movement and blinking [203]. BCI may open a new communication solution for these patients with sufficient intact cognitive abilities [204, 205]. It is in this perspective that Guger and colleagues compared these two paradigms

to assess whether vibrotactile P300 outperformed MI in a communication system for LIS patients [193]. The use of haptic-based P300 for the control of an object of the everyday environment has also been studied, in particular for the control of wheelchair because the visual feedback limits the user interaction with the external environment [113]. Recently, a spelling application with the use of tactile stimulation on the finger tips was developed by Van der Waal et al. [195], with spelling rates resulting similar to visual spellers. Kaufmann and colleagues [206] described an experiment in which they tested healthy users steering a virtual wheelchair in a building. The four navigation directions were associated with different tactor locations on the body. Out of the 15 participants, 11 successfully navigated a route along four waypoints supporting the view that haptic P300 paradigm have potential for medical applications.

Steady-State Somatosensory Evoked Potential (SSSEP)

SSSEP are a steady-state component of brain signals evoked by sustained repetitive vibrotactile stimulation within the frequency range of (17-35 Hz) [212]. The idea behind the use of such method is to increase the information transfer rate (which is slower with SMR-based paradigms because it requires some second to establish ERD patterns) without loading the eyes gaze [207]. SSSEP also represent an alternative to visual-based P300 or Steady-State Visual Evoked Potential (SSVEP). Because the stimuli paradigm is based on vibrations, most studies use tactile interfaces with a vibrator to deliver the stimulus (cf Table 2.3). The first appearance of SSSEP within a haptic-based BCI environment is found in the study by Müller-Putz and colleagues [207], in which the authors investigated whether SSSEP is an efficient as BCI paradigm. Tactile stimulus was provided by vibrotactile stimulators placed on both indexes and the user had to concentrate on one stimulus (right or left). They reported that on four healthy subjects only half reached classification accuracy of 70%. The placement of the vibrotactile stimulators in SSSEP-based BCI differs between studies even if in most cases is concentrated on the hands of the user (fingers, wrist) or its feet [211], being the discrimination of different vibration frequencies higher when the tactors are placed in these locations. Comparison between paradigms has also been investigated: for example, Severens and colleagues [213] studied the difference of performance between SSSEP and P300 reporting that P300 outperformed SSSEP and the combination of both did not result in better performance than P300 alone. These results show the limitation of this paradigm, the comfort of the subject being low (he has to concentrate on one of two or more tactile stimuli) [214], which is not the case with SSVEP where the eye position primarily determines the target [207]. The combination of SSSEP with other paradigms could be more promising. Ahn and colleagues [215] combined the SSSEP (left and right finger) with an imagined movement BCI paradigm. Kim and colleagues [211] designed a wheelchair driving system which provide three vibrotactile stimulators to control different directions indicating that this system has potential to help Amyotrophic Lateral Sclerosis (ALS) patients or other patients with LIS to gain independence in their daily activities.

Table 2.2: P300 based haptic; K: Kinaesthetic, H: Hand, W: Wrist, FF: Force Feedback F: Finger(s) P: Portable, G: Grounded, D: Discrete, C: Continuous, PP: Physical practice, *: MEG., T-Vib: Tactile vibrotactile, E-T: Electrotactile V: Visual, T: Thumbs, I, Index, M: Middle finger, NP: Number of patient, NS: Number of subjects, SP: Stroke patients, (C)LIS: : (Complete) Locked-In Syndrome, FC: Feedback comparison, HI: haptic influence, HD: haptic design

Haptic sensation	Actuator technology	Portability	Multimodality	Haptic Gain	Paper Purpose	NP/NS	References
T-Vib	Mechanical vibrators H or W	P	V	Inf	Research FC	-/18	[190]
T-Vib	Mechanical vibrators (waist)	P	none	N/A	Research HD	-/10	[19]
T-Vib	Mechanical vibrator (L/R W)	P	none	N/A	Rehabilitation	11/- LIS	[191]
T-Vib	Mechanical vibrators (L/R W)	P	none	Sup in communication speed	Research FC (auditory and MI)	-/10	[192]
T-Vib	Mechanical vibrators (L/R W + shoulder)	P	none	N/A	Rehabilitation	12/- LIS/CLIS	[193]
T-Vib	Mechanical vibrators (4 on arm)	P	none	Sup	Rehabilitation/ Research FC	1/- LIS	[114]
T-Vib	Mechanical vibrators (torso)	P	V	Bimodal = unimodal	Research	-/10	[108]
T-Vib	Mechanical vibrators (3 F)	P	Hex-O-Spell	Inf	Rehabilitation/ Research FC	6/5 ALS	[194]
T-Vib	Mechanical vibrators (knees, abdomen and neck)	P	none	N/A	Research HD	-/10 elderly subjects	[113]
T-Vib	Mechanical vibrators (F)	G	Hex-O-Spell	=	Research HD FC	-/12	[195]
T-Vib	Mid-air stimulation	G	none	N/A	Research HD	-/13	[196]
T-Pressure	solenoids (F: I,M,R)	G	V	N/A	Research HD	-/5	[197]
K	H FF	G	none	N/A	Research HD	-/7	[198]

Table 2.3: Haptic based-SSSEP; P: Portable, G: Grounded, D: Discrete, C: Continuous, PP: Physical practice, *: MEG., V: Visual, T-Vib: Tactile Vibrotactile

Haptic sensation	Actuator technology	Portability	Multimodality	Haptic Gain	Paper purpose	NP/NS	References
T-Vib	Mechanical vibrator (1 F)	P	none	N/A	Research	-/4	[207]
T-Vib	Mechanical vibrator	P	none	N/A	Research	-/14	[208]
T-Vib	Mechanical vibrator (W)	P	V (cue)	N/A	Research	-/57	[209]
T-Vib	Mechanical vibrator (2 F)	G	none	N/A	Research	-/16	[210]
T-Vib	Mechanical vibrator (L/R foot)	P	none	N/A	Research/ Rehabilitation	-/5	[211]

2.4 Discussion and Perspectives

Haptic-based BCI/NF applications have gained increasing interest in recent years. Researchers using haptic as to provide feedback or stimulation have focused on 3 different paradigms: (1) haptic-based SMR where kinaesthetic feedback is mostly employed and used for stroke rehabilitation, (2) haptic-based P300 where tactile stimuli are generally used to elicit a brain response for the control of an object and (3) haptic-based SSSEP where vibrotactile stimulus are employed. In each of the paradigms presented in this review, clinical applications have been tested with promising results. Nevertheless, there are limitations and challenges that must be addressed by the haptic-based BCI community. In this section, we will discuss some of these points regarding the design of haptic systems adapted to BCI, the utility and interest of haptic feedback for BCI and NF applications (with respect to other modalities) and limitations of current solutions.

Most of the BCI studies involving haptic have used the MI paradigm and often conjointly with visual feedback. This general trend is mostly explained by the fact that in MI task, closing the sensorimotor loop has potential to improve the quality and pertinence of the feedback provided, thus enhancing user engagement and NF performance. On the other hand, for SSSEP or P300 paradigms, haptic feedback is seen more as an alternative to the visual channel. Concerning the applications of haptic BCI/NF, this review indicate that there is a major tendency on using these systems for rehabilitation, especially for stroke patients, and that the vast majority of studies used a kinaesthetic feedback, with the rationale of reproducing a real and complex movement. On the other hand, tactile feedback is mainly used with the aim of restoring comfort for patients with LIS syndrome or patients with visual impairments, rather than for rehabilitation purposes. The majority of kinaesthetic feedback involves the upper limb with orthoses placed either on the hand or arm; this is not necessarily the case of tactile feedback that can be placed on different parts of the body. The visual modality is also commonly employed in these studies, either as a visual clue (i.e. to know if the user has to imagine a right or left movement), or as feedback complementary to the haptic feedback. The visual feedback metaphor is either classic (a bar or thermometer) or a more realistic proprioceptive feedback representing for instance a hand. The gain of the haptic with respect to the visual modality in different paradigms remains to be more accurately assessed, even though several studies have cleared the ground and seem converging on the fact that haptic is either equivalent or more effective than visual feedback from some applications.

Haptic-based P300 is mostly based on tactile vibration as a stimulus and rarely with other modalities. Visual stimuli is used together with haptic stimulation in P300 paradigm mainly to assess the gain of a haptic stimulus. The consensus around this gain is also still unclear because some studies show an equivalent effect on the classification performance while in others haptic-based paradigms have reduced performances with respect to visual ones. The use of a haptic stimulus is often motivated by the fact that haptic remains the only possible communication channel for some patients (LIS, CLIS) where the use of the visual channel is not always possible. Contrary to haptic-based SMR paradigms, for P300 applications there is a richer literature dealing specifically with the design of the haptic interface.

Applications based on haptic SSSEP are very similar to P300 paradigms but very limited research has been done on the design of such systems. Since P300 and SSSEP share similar objectives, it would also be interesting to compare these 2 paradigms in future studies.

2.4.1 Design of Haptic based BCI/NF

The integration of haptics in BCI/NF environment can be complex and entails some challenges at different levels. This is also because haptic-based BCI/NF studies are usually designed by imitating visual feedback protocols, even if the design may be sub-optimal for the haptic modality. In the following section, we will address some issues that should be addressed in the design of haptic BCI/NF protocols adapted to specific applications.

When and how should the feedback be provided?

The basis of human-computer interaction is the use of a feedback, which underlies the interaction phenomenon occurring between the user and the system [216]. A recurring question in the BCI community is the frequency at which the feedback is provided. The feedback can be given is two different ways: continuously or discretely. It would seem more natural in a BCI environment to give the feedback at the end of a successful trial than continuously. Conversely, in NF paradigm, the feedback is an indicator for the user of its own cerebral activity: here it would seem more appropriate to give haptic feedback in real time. A recent study from [217] indicated that improvement of MI task could appear if a vibrotactile stimulation of the non-dominant hand or the paretic hand for the patients is performed during MI, hence in real-time alerting on the importance of defining the feedback delivery modality depending on the desired application.

Haptic interfaces Induced Artifacts

In haptic BCI NF applications different artefacts can contaminate the signal; these artefacts can be generated by the devices controlled with the haptic feedback (i.e. noise generated by actuators based on electric/magnetic neurostimulation, on robotic devices [181, 218]) or have a physiological origin (i.e. compensatory movements, cranial and neck muscle activity, eye movements, swallowing, etc). The question of whether the haptic feedback introduce additional artefacts thus influencing BCI performance is still debated and highly depends on which haptic system has been tested. For tactile feedback, some studies showed that no interference with electric signal has been found [117, 219]. For example, Leeb and colleagues demonstrated no significant difference during the rest and the stimulation with a vibrotactile feedback [181]. However, Hommelsen and colleagues [220] showed that FES feedback was a considerable source of false positives when the mu rhythm was used for the detection of efferent commands. We suggest that a thorough study of the influence of haptic feedback, whether tactile or kinaesthetic, should be conducted to determine artefacts induced by vibratory feedback and feedback with an orthosis.

Features extraction and feedback calculation

According to recent findings from Bashashati et al. [221] the choice of the classifier for a BCI system depends on the feature extraction method used. We also suggest that the choice of the classifier and the choice of the feature must take in account the specific feedback modality employed, e.g. an optimal classifier for a haptic feedback may be not efficient for a visual feedback. The majority of EEG classification algorithms are developed for vision-based BCI/NF while neurophysiological responses to tactile stimuli may differ: a research effort in defining methodological framework specific to the analysis of haptic features is therefore needed.

Haptic based BCI/NF vs haptic interfaces: a technological gap

To date, the BCI community uses haptic interfaces for sensory feedback or as stimulation systems that are generally simple and sometimes dated. The haptic interfaces have hugely progressed in recent years and it would probably be interesting to integrate these technological advancements into BCI/NF studies. If we consider for instance the DOF of such haptic devices, at present the majority of studies involving a kinaesthetic system are limited to only one DOF even if the device can provide more. Using more DOF may facilitate motor learning [222] and should be investigated for rehabilitation of stroke patients. For stroke rehabilitation, tactile or kinaesthetic devices already exist but not in a BCI environment, for example, Lin and colleagues [223] developed a haptic glove equipped with vibrotactile stimulators that interact with a virtual-reality environment. Other studies have focused more on the ergonomy of the user by designing exoskeletons with multiple DOF [224, 225]. However, the wearability is not often a priority while it must be taken in account to enable the user to optimally perceive and interact with the environment. For instance, In and colleagues [226] developed wearable hand interfaces, proposing a jointless hand exoskeleton weighting only 80 g. We suggest that portability of haptic feedback should be more central in future haptic studies design.

2.4.2 Haptic Vs other modalities

Visual feedback has historically dominated the field of BCI/NF and only in recent years other modalities to deliver information (auditory or haptic) have been explored [227].

The gain of haptic

The gain of haptic over the other modalities could be assessed looking at different parameters such as BCI/NF performance, comfort of the subject or its adaptation in a daily environment. For example, haptic feedback could enhance MI [217] by bypassing BCI-illiteracy. BCI-illiteracy represents a big challenge in BCI research [228] and currently available SMR-based BCI/NF may have reached the limitation of their performance, as approximately 30%

of healthy subjects [229] and 40% of stroke patients [230] can not reach the critical BCI accuracy of 70%. The recent work from Lukyanov and colleagues [227] suggest that after some training, the type of feedback (visual or tactile) does not affect the classification accuracy. It impacts however the comfort of the subjects who describes the tactile feedback as more natural. Moreover, there are still few studies that compare different modalities: for SMR paradigms it seems that visual and haptic are comparable in terms of BCI performance, however, for P300-based studies this is still not clear. The gain of the haptic must also be determined with respect to the decrease of visual workload since the feedback no longer occupies the visual channel.

In current approaches haptic feedback is delivered in a uni-dimensional way e.g the task performed by the user is usually binary: open/close, open/grasp. For stroke rehabilitation it could be a limitation since the mental task is often more complex in reality. Future studies should explore the possibility to include more than one task in order to provide a more complex training (bearing in mind that this would also increase the training time). We suggest that more research should be done on the design of more realistic haptic training.

Multimodality

In our daily environment we are faced with many simultaneous and multimodal stimuli, it might therefore seem interesting to test a multisensory feedback approach in a BCI context. We can hypothesise that multimodal feedback like visuohaptic or audiovisual feedback could be more effective than simple unimodal feedback [15]. In a clinical context it might also be interesting, i.e. vision can be compromised for LIS, CLIS or ALS patients and the use of additional sensory feedback might be a good alternative to uni-dimensional feedback. Several studies tested the impact of a multimodal visuo-auditory feedback for BCI-based SMR: overall the effect of a multimodal feedback is either similar to a visual unimodal feedback [231] or shows better results in the first session [107]. In some cases multimodal feedback could increase performance in some naive subjects [232]. For the visuohaptic modality, the investigation from Brouwer [19] showed that visual-tactile stimulation has better performance over uni-sensory stimulation. It has also been suggested that the feedback given to the subject could either be equally shared on different channels, or replicated on each of them [104] or even dynamically distributed between channels. Although the use of visual feedback in addition to haptic feedback is often systematic, it is not always justified. This suggest that further work is needed to shed light on the use of multimodal feedback and to assess the interest of a visuo-haptic feedback compared to unimodal ones, whether visual or haptic.

2.5 Conclusion

In this chapter we summarised and discussed the state-of-the-art research on haptic-based BCI/NF. We outlined different paradigms using haptic interfaces, such as SMR, P300 and SSSEP and methodologies for the design of pertinent haptic applications. We identified

major trends in the use of haptic in BCI and NF and limitations of current solutions. To date, there is no consensus on the effectiveness of haptic feedback for BCI and NF systems. This review shows that haptic interfaces have potential to enhance performance and increase the pertinence of feedback provided, in particular for SMR paradigm used in the context of motor rehabilitation. In the next sections we will assess the use of innovative haptic technologies for NF and the utility of haptic, used alone or in combination with other modalities.

Towards Multimodal Neurofeedback based on Visual and Haptic Stimulation

Study of Proprioceptive Haptic Feedback for EEG-based Neurofeedback

3

Preamble: *In this chapter we study the combination of visual feedback in virtual reality and proprioceptive haptic feedback for EEG-NF with the particularity of producing illusions of movement. To achieve this, we have conducted two experiments to find out which type of visual feedback is most appropriate for obtaining proprioceptive illusion and to find out what is the influence of such haptic feedback on EEG signals. These two studies are preliminary studies prior to the implementation of an NF study.*

Contributor: *This research was conducted in association with Salomé Lefranc (MD).*

3.1 Introduction

3.1.1 Context

Vibratory stimulation is already used in various medical applications such as pain management or proprioceptive rehabilitation after stroke [233, 234]. It has a powerful proprioceptive role [235] and when applied under strict conditions (frequency of 80-100 Hz, tendon target) [236], it can create illusions of movement also named kinesthetic illusions (or tendon vibration inducing illusion) [237] by apparently stimulating the brain motor areas [238]. There is a wide range of haptic stimulations, such as standard vibration, tendon vibration as described here, and pressure stimulation. Each tool has different influences on the sensory stimulation and the brain activity it triggers. In the literature concerning tendon vibration, we know that this kind of vibration could correspond to passive movements in term of cortical excitability in sensorimotor areas [239]. Vibratory sensation applied to a tendon, triggers the activation of local mechanoreceptors, which induces a visible elongation of this tendon. This phenomenon elicits a kinesthetic illusion antagonistic to the vibrated tendon and leads to a higher cortical activity in sensorimotor motor areas and a reinforcement of activation in the propriomotor loop [240–242]. The main advantage of this propriomotor loop is to be more effective than the visuomotor one, which is slower and less automatic in terms of neuronal activation [243]. This vibratory modality presents 3 main interests in the motor rehabilitation domain: the production of a kinesthetic illusion (probably through the stimulation of the motor areas), the strengthening of the sensorimotor loop, and a faster action than the visuomotor loop. It could be helpful for motor rehabilitation of neurological impairments such as stroke where attention, cognitive and visual disorders can disturb the rehabilitation program.

In the last twenty years, a growing number of studies have taken interest in developing Virtual Reality (VR) tools in various fields, such as social psychology [244], haptics [245]

and rehabilitation [246, 247]. Virtual reality immersion is the perception of being physically present in a non-physical world. The perception is created by surrounding the user with images, sounds or other stimuli that provide an immersive environment. The user can interact with a virtual environment that looks realistic enough to allow a greater feeling of immersion [248]. In this immersive state, the participant is no longer aware of their own physical state. The more immersive the virtual environment is, the more the participant adheres to it. Immersion has a special effect called "embodiment: the participant feels present in the virtual world and interacts with it as if it was real. Embodiment depends on the quality of certain factors such as appearance or point of view in the VR environment [249]. Some studies suggested that the detailed appearance of the body contributed to the construction of the body image in VR [250]. Kim and colleagues also demonstrated the importance of the correspondence between the properties of the real human body and the adaptation made in VR to obtain the best possible incarnation and therefore the best illusion [251]. The role of embodiment in VR seems valuable to immerse participants in a controlled environment and create kinesthetic illusions [252]. Combining VR interface combined with haptic devices tends to increase the feeling of embodiment described in the literature, by giving a congruent tactile feedback to a visual immersive environment [211]. Rinderknecht and colleagues (2013) also proved that the addition of the VR enhanced the perception of the illusory movement induced by tendon vibration in healthy participants [253]. Other studies have also demonstrated the interest of using a virtual environment congruent with the movement of our limb to allow a better illusion and feeling of embodiment [254], or the combination of visuomotor and visuotactile stimulation on the virtual body ownership illusion [255].

Another tool that can be used to stimulate brain motor areas is Motor Imagery (MI), which consists in imagining moving the limb without performing any actual movement. MI is already used for upper or lower limb rehabilitation in motor rehabilitation after neurological impairments [256, 257]. It is now well known that MI triggers brain structures sharing similar neural networks with motor execution, including the premotor, supplementary motor, cingulate, parietal cortical areas, the basal ganglia, and the cerebellum [258, 259]. There are 2 main types of MI: the so-called visual MI (in the third person) or the so-called kinesthetic MI (in the first person). Kinesthetic MI consists in performing the task mentally with the sensation of movement (motor and sensory). More difficult to elaborate than visual MI, it has been shown to activate the same neural networks as real movements in functional imagery [260] and is therefore to be preferred in rehabilitation. Associated with MI or used alone, Action Observation (AO) tasks have also shown their interest to activate the brain motor areas [261, 262]. This literature proves that watching one's own limb or another person's limb can improve motor learning and motor skills in healthy participants or neurologic patients.

In the literature, cortical activations have been uncovered using functional imaging and electroencephalography (EEG) recordings. EEG activity can be recorded during MI or tendon vibration from electrodes placed over the brain motor areas. It is then processed to extract relevant features from the recorded signals. Sensory-Motor Rhythms (SMR) consist of brain waves oscillations generated by the somatosensory and motor cortices and

recorded, mainly, from C3 (left motor area) and C4 (right motor area) electrodes. SMR are detectable at frequencies from 8-28 Hz [263, 264]. SMR rhythms are represented by Event Related Desynchronizations (ERD) and Event Related Synchronizations (ERS), which correspond to the attenuation or increase of the power of spontaneous EEG signals in the μ band (8–13 Hz) and β band (13-28 Hz), observed around the motor cortex in synchrony with the intent and/or execution of a MI task [265]. To summarise, SMR are modified while doing passive and active motor movements as well as preparation and imagination of the movement [266].

The effects of the combined association of visual kinesthetic illusion of movement and MI to stimulate brain motor areas have not been clearly described yet. The literature suggests some hypotheses like the fact that kinesthetic illusions and kinesthetic MI could share the same neural substrate mechanisms [267]. Chatterjee and al. (2007) found in a Brain-Computer Interface (BCI) study, some interesting results about an enhancement of μ rhythm desynchronization when a vibratory actuator was applied simultaneously on the upper limb concerned by the MI, but this study did not concern vibrations with illusion of movement [117]. Then, Yao and colleagues (2015) demonstrated in healthy participants that tendon vibration inducing an illusion of movement significantly increased the detection accuracy of MI when the vibration was applied just before the MI [268]. Finally, Barsotti and colleagues (2018) exposed that MI combined with tendon vibration seemed to increase the ERD threshold in motor areas in the context of BCI training in healthy participants [269].

The association of VR and tendon vibration seems to be a synergistic tool to enable the participant to perceive a movement illusion, by kinesthesia illusion (induced by tendon vibration) and by visual illusion (induced by the VR system in the same time) [253]. Therefore, we used tendon vibration associated with a VR environment in our research: first to obtain a potentiation of the illusion, and second because of the observation of a motor task playing a role in brain motor activations.

3.1.2 Objective of our Experiments

Related to this context, in this chapter we will present two experiments. The first on the design of a visuo-haptic feedback and the second on the effect of this novel visuo-haptic feedback on EEG acquisition. These two studies are preliminary studies prior to the implementation of an NF study.

The aim of **the first study** is to determine the optimal parameters that can enhance an illusion of movement obtained by using a vibration. If the technical parameters of the vibration are already determined [253, 270–272], the visual conditions facilitating and enhancing the creation of a kinesthetic illusion are not known yet. Some studies tend to prove that the kinesthetic illusion is more important when the subject receive a visual cue congruent with the kinesthetic illusion induced by the vibration [273–275] compared to the case of a lack of vision of the concerned target during the vibration period [276–278]. These studies focus on healthy controls with protocols using mainly the “illusion mirror

paradigm" [279] without using Virtual Reality tools during tendon vibration. On the other hand, Caola and colleagues showed that the illusions of ownership and movement were higher when concomitant synchronous visuo-tactile stimulation were provided using VR immersing [280]. Our research hypothesis is that a virtual visual condition congruent to the illusion of movement produced by a tendon vibration enhances the intensity of illusion rather than the lack of visual cue or an incongruent cue. Therefore, we tested in healthy controls 3 virtual visual conditions associated with wrist tendon vibration: a moving virtual hand, a static virtual hand and no virtual cue and evaluated the illusion of movement felt in each condition.

The aim of **the second study** is to evaluate using EEG whether a visuo-proprioceptive immersion (VPI) including tendon vibration (TV) and Virtual moving hand (VR) combined to MI tasks could be more efficient than VPI alone or MI alone, in term of cortical excitability of motor brain areas in healthy participants. Our research hypothesis is that a visuo-proprioceptive stimulation (including tendon vibration with illusion of movement and VR visual environment) combined with MI could increase the cortical excitability of brain motor areas compared to MI or visuo-proprioceptive stimulation separately taken, by the production of a virtuous closed-loop feedback. Improving and reaching the best cortical excitability as possible could allow an optimal brain plasticity and is an efficient mean of neurorehabilitation for patients.

3.2 Experiment 1: Influence of visual feedback on the illusion of movement induced by Proprioceptive Haptic feedback

3.2.1 Materials and Methods

Study Design

We conducted in 2019 a monocentric randomised controlled pilot study in the Rehabilitation Unit of Rennes University Hospital in France. The study was promoted by the Rennes University Hospital Centre and obtained the approval of the Ethics Committee of Strasbourg University, France, on October 8th, 2019 (record number: 19/62-SI 19.07.05.46737). An information letter was provided to the participants including: the aims of the study, the protocol, the involved risks and insurance notifications. Written consent was obtained from each participant prior to testing. This study has been recorded in Clinical Trials under the following record number NCT04130711. No changes to the study design were made after approval by the ethics committee. The participant in the picture (Figure 3.1.a) in this manuscript has given written informed consent to publish these case details.

Participants

Volunteer healthy participants were recruited using a public information in the Department of Rehabilitation unit of Rennes University Hospital and of the Medicine Department of Rennes University. A total of 30 healthy participants (Mean± Standard Deviation): 24.933.79 years old, Min = 21, Max = 35 participated to the study, with 22 men (73,33%) and 8 women (26,66%). All healthy participants fulfilled the following inclusion criteria: age between 18 and 80 years old; no previous history of neurological illness. We asked the participants if they had a neurological history such as brain injury, brain surgery, epilepsy. No specific questionnaire was used. Participants deprived of freedom and with a legal incapacity were excluded from the study. Concerning the number of participants, a cohort of 30 participants was sufficient to obtain a good statistical power when using a within design.

Experimental Procedure

Procedure Participants sat in a typical office chair with armrest and adjustment of seat height and backrest inclination in front of a computer screen. Their non-dominant arm was positioned in a shell to keep it on the edge (Figure 3.1.a and 3.1.b), with the hand hidden from view by a black cloth, without support at the top (Figure 3.1.a). Laterality was determined by an Edinburgh questionnaire. A vibrator set on their flexor carpi tendon. Tendon vibration was applied during 10 seconds consecutively at the frequency of 100 Hz in order to induce an illusory movement. For each tendon vibration trial, participants saw random visual conditions on the computer screen in front of them: a virtual hand moving in the same direction as the wrist extension (Moving condition) (corresponding to the movement that the participant could feel if the tendon vibration induced a correct illusory movement); no hand at all with an empty screen (Hidden condition); a static virtual hand (Static condition) (Figure 3.1.c, 3.1.c and 3.1.c). Immediately, after each trial the participants were asked to indicate on a virtual protractor the maximal angle to which the illusion of wrist movement had gone (Figure 3.1.c) and how much they felt the movement illusion by using a Likert scale [41] from 1 to 7 (with 1 = no illusion at all; 4 = moderate intensity of illusion of movement; 7 = strong intensity of illusion of movement). For each participant, 33 trials were conducted i.e. 11 trials per visual condition (Figure 3.1.c). The first three trials were not included in the analysis, and were useful to check on 3 consecutive vibrations if the vibrator was well positioned, and if the evaluation modalities were understood by the participant. At the end of the experiment, participants filled out a questionnaire to determine if the participants had already tried such vibrating devices, get subjective data on vibration comfort, get the preferred visual condition, understand if the intensity of illusion was sufficiently felt. First, we explained orally that the subject would receive bursts of vibration to their wrist, which might give them a feeling of movement. We did not specify which movement it might be (hand, finger, ...) nor in which direction it would occur. Then we explained to them that during these vibrations, they would see on a screen a virtual hand resembling theirs, which might move or not. Again, we did not describe the direction of the hand's movement on the screen. Then we gave our instructions in writing the same

way. We systematically reminded the subjects to concentrate well on their sensations. In this way, we avoided influencing participants on potential outcomes or biased information. We checked that they understood the instructions, and we checked the consistency of the answers on the protractor and the Likert scale on the first trial to be sure that they had understood the guidelines.

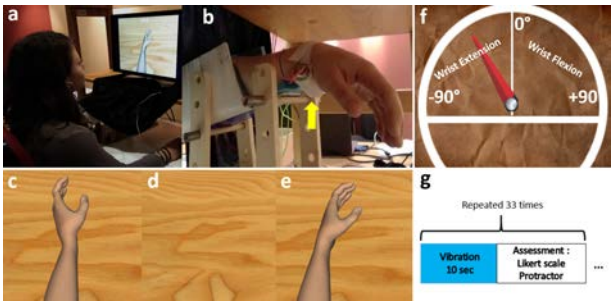

Figure 3.1: Apparatus used in the experiment (example for a right-handed participant). a-b) Set-up of the vibrator. A black curtain covered the forearm of the participant. c-d-e) Visualisation of the three virtual visual conditions (respectively Moving, Hidden, Static condition). A black arrow (not visible during the experiment) indicates the movement of the wrist in the Moving condition, from flexion to extension. f) Measure of sensation of displacement with the protractor. "−90" indicates an extreme wrist extension in the case of a left upper limb. The notes «values of degree» and « wrist extension, wrist flexion » are not visible by the participant during the experiment.

Visual Feedback Visual feedback of the performed mental task was given to the participants by using Unity software, and the virtual scene was composed of a homemade neutral and white skin upper limb avatar. The scene was displayed on a 17 inch-LCD monitor, was rendered from the point of view of the virtual avatar and the monitor was positioned in order to match participant's first perspective. The movement executed by the virtual hand was either: 1) Moving condition (Figure 3.1.c and 2): an extension of the non-dominant wrist with a total displacement of 30 degrees from the resting position, at speed of 3 degrees per second, congruent with the illusory movement which was expected by the application of a flexor carpi tendon vibration [8], or 2) Hidden condition (Figure 3.1.c): an empty surface corresponding to the space occupied by the virtual hand or 3) Static condition (Figure 3.1.c): a static virtual hand of the non-dominant wrist in front of the participant. The visual clue was available to represent a left or right hand depending on the laterality of the participant.

Vibratory Device The device used in this work is a UniVibe™ Model 320-105 vibratory unit (Figure 3.3), which was composed of an actuator with an adjustable position and orientation that can be finely positioned on flexor carpi tendon and maintained on skin with hook-and-loop fastener. We created a sound box by 3D print to protect the skin from the motor and allow a better sensation of vibration. An Arduino controls the vibration motor. Actuation was obtained by using an eccentric rotating mass actuator, allowing to accurately modulating the frequency patterns required for eliciting the motor illusion. The vibration frequency is determined by the rotation of the mass. The diameter of the skin tactor was 25 mm. In this study, we applied a frequency of 100 Hz, an amplitude of 5G,

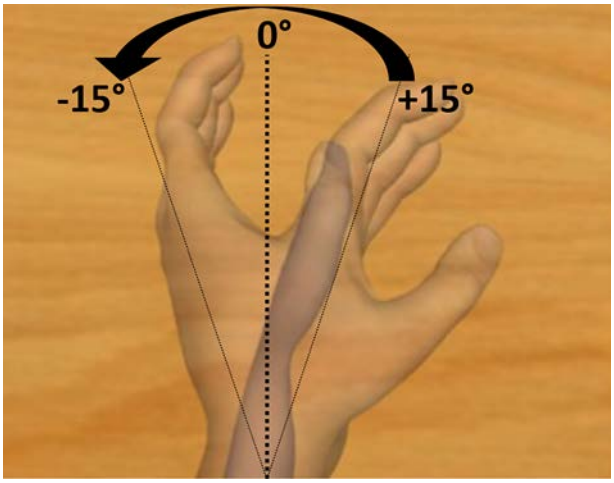

Figure 3.2: Description of the moving condition. Movement from wrist flexion to wrist extension, with a total displacement of 30 degrees around the rest position. The values and arrow are not visible by the participant during the experiment.

and voltage of 3.3 V based on the literature [236, 270, 271] to elicit movement illusion. We explained orally to the participants that they would receive bursts of vibration to their wrist, which might give them a feeling of movement. We did not specify which movement it might be (hand, finger...) nor in which direction it would occur.

Collected data

Primary outcome measure was the angle of motion felt in degrees during each vibration. The participants used a computer mouse (with their free hand) which allowed them to move the needle of the protractor. The participants could steer the needle from −90 (wrist in extension) to +90 (wrist in flexion) with all possible shades of degrees. They noted the direction of illusion of movement they felt on a protractor (Figure 3.1.c). An angle of 0 meant no illusion at all (resting position), while negative degrees meant a sensation of wrist's extension up to −90 and positive degrees meant a sensation of wrist's flexion up to +90. The protractor was available for right-handed or left-handed subjects, with negative degree values describing a wrist extension. On the screen, the virtual hand moved at an angle of 30 from a discreet wrist flexion to a discreet extension (Figure 3.2). Secondary outcome measures were the intensity of illusion of movement noted on the Likert scale [41] (with 1 = no illusion at all; 4 = moderate intensity of illusion of movement; 7 = strong intensity of illusion of movement) after each vibration and the preferred visual condition. Data was collected in Data Archiving and Networked Services (DANS) database.

Statistical Analysis

A descriptive analysis of all variables used in this study were performed. Qualitative variables were described with frequencies and their related percentages. Quantitative variables were divided into two groups:

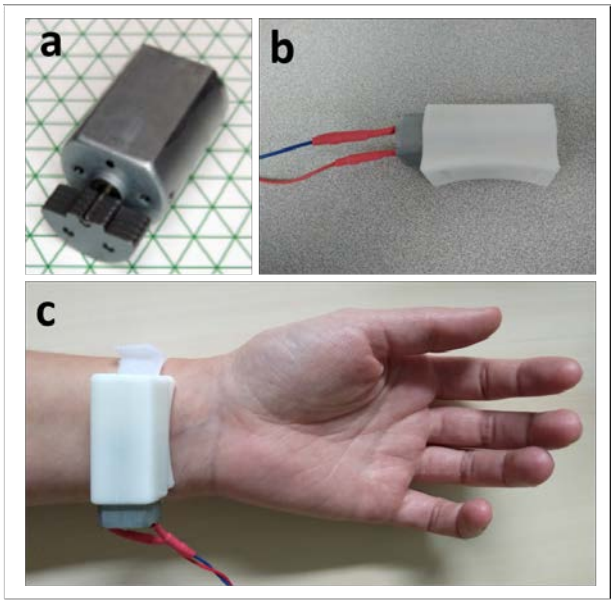

Figure 3.3: Pictures of the vibratory device UniVibe™. a) Raw vibration motor. b) Vibration motor device linked to the Arduino® and inside a sound box. c) Wrist placement.

- Variables following the normal distribution using the mean $\pm$ standard deviation
- Variables not following the normal distribution using the median and interquartile intervals.

Statistical tests were performed with SPSS Version 22 and R Version 3.6.2 software. The repeated measures analysis of variance (ANOVA) has revealed a violation of the assumption of sphericity according to Mauchly's test [42] in particular for one of the main judgement criteria (i.e., the difference in motion illusion in degrees): $\chi 2 = 113.40, p < 0.001$. Thus, a non-parametric approach was followed. A within-group analysis comparing the 3 visual virtual conditions (static condition, moving condition, hidden condition) was conducted using Friedman tests and then 2 by 2 conditions using post-hoc tests (Wilcoxon signed rank test) corrected with Bonferroni.

3.2.2 Results

Sensation of wrist's extension

The mean ($\pm$SD) sensation of wrist's extension was respectively -17.59 (24.77) for the Moving condition, -4.14 (27.31) for the Hidden condition and 0.44 (26.23) for the Static condition (Figure 3.4). Comparison of the repeated measures was performed using Friedman's test showing a statistically significant difference in the conditions, $\chi 2 = 113.40, p < 0.001$). Post-hoc analysis with a Bonferroni correction applied, showed that the Moving condition induced a higher sensation of wrist's extension than the Hidden condition and the Static condition ($p < 0.001$). The Hidden condition also induced a higher sensation of wrist's extension than the Static condition ($p < 0.01$). We then compared results between women and men. There were 8 women and 22 men. We did not find any significant results between

the groups in each condition (Kruskal Wallis test), respectively for the Moving condition ($H = 1.35, p = 0.24$), the Static condition ($H = 0.45, p = 0.50$), the Hidden condition ($H = 0.51, p = 0.48$).

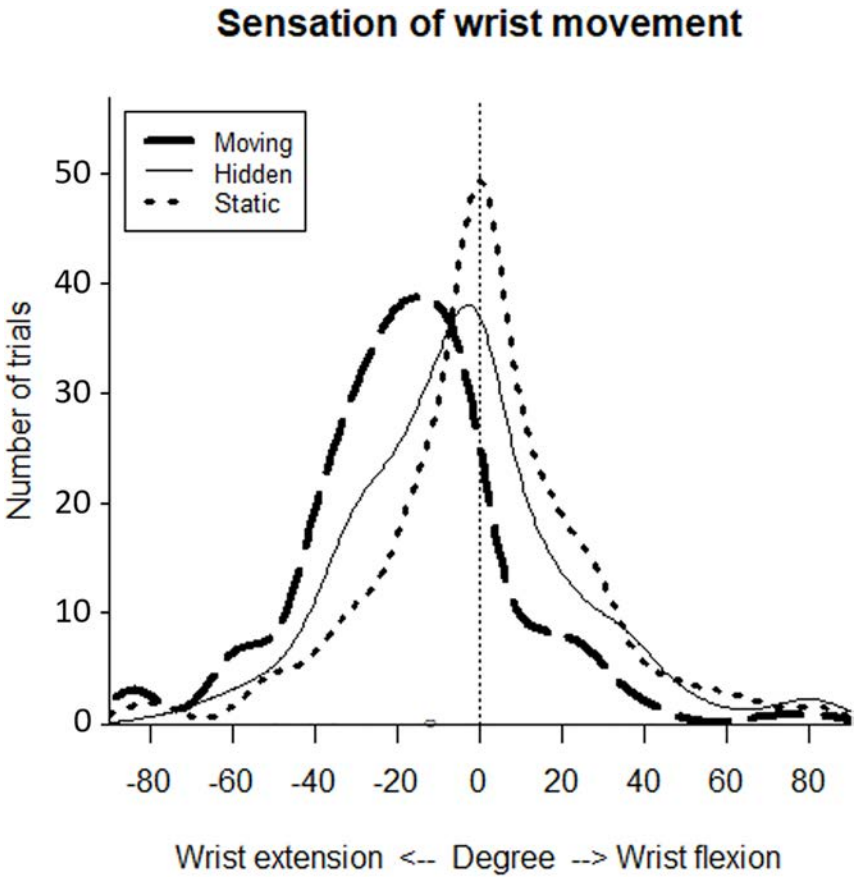

Figure 3.4: Smoothed histogram of the frequency of sensation of wrist displacement in each condition averaged in healthy controls. The vertical line represents the zero degree axis.

Intensity of the illusion of the movement

The mean (SD) Likert ranking were respectively 4.62 (1.51) for the Moving condition, 4.25 (1.60) for the Hidden condition and 3.86 (1.57) for the Static condition (Figure 3.2). There was a significant difference between the 3 visual conditions concerning the Likert scale ranking ($\chi 2 = 45.80, p < 0.001$). Post-hoc analysis showed that the Moving condition induced a higher intensity of illusion of movement than the Hidden condition ($p < 0.01$) and the Static condition ($p < 0.001$). The Hidden condition induced a higher intensity of illusion of movement than the Static condition ($p < 0.05$).

Subjective Reports of participants

Among our 30 participants, 27 were right-handed (90%) and 3 were left-handed (10%). Four participants had already had a small experience of illusion of movement induced by tendon vibration (13.3%). The participants' preferred condition to facilitate the illusion of

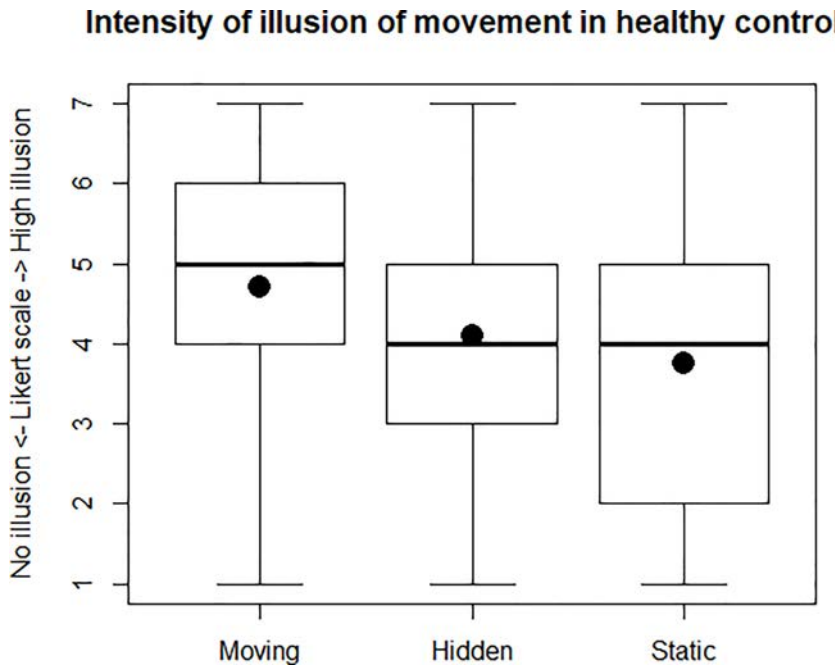

Figure 3.5: Boxplot about intensity of illusion of movement felt for each condition, averaged in all healthy controls (respectively for Moving, Hidden, Static condition). Likert scale from 1 to 7: 1 means "no illusion", 7 mean "very high intensity of illusion". The dots represent the means.

movement was the Moving one (Number of participants (n = 19, 63.33%), then the Hidden condition (n = 6, 20%), then the Static condition (n = 2, 6.67%), and some participants did not prefer any of the 3 conditions (n = 3, 10%). The type of illusion felt by the participants was mainly a wrist extension (n = 16, 53.33%), then a wrist flexion (n = 7, 23.33%), then a wrist spination (n = 6, 20%) and a fingers extension (n = 1, 3.33%). Most participants felt the illusion of movement easily while they experienced the Moving and Hidden conditions compared to the Static one (respectively 83.3% (n = 25), 66.7% (n = 20), and 40% (n = 12)). When participants felt an illusion of movement, it rather appeared at the onset of the vibration period in the Moving condition (n = 15, 50%), or at the middle of the vibration period in the Hidden and Static conditions (respectively n = 13, 43.33% and n = 12, 40%). The illusion of movement lasted approximately 10 seconds for the participants in the Moving condition (n = 12, 40%) whereas it lasted less than 5 second in the Hidden and Static condition (respectively n = 12, 40% and n = 14, 46.66%). During the experiment, some participants (n = 3, 10%) experienced a transient uncomfortable feeling of paresthesia or itching on their wrist and/or their hand, without any need to stop the experiment.

3.2.3 Discussion

This study investigated the contribution of virtual visual cues to improve the illusion of movement induced by wrist tendon vibration in healthy controls. The results confirmed our main hypothesis that the illusion of movement seemed higher when the movement of the virtual hand seen on the screen was congruent to the sensation of illusion felt. The Moving condition was significantly superior to the Hidden and Static condition in terms of

sensation of wrist extension (Figure 3.4), intensity of illusion (Figure 3.5) and comfort for the participants.

The Hidden condition was also superior to the Static condition in terms of sensation of wrist displacement and intensity of illusion of movement which was expected regarding the existing literature [277, 278, 281]. These results could be explained by the incongruent visual cue given to the participant and disturbing the production of illusory movements. The participants also indicated that the illusion of movement rather started after few seconds and lasted about 5 to 10 seconds. The onset of the illusion matched with the data found in the literature [271], i.e. approximately 5 seconds. The best duration of the illusion in the literature seemed to be between 10 and 30 seconds [271, 272, 282], which is consistent with our data. Surprisingly, we found that the illusion of movement felt did not only consist in a wrist extension in all participants, contrary to what is described in the literature [236, 278] when a vibration on the flexor carpi tendon is applied. Indeed, in our experiment, only 2 participants felt exclusively a wrist extension during the entire vibration period. All other participants felt a wrist extension, but also a wrist flexion, even a wrist supination sometimes, without any movement of the subject or the vibratory during the experiment. All these sensations seemed random, not depending on a specific visual condition, except for the Moving condition which more frequently induced a sensation of wrist extension. In this virtual Moving condition, the illusion of movement seemed lower when the subjects felt another illusion that wrist extension, because the illusion became incongruent to the visual cue, regarding to the reports of the participant. Nevertheless, even though the goal of tendon vibration was a wrist extension in this study, the illusion of movement was well present in all participants in the Moving condition, and could be also effective in stimulating brain motor areas [239]. The interest of stimulating the wrist extension was to be close with the aim of motor rehabilitation in stroke patients who suffer from motor control deficiency and often spasticity in their upper limb extremity [283]. It could lead to a closed fist, and one main goal of the rehabilitation care is to open the hand and stretch the wrist in order to avoid vicious deformations [284, 285]. We tested the participants with their non-dominant upper limb. First, we found in the literature that the illusion of movement induced by tendon vibration could be higher on the non-dominant limb [271]. Then, the aim was to match a healthy population with a chronic stroke population. The post-stroke subjects often need to re-lateralise themselves to use the non-injured upper limb in case of incomplete recovery.

However, our experiment presented some methodological limitations. Above all, the between-design was not applicable here. Each participant had 33 vibration tests (10 in each condition). All the tests were performed in a randomised order, so that the first vibration tests could be randomly any of the 3 conditions repeated several times in a row. Moreover, as explained below, to feel an illusion of movement induced by tendon vibration, the participants needed to be completely relaxed. Subjects at the beginning of the study tended to not be relaxed due to experiencing new vibrations. It also took them some time to adjust to the virtual world and to immerse themselves into the VR tool. Sometimes, they became distracted by the investigator due to repositioning the vibrator, particularly during the first tests. They also needed some time to understand the measurement system with the Likert

scale and the protractor. For all these reasons, it was necessary to remove these initial tests from the main analysis and therefore not do a between-design analysis.

One explanation concerning the unexpected sensation of wrist flexion and supination during tendon vibration could be the complexity of the wrist anatomy. Flexor carpi tendon are numerous in a very little area in the wrist and some of them have several functions as flexion but also supination. The vibratory device used in this experiment conformed with the device found in the literature, with a size including the width of the wrist. This type of device cannot be precise to the point of targeting a single tendon. Further studies would be necessary to develop more precise vibratory devices. Then, during the experiment some participants tended to tense up when they received the vibration, and could develop some Tonic Vibration Reflex (TVR) events inducing flexion illusions [276].

Next steps will be to test the same hypothesis with stroke patients to quantify if and how an illusion of movement could be obtained in the same conditions. Chancel et al. [286] tested in elderly the ability to perceive self-hand movements based on multisensory feedback with vibration on thumb. Results showed that the illusion of movement induced by a tendon vibration was slower and weaker to appear in elderly people that in a younger population. Stroke patients are mainly older than our study population [2], thus we can expect a weaker illusion of movement felt with stroke patients. In addition, stroke people often suffer from others symptoms such as attention disorder which can decrease the ability to focus or hypoesthesia. Sensory inputs and sensorimotor integration can be disrupted. The current literature [287, 288] remains unclear about the effectiveness of central integration of peripheral vibration in this population.

In conclusion, our results showed that virtual visual cues congruent to the illusion of expected movement enhanced the illusion of movement induced by tendon vibration. Our study is the first which demonstrates the benefits to use VR cues with tendon vibration to improve the illusion of movement in healthy subjects. Moreover, it confirms that congruent visual cue is greater than hidden object or even static visual cue.

3.3 Experiment 2 : Influence of Visuo-haptic and Motor Imagery of wrist on EEG cortical excitability

3.3.1 Materials and Methods

Study Design

We conducted, from October to November 2019, a monocentric randomised controlled pilot study in the Rehabilitation Unit of Rennes University Hospital in France. The study was promoted by the Rennes University Hospital Centre and obtained the approval of the Ethics Committee of Strasbourg University, France, on October 8th, 2019 (record number: 19/62-SI 19.07.05.46737). An information letter was provided to the participants including:

the aims of the study, the protocol, the involved risks and insurance notifications. Written consent was obtained from each participant prior to testing. This study has been recorded in Clinical Trials under the following record number NCT04130711. No changes to the study design were made after approval by the ethics committee. The participant in the picture (Figure 3.6.a) in this manuscript has given written informed consent to publish these case details.

Participants

Volunteer healthy participants were recruited using a public information in the Department of Rehabilitation unit of Rennes University Hospital and of the Medicine Department of Rennes University. A total of 20 healthy participants (Mean$\pm$ Standard Deviation): 31.309.86 years old, $Min = 22$, $Max = 61$ participated to the study, with 11 males (55%) and 9 females (45%). All healthy participants fulfilled the following inclusion criteria: age between 18 and 80 years old; no previous history of neurological illness (brain injury, brain surgery, epilepsy), right-handed. Participants deprived of freedom and with a legal incapacity were excluded from the study. Concerning the number of participants, the corresponding literature motivating the research hypothesis includes studies involving about 15 or 16 participants [269].

Experimental Procedure

Procedure The participants sat in a typical office chair in front of a computer screen in a quiet room. The EEG cap was positioned on their scalp and the vibratory on the flexor carpi tendon of their non-dominant arm (left arm), positioned in a shell and hidden from view (Figure 3.6.a and 3.6.b). This experiment occurred on the non-dominant left limb, because the findings of a previous study showed that the illusion of movement was greater when the tendon vibration was applied on non-dominant limb [271]. Laterality was determined orally and then checked by an Edinburgh questionnaire. This experiment was composed of 3x3 randomised conditions of 3 minutes 20 seconds each and we recorded the EEG signals of the participant in each session of 3'20 minutes without any additional feedback. The first condition consisted of MI (MI condition). The second condition (visuo-proprioceptive condition VPI) consisted of applying a wrist tendon vibration on the wrist of the non-dominant arm of the participant while he could see a virtual moving hand, the movement of which was congruent to the illusion of movement induced by the actuator . The third condition combined the MI task with the visuo-proprioceptive illusion (Combined condition=MI+VPI)) (Figure 3.7 and 3.3). We decided to use this virtual cue because of the results of a previous experiment [253](Le Franc et al, article submitted in 2020) the results of which confirmed that virtual visual congruent cues associated with tendon vibration could increase the illusion of movement and the feeling of immersion felt by the participants.

Each block of MI tasks or VPI or combined conditions lasted 10 seconds and was separated from the next one by 10 seconds of rest. Each block was repeated 10 times to fulfil one

session of 3 minutes and 20 seconds (Figure 3.7.b). MI task: The instruction the participants was to imagine a movement similar to the one they will have seen on the screen. After MI task (in combined or MI condition), a Likert scale from 1 to 7 (1 = easy, 7 = difficult) appeared on screen in order to quantify the difficulty of performing the MI tasks. At the end of the experiment, all the participants filled out a questionnaire to determine if the participants had already tried such vibrating devices or MI, get subjective data on vibration comfort, and get some information about the illusion of movement felt. Then, we analysed the ERD rate for each condition in order to determine which one was the best to improve cortical excitability and if visuo-proprioceptive stimulation could trigger motor areas activation during MI. After VPI or combined condition, a Likert scale from 1 to 7 appeared on screen in order to quantify the intensity of the illusion (with 1 = no illusion at all; 4 = moderate intensity of illusion of movement; 7 = strong intensity of illusion of movement).

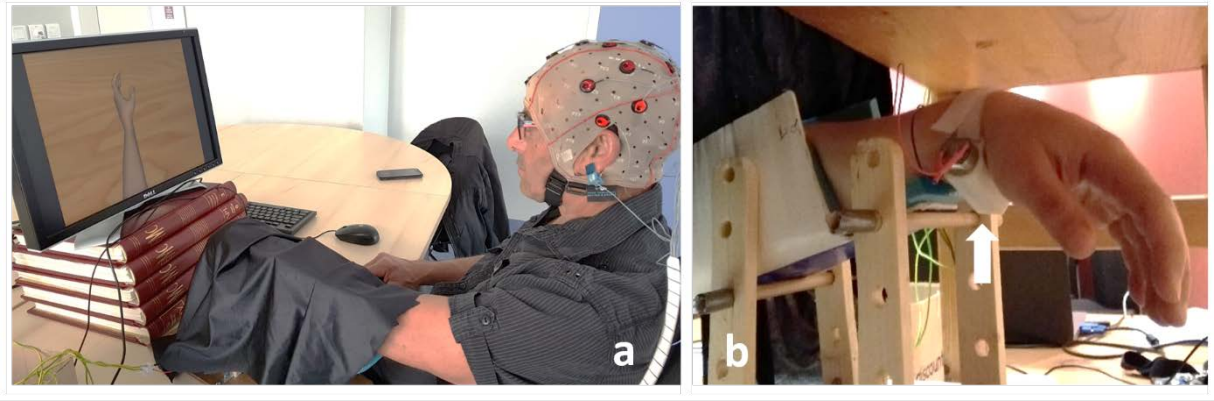

Figure 3.6: Apparatus used in the experiment. a) Set-up of the participant during EEG recording. The vibrator was positioned on the left non-dominant wrist, hidden from view of the participant by a black cloth. b) Set-up of the vibrator on the flexor carpi tendon. The forearm was positioned in a shell. The white arrow indicates the vibrator.

Visual Feedback

Visual feedback of the performed mental task was given to the participants by using Unity 3.5 software, and the virtual scene was given to the participants by using Unity 3.5 software and composed of a moving homemade neutral and white skin upper limb hand avatar. The scene was displayed on a 17 inch-LCD monitor, was rendered from the point of view of the virtual avatar and the monitor was positioned in order to match the participant's first perspective. The movement executed by the virtual hand was an extension of the non-dominant wrist with a total displacement of 30 degrees from the resting position, at a speed of 3 degrees per second, congruent with the illusory movement that was expected by the application of a flexor carpi tendon vibration (Figure 3.7.a and 3.3) [289].

Vibratory Device

We used the same vibrator as in experiment 1. The more precise characteristics are documented in the section 3.2.1.

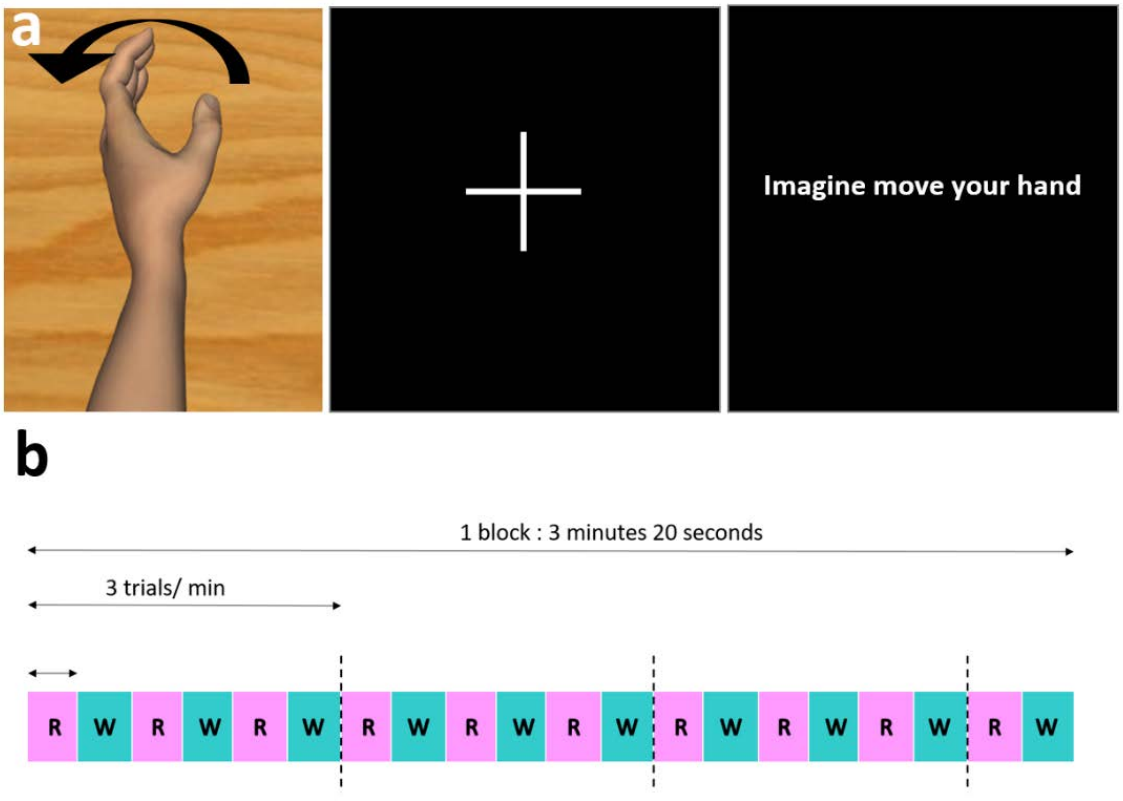

Figure 3.7: Description of the recorded sessions. a) Visualisation of the condition on the screen: a virtual moving hand during the vibration period (combined condition and visuo-proprioceptive condition), or a cross on the screen for rest period, or a visual instruction on screen to do motor imagery (MI condition). b) Descriptive diagram of one block process. « R » means rest period and « W » means indifferently visuo-proprioceptive stimulation, Motor Imagery period or combined stimulation.

EEG data acquisition

We recorded EEG data in an extended 10-20 system with g.Tec® cap and g.Amp amplifier. The data was processed using a custom-made processing algorithm using the OpenViBE software. A pattern of 16 electrodes was placed over the scalp: Fpz, Fz, Cz, Pz, Fc1, Fc2, Fc5, Fc6, C3, C4, T7, T8, Cp1, Cp2, Cp5, Cp6. The passive ground electrode was placed on AFz and all channels were referenced to a right ear lobe electrode.

EEG data analysis

The EEG analysis was performed on the electrodes Cz, Fc1, Fc2, Fc5, Fc6, C3, C4, Cp1, Cp2, Cp5, Cp6 (with respect to the motor areas). EEG recordings were band-pass filtered from 0.5 to 40 Hz and then digitally converted with sample frequency of 512 Hz (using a Butterworth zero phase filter with a 48 dB slope). All EEG recordings were inspected

visually and electrodes with too high impedance (>30 kHz) or poor signal quality were excluded from further analysis.

Imagined movement in sensorimotor rhythms paradigms causes ERD in μ (8-13 Hz) and β (13-28 Hz) rhythms, known to be involved in movement imagination, preparation or active tasks and observed in the primary motor cortex, contralateral to the limb involved in the task, mainly related to C3 and C4 electrodes [263]. The ERDs were extracted from a Riemannian distance [290]. We did not include a spatial filter in the analysis and directly observed the entire signal strength of the electrodes. This relative power change is calculated according to: With taskE and restE denoting the average power in the frequency range of electrode E during task condition and rest, respectively. Positive power changes will be referred to ERS whereas negative changes will be referred to ERD. ERD and ERS are percentage values, the reference value being calculated according to the rest task. Results were visualised for the alpha (8-13 Hz) and beta (13-28 Hz) band as topoplot maps.

Collected data

Primary outcome measure was the ERD rate measured in μ and β bands regarding the C4 electrodes in each condition (MI condition, visuo-proprioceptive condition, combined condition). Secondary outcome measures were the intensity of illusion of movement felt during tendon vibration noted by a Likert scale (from 1 to 7 with 1=no illusion at all; 4=moderate intensity of illusion of movement; 7=strong intensity of illusion of movement) and the difficulty of doing MI tasks (from 1 to 7 with 1=easy to 7=difficult). The participants had a computer mouse (with their free right hands) which allowed them to quote on the Likert scale on the screen after each block. Data were collected in Data Archiving and Networked Services (DANS) database.

Software and statistical analysis

Data processing, analysis signal analysis were performed using MATLAB R2017a (MathWorks, Inc., Natick, MA, United States). The results from the spatial activation pattern are given as the relative power change from baseline $\pm$ standard deviation (SD). Topographical plots were created using a custom-made MATLAB function. We used percentages to describe qualitative variables, and mean $\pm$ standard deviation to describe quantitative variables for parametric data. We also used median and interquartile intervals to describe non-parametric data. All data were analysed by statistical tests using the R and MATLAB software. According to Shapiro-Wilk test, our data followed a normal distribution (p=0.25, p=0.73, p=0.11 respectively for the combined condition, for the visuo-proprioceptive condition and for the MI condition). According to Mauchly's Test of Sphericity, our data set violated the assumption of sphericity, for the main judgement criteria: $\chi 2 = 24.47$, $p < 0.001$. Thus, we used a non-parametric approach. A within-group analysis comparing the 3 conditions was performed using Friedman test and then 2 by 2 conditions using post-hoc tests (Wilcoxon signed rank test) corrected with Bonferroni. P-values<0.05 were

considered statistically significant. We also used the paired Student test and Kruskal-Wallis test to compare data on the Likert scale as a function of conditions and a two sample Student t-test to compare the ERD data.

3.3.2 Results

This is the flowchart of the experiment Figure 3.8 .

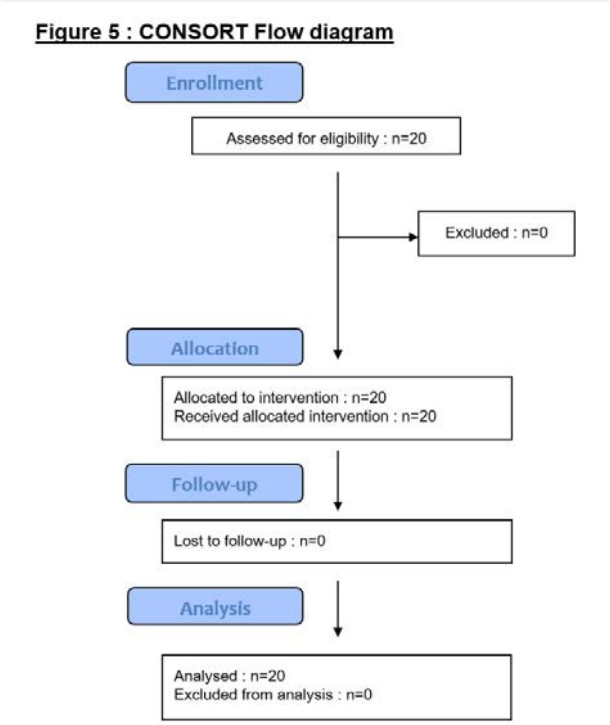

Figure 3.8: Flowchart of the experiment.

EEG data

The mean ERD in percentage $\pm$ Standard Deviation was 38.00$\pm$10.08 for the combined condition, 33.04$\pm$9.93 for the visuo-proprioceptive condition and 13.34$\pm$12.08 for the MI condition. (Figure 3.9.a). There was a significant difference between the 3 conditions ($\chi 2 = 24.47, p < 0.001$) according to the ERD percentage. There was no significant difference between the combined condition and the visuo-proprioceptive condition ($p = 0.59$), but there was a significant difference between the combined condition and the MI condition ($p < 0.001$) and between the visuo-proprioceptive condition and the MI condition ($p < 0.001$).

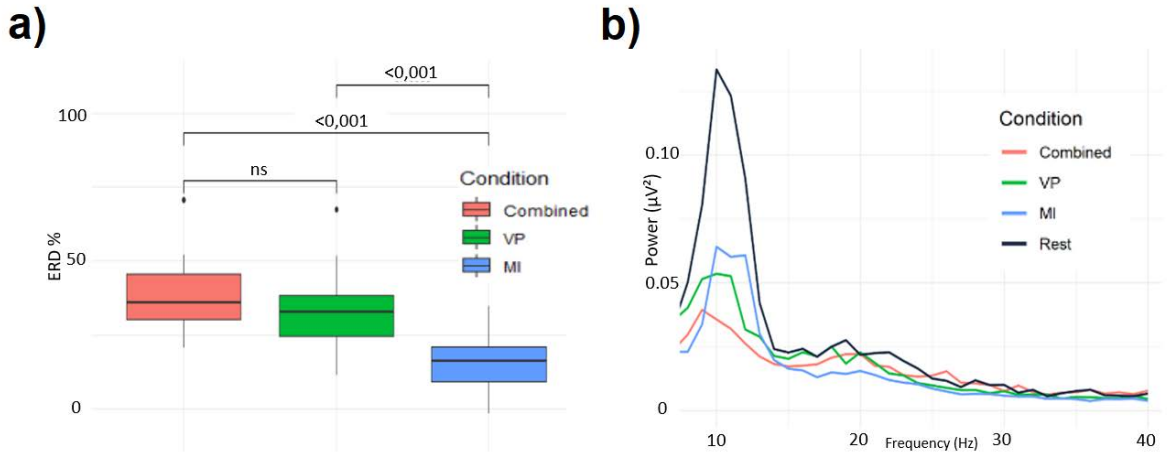

Figure 3.9: EEG Results. a) Boxplot of ERD percentage measured in each condition in the 8-28 Hz bands. The left boxplot represents the ERD percentage in the combined condition ("Combined"), the second boxplot concerns the visuo-proprioceptive condition ("VP"), the right boxplot concerns the MI condition '"MI"). The crosses represent the means of ERD. NS means "no significant". b) Power spectrum density analysis. Representation of each condition as a function of the signal power in the 8-28 Hz frequency bands on C4 electrode. Each line represents one condition. Black: Rest state, red: combined condition, green: visuo-proprioceptive condition (VP), blue: MI condition.

According to these data, the topoplots represented the power of ERD measured in the 8-28 Hz bands (μ and β bands) around the scalp averaged in all the participants of the study (Figure 3.9.b).

Among the participants who preferred to perform the MI tasks during vibration (n=9), ERD average was 41.85% $\pm$ 11.11, while in the population of participants who found MI more difficult to do when visuo-proprioceptive stimulation was present at the same time (n=11), the result was 34.86% $\pm$ 8.41. There was no significant difference between the two groups (Kruskal-Wallis test, $K = 0.24$, $p = 0.62$). Among the 5 participants who had previously performed MI (See subjective reports), the ERD rate was 5.82% $\pm$ 27.45 in the MI condition compared to the other participants who had never performed it before 16.05% $\pm$ 6.94. There was no significant difference between the groups (Kruskal Wallis test, K=0.47, p=0.49). We did not find any correlation between the intensity of movement illusion felt by the participants and the level of cortical activation represented by the ERD in the visuo-proprioceptive condition (Pearson's test, r=-0.08, p=0.72) or in the combined condition (r=-0.07, $p = 0.77$).

A power spectrum density (PSD) analysis showed the evolution of the signal power as a function of the frequency bands of interest in the 8-28 Hz on C4 electrode, according to each condition and in comparison with the rest state (Figure 3.10.c). There was a significant difference between the 3 conditions (χ2= 12.77, p<0.01) according to the PSD values. There was no significant difference between the combined condition and the visuo-proprioceptive condition ($p = 0.24$), but there was a significant difference between the combined condition and the MI condition ($p < 0.01$) and between the visuo-proprioceptive condition and the MI condition ($p < 0.001$). We compared the values in each condition between the task and the corresponding rest: we found a significant difference in each condition: Combined condition, Visuo-proprioceptive condition and MI condition ($p < 0.001$).

A time-frequency analysis was performed for each condition, with the average results of all study participants averaged over the 10-second period of stimulation in the 8 to 28 Hz frequency bands (Figure 3.10.d).

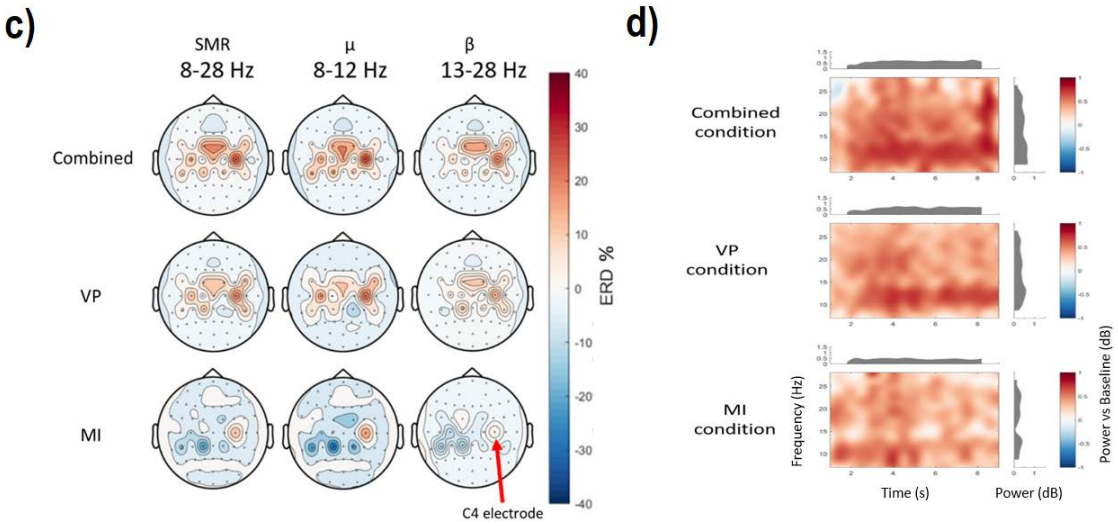

Figure 3.10: EEG Results. c) Topoplots of ERD percentage measured in each condition. The topoplots were averaged in all the participants. They are separated in rows, according to each condition tested (combined condition, visuo-proprioceptive condition (VP), motor imagery condition (MI)), and in columns according to the 8-28Hz (μ-β bands), 8-13Hz (μ bands), 13-28Hz (β bands). The red arrow locates the position of the C4 electrode. Red represents ERD; blue represents ERS. d) Time frequency analysis. Representation of signal power as a function of task completion time (10 seconds) in the 8-28 Hz frequency bands under each condition. From top to bottom: combined condition, visuo-proprioceptive condition (VP), MI condition. The red colour represents a greater decrease in signal power. d) Time frequency analysis. Representation of signal power as a function of task completion time (10 seconds) in the 8-28 Hz frequency bands under each condition. From top to bottom: combined condition, visuo-proprioceptive condition (VP), MI condition. The red colour represents a greater decrease in signal power.

Intensity of the illusion of movement

The mean±SD Likert ranking was respectively 4.91±1.63 for the visuo-proprioceptive condition and 4.951.16 for the combined condition. There was no significant difference between the conditions (paired t-test, $t = 0.15$, $p = 0.88$, Cohen's $d = 0.03$). The intensity of illusion of movement was also measured across time by the Likert ranking. For each condition, we analysed the Likert ranking measured at the onset of the experiment compared to the values at the end of the experiment. The mean was 4.50 (in the session 1 of the condition i.e. the 3 first recorded minutes) and then 5.05 (in the session 3 of the condition i.e. the 3 last recorded minutes) for the visuo-proprioceptive condition. There was no significant difference between the session 1 and 3 (paired t-test, $t = 1.09$, $p = 0.29$, Cohen's $d = 0.06$). The mean was 4.85 (in the session 1 i.e. the 3 first recorded minutes) and then 4.95 (in the session 3 i.e. the 3 last recorded minutes) for the combined condition (Figure 3.11). There was no significant difference between the session 1 and 3 (paired t-test, $t = -0.25$, $p = 0.81$, Cohen's $d = 0.01$).

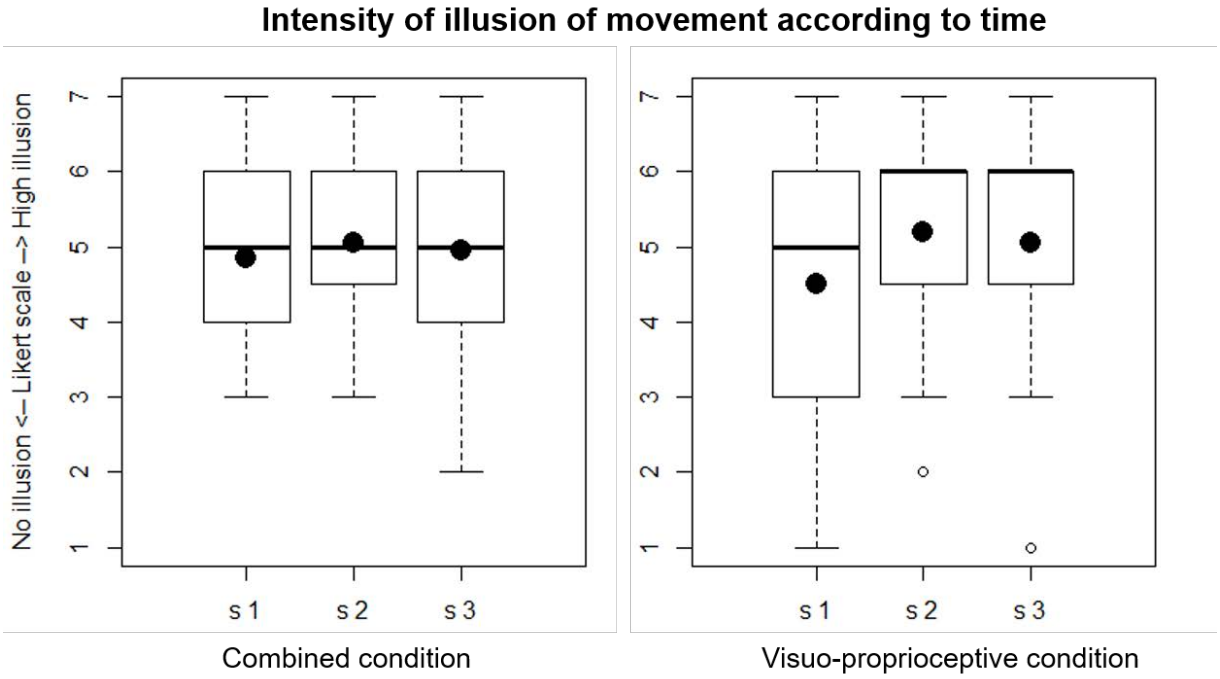

Figure 3.11: Intensity of illusion of movement according to time. Boxplot representations of the intensity of illusion of movement in combined condition (left boxplot) and in visuo-proprioceptive condition (right boxplot). The dots represent the means on the Likert scale ranking.

Perceived ability to perform MI tasks

The mean±SD Likert ranking was respectively 3.811.21 for the MI condition and 4.15±1.58 for the combined condition. There was no significant difference between the conditions (paired t-test, $t = 1.41$, $p = 0.16$, Cohen's $d = 0.24$). The perceived aptitude of doing MI was also measured according to time by the Likert ranking. For each condition, we analysed the Likert ranking measured at the onset of the experiment compared to the values at the

end of the experiment. The mean was 4.10 (in the session 1 of the condition i.e. the 3 first recorded minutes) and then 3.70 (in the session 3 of the condition i.e. the 3 last recorded minutes) for the MI condition. There was no significant difference between the session 1 and 3 (paired t-test, $t = 1.05$, $p = 0.31$, Cohen's $d = 0.05$). The mean was 4.45 (in the session 1 i.e. the 3 first recorded minutes) and then 3.80 (in the session 3 i.e. the 3 last recorded minutes) for the combined condition (Figure 3.12). There was no significant difference between the session 1 and 3 (paired t-test, $t = 1.58$, $p = 0.13$, Cohen's $d = 0.04$).

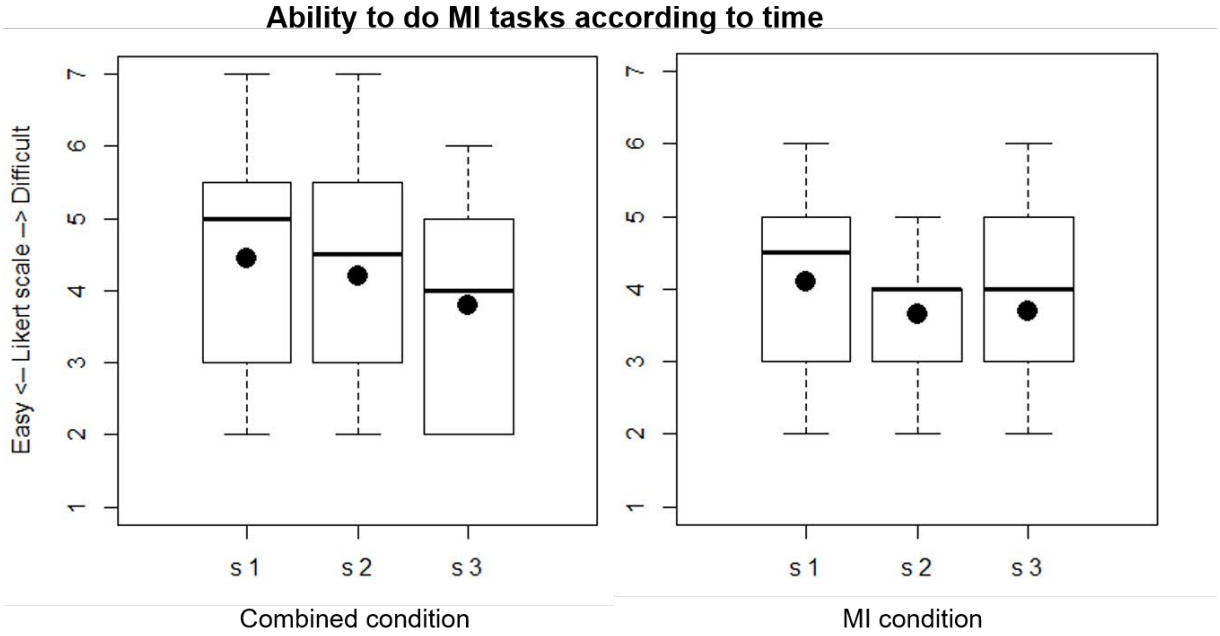

Figure 3.12: Perceived ability to do motor imagery according to time. Boxplot representation of the perceived ability of doing motor imagery in combined condition (left boxplot) and MI condition (right boxplot). The dots represent the means on Likert scale ranking.

Subjective Reports of participants

Among our 20 participants, 5 participants (25%) had already experimented MI tasks at least once. Most of our participants felt tired at the end of the experiment ($n = 13$, 65%), but 16 participants (80%) thought that there was enough resting periods during the protocol. Nine participants (45%) thought that their MI performance was better and easier when the tendon vibration was applied simultaneously.

3.3.3 Discussion

The main aim of our experiment was to evaluate whether a visuo-proprioceptive stimulation including tendon vibration illusion, VR environment and MI tasks could be more efficient in terms of sensorimotor areas cortical excitability than either MI or visuo-proprioceptive stimulation alone.

First, the results demonstrated that the combined condition was significantly better than the MI condition in terms of ERD rate around brain motor areas. However, we did not find any significant difference between the combined condition and the visuo-proprioceptive condition (Figure6a, 6c). To go further, contrary to the existing literature, we did not find any evidence of a clear synergistic effect of MI and visuo-proprioceptive illusion to enhance motor cortical excitability in healthy participants. This conclusion assessment should be qualified by other results. In time-frequency analyses, we observed greater ERD peaks in the combined condition than in the other conditions, in the μ bands (8-13 Hz), over the stimulation time (Figure6d). In power spectrum density graphic, we also found a greater decrease in ERD power in the combined condition than in the other conditions and relative to the rest state (Figure6c). We might therefore hypothesise a partial synergy of the visuo-proprioceptive and MI conditions when temporality was taken into account. Based on the literature, our analyses focused on the C4 electrode, recognised as the main electrode representing the motor cortex [83, 291].

Those key findings contradicted those found in the existing literature on the topic. Barsotti et al (2018) found in their study higher BCI performance when the kinesthetic illusion induced by vibrational feedback was present [282]. Although they are two different techniques, MI and tendon vibration (involving illusions of movement) share some common neural substrates. Several studies using functional brain imaging have shown that similar areas were activated by these two techniques [240, 256]. Other studies also proved that one tool could interact with the other one to improve it. For example, Shibata and al. (2017) demonstrated that the velocity of perceived movement was significantly higher when the participant performed MI at the same time than a vibration stimulation compared to a vibration stimulation alone [292]. Similarly, Kitada and al. (2002) found that the type of MI performed (i.e. congruent or incongruent) influenced the maximum perceived angle of wrist flexion during the tendon vibration. If the MI were congruent with the illusion induced by the tendon vibration, the perceived angle of wrist was higher than if the MI were incongruent [293]. On the other hand, MI performance was improved when tendon vibration with illusion of movement was done immediately before it in Yao and al's study [268]. To reinforce this activation, we combined, in this experiment, tendon vibration with an immersion in a VR environment.

One hypothesis that may explain the lack of evidence of superiority of the combined condition involving MI and visuo-proprioceptive stimulation is the possible absence of physical accumulation of ERD from different origins, and the difference in the modulation behaviour of ERD/ERS. The results of the Rimbert et al.'s study showed that a median nerve stimulation when combined with MI modulated the generation of ERD and ERS differently than MI alone or electrical stimulation alone. On the one hand, ERD visible in MI and electrical stimulation alone did not seem to accumulate. On the other hand, ERS were significantly amplified in the same condition [294] and our stimulation was not targeted to the nerve but consisted of a tendon vibration, with potential EEG recording artefacts related to the vibrational force [117, 220]. Rimbert et al.'s work also suggested that ERD and ERS produced by MI were modulated according to the time allocated to that MI. In their study, EEG recordings were made while healthy participants performed

MI tasks that were either "continuous" (repetitive for 4 seconds) or "discrete" (one time during 1000 ms). It appeared that detectable ERD/ERS in the category of discrete MI were of higher consistency and more easily detected compared to continuous MI, with ERD found particularly lower in continuous MI [295]. These phenomenon suggests that the ERD and ERS components overlapped over time in continuous MI [296]. We could deduct from this study that the detection of ERDs under MI conditions was not optimised by overlapping these repeated ERD/ERS phenomena in our study. Unlike the BCI studies, where ERD measurements are often recorded some 500 milliseconds before the start of the MI instruction and over periods of 2 to 4 seconds, our ERDs were recorded from the time the set-point was given and for a duration of 10 seconds. On the other hand, the combined condition could not have been achieved over shorter duration, since the illusion of motion induced by the vibration generally requires more than 5 seconds to appear and more than 10 seconds to be optimal [271].

In the vibration condition (Figure 3.9.b), we found bilateral activations (ERDs) over parietal areas that were more intense on the contralateral side of the vibration. These results are in line with the literature, which has already described bilateral activations of the parietal operculum [239] and bilateral activations at the onset of the execution of movement [297]. We also found significant ERSs over the left (ipsilateral) hemisphere related to the hand MI. ERSs were detectable in both μ and β rhythms, matching with the current literature that reports significant ERSs over the ipsilateral side in the 5 seconds after the onset of the exercise [264]. The ERD activity related to the pre-frontal cortex (FC1-FC2 electrodes) seemed increased in both the vibratory conditions. It could be explained by the stimulation of prefrontal medial regions involved in the awareness of illusory movements as described in the literature [298, 299].

We also observed a significant difference in the ERDs between the visuo-proprioceptive and the MI conditions, in favour of the visuo-proprioceptive condition (Figure 3.9.b). These results were expected because stimulation such as vibration, which is powerful, causes a strong cortical response as can functional electrical stimulation. This is due on the one hand to the triggered sensitive response, but also because of the EEG artefacts caused by the vibration. MI, which has a lower consistency, was comparatively less effective. These results may give interesting arguments in favour of using one tool rather than the other one in rehabilitation. Based on these results, it may seem more useful to use external stimulation such as vibration to generate greater cortical responses. This visual and proprioceptive immersion allows both sensory-motor and visuo-motor loop reinforcement. On the other hand, an intrinsic stimulation such as mental imagery, generated by the subject, introspective, controlled and more "active", is a more dynamic modality from a rehabilitative point of view.

In our study, 9 participants (45%) thought that their MI performance was better and easier when the visuo-proprioceptive illusion was applied simultaneously to their MI, while the others thought that the visuo-proprioceptive illusion was disturbing. This subjective result could be explained by the positive effect of repeated tendon vibrations inducing illusory movement while the participant had to perform MI tasks, to enhance their MI performance, as noticed by Yao and al. [268]. In this study, the participants improved

their MI performances and accuracies evaluated using EEG, by repeated tendon vibration inducing illusion during the MI tasks. Another correlate of this result could be done with the action-observation task : some studies showed that the MI performance and accuracy was enhanced when the participants could see in the same time or just before the real representation of their imagining movement [300, 301]. By using the VR system of a virtual-own hand, the participants saw the hand movement and could mature their MI performance in our experiment. However, the ERDs were not higher for the participants who experienced facilitated MI during tendon vibration compared to those who felt disturbed MI during tendon vibration. This could mean that the perceived ability to perform MI tasks is very subjective and cannot predict the modulation of ERDs. Our results also demonstrated the subjective difficulty of doing MI for naive users (Figure 3.12). These data matched with the broad literature on the topic. The participants needed to practice MI tasks many times to complete the exercise more easily [183, 302, 303].

We also found that the sensation of illusion induced by tendon vibration was constant all the time of the experiment, without any habituation of the participants (Figure 3.11). By using short periods of tendon vibration in our protocol (10 seconds for each trial, repeated 60 times), we were in accordance with the current literature where were described short periods of vibration (10-60 sec) to induce a high sensation of illusion of movement over the entire period tested, without habituation effect [271, 304].

However, our study presents some methodological limits. First, we included a small population of 20 healthy participants. This could have induced a lack of power in our statistical results. However, the mean number of participants included in the existing literature was about 15 participants [262, 269]. Second, we used a 16 electrodes cap which is still common practice in MI analysis [305] allowing us an easier set-up. In the future, it might be interesting to use a cap with more electrodes allowing a more precise analysis with regard to the sensory-motor areas.

It could be interesting to test in further studies to test the same hypothesis with stroke patients to see if similar results could be obtained. This population is often older [2] than the healthy participants included in our study. The elderly have more difficulties to perceive illusion of movement induced by tendon vibration [286] and we can expect a weaker illusion of movement felt with stroke patients because some of them will additionally present cognitive troubles such as attentional ones or sensitive disorders. The current literature [306, 307] remains unclear about the effectiveness of central integration of peripheral vibrations in this population.

BCI studies can use MI as a substrate, and there is an wide literature on the haptic feedback used [308]. Vibration-type haptic feedback can give artefacts of signal interpretation and it is necessary to understand how to give this feedback for more effective results and to make the difference between cortical activity from vibration and from MI in the BCI system..

In conclusion, it seems that there is a synergistic effect between MI and visuo-proprioceptive stimulation, although this cannot be showed in this study. The use of these both tools could maximise motor cortical activations and be used in BCI systems. Further studies would be needed to confirm this conclusion. Overall, our results pave the way to the design of

new tools in rehabilitation using VR associated with brain computer interface and haptic stimulation.

3.4 Conclusion

In this chapter we have conducted two studies, the first on the design of a visuo-haptic feedback and the second on the effect of this novel visuo-haptic feedback on EEG acquisition. Theses two studies demonstrated firstly that virtual visual cues congruent to the illusion of expected movement enhanced the illusion of movement induced by tendon vibration and secondly that using MI and visuo-proprioceptive illusion rather than MI or visuo-proprioceptive illusion alone could increase cortical excitability in brain motor areas. These two studies are preliminary studies prior to the implementation of an NF study. This novel visuo-haptic feedback will be used in a fMRI-NF study presented in the next chapter.

Study of Proprioceptive Haptic Feedback for fMRI-based Neurofeedback

4

Preamble: *This chapters presents the results of the first fMRI-Neurofeedback study that uses a visuo-haptic feedback. The aim of this study is to compare the NF performance between unisensory and multisensory feedback. To do this we compare three conditions: visual alone, haptic alone or the combination of both (visuo-haptic). The visuo-haptic feedback is design-based on the results of the previous chapter: the haptic feedback is delivered through a pneumatic vibrator which is MR-compatible and the visual feedback is a virtual hand.*

Contributor: *This work was conducted with Pauline Cloarec (Master Student in Radiology)*

4.1 Introduction

As the fMRI-NF is still in its early days, there are many open questions about the optimal methodology. One of them concerns the feedback modality. Indeed, one of the cornerstones of NF and BCI is the feedback given to the subject whom relies on it to regulate, learn and improve his or her mental strategy. However, to date, most fMRI-NF protocols have only relied on visual feedback [85, 186], and its use may seem questionable in some cases. As suggested by Stoeckel and colleagues, some people or population might benefit from haptic, auditory, virtual reality/immersion, or the combination of some of these modalities for NF [27, 309]. Although suggested, few studies have focused on the value of using other feedback modalities. This lack of studies is not apparent in the EEG-NF, where many studies used haptic as feedback modality [18, 153].

Even if visual feedback has been shown to be the type of sensory input that produces the best learning processes [106], there are arguments that would support haptic as a feedback modality. For example, visual feedback may not be suitable for individuals with impaired vision or during a mental motor imagery task, which requires great abstraction from the subject. In this case, a haptic feedback could seem more appropriate and more natural than visual feedback [104]. Besides, it has been suggested that providing haptic feedback could improve the sense of agency, a technology acceptance-related factor, in motor imagery (MI) BCI's [108]. Nevertheless, the combination of multiple types of feedback, referred to as multisensory feedback, is expected to provide enriched information [310]. However, to be efficient, feedback should not be too complex and should be provided in manageable pieces [311]. Perceptible gains from the use of different modalities are still little known, no studies have addressed the role of feedback in fMRI-NF.

Applications related to haptic-based BCI are multiple, such as rehabilitation and entertainment. The majority of the clinical papers focus on stroke rehabilitation, because haptic-based BCI/NF seems to be a promising way for motor rehabilitation, as this non-invasive

technique may contribute to closing the loop between brain and effect [308]. The haptic feedback presents 3 main advantages for motor rehabilitation : the production of a kinesthetic illusion, the strengthening of the sensorimotor loop, and a faster action than the visuomotor loop [312]. Moreover, there is frequently a visual handicap (homonymous lateral hemanopsy) linked to the location of the stroke with motor deficit in the upper limb. By providing immediate sensory feedback contingent upon the contraleteral brain activity, we hypothesised that reestablishing contingency between ipsilesional cortical activity related to planned or attempted execution of finger movements and proprioceptive (haptic) feedback, such feedback will strengthen the ipsilesional sensorimotor loop fostering neuroplasticity that facilitates motor recovery.

As already mentionned in Chapter 2, haptic systems are categorised into : tactile feedback and kinaesthetic feedback. However, many haptic systems suffer from problems related to MR-compatibility or are difficult to set up. Vibration stimulation seems to be a good starting point for the creation of MR-based feedback as many technologies allow its introduction into the MR environment (piezoelectric or air pressure devices). Moreover, vibratory stimulation is already used in various medical applications such as pain management or proprioceptive rehabilitation after a stroke [233, 234]. Its role is not only tactile but also proprioceptive because if applied under certain conditions (frequency of 60-100 Hz, tendon target)[112], it can create movement illusions also called kinaesthetic illusions by stimulating the brain motor areas [238].

The multisensory aspect of feedback seems to be a way to improve the design of NF studies. However, multisensoriality should not just be additive but coherent and synergistic. That is why the association of a virtual hand and the tendinous vibration on the wrist of this same hand seems to be an ecological tool for an MI task. It allows the user to perceive a vibration at the level of his hand (with potential hand movement illusion) while having a visual illusion. In this study, we used tendon vibration associated with a VR environment as a multisensory feedback with a twofold rational: firstly to obtain a potentiation of the illusion, and secondly because of the observation of a motor task playing a role in brain motor activations.

To the best of our knowledge, this is the first time an fMRI-NF study has introduced haptic feedback as well as visuo-haptic feedback. The current study aims therefore to expand this search area by (1) testing the feasibility of the use of haptic as a feedback for MI based fMRI-NF, (2) developing an ecological multisensory approach by combining both immersive visual feedback and haptic feedback, and finally by (3) evaluating the differences in performance between unisensory and multisensory feedback. This was achieved using a MR-compatible vibrotactile device as haptic feedback. We hypothesise that our approach could lead to (1,3) the creation of new, more immersive and environmentally friendly feedback, as well as helping subjects to regulate and learn NF through multisensory feedback (2).

4.2 Materials and Methods

4.2.1 Participants

15 healthy adult volunteers were involved in this study (5 women, $M = 27$, $SD = 3.26$). All healthy participants fulfilled the following inclusion criteria: aged between 18 and 80 years, no previous history of neurological illness (brain injury, brain surgery, epilepsy), right-handed. Exclusion criteria included left-handedness and vision impairments exceeding -3 to +3 diopters (when correction by contact lenses was not possible). We decided to choose right-handed volunteers because the majority of the population is right-handed.

4.2.2 MRI Acquisition

All MR images were acquired from a Siemens 3T scanner (MAGNETOM Prisma, Siemens Healthineeers, Erlangen, Deutschland) with 64-channel head coil. MRI data were acquired on the Neurinfo MRI research facility from the University of Rennes I.

Functional data is obtained with a T2*-weighted single-shot spin-echo EPI with the following parameters [313]: repetition time (TR) / echo time (TE) = 1000/30 ms, Field-Of-View (FOV) = 210 × 210 mm^2, 42 slices, voxel size = 2.5×2.5×3mm^3, matrix size = 105 × 105, flip angle = 65°, multiband acceleration factor 3. As a structural reference for the fMRI analysis, a high resolution 3D T1 MPRAGE sequence was acquired with the following parameters: TR/TI/TE = 1900/900/2.26 ms, GRAPPA 2, FOV = 256 × 256 mm2 and 176 slabs, voxel size = 1 × 1 × 1 mm^3, flip angle = 9°.

fMRI data were pre-processed online for motion correction, slice-timing correction and fMRI NF features were then computed in the NF control unit using a custom made script developed in Matlab 2017 and SPM12 (The Math-Works, Inc., Natick, Massachussets, United States).

4.2.3 Experiment Design

The overview experimental design is summarised in *Figure*4.1. All participants were engaged in one fMRI-NF session on one day. Each participant performed 3 training blocks, in which they received Visual (NF-V), Haptic (NF-H) and Visuo-Haptic (NF-VH) feedback, using a counterbalanced order across participants who were blinded to the order [314].

An oral information was given just before the session about motor imagery (MI), NF and movement illusion. Instructions for MI oriented the volunteers towards a kinesthetic MI, without mentioning a specific strategy. Participants were naive with respect to the purpose of the experiment.

A pneumatic vibrator was set on the flexor carpi tendon of the right hand (dominant hand) at the beginning of the session when the volunteer was lying in the MRI. It was maintained

on skin with velcro strip (Figure 4.1 *NF-H*). An important point is that the hand was in a resting position, and did not touch anything around.

The session consisted of five MI functional runs and an anatomical scan (T1 MPRAGE). Each functional run consisted of 8 blocks of rest (20 s) and tasks (20 s). During the 1st run, the participant did not receive any feedback (first no-feedback) but only instructions: *"Imagine moving your right hand"* for the task and a dark grey cross for the rest. During the runs 2 to 4, the various feedback on the activation level of the selected target region were given (feedback runs). After the training runs, participants were engaged in one last run in which again no feedback was given (last no-feedback). Randomised condition orders were equally balanced over all sessions of all participants.

At the end, each participant filled a post hoc questionnaire, gathering qualitative information about the different feedback. In the questionnaire, subjects had to express their degree of agreement about each affirmation by using a Likert-scale from 1 to 6 (1 = totally disagree, 6 totally agree).

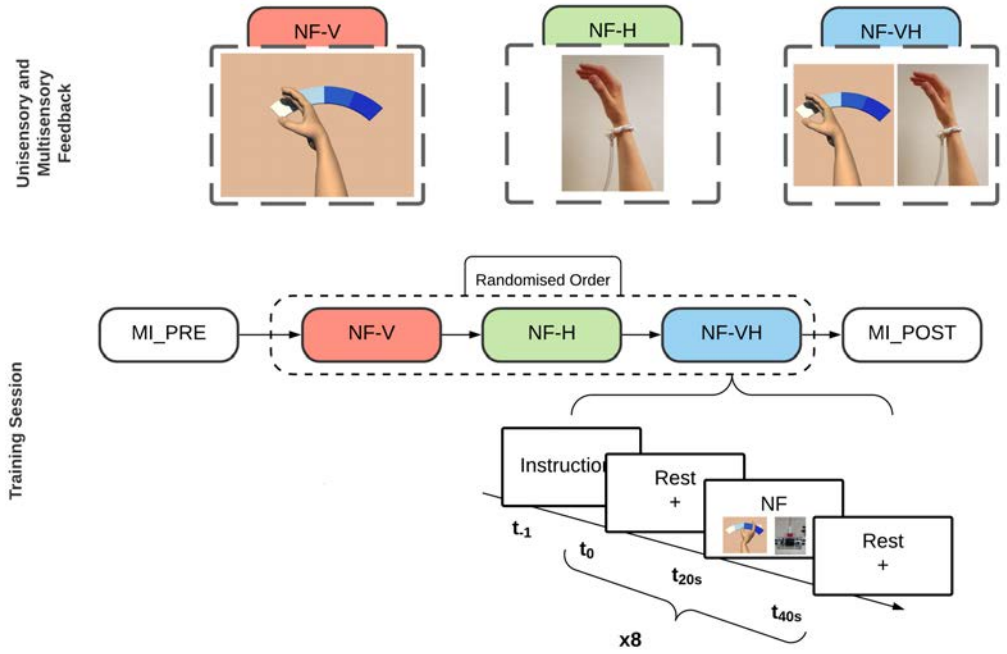

Figure 4.1: A schematic of the experimental protocol. The first row represents the feedback that will presented to the subject during the training runs, with NF-V is the visual feedback, NF-H the haptic feedback and NF-VH the multisensory feedback combining visual and haptic feedback. The second row represents the training session, it should be noted that the three NF runs are randomised for each subject in accordance with a Latin square.

4.2.4 Region-of-Interest (ROI) and Calibration

For the fMRI calibration and the definition of ROIs, data of the motor imagery session (no-feedback) were pre-processed for motion correction, slice-time correction, spatial

realignment with the structural scan and spatial smoothing (6 mm FHWM Gaussian kernel). A first-level general linear model (GLM) analysis was then performed. The corresponding activation map was used to define two ROIs around the maximum of activation in left M1 and left SMA. To this end, two large apriori masks were defined and the respective ROIs identified taking a box of 9 x 9 x 3 voxels (20 x 20 x 12 mm^3) centered around the peak of activation (thresholded T-map $task > rest, p < 0.001, k > 10$) inside the apriori masks. The position of the ROIs was validated by a clinician. A weighted sum of the BOLD activity in the two ROIs was then used to compute the fMRI NF (Section 4.2.5). Also for the fMRI NF, a threshold was set by estimating the value reached 30% of the time during the calibration session.

4.2.5 Real-time fMRI system and NF calculation

Real-time NF calculation, which has been described in detail here: [12], was performed by a dedicated computer (Intel Core I7, 16 GB RAM, Windows 10). The fMRI NF feature (following equation) was calculated as the difference between percentage signal changes in the two ROIs (SMA and M1) and a large deep background region whose activity is not correlated with the NF task (slice 3 out of 42), in order to reduce the impact of global signal changes (i.e., breathing, heart-rate changes and head movements; [53]). This feature was according to the following equation:

$$fMRI_{nf}(t) = \frac{B_{sma}(t)}{2 \times B_{sma}(prev - rest)} + \frac{B_{m1}(t)}{2 \times B_{m1}(prev - rest)} - \frac{B_{bg}(t)}{B_{bg}(prev - rest)},$$

B_{sma} is the average bold signal in the SMA ROI, B_{m1} in the M1 ROI and B_{bg} in the background slice. $B_x(prev - rest)$ is the ROI x baseline obtained by averaging the signal in the ROI x from the fourteenth to the nineteenth second (to account for the hemodynamic delay) of the previous rest block. The same weight is given to both ROIs. The fMRI feature was smoothed over the three last volumes, divided by the individual threshold and eventually translated as feedback every repetition time (1 s).

4.2.6 Set-up: Unisensory and Multisensory feedback

Visual Feedback

Visual feedback of the performed mental task was given to the participants by using Unity software (version 3.5), and the virtual scene was composed of a homemade neutral and white skin upper limb avatar (cf. 4.1 *NF-V*). The feedback was a right hand rendered from the point of view of the virtual avatar and moving along a coloured band on a blue scale.

The movement executed by the virtual hand was an extension of the right wrist which is congruent with the illusion of movement caused by the haptic feedback [289].

Haptic Feedback

MR-compatible Vibrator The haptic feedback is a tactile interface based on vibrotactile stimulation. Vibrations are delivered through a pneumatic vibrator which is MR-compatible. The body of the vibrator is a cylinder made of non-magnetic materials, and it contains a wind turbine to which an off-centered mass is attached. The rotation of the off-centered mass generates tangential vibrations transmitted to the vibrator body. The vibration frequency and amplitude depend on the angular velocity of the rotor, which is proportional to the air inflow. The device is controlled through a system placed outside the scanning room. The maximum frequency intensity of a pneumatic vibrator is dependent on the input air pressure. In our case, the system was capped at 4 bar, which allows a maximum frequency of 60Hz.

Semi-continuous feedback The vibration frequency of the pneumatic vibrator was used as feedback, frequencies were allocated to map the whole range of NF scores. The vibration was delivered continuously and in order to ensure that the user could perceive the frequency changes. The frequency was selected according to the *just noticeable difference* of the vibrotactile perception (20% between each frequencies) [315]. Four frequency steps were then allocated as follows:

$$Nf_{scores} = \begin{cases} [0, 40[& f = 0\,\text{Hz} \\ [40, 60[& f = 30\,\text{Hz} \\ [60, 80[& f = 50\,\text{Hz} \\ \geq 80 & f = 60\,\text{Hz} \end{cases}$$

In order to avoid getting occurrences of BOLD reactions in motor cortex and to reward MI task above all. The vibration frequency is 0Hz up to 40% NF scores. The interest is that the subject must be fully engaged in the task before receiving the feedback.

Visuo-Haptic feedback

The visuo-haptic feedback is the combination of the visual and haptic feedback respectively. Visual feedback being a representation of the illusion of movement induced by haptic feedback. Hence, if the virtual hand moves towards the dark blue area, the vibration will be greater and thus the illusion of movement will be intense.

4.2.7 Offline Data Analysis

Functional MRI Preprocessing

Structural and functional MRI data were pre-processed and analysed with AutoMRI, a proprietary software using SPM12 and Matlab. The structural 3D T1 images was segmented into tissue class images (grey and white matter, cerebrospinal fluid compartments, soft tissue, bone and others) and normalised to the Montreal Neurological Institute (MNI) template space. The preprocessing of fMRI included successively a slice-timing correction, a motion correction, a coregistration to the 3D T1 and a spatial normalisation to the MNI space, followed by a spatial smoothing with a 6-mm FWHM Gaussian kernel.

First-Level Analysis

For the first-level GLM analysis, the regulation blocks were modeled as boxcar functions convolved with the canonical hemodynamic function of SPM12. In the GLM, the six parameters of movement (translation and rotation) were included as covariates of no interest. For each run of each participant, a positive contrast between NF regulation and baseline (rest) blocks was applied.

Whole-brain Analysis

To investigate common de-/activations across participants, second-level whole-brain GLM analysis included one-sample t-tests for the first and last training runs and for the first and last no-feedback runs. Contrast images were thresholded at $p < 0.001$ and a family-wise error correction for multiple comparisons was performed using Monte Carlo based simulations to calculate cluster sizes that lead to an overall corrected significance level of $p < 0.01$. Group-level images were visualised in a sliced brain using Nilearn (`http://nilearn.github.io/`).

Offline ROI Analysis

Average contrast values of each ROI were extracted using MarsBaR (`http://marsbar.sourceforge.net` ; [316]).

Statistical Analysis

For each feedback (NF-VH, NF-V, NF-H), we conducted non-parametric Wilcoxon signed-rank tests (signrank Matlab function) between NF and the no-feedback condition with Bonferroni correction (corrected p-value threshold: 0.05 /2 conditions = 0.025). For between group comparison we computed a Wilcoxon test (ranksum Matlab function, equivalent to Mann-Whitney U-test) on NF.

Questionnaires

All data were analysed by statistical tests using Jamoji 1.1.9.0 and RStudio. Qualitative variables are represented with numbers and percentages, and quantitative variables are represented with means (standard deviations). A within-group analysis comparing the 3 conditions have been performed using Friedman tests (the non-parametric approach was used because N is relatively small).

All obtained results (except by individual-level whole-brain maps) and scripts used for the data analysis are available on the public GitHub repository: `https://github.com/MathisFleury/fMRI_NF_Multisensory.git`. A checklist summary of the consensus on the reporting and experimental design of clinical and cognitive-behavioural neurofeedback studies (CRED-NF) was included as supplementary material.

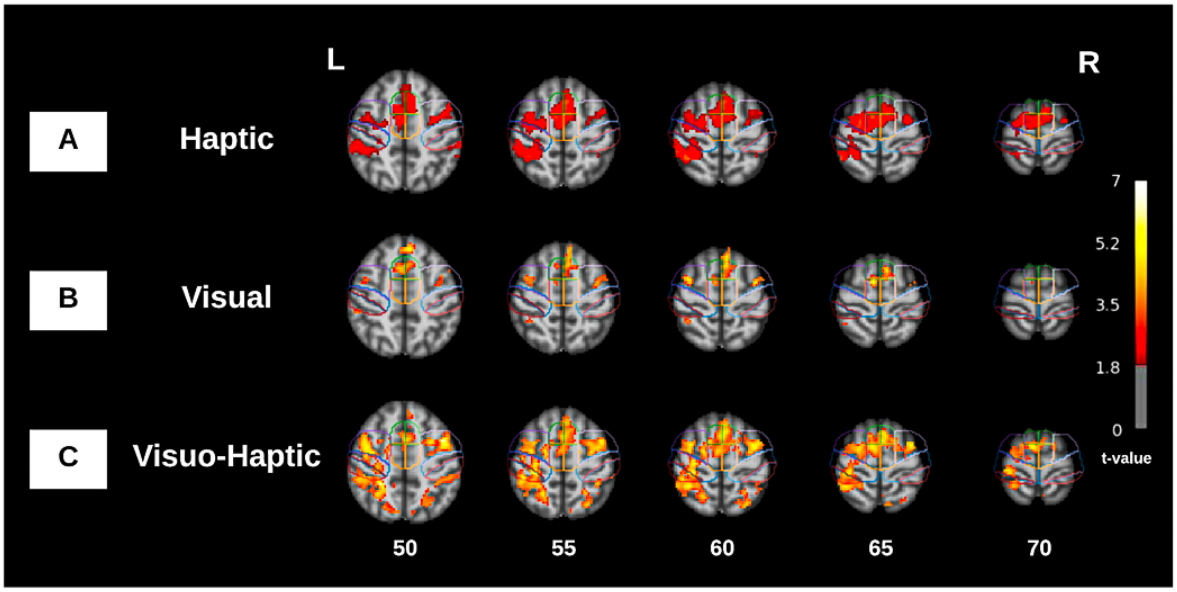

Figure 4.2: Group activation maps of the training runs in MNI coordinates ($p < 0.001$, uncorrected). The outline of the motor areas of interest based on the HMAT atlas is indicated: preSMA (green) SMA (orange), PMC (purple), M1 (blue) and Sensory motor cortex (red).

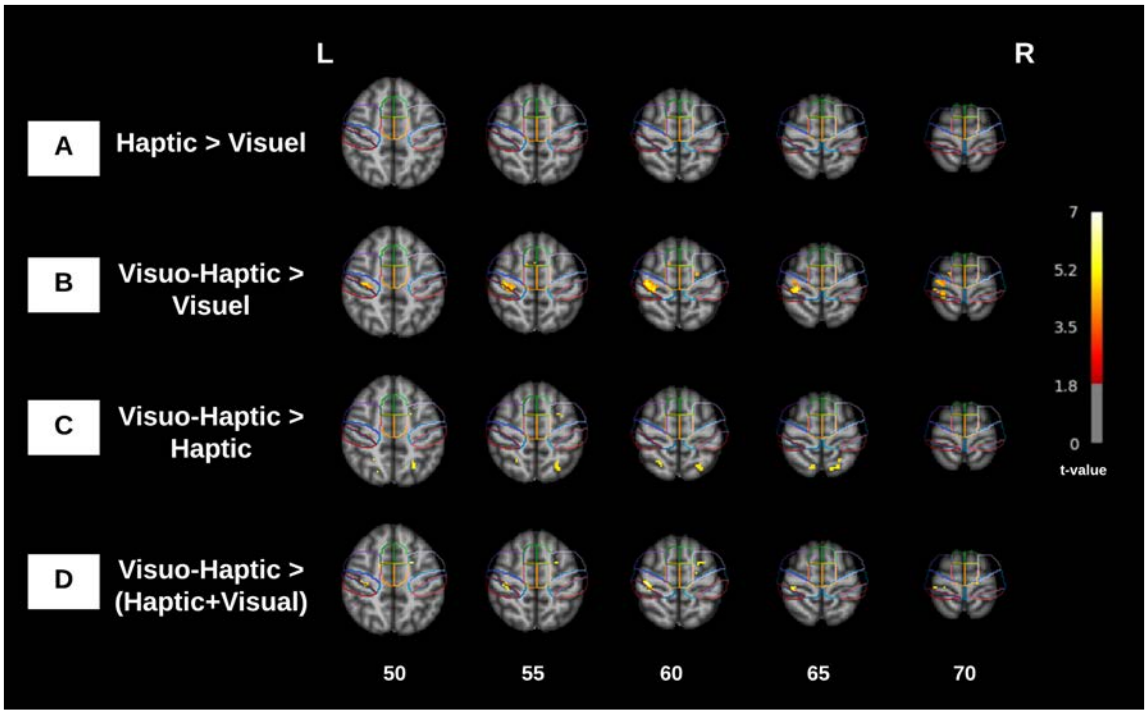

Figure 4.3: Group activation maps of the training runs in MNI coordinates ($p < 0.001$, uncorrected). The outline of the motor areas of interest based on the HMAT atlas is indicated: preSMA (green) SMA (orange), PMC (purple), M1 (blue) and Sensory motor cortex (red)

4.3 Results

The following section shows a comparative analysis between visual, haptic and visuo-haptic session in terms of NF performance and fMRI ROI analysis.

4.3.1 Excluded participants

Two participants were excluded from the offline analysis : a wrong NF score was presented to the subject during the whole session after the calibration step. For the first excluded participant, the activation during the first no-feedback run in his left visual area was higher than in left M1. This visual area was unfortunately included in the mask around left M1 and was recognised as the ROI. The NF score was consequently calculated on visual area and not on M1 area.

For the other excluded participant, there was no activation in left SMA during the first no feedback run. The NF score was only determined on the activation in M1 ROI, i.e. the NF score could not go beyond 50% anyway.

4.3.2 NF Performance

In the offline data analysis, we found a significant difference ($p < 0.001$) in activation in the left M1 ROI between rest and task by studying all runs and all subjects together.

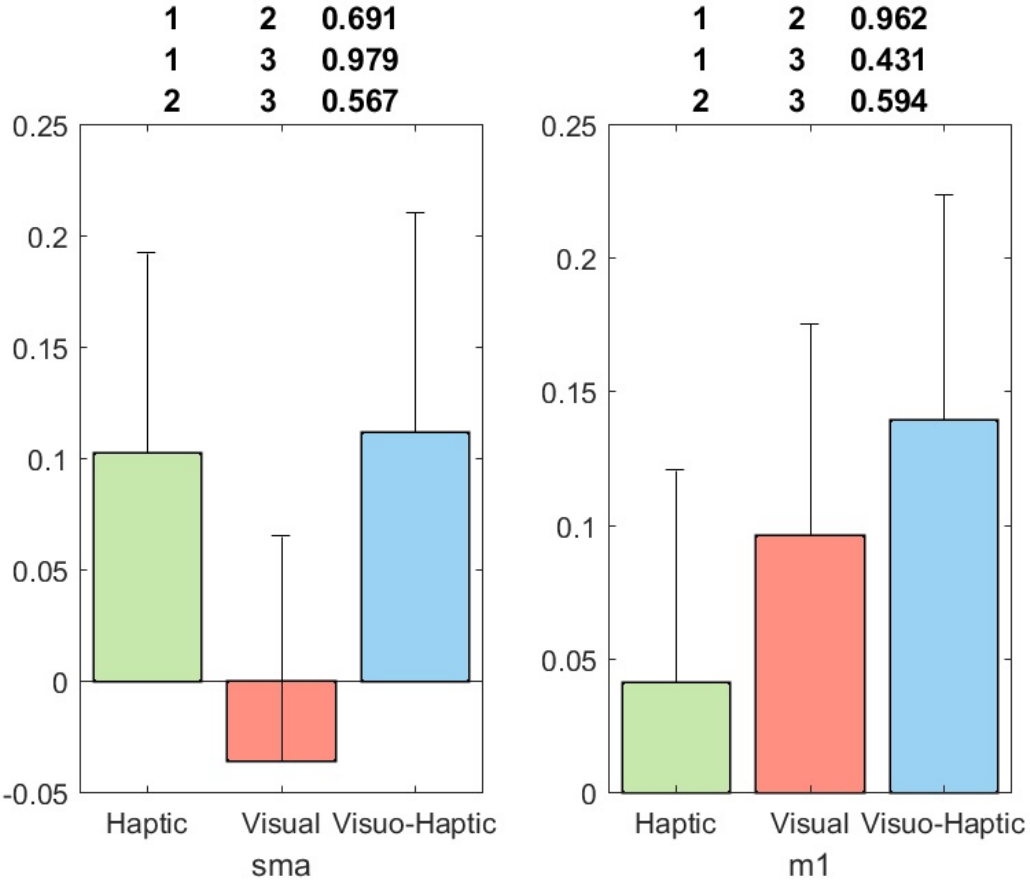

Figure 4.4: fMRI NF scores values (meanstandard error across subjects and NF runs) with relative statistics;*indicates statistically significant difference ($p < 0.01$) between rest and NF task as assessed with a Wilcoxon test across subjects.

Concerning the NF score of M1 and SMA during the three NF runs, the activity within SMA during the NF-H and NF-VH runs was significantly higher than NF-V ($p < 9,58e-10$, Kruskal-Wallis test) but no difference was found between NF-H and NF-VH ($p < 0,99$, Kruskal-Wallis test). The activity within M1 during NF-VH was significantly higher than NF-V ($p < 0,05$, Kruskal-Wallis test) and NF-H ($p < 1,72e-07$, Kruskal-Wallis test), NF-V is also significantly higher than NF-H ($p < 0.004$, Kruskal-Wallis test).

4.3.3 ROI analysis

When we studied the group activation maps of the training runs (with $p = 0.001$ uncorrected), it revealed common activation during the task (Figure 4.2 A,B,C). Concerning the NF-H run, we found significant activation in bilateral preSMA and SMA, in bilateral

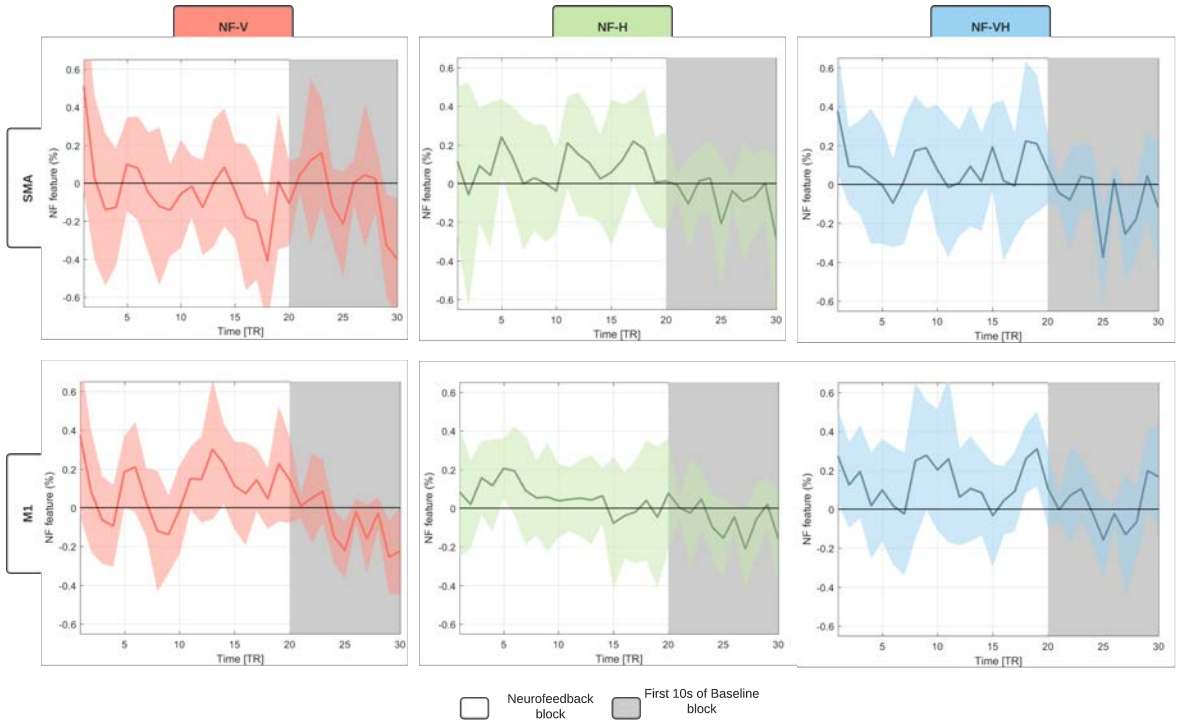

Figure 4.5: Average percent signal change (PSC) times courses in SMA or M1 for each feedback. Shaded areas represent the confidence interval (95%). The background colour represent the neurofeedback block (white) and part of the baseline block (dark grey).

PMC and in left sensory motor cortex, and left M1, with a T-value between 1.8 and 3.5. During the NF-V run, we found significant activation in bilateral preSMA, bilateral PMC and left SMA. The extent of significant activation was more restricted than the haptic feedback run but with a higher T-value (between 3.5 and 5.2) (Figure 4.2B). Finally during the NF-VH run, we found significant activation in bilateral preSMA and SMA (with a left-predominance for SMA), bilateral PMC, and left M1 and Sensory motor cortex. In this run, the significant activation was more extensive, with a T value between 3.5 and 5.2 (Figure 4.2C).

When we studied the group activation maps of the contrast between training runs (with $p = 0.001$ uncorrected) (Figure 4.3), the contrast between haptic and visual did not reveal any significant activation (Figure 4.3A). The contrast between VH and V showed significant activation in the left M1 (Figure 4.3B). The contrast between VH and H revealed activation in the parietal lobe (Figure 4.3C).

4.3.4 Learning the voluntary control of M1 and SMA

When we focused on M1 and SMA, the two regions of interest in the perspective of reeducation, we found an activation in bilateral SMA during the three run (NF-H, NF-V and NF-VH) and in left M1 only during NF-VH run (Figure 4.2). When we compared the different feedback (thanks to the contrast created by the difference of activation between

two runs), we found a significant activation in left M1 on the contrast VH-V (Figure 4.3B). ROI time courses locked to the onset of neurofeedback training illustrates the activity between each run (Figure 4.5).

4.3.5 Mental strategies underlying self-regulation and questionnaires

Among 15 participants, 12 were naive about MI (80 %). We reported the different mental strategies underlying self-regulation : 10 reported having performed a kinesthetic MI (66,7 %). Some reported strategies were opening a door lock with a key, tapping, rotating flexing or extending the wrist.

Concerning the visual feedback, the participants reported a weak appropriation of the virtual hand (Mean = 2.64, DS = 2). The frequently proposed modification for better appropriation was a gesture modification of the hand.

Concerning the haptic feedback, the participants did not report any discomfort with the vibrator. Especially on the affirmation *"the sensation of vibration becomes uncomfortable"*, they did not agree with a mean (SD) likert ranking at 1,53 (1.41). Some participants reported however a transient feeling of paresthesia on their wrist and/or their hand, without any need to stop the experiment.

Concerning the visuo-haptic feedback, they did not agree with the affirmation *"I found the association of two information too difficult to integrate"* with a mean (SD) likert ranking at 2.53 (1.77). Subjects reported to have paid more attention to haptic feedback for 33.3% (N=5), to visual feedback for 13.3% (N=2) and for visuo-haptic feedback for 53.3% (N=8). The degree of agreement about the affirmation *"I found the multisensorial feedback more natural than unisensory feedback"* was equal to a mean (SD) likert ranking at 3.87 (1.60).

Finally, there was no statistical difference between the 3 feedbacks to perform in MI (x2 = 1.32 p =0.517) or concerning the feedback's reliability during the MI (x2 = 2.21 p =0.074). But to improve the performance of the MI in further experimentation, the most useful feedback among the subjects would be VH for N=9 (60), H for N= 5 (33.3), and V for N = 1 (3.7).

4.4 Discussion

In this work we proposed the use of a multisensory feedback based on visual and haptic as a semi-continuous feedback for MI-NF. We investigated its contribution in terms of NF performance and ROI analysis. In order to obtain this multisensory feedback that is congruent with the MI-task, the kinaesthetic feedback was delivered to the subjects coupled with the visual feedback of a virtual arm. The novelty of this approach lies in the creation of continuous MR-compatible haptic feedback, that is provided accordingly to the subject's MI performance.

The choice of the region-of-interest (ROI) is quite important from the perspective of motor rehabilitation. Kinaesthetic motor imagery seems to be able to activate the same neural networks as real movements in functional imagery [260]. While the primary motor cortex (M1), which directly controls the execution of the movement, has been suggested to be the most promising target for an efficient motor recovery [317], supplementary motor area (SMA), which coordinates and plans the movement, seems to be easier to engage during motor imagery [85] and more robust than M1.

Subjectively, participants tend to the multisensory feedback : 60 % will choose the multisensory feedback to improve their performance in MI-NF in further experimentation. The NF scores and ROI analysis support this trend to the multisensory. We found a significant higher activation in left M1 on the contrast VH-V.

In a future study it would be interesting to increase the power of vibration in order to obtain more intense illusions of movements, because technical limitations only allowed us to deliver a frequency of 60Hz, which is barely sufficient to deliver an illusion of movement, hence the fact that few subjects ($N = 2$) reported having one. It should also be noted that the statistics should be taken with caution as the number of subjects in this study is low ($N = 15$), which is relative given the purpose of the experiment and the cost of acquiring an MRI session.

It could be interesting to test in further studies the same hypothesis with stroke patients to see if similar results could be obtained. This population is often older [318] than the healthy participants included in our study. We know that the elderly have more difficulties to perceive illusion of movement induced by tendon vibration [319] and we can expect a weaker illusion of movement felt with stroke patients because some of them will additionally present cognitive troubles such as attentional ones or sensitive disorders. The current literature [287, 288] remains unclear about the effectiveness of central integration of peripheral vibrations in this population.

4.5 Conclusion

In this chapter, we evaluated the performance of our novel visuo-haptic feedback for fMRI-NF with a MI task on 15 participants. We compared three conditions: visual alone, haptic alone or the combination of both. The haptic feedback is delivered through a pneumatic vibrator which is MR-compatible. For the visual feedback we used the same virtual hand as in Chapter 3, the movement executed by the virtual hand was an extension of the right wrist. We then compared the BOLD activations as well as the NF scores for the three conditions. The results showed that a visuo-haptic feedback could enable more intense activation of motor regions rather than visual or haptic alone.

Towards Multimodal Neurofeedback based on EEG-FMRI for Stroke Rehabilitation

Automated Electrodes Detection for multimodal EEG/fMRI Acquisition

5

Preamble: *The coupling of Electroencephalography and functional magnetic resonance imaging enables the measurement of brain activity at high spatial and temporal resolution. The localisation of EEG sources depends on several parameters including the knowledge of the position of the electrodes on the scalp. In this chapter we will describe a new automated method for detecting electrodes for bimodal EEG-fMRI that may be useful for NF.*

5.1 Introduction

As mentionned in Chapter 1, Electroencephalography (EEG) measures the electrical potential generated by the neuronal activity over the scalp with electrodes placed on the surface of the scalp [320–322]. Usually electrodes are placed thanks to a flexible cap and positioned according to anatomical points enabling optimal covering of brain regions regardless of the size and shape of the subject's head. Currently, when acquiring EEG and functional magnetic resonance imaging (fMRI) simultaneously, the position of the electrodes is calculated according to fiducial points (anatomical points of the skull) such as inion, nasion and vertex [323]. The localisation of EEG sources in the brain depends on several parameters including the position of the electrodes on the scalp. A precise knowledge of these positions is important because inaccurate information on EEG electrodes coordinates may affect EEG inverse solution [324]. This knowledge is even more crucial in the case of simultaneous EEG and fMRI study, when the sessions are conducted repeatedly over a long period of time. Approximations in the positioning of the electrodes are then made in each session and will give rise to important inaccuracies in the measured evoked potential [325]. As a matter of fact, magnetic resonance (MR) images and EEG need to be registered to be able to compare activations given by fMRI and by EEG. This simultaneous acquisition allows the concordance of two different kind of information, a high temporal resolution in the order of a millisecond with EEG, and a high spatial resolution in the order of millimetre with MRI.

In this chapter an automated and efficient method to determine EEG electrodes positions based on a specific MR sequence is presented and evaluated. Compared to other existing approaches, the proposed method does not need additional hardware (like 3D electromagnetic digitizer devices [326, 327], artificial electrode markers [328] or laser scanner [329, 330], which might be uncomfortable for the subject if he must stay still during acquisition [331] and add time to the preparation of the patient. Semi-automated electrodes localisation methods exist [332, 333], which require a manual fiducial landmark identification to guide co-registration without any markers but these approach relies on the efficiency of the accuracy of the operator. Another automated method was recently developed and shown great results with an anatomical MR image [334], however, this method is only working

with a high density cap also compatible with MRI: the GES 300 from Geodesic EEG Systems. Since this kind of cap includes plastic around electrodes and contain hydrogen protons, it can be visible on T1-w image. For seek of genericity (i.e. able to operate on all types of caps when artefacts do not appear on T1-w images), we propose to make use of a MR sequence with radial k-space sampling named UTE for Ultra-short Echo-Time. It allows to visualise the tissues with a very short T2 and T2*, such as cortical bone, tendons and ligaments [335, 336]. This sequence is all the more interesting in our context because it enables the visualisation of the MR compatible electrodes [333, 337] on the scalp with a capability to be performed rapidly enough to not overwhelm the whole MRI protocol.

This chapter proposes a fully automated method, which provides reliable and reproducible results for the detection and labelling of a MR compatible EEG cap into the MR space.

5.2 Methods

The retrieval of the electrodes consisted in two parts; firstly, we provided a mask that includes the volume where the electrodes are located; secondly, we performed the electrode detection inside this volume of interest (VOI). Figure 5.1 presents a flowchart of the method's main steps. We hypothesised that electrodes would appear as spheres inside the UTE volume and it allows us to perform a Hough transform in a consistent manner across subjects.

5.2.1 Scalp segmentation

Several reliable scalp segmentation methods exist for T1-w imaging. Because UTE images are noisier, we performed the scalp segmentation on the T1-w images and co-registered the UTE images with the T1-w images to apply the mask. The T1-w is first registered on the UTE and the anatomical T1 image is then segmented using FSL, an open-library of analysis tools for MRI and its function BET (Brain Extraction Tool) [338]. A mask of the scalp is computed from the segmentation. Since electrodes are located around the head of the subject, the scalp mask is dilated toward the periphery in order to isolate this layer. What is outside the dilated mask is subtracted in order to isolate only the layer where the electrodes are located.

5.2.2 Detection of electrodes with the Spherical Hough transform

A 3D Hough transform was used to segment the electrodes inside the VOI. Hough transform is typically used to detect circles or lines in 2-dimensional data sets, but was recently extended to detect spheres in 3-dimensional data sets [339, 340]. As the shape of an electrode can be assimilated to a sphere, the Spherical Hough Transformation algorithm seemed particularly well adapted to this task. The VOI image is first smoothed using a Gaussian kernel, with a FWHM (Full Width at Half Maximum) adapted to the size of

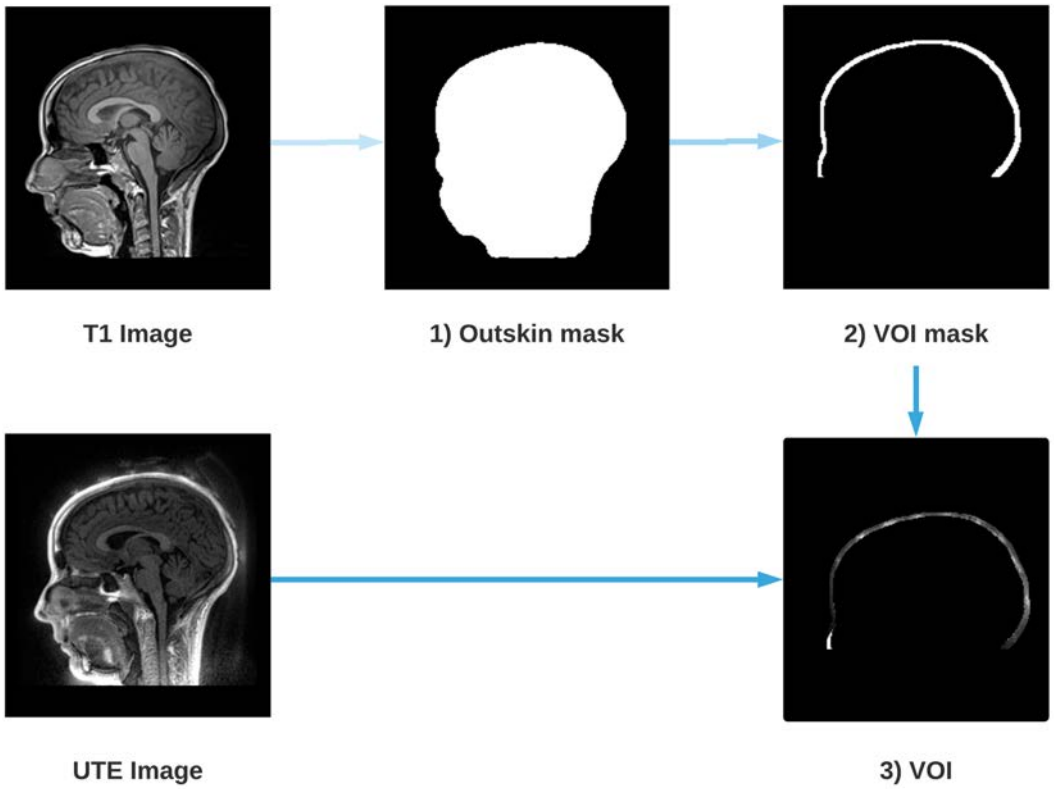

Figure 5.1: Steps for the extraction of the Volume Of Interest (VOI). An outskin mask is performed from the T1 image (1), then a dilation and a removal of the mask is performed (2) in order to obtain the layer where the electrodes are located. Finally, the UTE image is masked by the dilated mask (2) which gives us the VOI (3).

the electrode (10 mm) in order to reduce the noise of the image while saving electrode information. Then, the Hough algorithm is performed and provides a list of n potential electrodes, $D = [d_1, \ldots, d_n]$. Figure 5.2 shows an example of such detections on a 2D slice of the VOI. Because the VOI includes also anatomical structures (nose, ears) and noise (artefacts due to the cap or gel), the number of potentially detected electrodes is substantially higher than the number of "true" electrodes N, in our case 64.

5.2.3 Selection of detected electrodes

The detected electrodes are then filtered to get rid of the potential false detections given by the Hough transform. A 64 electrodes spherical EEG template p_j $(1 \leq j \leq 64) \in P$ was given by the cap manufacturer, indicating theoretical positions of every electrodes relatively to each other. Due to the non-sphericity of the head and the elastic deformations of the cap, these positions are not sufficient enough to give a reliable detection by itself. However, this template will be used to identify outliers in our detections. This spherical template is registered onto the detected electrodes from previous section, through the Iterative Closest

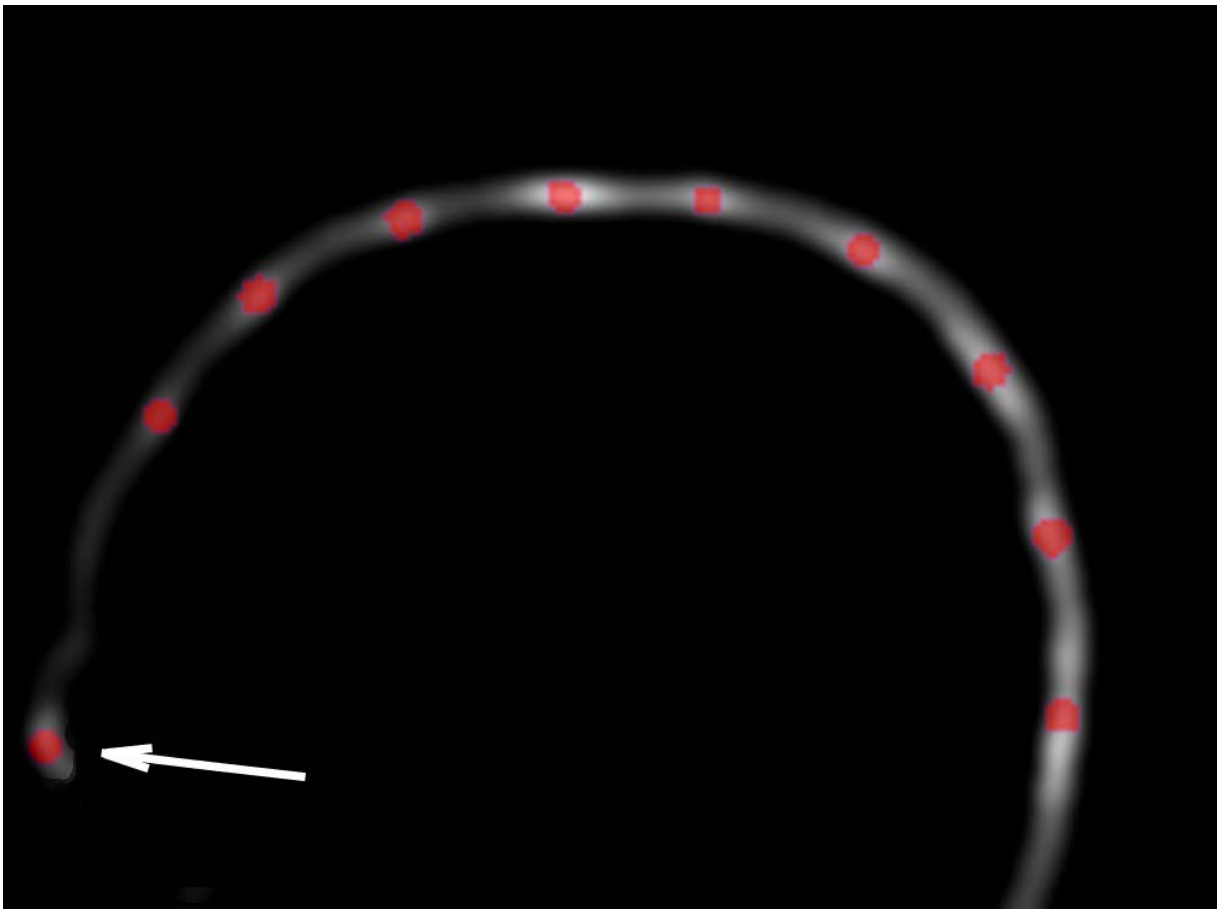

Figure 5.2: Example of Hough transform detection (red dots) on the VOI smoothed image. Hough transform detects also anatomical parts (arrow), which will be excluded in the filtering steps (cf. section 5.2.3.

Point (ICP) algorithm, a well-known algorithm for registering two-cloud of points [341, 342]. The algorithm takes a first point cloud which will be kept fixed, while the other one will be spatially transformed in order to best align the reference. The goal is to iteratively minimise a metric error, usually the distance between the two sets of points, by modifying the transformation applied to the source.

In our case, the ICP will find the optimal rotation, translation and scale to fit the data point set D obtained with the Hough transform and the model point P. The algorithm is divided into 2 steps. The first step consists in estimating correspondences between the two set of points. During this step, for each point p_j, in the reference set P, the closest point d_i of the detected points set D is computed. This point will be noted c_j and therefore defined as follows:

$$c_j = \underset{d_1,\ldots,d_n}{\arg\min}\, \mathrm{dist}(d_i, p_j), \quad \forall j \in [1, \ldots, N]. \tag{5.1}$$

The second step consists in computing the similarity transform that best aligns every c_j to

the corresponding p_j. The minimisation is expressed by:

$$(R^*, S^*, t^*) = \underset{R,S,t}{\arg\min} \sum_{j\in[1,\dots,N]} \|c_j - SR\,p_j - t\|^2, \tag{5.2}$$

where R is a rotation matrix (3×3), t is a translation vector (3×1) and S is a scale matrix ($S = s * Id,\ 3 \times 3$). The ICP runs until convergence. The registered template $P^{'}$ can then be written as:

$$p_j^{'} = SR\,p_j + t. \tag{5.3}$$

Once the ICP is completed, a two-part filtering phase is implemented. The first one consists in taking the closest point of the Hough transform data set; for each of the N electrodes of the registered model P', the closest detected point c_j is selected. Unselected points are discarded and, after this first filtering step, the number of electrodes is therefore equal to N, the total number of electrodes desired (64 in our case). Figure 5.3 illustrates the impact of this step.

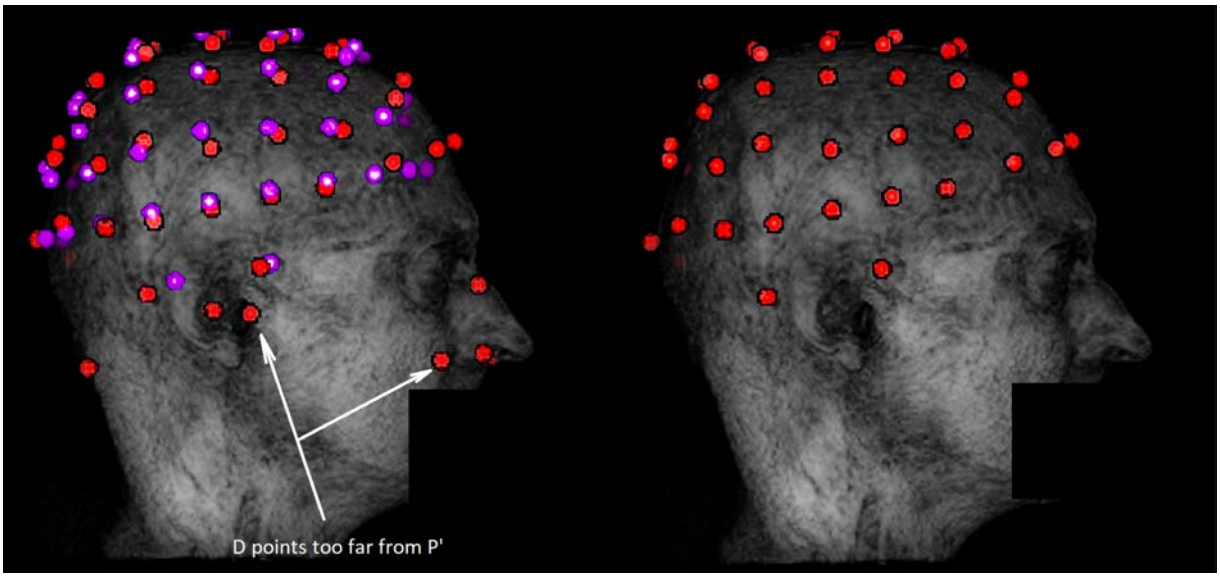

Figure 5.3: Example of outliers removal in potential electrodes data set D with the ICP algorithm. The dataset D is represented in red on the left along with the registered template P' in purple. The data set obtained after the first filtering step is in red on the right. Outliers are mostly due to external anatomical parts or noise not taken in account during the segmentation. These outliers are discarded by the filtering step because they are too far from P'.

For the second and final step, all points c_j, which are too far from the closest point of the template $P^{'}$, are removed. A threshold equals to four times the Median Absolute Deviation (MAD) of all distances is applied. For each removed point, a replacement is determined by a new detection from the local maxima on the VOI image around the theoretical position given by the registered template (cf. Figure 5.4). The new data set D' is obtained and the N electrodes are then labeled using the template.

5.2.4 Validation of the method

A manual selection of the electrodes positions was done on the UTE sequence and the quality of our detection was assessed using this manual selection as a ground truth. Instead of selecting the center of each electrode in a 3D image, we choose to use a more convenient procedure for the manual detection. Following [333], the manual detection was performed by picking up the Cartesian position (x_i, y_i, z_i) of each 64 electrodes for each subject on a pancake view, which is roughly a 2D projection of the scalp [332].

The performance indicators of our automated detection will be the position error (PE) and the positive predictive value (PPV). The position error is the average Euclidean distance between each pair of electrodes (the manually selected one, considered as the ground truth, and the detected one) and the PPV is the percentage of electrodes that have been well detected. We considered that a detected electrodes is well localised when the PE is below 10 mm, which corresponds to the diameter of the electrode [343].

We also compared the performance of our method against a more traditional semi-automatic one: five fiducial points were selected manually and the spherical template was adjusted to these points [344]. This method, although not recent, is still used by many studies (e.g. [345–347].

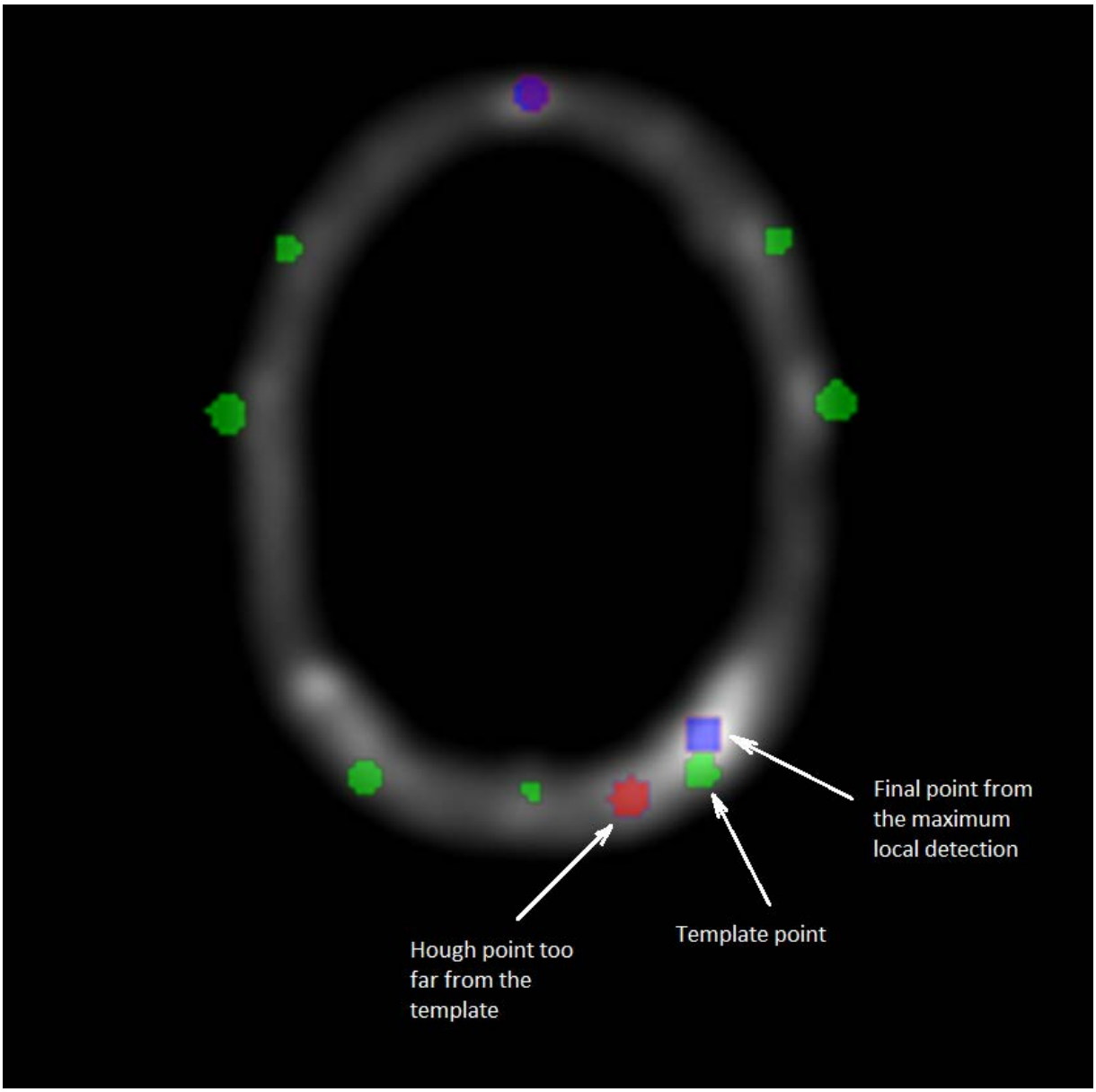

Figure 5.4: Cross section of the VOI image. Green points are corresponding to the template data set P', blue points to the maximum local detection and the red one are the outliers from D. The second and final filtering step consists in replacing any point from the Hough data set too far from the registered template P'. The substituted point comes from a detection by local maxima, closest to the template P'.

5.3 Materials

5.3.1 Subjects and EEG equipment

After IRB approval, eight healthy volunteers provided written informed consent to take part in the study. They all underwent a simultaneous EEG/fMRI examination (fully described in [62]. EEG was acquired using two 32-channel MR compatible amplifiers (actiCHamp, Brainproduct, Gilching, Germany) and a cap providing 64 Ag/AgCl electrodes positioned according to the extended 10-20 system and one additional ground electrode. Electrodes are attached to small cups with inner diameter of 10 mm and 4 mm height, inserted in the cap and filled with gel to minimise the contact impedance. All subject wore a large (circumference between 56-58 cm) MR compatible cap from Brainproduct (Gilching, Germany) and a particular attention was given to its positioning according to standard fiducial points.

5.3.2 UTE sequences parameters

All MR data were collected on a 3T Siemens Verio MR scanner (VB17, Siemens Healthineers, Erlangen, Germany). Specifically, the UTE sequence using 3D radial k-space sampling was performed with the following parameters: repetition time (TR) = 3.45 ms, echo time (TE) = 0.07 ms, flip angle (FA) = 14° and voxel size $1.33 \times 1.33 \times 1.33\,mm^3$. A 3D T1 MPRAGE was also performed: TR = 1900 ms, TI = 900 ms, TE = 2.26 ms, FA = 9° and voxel size $1 \times 1 \times 1\,mm^3$. Two additional UTE sequences with lower sampling resolution were acquired in order to decrease the acquisition time and to investigate the impact on electrodes detection. To reduce the acquisition time, the number of spokes has to decrease; from 60000 spokes (60K) for the original, to 30000 (30K) and 15000 (15K) spokes for the additional ones. The UTE acquisition time goes down from 5 min 35 s to 2 min 47 s and 1 min 23 s. A comparison between these acquisitions is shown in Figure 5.5.

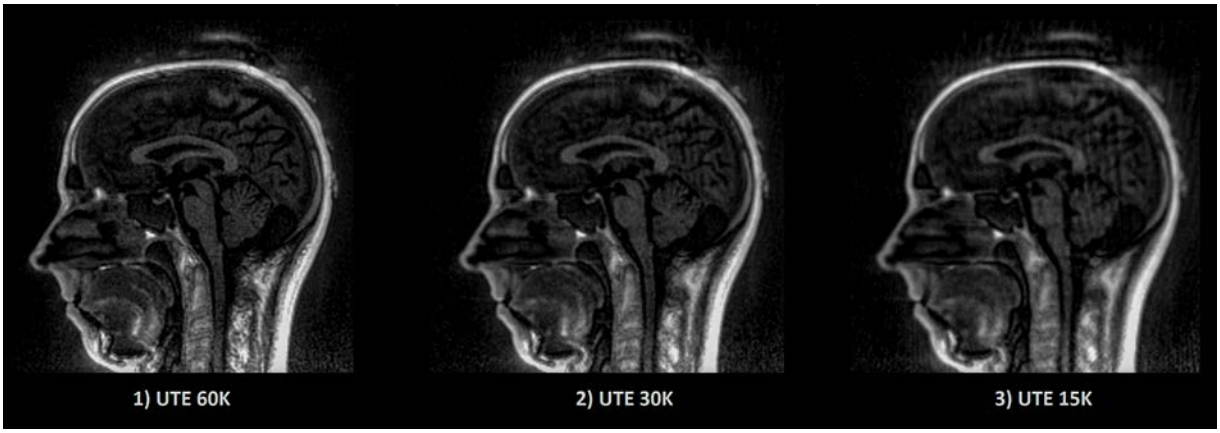

Figure 5.5: Example of UTE images with different sampling. The image quality as well as the acquisition time decrease linearly according to the sampling. Acquisition time for 1) 5 min 35 s, 2) 2 min 47 s, 3) 1 min 23 s.

5.4 Results

The creation of an image (VOI) containing only the information related to the electrode allows to remove external noise while protecting the information related to the electrode. This image enables robust detection of the position of the electrodes for all subjects. Furthermore, since our method always detects exactly N (64 in our case) electrodes, the number of false negatives (missed electrodes) will automatically be equal to the number of false positives (wrongly detected electrodes). Table 5.1 presents the mean position error (PE), the standard deviation of the PE and the maximum PE of our detections for each of the eight subjects. The max PE reflected a high difficulty to detect the electrodes near anatomical parts or in posterior regions where the head apply a pressure on the EEG cap inside the MRI. Our UTE-based electrode detection showed an average PE of 3.1 mm for all subjects. The detection accuracy, represented by the positive predictive value (PPV), is also shown and corresponds to the percentage of electrodes correctly found. The average PPV for all subjects was 94.22%.

Table 5.1: Position error (PE) and positive predictive value (PPV) for each subject (S1-S8) for UTE-MR electrodes detection. The PPV is the percentage of electrodes that have been detected. We consider that an electrode is well localised when the PE is below 10 mm, which represents the diameter of an electrode. The mean PE on all subject is equal to 3.1 mm and the mean PPV to 94.22%.

Subjects	Mean PE (mm)	Std PE (mm)	Max PE (mm)	PPV (%)
S1	2.73	2.83	17.32	95.38
S2	2.41	2.38	12.43	96.92
S3	2.66	2.43	13.62	95.38
S4	4.10	3.97	21.3	89.23
S5	3.32	3.38	14.45	90.7
S6	2.85	3.24	17.57	95.38
S7	2.76	2.51	15.90	96.92
S8	3.69	5.13	26.24	93.84

We then compared the performance of our method with the semi-automatic one presented in section 5.2.4 (FID). The PE and PPV were calculated in the same way. The results are shown in Table 5.2 and Figure 5.6 shows, for each subject, a comparison of the PEs obtained by the two methods. The mean PE on all subject is equal to 7.7 mm and the mean PPV to 79.41%. Moreover, for every subjects, our method produced smaller PE and better PPV. A paired t-test was computed between the two PEs sets and a significant difference was obtained ($p<0.0001$).

Finally, we investigated the impact of lower sample UTE sequences, which allow reducing the acquisition time, on electrode detection. We tested two others UTE sequence (cf. Section 5.3.2. We applied our detection method on the three different UTE images and compared the quality of the detections. Table 5.3 reports the mean PE and mean PPV obtained for the three UTE sequences on seven subjects (the first subject did not receive the additional sequences). As expected, the mislocalisation, as well as the position error, increase according to the decrease of the sampling. However, our results are still clearly

Table 5.2: Positive predictive value (PPV) and position error (PE) for each subject (S1-S8) for semi-automated electrodes detection based on manual delineation of fiducial landmark (FID). The PPV is the percentage of electrodes that have been detected. We consider that an electrode is well localised when the PE is below 10 mm, which represents the diameter of an electrode. The mean PE on all subject is equal to 7.7 mm and the mean PPV to 79.41%.

Subjects	Mean PE (mm)	Std PE (mm)	Max PE (mm)	PPV (%)
S1	7.60	3.09	15.31	76.92
S2	7.79	2.85	14.63	72.30
S3	6.15	2.71	13.45	90.76
S4	7.70	3.41	17.78	73.84
S5	6.08	2.78	16.36	90.76
S6	6.54	3.40	17.47	87.69
S7	6.88	3.39	17.10	87.69
S8	12.55	6.36	30.6	55.38

better than the semi-automatic one for the 30k sequence (half the acquisition time than the original one) and are slightly better for the fastest sequence.

Table 5.3: Mean of position error (PE) and mean positive predictive value (PPV) for three different sampling resolutions of the UTE sequence. Shorter acquisition time implied lower SNR and lower detection accuracy. Results are still better than the semi-automatic method.

	UTE 60K	UTE 30K	UTE 15K
Acquisition time	5 min 35 s	2 min 47 s	1 min 23 s
PE (mm)	3.12	4.02	6.56
PPV (%)	94.22	88.13	80.43

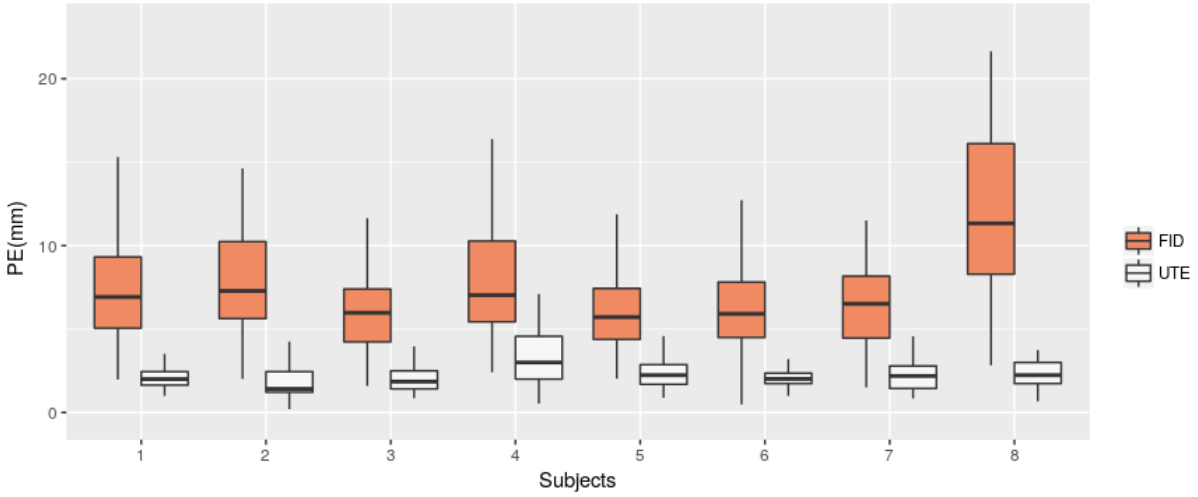

Figure 5.6: Position Error (PE) for UTE-based electrodes detection method (UTE) and the semi-automatic method based on fiducial points (FID). Box-plots for the eight subjects are shown.

5.5 Discussion

We have proposed an automated method for detecting and labelling EEG electrodes based on UTE MR images without using any external sensors. Previous results indicate that a localisation technique using electromagnetic digitisation technology is time-consuming [348] and others techniques such as 3D digitisation can be affected by errors of registration and projection of EEG electrodes on the head model. We have shown that our method offers constant and precise results. Moreover, the proposed method provides the position of the electrodes directly into the MR-space, which is crucial in case of simultaneous EEG/fMRI acquisitions.

Furthermore, for seek of genericity, the proposed method is able to operate on all types of caps and does not need specific electrodes, unlike a recent work from [334] for example. To the best of our knowledge, this is first automated electrodes detection method implying non-visible electrodes on anatomical MR sequence.

The method presented here requires only an additional sequence (the UTE acquisition sequence) without any additional equipement in the experimental protocol. This acquisition takes from 1 to 5 min. From our experiments, a good compromise between acquisition time and detection quality can be achieved with a 2 or 3 min sequences. Further optimisation of the sequence parameters could enable an improvement of the images without increasing the acquisition time.

5.6 Conclusion

We presented a method to automatically detect and label EEG electrodes during an EEG/fMRI acquisition. We used a UTE MR sequence to obtain electrodes positions on

a MR-volume. This method only has for additional cost the acquisition time of the UTE sequence in the MR protocol. We have demonstrated that our method achieves a significantly more accurate electrode detection compared to a semi-automatic detection one that is more commonly used during EEG/fMRI protocols. We believe that this method will be useful to improve the fusion of EEG and fMRI signals.

Multimodal EEG-fMRI Neurofeedback for Stroke Rehabilitation

6

Preambule: *In this chapter, we propose to test the feasibility of the multisession EEG-fMRI NF training in stroke patients, in view of designing a randomised controlled trial on chronic stroke patients involving a longer training protocol. Secondly, we aimed at testing if the multi-target bimodal strategy was implementable and efficient in guiding the patients towards the upregulation of the ipsilesional M1. The relation between NF training efficacy and the integrity of the ipsilesional corticospinal tract (CST) reconstructed from diffusion tensor imaging (DTI) imaging was also investigated. Finally, functional tests were performed in order to evaluate the potential for clinical improvement of multi-target, bimodal NF training.*

Contributors: *This work has been conducted in a team, especially with Giulia Lioi (PhD) and Simon Butet (MD-PhD)*

6.1 Introduction

Recent studies have revealed the potential of Neurofeedback (NF) training for Stroke rehabilitation [81], as an alternative or in aid to traditional therapies [5], to stimulate neural plasticity and support functional improvement [349]. These works have implemented unimodal EEG or fMRI NF. In this exploratory study, and for the first time in literature, multisession bimodal EEG-fMRI NF for upper limb motor recovery was tested in four stroke patients. The bimodal training sessions were alternated to unimodal EEG-only NF sessions, in order to guarantee a suitable cumulated training time to the patients. We expected that during bimodal EEG-fMRI NF training the patient, receiving richer and specific information, could develop a strategy and then "transfer" to unimodal EEG sessions, to reach a sufficient training intensity.

The choice of the cortical target of NF training has a critical impact on the rehabilitation outcome. If ipsilesional primary motor cortex (M1) has been suggested as the most promising target for an efficient motor recovery [317], supplementary motor area (SMA) may be easier to engage during motor imagery [85, 350] than M1 [84, 351, 352] and may have an important role to restore motor function in more severely affected patients [353, 354]. The second important novelty of this study is the definition of an adaptive, multi-target training that more strongly rewarded SMA activation in the first NF training session and then increased the M1 activation contribution in the final NF session. To this end, we defined an adaptive cortical region of interest (ROI) equal to a weighted combination of ipsilesional SMA and M1 activities and then varied the weights in order guide the patient training towards an improved activation of M1. In particular, while several studies have shown robust SMA activation during kinesthetic motor imagery, it is still unclear whether M1 can be consistently

activated. Some motor imagery studies reported significant activation [350], however, fMRI NF studies found non-conclusive results at group level [351, 352] and one recent study showed deactivation of M1 during kinesthetic motor imagery-based upregulation training of the SMA and M1 [85].M1 involvement may depend on the subject and the nature of performed motor imagery task and there is no evidence that it is consistently activated, at least in short training protocols [355]. On these premises, the second important novelty of this study is the definition of an adaptive, multi-target training that more strongly rewarded SMA activation in the first NF training session, yet increased the M1 contribution in later sessions. To this end, we defined an adaptive cortical region of interest (ROI) based on a weighted combination of ipsilesional SMA and M1 activities. We varied the weights across the training sessions in order to guide the patient training towards an improved activation of M1 and neighbouring ipsilesional motor areas.

The first aim of this pilot work was to test the feasibility of the multisession EEG-fMRI NF training in stroke patients, in view of designing a randomised controlled trial on chronic stroke patients involving a longer training protocol. Second, we aimed at testing if the multi-target bimodal strategy was implementable and efficient in guiding the patients towards the upregulation of the ipsilesional M1. The relation between NF training efficacy and the integrity of the ipsilesional corticospinal tract (CST) reconstructed from diffusion tensor imaging (DTI) imaging was also investigated. Finally, functional tests were performed in order to evaluate the potential for clinical improvement of multi-target, bimodal NF training.

6.2 Methods

6.2.1 Participants

Four chronic stroke patients (aged between 54 and 76 years, 2 females) with mild to severe left hemiparesis (Fugl-Meyer score in the range 14-50) and without major cognitive deficits participated to the study (Table 1). All participants gave their written informed consent and the study was approved by the institutional review board Poitiers III Ouest (NCT01677091).

Table 6.1: Patients' demographics, stroke characteristics, and clinical outcomes.

ID	Age	Time since stroke	Stroke type	FA asymmetry	FMA-UE		
					PRE	POST	Change
P01	62	5 years	Hemorrhagic-subcortical	0.105	14	14	0
P02	76	3 years	Ischemic-subcortical	0.0358	19	25	+6 (+31.5%)
P03	68	1 year	Hemorrhagic-subcortical	0.064	50	53	+3 (+6.0%)
P04	51	1 year	Ischemic-cortical	0.05	41	37	−4 (−9.7%)

6.2.2 NF training protocol

The experiments took place at the Neurinfo platform and in the Physical and Rehabilitation Medicine Department (CHU Rennes, France). The NF training protocol included two bimodal EEG-fMRI NF sessions interleaved with three unimodal EEG NF sessions (Figure 1) and a final motor assessment, within ten days from inclusion. Patients were informed at the inclusion, verbally and by an explanatory note, about the goals and the program of the study. Instructions were repeated before each training session. Concerning the instructions for mental imagery, we oriented the patients towards a technique of kinesthetic motor imagery, without mentioning a specific strategy. For each bimodal NF session, the protocol included a calibration step (motor imagery of hemiplegic hand) and three NF training runs (5 minutes 20 s each). Each NF run consisted of epochs of rest (20 s) alternated to period of closed-loop motor imagery training (20 s). Details about the protocol have been previously published by our group [12]. Similarly, the unimodal EEG NF sessions consisted in a calibration period followed by three NF runs with a block-design alternating rest and task during 5 minutes, with an amount of training time and protocol structure equivalent to bimodal training sessions.

6.2.3 Data acquisition and experimental setup

EEG and fMRI data were simultaneously acquired with a 64-channel MR-compatible EEG solution from Brain Products (Brain Products GmbH, Gilching, Germany) and a 3T Prisma Siemens scanner running VE11C with a 64-channel head coil. EEG data were sampled at 5kHz with FCz as the reference electrode and AFz as the ground electrode. fMRI acquisitions were performed using echo-planar imaging (EPI) with the following parameters: repetition time (TR) / echo time (TE) = 1000/23ms, FOV = 230 × 230mm2, 16 4mm-slices, voxel size = 2.2×2.2×4mm3, matrix size = 105 × 105, flip angle = 90°. During rest, the screen displayed a cross and participants were asked to concentrate on the cross and not on the task. During task, the screen showed the NF metaphor. The feedback was visual and consisted of a yellow ball moving in a one-dimensional gauge proportionally to the average of the EEG and the fMRI features (Figure 2). As a structural reference for the fMRI analysis, a high resolution 3D T1 MPRAGE sequence was acquired with the following parameters: TR/TI/TE = 1900/900/2.26 ms, GRAPPA 2, FOV = 256 × 256 mm2 and 176 slabs, voxel size = 1 × 1 × 1 mm3, flip angle = 9°. The EEG/fMRI-NF platform in place at Neurinfo integrates and synchronise EEG and fMRI data streams by means of a NF control unit [62]. EEG data were pre-processed on-line with BrainVision Recview software 2.1.2 (Brain Products GmbH, Gilching, Germany) for gradient and BCG artefact correction [356] and sent to the NF control unit for further processing. fMRI data were pre-processed online for motion correction and EEG and fMRI NF features were then computed in the NF control unit using a custom made script developed in Matlab 2017 and SPM8 (The Math-Works, Inc., Natick, Massachussets, United States) and translated as a visual feedback with Psychtoolbox 3 (`http://psychtoolbox.org/`).

6.2.4 Calibration

At the beginning of each experimental session, a motor imagery task without NF was performed to calibrate both fMRI and EEG signals. Immediately at the end of this motor imagery run, EEG and fMRI data were pre-processed and analysed to estimate subject-specific EEG and fMRI NF calibration features.

For the EEG calibration, only 18 channels located over the motor regions were selected for further analysis. The power in the 8–30 Hz frequency band was computed and a Common Spatial Pattern (CSP; [357]) filter was estimated. In cases where the CSP filter did not look physiologically plausible [visual inspection to check if the Event-Related Desynchronization (ERD) computed from filtered data was correlated with the task [263]], we used a laplacian filter over the ipsilesional motor electrode C4 (more details in [12]). An ERD feature was then computed from filtered data and the threshold for the EEG NF was set equal to the ERD value reached at least 30% of the time. The threshold was computed with the rationale of adapting the NF difficulty to individual performances for each session and make the training engaging.

For the fMRI calibration and the definition of ROIs, data of the motor imagery session were pre-processed for motion correction, slice-time correction, spatial realignment with the structural scan and spatial smoothing (6mm FHWM Gaussian kernel). A first level general linear model analysis modelling the task was then performed. The corresponding activation map was used to define two ROIs around the maximum of activation in the ipsilesional M1 and SMA respectively. To this end two apriori masks were defined (see Figure 2) and the respective ROIs identified taking a box of 9x9x3 voxels (20×20×12 mm3) centered around the peak of activation inside the apriori masks. A weighted sum of the BOLD activity in the two ROIs was then used to compute the fMRI NF (Figure 2). Also for the fMRI NF a threshold was set by estimating the value reached 30% of the time during the calibration session.

6.2.5 NF online calculation

Calibration parameters were estimated before the first NF training run for each training session in order to properly compute the NF features. NF calculation, which has been described in detail elsewhere [12], was performed on the two synchronised data streams (EEG and fMRI) in the NF control unit. EEG data were firstly filtered with the subject specific spatial filter selected during the calibration phase. The band power (BP) in the 8-30 Hz band was then computed and normalised with respect the power in the last 5 seconds of the previous rest block (prev-rest) with the following event related desynchronization (ERD) [263] formula:

EEG-NF values were smoothed, divided by the calibration threshold and normalised between 0 and 1 in order to return only positive values to the subject. The EEG feature was eventually translated as visual feedback (position along the gauge) every250 ms.

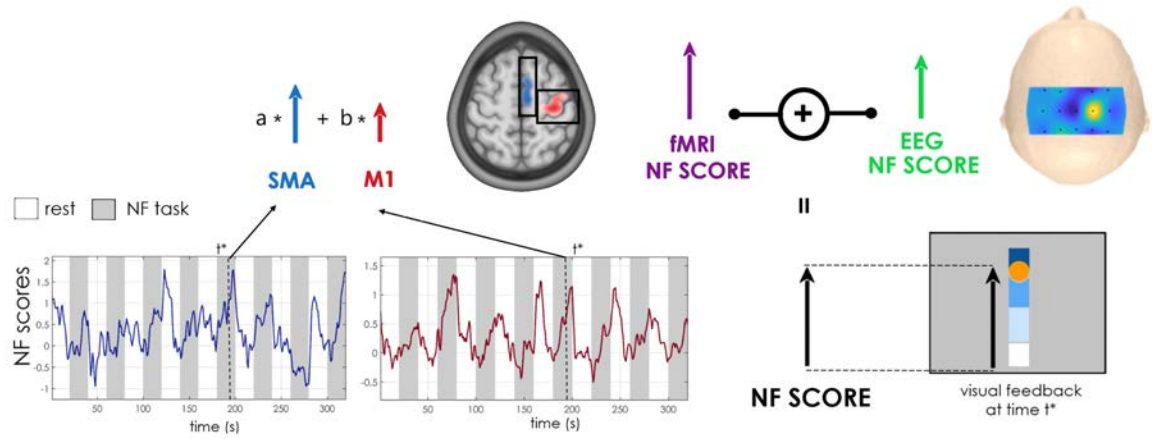

Figure 6.1: NF calculation schematic. The visual NF at time ∗ is equal to the average of EEG and fMRI NF scores, updated respectively every 250 ms and 1 s. The fMRI NF score, in turn, is equal to the weighted sum of blood-oxygen-level-dependent (BOLD) activations (contrast NF TASK > REST) in the supplementary motor area (SMA) and primary motor cortex (M1) regions of interest (ROIs) (in blue and red on a normalised anatomical scan, with calibration a priori masks in black). The weights assigned to the two contributions M1 and SMA vary from the first training session ($a = 0.5$,$b = 0.5$) to the second ($a = 0.25$,$b = 0.75$). The EEG score was obtained computing the Event Related Desynchronization (ERD) on a combination of electrodes given by Common Spatial Pattern (CSP) or Laplacian filter weights.

The fMRI NF feature (equation 2) was calculated as the difference between percentage signal change in the two ROIs (SMA and M1) and a large deep background region (slice 3 out of 16) whose activity is not correlated with the NF task, in order to reduce the impact of global signal changes (i.e., breathing, heart rate changes and head movements; [53]).

Bsmais the average bold signal in the SMA ROI, Bm1in the M1 ROI and Bbgin the background slice. During the 1st week,the same weight was given to both ROIs ($a = b = 0.5$) while in the second session a higher weight was assigned to the BOLD signal of the M1 ROI ($a = 0.25$,$b = 0.75$), in order to guide the training towards upregulation of the ipsilesional motor cortex. The fMRI feature was smoothed over the previous three volumes, divided by the individual threshold and eventually translated as visual feedback every repetition time (1 s). The total position of the ball on the gauge was at every instant equal to the mean between the EEG and fMRI NF features (Table 6.1).

6.3 Unimodal EEG-NF

We used the Mensia Modulo (Mensia Technologies) hardware solution to perform the unimodal EEG-NF sessions. Mensia Modulo is equipped with an 8-channel EEG cap that can be rapidly set up and is designed for a high number of training sessions. The patient received the visual feedback metaphor on a computer screen. The gauge was accompanied by a puzzle game that was completed less or more rapidly depending on the feedback score. Pre-processing included filtering and eye blink artefacts removal (details about the data pre-processing pipeline can be found in the patent US 2017/0311832). An analysis based on the covariance matrix of the ipsilesional motor channels EEG signals was then applied and

the ERD NF score was extracted based on the Riemannian distance [290] between motor imagery task and resting blocks.

6.3.1 Evaluation of Outcome Measures

Clinical Outcomes

Before and after the NF training protocol upper limb motor function was assessed by a certified physiotherapist by means of the Fugl-Meyer upper extremity test (FMA-UE; [358]), which evaluates motor activity skills and selectivity of the movement. The FMA-UE score ranges between 0 and66, with scores lower than 20 indicating severe deficit and scores higher than 48 associated with mild motor impairments [359]. Subjective ratings on motivation and satisfaction with NF protocol features (i.e., number and length of training sessions, NF metaphor) were evaluated with qualitative questionnaires, based on a 5-point Likert scale [360]. Additional comments mainly regarding the motor imagery strategy were noted too.

Assessment of Corticospinal Tract Integrity

The integrity of the CST is a well-established predictor of the potential for motor improvement [361]. In order to assess the asymmetry between the ipsilesional and contralesional CST, diffusion imaging (TR/TE = 11,000/99 ms, FOV 256×256 mm^2, 60 slices, matrix 128×128, voxel size, 2×2×2 mm^3, 30 directions,b= 1,000 s/mm^2) was performed at inclusion. The diffusion tensor model was estimated and the fractional anisotropy (FA) calculated. The CST was then reconstructed using the method of Lee et al. [362] using the software medInria3: After estimating the FA maps, two regions of interest were segmented to isolate the CST: the posterior limb of the upper internal capsule and the CST at the lower pons. FA asymmetry between the affected and unaffected CST was then calculated. FA is a measure of white matter fibbers integrity and a disruption of the structural fibers is associated with an FA decrease. An index of FA asymmetry = (FAcontralesional-FAipsilesional)/(FAcontralesional+FAipsilesional) gives therefore important indications about the structural deficit in the ipsilesional CST. Such an index ranges between -1.0 and +1.0, where positive values indicate reduced FA in the affected CST, and a value of 0 indicates symmetrical FA, i.e. preserved ipsilesional CST. In particular it has been shown that a FA asymmetry index value greater than 0.15 is a "point of no return," beyond which limited capacity for recovery is expected [361, 363].

6.3.2 fMRI and EEG outcomes

For each patient, in order to evaluate the effect of NF training on upregulation of BOLD activity, we assessed the difference between SMA and M1 NF scores in session b-s1 and b-s5 by means of a Wilcoxon test across NF runs. We also computed equivalent NF scores for a

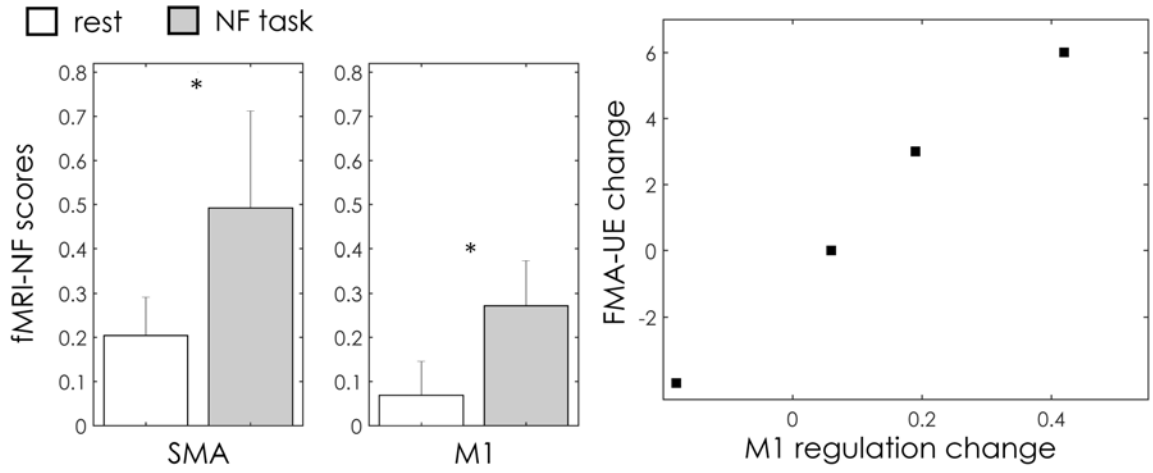

Figure 6.2: Group results. **(A)** fMRI NF scores values (meanstandard error across subjects and NF runs) with relative statistics; ∗ indicates statistically significant difference ($p < 0.01$) between rest and NF task as assessed with a Wilcoxon test across subjects. **(B)** Scatter plot relating change in the clinical outcome (FMA-UE score) and ipsilesional M1 BOLD regulation for the four patients.

"neutral" ROI, whose activity is not expected to be up regulate after the motor NF training. Using the Montreal Neurological Institute (MNI) atlas, a 9×9×3-voxel ROI around the peak of activation in the right medial superior frontal cortex was identified: NF scores were then computed applying the same algorithm as for SMA and M1.A whole-brain analysis was also performed to characterise cortical areas engaged during NF and describe the reorganisation of motor maps at the end of the protocol. Pre-processing (slice-time and motion correction, co-registration to the 3D T1, followed by spatial smoothing with a 6 mm FWHM Gaussian kernel and normalisation to MNI template) and a first-level general linear model analysis were performed. The activations maps were voxel-wise Family-Wise error (FWE) corrected ($p < 0.05$). Similarly, for the EEG analysis data were first pre-processed offline with a semi-automatic artefacts rejection procedure implemented in Brain Products Analyzer (version 2.1.1.327) and fieldtrip; data were then filtered between 8 and 30 Hz using a Butterworth zero-phase filter (48 dB slope). For each subject, mean NF scores per session and the ERD scalp distributions over motor channels were computed for both the bimodal and unimodal training sessions.

For additional details on the methodology of acquisition,processing and analysis of data, including toolbox and software used see Mano et al. [62]; Perronnet et al. [12, 86]. Data and materials are available upon request to interested researchers

6.4 Results

Overall, in all the patients motor imagery elicited activation,with respect to rest, in the SMA ($p = 0.004$, Wilcoxon test)and M1 ($p = 0.006$, Wilcoxon test) areas (Figure 3A). Two over four patients showed a significant increase in ipsilesional M1 activation (NF score) in the second training session as compared to the first one (Table 2). Interestingly these two also

Table 6.2: Multi-target fMRI control: individual results of blood-oxygen-level-dependent Neurofeedback (BOLD NF) scores (normalised percent signal change from baseline-rest)

ID	Ipsilesional M1 regulation			SMA regulation			Frontal Sup regulation
	s1	s5	Change	s1	s5	Change	Change
P01	0.10 + 0.25	0.16 + 0.31	+0.06	0.51 + 0.48	0.20 + 0.37	**−0.30**	−0.14
P02	0.23 + 0.37	0.65 + 0.42	**+0.42**	0.19 + 0.27	0.42 + 0.44	**+0.23**	**−0.18**
P03	0.18 + 0.27	0.37 + 0.36	**+0.19**	0.27 + 0.38	0.28 + 0.35	+0.01	−0.05
P04	0.30 + 0.33	0.23 + 0.33	−0.08	0.13 + 0.23	0.21 + 0.25	+0.07	0.05

improved their clinical FMA-UE score (Figure 3B). The fourth patient, on the other hand, significantly increased its activation in the SMA area, but decreased it in the ipsilesional M1, and showed a decrease in FMA-UE score. Changes in regulation of the "neutral" ROI in the frontal superior cortex were not significant or in contrast with the upregulation of the motor areas.Qualitative questionnaire results indicated that generally patients were highly motivated to engage in NF training and very interested by this type of reeducation, which they found complementary with traditional rehabilitation therapies. They were also satisfied with the visual feedback appearance and how it translated their motor imagery effort. Concerning the strategies employed by the patients to control the ball movement, they all used motor imagery of the affected limb. While some of the evoked simple and repetitive tasks (i.e., P01: thought of opening and closing the hand, P04: holding something with the hand),some others engaged in the imagery of a more complex task (P02: imagined hair combing, P03: ironing). Interestingly enough, these more elaborated strategies were also the most effective.

6.4.1 Individual Results

P01

The patient was a 62 years old male with right ischemic capsulo-lenticular lesion (Figure 4D) with important loss of ipsilesional CST integrity (Figure 4C) at the level of the posterior limb of the internal capsule (FA asymmetry index = 0,105). Time since stroke was 5 years and the initial FMA-UE score was14. This patient increased his NF score in the ipsilesional M1 in the second session as compared to the first one, but its activation was relatively weak (Figures 4A,B). The whole-brain analysis revealed a bilateral activation of M1 and SMA during the NF training (Figure 4E). Its EEG activation was bilateral too, and he showed a positive, relatively strong ERD across the three unimodal training sessions (Figure 4G). EEG acquired during the bimodal NF sessions was particularly noisy in session b-s1, and the ERD calculated over ipsilesional electrodes (C2, C4, C6) was negative. In the second session b-s5the average ERD was positive but relatively small (Figure 4F).No changes in the FMA-UE score were observed at the end of the training.

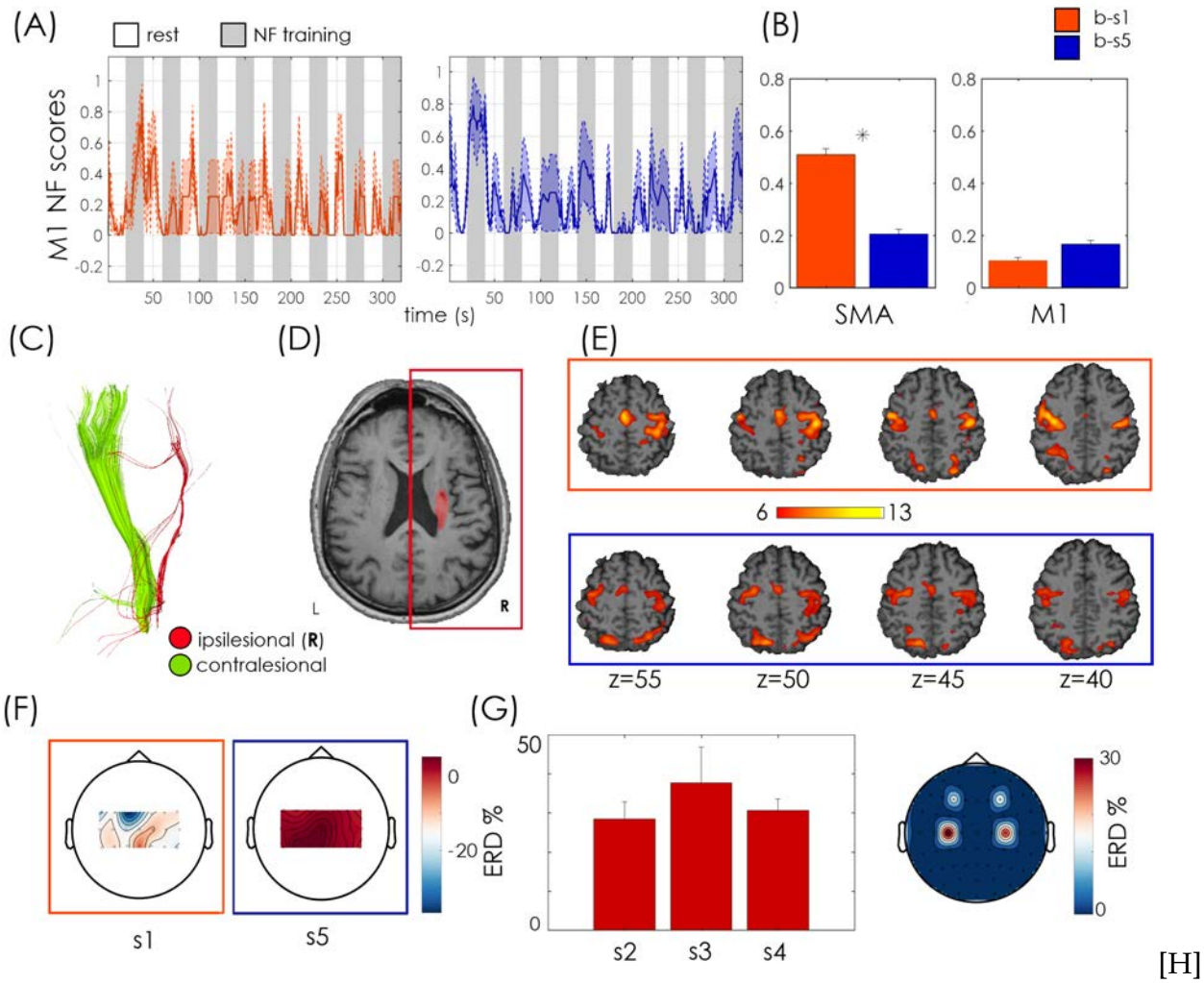

[H]

Figure 6.3: Patient P01 outcome measures. **(A)** M1 regulation during NF training: Normalised NF scores as showed to the patient (mean + standard error across NF sessions—NF1, NF2, NF3- for sessions b-s1 (orange) and b-s5 (blue). Resting blocks are indicated in white, NF training blocks in grey. **(B)** Bar plots of mean normalised NF scores in SMA (left bar plot) and M1 (right) with relative standard error and statistics for b-s1 and b-s5. *Indicates statistically significant difference ($p < 0.01$) between b-s1 and b-s5 as assessed with a Wilcoxon test across blocks of the same training session.**(C)** Corticospinal tract (CST) reconstruction from diffusion MRI imaging. Ipsilesional CST is represented in red and contralesional CST in green. **(D)** Manual Lesion Segmentation (in red) on an anatomical scan. **(E)** Individual contrast activation maps (NF TASK > REST, voxel-wise Family-Wise error (FWE) corrected,$p < 0.05$) during NF training in session b-s1 (orange) and b-s5 (blue).(F)Scalp plots of mean EEG ERD (across NF runs) in b-s1 (left) and b-s5 (right; bimodal EEG-fMRI sessions).**(G)** Unimodal EEG-NF outcomes: mean and standard error ERD estimated from the ipsilesional motor electrode (C4) for the three unimodal EEG-NF training sessions (left) with topoplot of the mean ERD values over motor electrodes (right). Results shown in panels **(F,G)** were obtained offline. For each motor channel (18 for the bimodal sessions, five for the unimodal EEG-NF runs) ERD was computed as the normalised difference in the 8–30 Hz band power (BP) between the rest block and the following training block. The mean ERD value for each channel is displayed in scalp plots representing "ERD activation maps". For panel **(G)**, in order to have a synthetic view of the ERD across the three unimodal sessions, only the ERD from channel C4, the electrode corresponding to the ipsilesional M1, was shown.

P02

Patient 2 was a 76 years old woman with a right ischemic capsulo-lenticular lesion with a high ipsilesional CST integrity(FA asymmetry index = 0.04; Figures 5C,D). Time since stroke was 3 years and initial FMA-UE score was of 19.Even if showing a vast bilateral activation during motor imagery (Figure 5E), the patient significantly improved volitional control of ipsilesional M1 at the end of the training ($p < 0.001$, Wilcoxon test across 24 training blocks, Figures 5A,B) exhibiting very effective and robust NF trends in the second bimodal training session b-s5. ERD maps of unimodal EEG NF indicate a positive and bilateral activation of the motor channels and ipsilesional ERD was positive for all the unimodal sessions (Figures 5F,G). These functional changes were accompanied by a clinically relevant [364] increase in the FMA-UE score from 19 to 25 (Table 6.2).

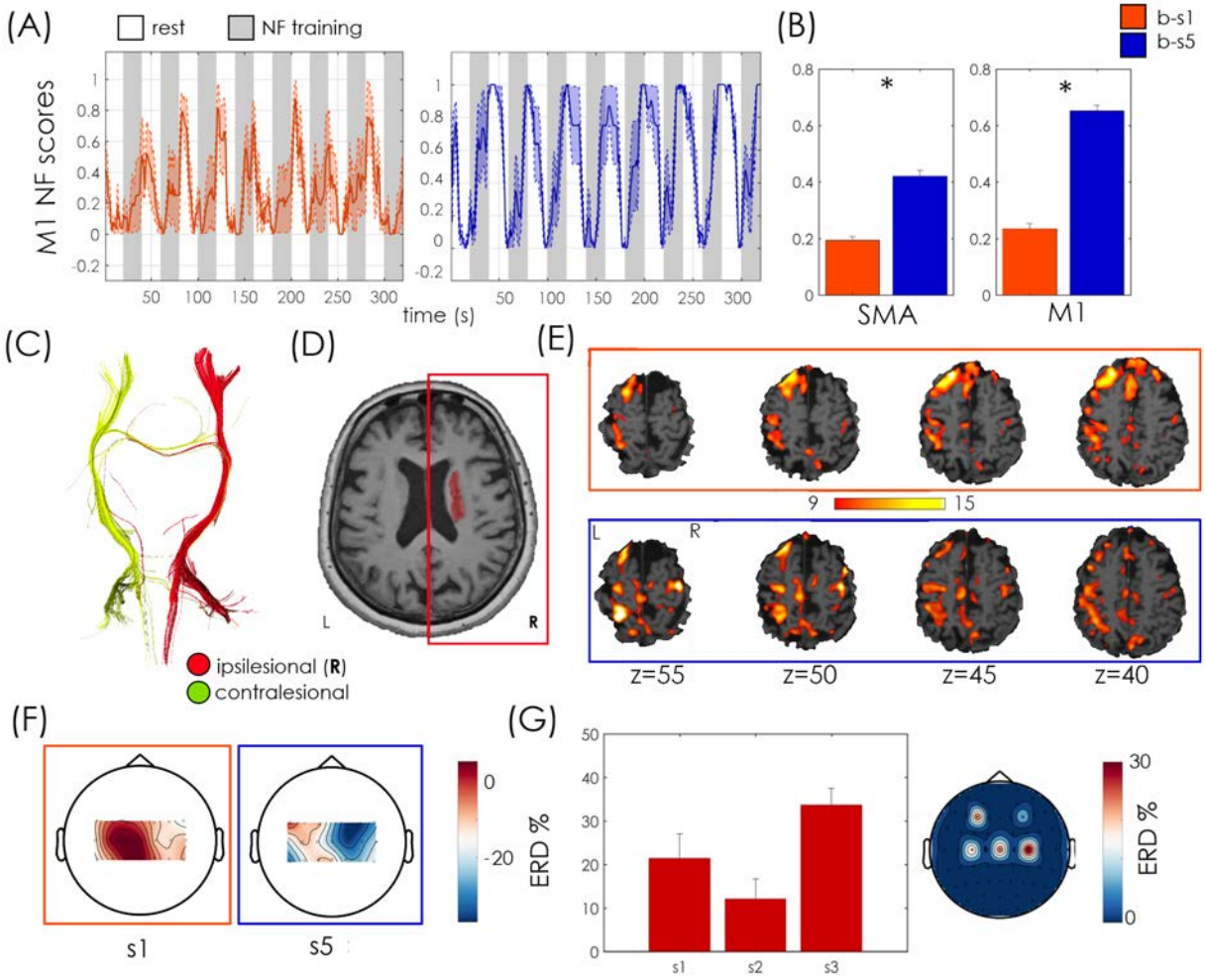

Figure 6.4: Patient 02 outcome measures. Legend as for 6.3

P03

Patient 3 was a 68 years old woman with a right hemorrhagic subcortical lesion (Figure 6D) and a mild hemiparesis (FMA-UE score 50). Time since stroke was 1 year and the symmetry

of CST quite well preserved (FA asymmetry index = 0.06,Figure 6C). The patient showed a strong SMA activation, which increased along with the two sessions, as revealed by the BOLD analysis. She significantly increased the activation of the ipsilesional M1 at the end of the training ($p < 0.001$, Wilcoxon test,Figures 6A,B) and exhibited a larger involvement of the ipsilesional motor and premotor areas, with respect to contralesional ones,during the second NF training, as revealed by BOLD activation maps in Figure 6E. The fMRI NF scores during the second session exhibited higher regularity and amplitude,with respect to the first one. During both unimodal and bimodal training, EEG activation was higher for midline motor electrodes (Figures 6E–G). These functional changes were associated with an increase of 3 points of the FMA-UE score(Table 2).

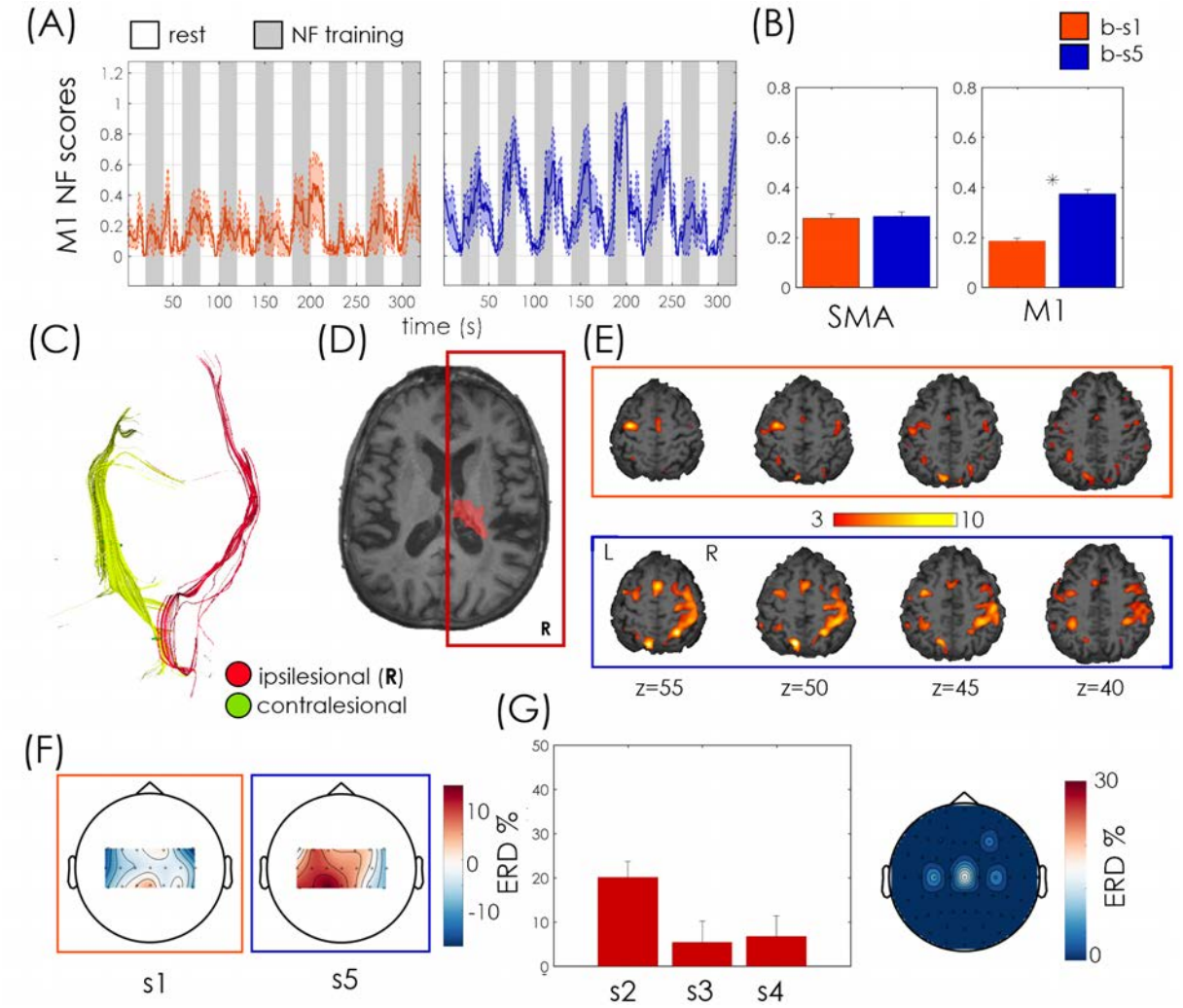

Figure 6.5: Patient 03 outcome measures. Legend as for 6.3

P04

Patient 4 was a 51 years old male affected by a right ischemic-cortical stroke (Figure 7D), which occurred 12 months before the onset of the study. His initial FMA-UE score was 41 and he showed high integrity of the ipsilesional CST, with an FA asymmetry index of

0.05. This patient showed a relatively weak BOLD motor activation during NF training, in particular in the ipsilesional motor cortex(Figure 7E). He exhibited an increase in SMA activation in the final session associated however with a down-regulation of ipsilesional M1 activation, in contradiction with the designed training strategy (Figures 7A,B). This was associated with a negative ipsilesional EEG ERD during the second bimodal NF training session (Figure 7F), and to scarce performances during unimodal EEG sessions (in one session the average ERD was negative and average scalp plot revealed an ERD smaller than 20%,Figure 7G). These counteractive functional changes were associated with a modest deterioration (-9, 7%) of the FMA-UE score.

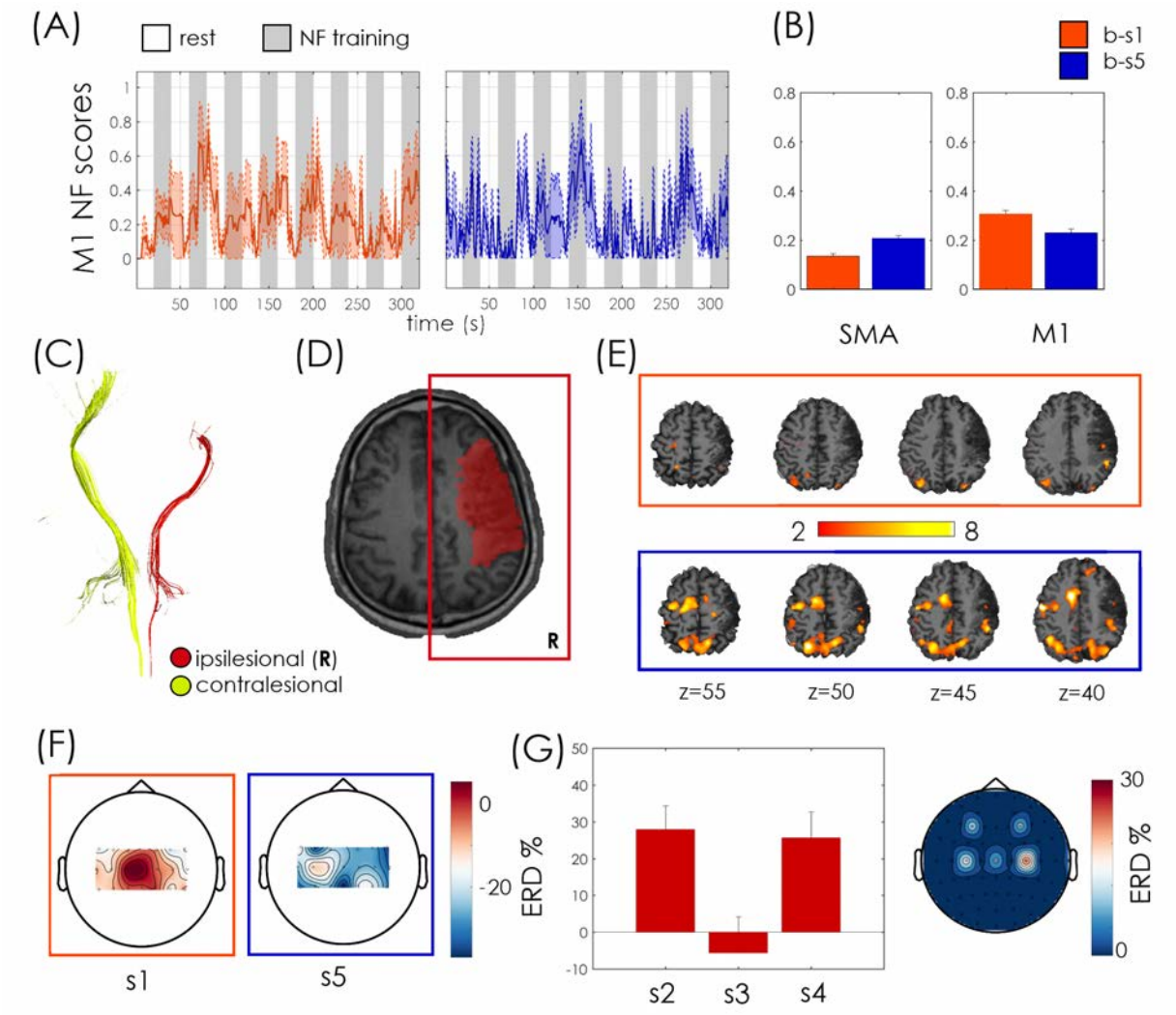

Figure 6.6: Patient 04 outcome measures. Legend as for 6.3

6.5 Discussion

In this exploratory study, the feasibility and efficacy of multisession bimodal EEG-fMRI NF training for upper limb motor recovery after stroke was tested. The pilot study involved four chronic patients with various degrees of motor impairment and stroke characteristics.In

recent years, few studies have explored the potential of real-time NF for improving motor performances in stroke using different imaging modality such as fMRI [365], EEG [105] or functional Near-Infrared Spectroscopy -NIRS [366]. A recent systematic review on fMRI NF for motor training in healthy subjects and stroke patients [5] indicated that real-time fMRI is effective in promoting self-regulation of targeted areas and has potential to improve motor outcomes.However, the efficacy of fMRI-NF was shown in some but not all studies and depended on function and respective cortical areas engaged. Another factor that severely limits the efficacy of fMRI training is that, due to the cost of MR scanning, in most fMRI-NF studies only short training protocols are usually implemented or tested. This, together with the high complementary of EEG and fMRI techniques, motivated our effort to integrate these two modalities in view of designing more specific, feasible and effective multi-session training protocols for upper limb motor recovery after stroke.

6.5.1 Feasibility of Bimodal NF

or the first time in literature, we tested bimodal EEG-fMRI for stroke rehabilitation. Bimodal EEG-fMRI NF poses various challenges: technological (as it requires a complex and high-performance installation), practical (for the relatively long preparation time of the patients, of around 40 min) and mental for the participants (NF is cognitively demanding,particularly in the unfamiliar MRI environment, that the patients usually associate with negative emotions). Results confirmed the feasibility and safety of this protocol on stroke patients with mild to severe hemiparesis: patients managed to upregulate the BOLD activity in the targeted motor areas during NF training. The EEG activity was harder to modulate during bimodal sessions, but all patients successfully up regulated the activity recorded at motor electrodes during unimodal EEG-NF sessions.

In general, a positive response to the training protocol emerged from the questionnaires. Patients were interested and motivated by NF training and the associated challenge and very satisfied with the NF metaphor. They also perceived this type of training as potentially complementary to traditional rehabilitation techniques.

6.5.2 Multi-target Strategy and Its Relation to Stroke Deficit

One crucial aspect when designing an NF protocol is the choice of target regions. Whether the M1 is activated during motor imagery is still debated [351, 352], while SMA seems to be more robustly and easily recruited. This work provides new pieces of evidence that M1 can be activated during motor imagery, especially when the patient is guided to this target through NF.

In this pilot work, we proposed a novel multi-target strategy for a guided rehabilitation of ipsilesional primary motor areas.Such a selective regulation of motor areas is only possible for the fMRI modality, which allows for a more precise spatial identification of activated areas than EEG. The multi-target training was effective in three out of four patients, who

improved the activation of ipsilesional M1 in the second training session with respect to the beginning of the protocol. Remarkably, if we consider that the protocol was 1 week long, for two of these patients the improvement of ipsilesional M1 control was associated with an increase of motor performances, as assessed by the FMA-UE score (Figure 3B).

Those two patients exhibited a high degree of symmetry of the CST, and therefore a preserved ipsilesional CST. On the other hand, the patient having a severely impaired CST, with an FA asymmetry index close to the threshold indicating very poor recovery potential, did not exhibit functional improvement.Patient 04 showed a high integrity of the ipsilesional CST but did not exhibit functional improvement. He presents a large cortical lesion including M1. In addition, the CST (segmented between the posterior limb of the internal capsule and the lower pons) does not seem to reach M1 (Figure 7C). This may be the main reason why the patient fails to activate M1, which is severely damaged while being able to activate SMA (preserved because vascularised by the anterior cerebral artery).

It has been shown that the recovery after partial lesion of M1 at the chronic stage of stroke is associated with reorganisation within the surrounding motor cortex [367]. We can hypothesise that, in patients with a large cortical stroke including M1, either recovery of ipsilesional activation would certainly require a much longer NF training, or we should consider changing the cortical target. In this case, contralesional M1 (via the cortico-reticulo-propriospinal pathway) would be a relevant alternative target [368].These findings highlight the importance of taking into account various factors when designing a clinical protocol.In particular, they confirm the critical role of the preserved neural pathways (the so-called "structural reserve"; [354] in the recovery process and indicate that this is importantly related also to functional brain regulation of the ipsilesional motor cortex, giving useful indications for future studies inclusion criteria.

6.5.3 Limitations

This is an exploratory work and presents various limitations.The first concerns the challenge of obtaining good quality EEG recordings in the noisy environment of fMRI, which represents the main issue in simultaneous EEG-fMRI recording. Great effort was put to reduce the impedance of the electrodes during patient preparation, strictly following the manufacturer guidelines. However, completely getting rid of BCG and motion artefacts in real-time remains a challenge. BCG artefact correction maybe even more challenging for stroke patients, as they are often affected by atrial fibrillation and therefore have an irregular heart rate, in comparison with the healthy population. The development of more efficient real-time methods to correct these artefacts is the object of current research [59] and will considerably improve the quality of bimodal EEG-fMRI NF in the near future. Artifacts and noise are part of the reason why EEG activity regulation during bimodal NF is more challenging if compared to fMRI [86]. Electrophysiological activity may also be intrinsically harder to control than metabolic activity since brain "naturally" regulates and processes feedbacks(i.e., blood pressure or flow) from the vascular system, while there are no equivalent "sensors" for brain electrophysiological activity [369].

Another limitation of this study was that we did not control for movements of the affected limb during the motor imagery task by measuring the electromyographic (EMG) signal. This choice was made not to increase the burden and complexity of the simultaneous EEG-fMRI setup, as measuring EMG requires the installation of an additional amplifier at the bottom of the MR bore and, to arrange cables in a straight line, needs custom cable lengths for each individual in order to fulfil the safety regulations and follow the manufacturer guidelines. We have therefore decided to monitor upper limb movements by means of a camera inside the MR bore and repeatedly instructed the patients to remain still during NF training.

Here we present results from a pilot study and further research is required to validate its findings and assess the efficacy of bimodal EEG-fMRI for stroke rehabilitation. The lack of blinded assessment and the absence of a control group (for instance a group receiving sham NF or a treatment-as-usual group) does not allow to rigorously assess if patients up regulated their brain activity by means of the NF training neither to determine if the observed clinical effects are a result of the NF intervention, as the observed improvement may be related to other uncontrolled factors [370].

This is an exploratory study whose main aims were to test the feasibility of the bimodal EEG-fMRI NF training in stroke patients and identify critical aspects for the design of a randomised controlled study. Our preliminary results are however encouraging and indicate that motor improvements were obtained after a relatively short training duration (1 week) in two out of four chronic patients at more than 1 year from the stroke episode, where spontaneous recovery has stopped.They also support the hypothesis that in these patients NF may trigger functional reorganisation of the affected motor areas by exploiting the residual brain plasticity. Finally, this pilot study was useful to identify crucial aspects and inclusion criteria for the design of a larger randomised controlled trial on chronic stroke patients.

6.6 Conclusion

In this chapter, we studied the feasibility and efficacy of bimodal EEG-fMRI NF training for upper limb motor recovery, which we tested on four chronic stroke patients. Preliminary results indicate that success in upregulating the activity of target motor areas depends on the type and severity of the stroke damage and emphasize the importance of taking into account the variability of the stroke patients' population when designing a clinical protocol. These findings give useful indications for the design of future clinical studies with NF.

Conclusion 7

General Conclusion

In this thesis the approach of multimodality within the Neurofeedback was put forth, experiments were developed and tested in a rehabilitation context. We particularly studied the input and output of multimodality for Neurofeedback, i.e. the use of multiple different neuroimaging techniques, in the interest of enriching the quality of information given to the user and the use of multisensory feedback.

We started from a state of the art of scientific literature on multimodality in neurofeedback. This state of the art was divided into two parts.

In Chapter 1, we presented the input of multimodal neurofeedback (NF) and more precisely with the combination of EEG and fMRI for NF. We focused on the general properties of the EEG and fMRI, such as their spatial and temporal resolution characteristics. Then, we analysed the different approaches for the integration of EEG-fMRI data for NF: symmetric or asymmetric approaches and activation or connectivity analyses. We studied the different studies using EEG and fMRI for NF. We proposed a classification of EEG-fMRI based NF studies, by particularly insisting on the simultaneous use of EEG-fMRI and EEG-informed fMRI. Finally, we analysed the most commonly used paradigms in these studies: the Motor Imagery Paradigm and the Emotion Network Paradigm.

In Chapter 2, we focused on the output of multimodal NF and more precisely on the use of haptic for NF. We focused firstly on human haptic perception before describing the different properties of haptic interfaces, whether tactile or kinaesthetic. Then, we analysed the different applications of haptic for NF and brain-computer interfaces. Two families of paradigms were studied: the motor imagery paradigm and external stimulation paradigms, such as the P300 and the steady-state somatosensory evoked potential. Finally, we discussed the contribution and utility of haptic feedback for NF.

With regard to these possibilities, we proposed in *Part 2*, a visuo-haptic feedback for the NF that is expected to be ecological and immersive. We chose to combine a visual feedback in virtual reality and a proprioceptive haptic feedback with the particularity of producing illusions of movement.

In Chapter 3, two studies have been carried out and are preliminary studies prior to the implementation of an NF study. On one hand we have characterised what would be the visual feedback that would induce the greatest illusion of movement during a vibration at the wrist. The results showed that a virtual hand moving in the direction of the illusion of movement (therefore congruent) was the feedback that gives the most intense illusion. In a second step, by using EEG, we evaluated whether our visuo-haptic feedback combined to motor imagery (MI) tasks could be more efficient than haptic alone or MI alone. We

showed that using MI and visuo-haptic feedback could increase cortical excitablity in brain motor areas, rather than using solely MI or visuo-haptic feedback.

In Chapter 4, we evaluated the performance of our visuo-haptic feedback for fMRI-NF with a MI task. To do this we compared three conditions: visual alone, haptic alone or the combination of both. The haptic feedback is a tactile interface based on vibrotactile stimulation and vibrations are delivered through a pneumatic vibrator which is MR-compatible. For the visual feedback we used the same virtual hand as in the Chapter 3, the movement executed by the virtual hand was an extension of the right wrist. We then compared the BOLD activations as well as the NF scores for the three conditions. The results showed that a visuo-haptic feedback could enable more intense activation of motor regions rather than visual or haptic alone.

In *part 3*, we studied the input of multimodal NF. We studied the combined use of EEG and fMRI for clinical NF, and particularly with stroke patients.

In Chapter 5, we presented a new technique for detecting the position of electrodes in fMRI. To detect these electrodes, we proposed a fully automated method based on a segmentation step followed by a Hough transform in order to select the positions of MR-compatible electrodes in a MR volume using the UTE (ultra-short echo-time) sequence. This method only has for additional cost the acquisition time of the sequence in the MR protocol. We demonstrated that our method achieves a significantly more accurate electrode detection compared to a semi-automatic detection one that is more commonly used during EEG/fMRI protocols.

In Chapter 6, we presented a NF pilot study on stroke patients with EEG/ fMRI. In an effort to advance the understanding of NF in the context of neurorehabilitation, we investigated the impact of NF on four stroke patients with EEG/fMRI. The objective of this pilot work was to test the feasibility of the EEG-fMRI NF training on stroke patients over several sessions, with the intention of designing a randomised controlled trial on stroke patients, this time involving a longer training protocol.

To conclude, we have developed new approaches for multimodal NF and applied them to study their prevalence in healthy subjects as well as on patients. The new proposal for visuo-haptic feedback can be carried out as part of a clinical study for stroke patients. The pilot study of the EEG-fMRI NF in stroke patients has shown the feasibility of using EEG-fMRI for stroke patients.

Future Works and Perspectives

At the end of this work, there are many paths for research and improvement for a short-term as well as long-term perspective on input or output of multimodal NF:

NF based Visuo-Haptic Feedback for Stroke Patients. Considering Chapter 3, it could be interesting to test in further studies to test the same hypothesis with stroke patients to see if similar results could be obtained. In particular, it would be interesting to know whether the quantification of movement illusions under the same conditions is similar with healthy subjects, as this population is often older than average and elderly have more difficulties perceiving the illusion of movement induced by tendon vibration.

Considering Chapter 4, it would also be desirable to propose a visuo-haptic-based fMRI-NF training protocol for this population. To evaluate it with other studies using unisensory feedback. In a second step it would also be interesting to test new ways to build the haptic feedback, in our method we used a semi-continuous method to fed-back the NF score but a continuous method could be more appropriate for the user.

Source Localisation during EEG-fMRI-NF. Considering Chapter 5, the new automated method to detect the position of the electrodes within MR is not yet used in an NF study. It could be interesting to use this information in order to better estimate brain sources and thus to provide better spatial resolution for fMRI-EEG-NF.

A Clinical Study for Stroke Patients using Bimodal EEG-fMRI. Considering Chapter 6, we presented a feasibility study of bimodal EEG-fMRI-NF for stroke rehabilitation. However, in order to observe clinical effects and to ensure that these are indeed the effects of NF, a study should be carried out on a larger number of subjects and with a control group.

The use of fNIRS as Neuroimaging Modality. During EEG-fMRI-NF sessions, one of the most disabling drawbacks is the portability of the system. It would indeed be more interesting to have more mobility for NF training, especially in a context of rehabilitation. The fNIRS could be an interesting alternative to the fMRI, thanks to the possibility of measuring the haemodynamic response. Moreover, EEG can be used simultaneously with fNIRS without major technical difficulties. However, fNIRS cannot be used to measure cortical activity more than 4 cm deep due to limitations in light emitter power and has more limited spatial resolution. This limits its use for NF protocols targeting the amygdala, for example. Nonetheless, it could be very interesting for NF based MI protocols.

Multimodal Data Integration. In Chapter 1, we presented possible levels of integration of EEG and fMRI bor bimodal NF. We reported two main EEG-fMRI data integration/fusion methods that have been described in the literature: asymmetric / symmetric fusion and activation / connectivity analyses. Asymmetric approaches which consist in using one modality to inform the other rely on the assumption that EEG and fMRI share common neuronal sources and therefore do not fully exploit their complementarity and symmetric approaches that try to analyse both modalities at the same time, data-driven methods for example on ICA, partial least square, or cannonical correlation analysis are interesting in that they leverage fully the information from both modalities while making little assumption

about the nature of the underlying data. However, none of the existing EEG-fMRI fusion method are currently applicable in real-time, but constitute a real challenge for bimodal EEG-fMRI. Activation and connectivity analysis, is the distinction between studies that locate activation patterns and those that investigate functional connectivity between regions. Although the majority of the studies are activation based, it is also interesting to see how specific brain regions interact together. Indeed, many cognitive processes require more than one active brain area and if brain areas interact they will show correlated activity. In fact, most of the processes so far examined with fMRI studies (e.g.,emotion processing, motor response, language,pain perception, etc.) include the coordinated activity of several brain region [37, 48].

In fine, in this thesis, we hope that we showed the importance of multimodality within NF studies, whether in input or output. Furthermore, we showed the complexity of the problem, opened up some new avenues that still needs to be done to master all the multimodal aspects.

Author's Publications

Journal articles

- A Survey on the Use of Haptic Feedback for Brain-Computer Interfaces and Neurofeedback Mathis Fleury, Giulia Lioi, Christian Barillot, Anatole Lécuyer; Frontiers in Neuroscience, Frontiers, 2020, 1, ⟨10.3389/fnins.2020.00528⟩
- Influence of virtual reality visual feedback on the illusion of movement induced by tendon vibration of wrist in healthy participants; Plos One, 2020, <10.1371/journal.pone.0242416>
- A Multi-Target Motor Imagery Training Using Bimodal EEG-fMRI Neurofeedback: A Pilot Study in Chronic Stroke Patients Giulia Lioi, Simon Butet, Mathis Fleury, Elise Bannier, Anatole Lécuyer, Isabelle Bonan, Christian Barillot ; Frontiers in Human Neuroscience, Frontiers, 2020, pp.1-13. ⟨10.3389/fnhum.2020.00037⟩
- Automated Electrodes Detection during simultaneous EEG/fMRI Mathis Fleury, Christian Barillot, Elise Bannier, Marsel Mano, Pierre Maurel ; Frontiers in information and communication technologies, Frontiers Media S.A., In press, pp.1-15. ⟨10.1101/395806⟩

Conference papers

- Bimodal EEG-fMRI Neurofeedback for upper motor limb rehabilitation: a pilot study on chronic patients Giulia Lioi, Simon Butet, Mathis Fleury, Claire Cury, Elise Bannier, Anatole Lécuyer, Isabelle Bonan, Christian Barillot ; rtFIN 2019 – Real Time Functional Imaging and Neurofeedback, Dec 2019, Maastricht, Netherlands. pp.1-2
- Influence of visual feedback on the illusion of movement induced by tendon vibration of wrist in healthy subjects Salomé Le Franc, Mathis Fleury, Mélanie Cogné, Simon Butet, Christian Barillot, Anatole Lécuyer, Isabelle Bonan ; SOFMER 2019 – 34ème congrès de la Société Français de Médecine Physique et de Réadaptation, Oct 2019, Bordeaux, France
- Efficacy of EEG-fMRI Neurofeedback in stroke in relation to the DTI structural damage: a pilot study Giulia Lioi, Simon Butet, Mathis Fleury, Anatole Lécuyer, Isabelle Bonan, Christian Barillot ; OHBM 2019 – 25th Annual Meeting of the Organization for Human Brain Mapping, Jun 2019, Rome, Italy. pp.1-4

Poster communications

- Bimodal EEG-fMRI Neurofeedback for stroke rehabilitation Giulia Lioi, Mathis Fleury, Simon Butet, Anatole Lécuyer, Christian Barillot, Isabelle Bonan ; ISPRM 2018 -International Society of Physical and Rehabilitation Medicine, Jul 2018, Paris, France

Preprints, Working Papers, ...

- Learning 2-in-1: Towards Integrated EEG-fMRI-Neurofeedback Lorraine Perronnet, Anatole Lécuyer, Marsel Mano, Mathis Fleury, Giulia Lioi, Claire Cury, Maureen Clerc, Fabien Lotte, Christian Barillot ; 2020
- Deep learning-based localization of EEG electrodes within MRI acquisitions Caroline Pinte, Mathis Fleury, Pierre Maurel; (Submitted in Frontiers) 2020

List of Figures

List of Tables

Appendix

Questionnaire from the studies described in Chapter 3

Questionnaire de satisfaction

Nous vous remercions d'avoir participé à l'étude HANDS.

Date :

Identifiant : └__┘__┘

Année de naissance : └__┘__┘__┘__┘

L'échelle de notation des affirmations est la suivante :
1 = Pas du tout d'accord
2 = Pas d'accord
3 = Ni en désaccord, ni d'accord
4 = D'accord
5 = Tout à fait d'accord

1) Avez-vous déjà une expérience sur la vibration induisant l'illusion de mouvement ? ***Cochez une seule case.***

□ Oui

□ Non

2) La meilleure condition visuelle pour ressentir une illusion de mouvement : ***Cochez une seule case.***

□ La main animée

□ La main statique

□ La main absente

□ Aucune

3) Pourquoi?

……

……

4) Décrire l'illusion de mouvement que vous avez ressenti : (par exemple une flexion des doigts, une extension du poignet…). ***Plusieurs choix sont possibles.***

……

……

5) Lors de la séance, la sensation de vibration est suffisamment perceptible. ***Cochez une seule case.***

	1	2	3	4	5	
Pas du tout d'accord	◯	◯	◯	◯	◯	Tout à fait d'accord

6) Lors de la séance, la sensation de vibration est inconfortable. ***Cochez une seule case.***

	1	2	3	4	5	
Pas du tout d'accord	◯	◯	◯	◯	◯	Tout à fait d'accord

7) J'ai facilement ressenti l'illusion du mouvement du poignet lorsque la main virtuelle est animée (de manière générale) : ***Cochez une seule case.***

□ Oui

□ Non

8) J'ai facilement ressenti l'illusion du mouvement du poignet lorsque la main virtuelle est statique (de manière générale) ***: Cochez une seule case.***

□ Oui

□ Non

9) J'ai facilement ressenti l'illusion du mouvement du poignet lorsque la main virtuelle est absente (de manière générale) : ***Cochez une seule case.***

□ Oui

□ Non

10) Lorsque la main virtuelle est animée, l'illusion de mouvement apparaît (de manière générale) : ***Cochez une seule case.***

□ Dès le début de la stimulation

□ Vers le milieu de la stimulation

□ Vers la fin de la stimulation

□ Je n'ai pas eu d'illusion de mouvement

11) Lorsque la main virtuelle est statique, l'illusion de mouvement apparaît (de manière générale) : ***Cochez une seule case.***

□ Dès le début de la stimulation

□ Vers le milieu de la stimulation

□ Vers la fin de la stimulation

□ Je n'ai pas eu d'illusion de mouvement

12) Lorsque la main virtuelle est absente, l'illusion de mouvement apparaît (de manière générale) : ***Cochez une seule case.***

□ Dès le début de la stimulation

□ Vers le milieu de la stimulation

□ Vers la fin de la stimulation

□ Je n'ai pas eu d'illusion de mouvement

13) Lorsque la main virtuelle est animée, l'illusion de mouvement dure : ***Cochez une seule case.***

□ Plutôt 1-3 secondes

□ Plutôt 5 secondes

□ Plutôt 10 secondes

□ Je n'ai pas eu d'illusion de mouvement

14) Lorsque la main virtuelle est statique, l'illusion de mouvement dure : ***Cochez une seule case.***

□ Plutôt 1-3 secondes

□ Plutôt 5 secondes

□ Plutôt 10 secondes

□ Je n'ai pas eu d'illusion de mouvement

15) Lorsque la main virtuelle est absente, l'illusion de mouvement dure : ***Cochez une seule case.***

□ Plutôt 1-3 secondes

□ Plutôt 5 secondes

□ Plutôt 10 secondes

□ Je n'ai pas eu d'illusion de mouvement

Commentaires éventuels :

……

……

Questionnaire de satisfaction

Nous vous remercions d'avoir participé à l'étude HANDS.

Date :

Identifiant : └┘└┘

Année de naissance : └┘└┘└┘└┘

L'échelle de notation des affirmations est la suivante :
1 = Pas du tout d'accord
2 = Pas d'accord
3 = Ni en désaccord, ni d'accord
4 = D'accord
5 = Tout à fait d'accord

1) J'ai déjà réalisé des expériences avec de l'imagerie mentale en EEG : ***Cochez une seule case.***

□ Oui

□ Non

2) La durée totale de l'expérience est trop longue : ***Cochez une seule case.***

	1	2	3	4	5	
Pas du tout d'accord	◯	◯	◯	◯	◯	Tout à fait d'accord

3) J'étais fatigué(e) à la fin de l'expérience : ***Cochez une seule case.***

	1	2	3	4	5	
Pas du tout d'accord	◯	◯	◯	◯	◯	Tout à fait d'accord

4) La sensation de vibration devient inconfortable à la fin de l'expérience. ***Cochez une seule case.***

	1	2	3	4	5	
Pas du tout d'accord	◯	◯	◯	◯	◯	Tout à fait d'accord

5) J'ai facilement ressenti une illusion de mouvement lorsqu'il y avait la vibration : ***Cochez une seule case.***

	1	2	3	4	5	
Pas du tout d'accord	◯	◯	◯	◯	◯	Tout à fait d'accord

6) La main virtuelle animée à l'écran m'a aidée à ressentir une illusion de mouvement : ***Cochez une seule case.***

	1	2	3	4	5	
Pas du tout d'accord	◯	◯	◯	◯	◯	Tout à fait d'accord

7) La main virtuelle animée à l'écran m'a aidée à réaliser une tâche d'imagerie mentale : ***Cochez une seule case.***

	1	2	3	4	5	
Pas du tout d'accord	◯	◯	◯	◯	◯	Tout à fait d'accord

8) J'ai trouvé que réaliser des tâches en imagerie mentale de mon membre supérieur pendant l'expérience était facile *: Cochez une seule case.*

	1	2	3	4	5	
Pas du tout d'accord	◯	◯	◯	◯	◯	Tout à fait d'accord

9) Ma capacité à faire de l'imagerie mentale était meilleure lorsqu'il y avait la vibration associée au poignet : *Cochez une seule case.*

	1	2	3	4	5	
Pas du tout d'accord	◯	◯	◯	◯	◯	Tout à fait d'accord

10) Le temps pour effectuer l'imagerie mentale (10 secondes) est trop court *: Cochez une seule case.*

	1	2	3	4	5	
Pas du tout d'accord	◯	◯	◯	◯	◯	Tout à fait d'accord

11) Le temps de pause entre les exercices est trop court : *Cochez une seule case.*

	1	2	3	4	5	
Pas du tout d'accord	◯	◯	◯	◯	◯	Tout à fait d'accord

12) J'ai pensé à la tâche d'imagerie mentale pendant les pauses : *Cochez une seule case.*

□ Oui

□ Non

13) Je pense avoir amélioré ma performance en imagerie mentale au cours de l'expérience : ***Cochez une seule case.***

□ Oui

□ Non

14) Décrire la stratégie d'imagerie mentale : (Quel(s) mouvement(s) pensiez-vous faire?)

……

……

Commentaires éventuels :

……

……

Questionnaire from the study described in Chapter 4

Questionnaire de fin de protocole

Nous vous remercions d'avoir participé à l'étude MR-HANDS.

Date (jj.mm.aaaa) :

Identifiant :

Age :

Genre (féminin ou masculin) :

L'échelle de notation des affirmations est la suivante :

1 = Pas du tout d'accord
2 = Pas d'accord
3 = Plutôt pas d'accord
4 = Plutôt d'accord
5 = D'accord
6 = Tout à fait d'accord

Concernant l'expérience en général

1) L'expérience vous a-t-elle semblé longue ? * Une seule réponse possible.

	1	2	3	4	5	6	
Pas du tout d'accord	☐	☐	☐	☐	☐	☐	Tout à fait d'accord

2) Combien de temps (en minutes) pensez-vous avoir passé dans l'IRM ?

...

3) J'étais fatigué(e) à la fin de l'expérience. * Une seule réponse possible.

	1	2	3	4	5	6	
Pas du tout d'accord	☐	☐	☐	☐	☐	☐	Tout à fait d'accord

4) J'ai réussi à me détendre totalement pendant l'expérience ? * Une seule réponse possible.

	1	2	3	4	5	6	
Pas du tout d'accord	☐	☐	☐	☐	☐	☐	Tout à fait d'accord

5) J'ai trouvé l'installation du bras droit inconfortable. * Une seule réponse possible.

	1	2	3	4	5	6	
Pas du tout d'accord	☐	☐	☐	☐	☐	☐	Tout à fait d'accord

6) J'ai réussi à m'investir pleinement dans l'expérience en oubliant le milieu environnant ? * Une seule réponse possible.

	1	2	3	4	5	6	
Pas du tout d'accord	☐	☐	☐	☐	☐	☐	Tout à fait d'accord

Concernant l'Imagerie Mentale

Il vous a été demandé d'imaginer un mouvement de votre main droite, d'en ressentir les sensations de mouvement sans la bouger réellement.

7) J'ai déjà réalisé des expériences avec de l'imagerie mentale. * Une seule réponse possible.

□ Oui □ Non

Je pense avoir amélioré ma performance en imagerie mentale au cours de l'expérience. * Une seule réponse possible.

□ Oui □ Non

>>> Concernant la tâche et sa réalisation

8) J'ai trouvé la tâche difficile. * Une seule réponse possible.

	1	2	3	4	5	6	
Pas du tout d'accord	☐	☐	☐	☐	☐	☐	Tout à fait d'accord

9) J'ai trouvé que la durée des périodes où l'on effectue la tâche était trop courte. * Une seule réponse possible.

	1	2	3	4	5	6	
Pas du tout d'accord	☐	☐	☐	☐	☐	☐	Tout à fait d'accord

10) Quel geste avez-vous imaginé pendant la période où vous deviez réaliser la tâche ? (le décrire le plus précisément possible)

…..

11) Il existe au moins deux manières d'imaginer le mouvement en imagerie mentale :

- **soit en imaginant une image visuelle du mouvement**
- **soit en imaginant les sensations physiques associées au mouvement.**

Par notre consigne, nous vous avons orienté(e) vers la sensation physique associée au mouvement de votre main droite. Avez-vous l'impression d'avoir réussi à produire ce type d'activité d'imagerie mentale ?

□ Oui j'ai plutôt réussi à imaginer les sensations de mouvement de ma main droite

□ Non j'ai plutôt réussi à imaginer une image visuelle du mouvement

>>> Concernant le repos

12) J'ai trouvé que la durée des périodes de repos était trop courte. * Une seule réponse possible.

	1	2	3	4	5	6	
Pas du tout d'accord	☐	☐	☐	☐	☐	☐	Tout à fait d'accord

13) Concernant ces périodes de repos, vous deviez fixer la croix. Décrivez ce à quoi vous avez pensé?

…….

15) J'ai pensé à l'imagerie mentale (c-à-d la tâche) aussi pendant les périodes de repos. * Une seule réponse possible.

	1	2	3	4	5	6	
Pas du tout d'accord	☐	☐	☐	☐	☐	☐	Tout à fait d'accord

Concernant le retour VISUEL

Les questions suivantes se rapportent à la période d'entrainement où vous ne receviez que le retour visuel seul (c-à-d la main virtuelle).

16) Ma capacité à faire de l'imagerie mentale était meilleure lorsqu'il y avait la main virtuelle animée. * Une seule réponse possible.

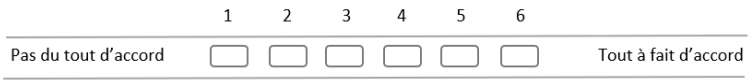

17) Si vous n'êtes plutôt pas d'accord avec l'affirmation précédente, pourquoi ce retour vous a-t-il dérangé ?

….

18) Je me suis approprié(e) le retour visuel de la main virtuelle, comme s'il s'agissait de ma propre main. * Une seule réponse possible.

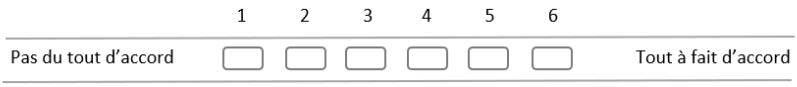

19) Si vous n'êtes plutôt pas d'accord avec l'affirmation de la question 18, quels types de retour visuel auriez-vous préférés ?

- **Modification du point de vue de la main virtuelle :** oui / non
- **Modification de l'apparence de la main virtuelle :** oui / non
- **Modification du geste de la main virtuelle** : oui /non
- **Modification de l'échelle de couleur de la gauge :** oui / non
- **Modification de la récompense lors de l'atteinte du seuil maximale de la gauge** : oui / non

20) Si vous n'êtes plutôt pas d'accord avec l'affirmation de la question 18, décrivez nous le retour visuel que vous auriez préféré?

…

21) J'ai trouvé que la vitesse de déplacement de la main virtuelle était satisfaisante. * Une seule réponse possible.

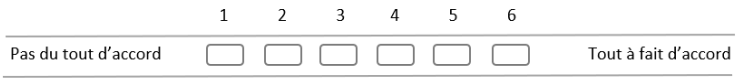

22) J'ai plus facilement ressenti une illusion de mouvement lorsqu'il y avait la main virtuelle, c'est-à-dire que j'ai eu l'impression que ma main bougeait (extension du poignet), alors que celle-ci était immobile. * Une seule réponse possible.

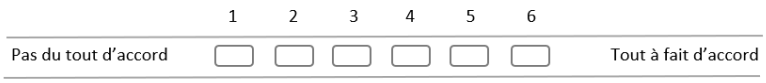

23) Le retour visuel m'a semblé être un indicateur fiable de la qualité de mon imagerie mentale. *Une seule réponse possible.

	1	2	3	4	5	6	
Pas du tout d'accord	☐	☐	☐	☐	☐	☐	Tout à fait d'accord

Concernant le retour HAPTIQUE (vibration)

Les questions suivantes se rapportent à la période d'entrainement où vous ne receviez que le retour avec le vibreur au poignet droit.

24) Ma capacité à faire de l'imagerie mentale était meilleure lorsqu'il y avait la vibration associée au poignet. * Une seule réponse possible.

	1	2	3	4	5	6	
Pas du tout d'accord	☐	☐	☐	☐	☐	☐	Tout à fait d'accord

25) Si vous n'êtes plutôt pas d'accord avec l'affirmation précédente, pourquoi ce retour vous a-t-il dérangé ?

….

26) La sensation de vibration devient inconfortable au cours de l'expérience. * Une seule réponse possible.

	1	2	3	4	5	6	
Pas du tout d'accord	☐	☐	☐	☐	☐	☐	Tout à fait d'accord

27) Le bruit du vibreur m'a perturbé pendant l'expérience. * Une seule réponse possible.

	1	2	3	4	5	6	
Pas du tout d'accord	☐	☐	☐	☐	☐	☐	Tout à fait d'accord

28) J'aurai aimé avoir une puissance de vibration plus importante. * Une seule réponse possible.

	1	2	3	4	5	6	
Pas du tout d'accord	☐	☐	☐	☐	☐	☐	Tout à fait d'accord

29) J'aurai aimé avoir un nombre de fréquences plus important dans le retour vibratoire reflétant mon activité cérébrale. * Une seule réponse possible.

	1	2	3	4	5	6	
Pas du tout d'accord	☐	☐	☐	☐	☐	☐	Tout à fait d'accord

30) J'ai plus facilement ressenti une illusion de mouvement lorsqu'il y avait la vibration, c'est-à-dire que j'ai eu l'impression que ma main bougeait (extension du poignet), alors que celle-ci était immobile. * Une seule réponse possible.

	1	2	3	4	5	6	
Pas du tout d'accord	☐	☐	☐	☐	☐	☐	Tout à fait d'accord

31) Le retour vibratoire m'a semblé être un indicateur fiable de la qualité de mon imagerie mentale. * Une seule réponse possible.

	1	2	3	4	5	6	
Pas du tout d'accord	☐	☐	☐	☐	☐	☐	Tout à fait d'accord

Concernant le retour VISUO-HAPTIQUE

Les questions suivantes se rapportent à la période d'entrainement où vous receviez à la fois le retour visuel et le retour haptique du vibreur au poignet droit.

32) Ma capacité à faire de l'imagerie mentale était meilleure lorsqu'il y avait la visualisation de la main virtuelle associée à la vibration au poignet. * Une seule réponse possible.

	1	2	3	4	5	6	
Pas du tout d'accord	☐	☐	☐	☐	☐	☐	Tout à fait d'accord

33) Si vous n'êtes plutôt pas d'accord avec l'affirmation précédente, pourquoi ce retour vous a-t-il dérangé ?

….

34) J'ai trouvé que l'association de ces 2 informations était difficile à intégrer, que cela faisait trop d'information. * Une seule réponse possible.

	1	2	3	4	5	6	
Pas du tout d'accord	☐	☐	☐	☐	☐	☐	Tout à fait d'accord

35) Mon attention s'est focalisée :

- ☐ **Vers le retour haptique et visuel de façon similaire**
- ☐ **Vers le retour haptique de façon préférentielle**
- ☐ **Vers le retour visuel de façon préférentielle**

36) J'ai trouvé que ce retour visuo-haptique était plus naturel qu'un retour visuel ou haptique seul

	1	2	3	4	5	6	
Pas du tout d'accord	☐	☐	☐	☐	☐	☐	Tout à fait d'accord

37) J'ai plus facilement ressenti une illusion de mouvement lorsqu'il y avait la visualisation de la main et la vibration associées, c'est-à-dire que j'ai eu l'impression que ma main bougeait (extension du poignet), alors que celle-ci était immobile. * Une seule réponse possible

	1	2	3	4	5	6	
Pas du tout d'accord	☐	☐	☐	☐	☐	☐	Tout à fait d'accord

38) Le retour combiné visuel et vibratoire m'a semblé être un indicateur fiable de la qualité de mon imagerie mentale. *Une seule réponse possible.

	1	2	3	4	5	6	
Pas du tout d'accord	☐	☐	☐	☐	☐	☐	Tout à fait d'accord

Au total :

39) Quel retour vous a semblé le plus utile pour améliorer la tâche d'imagerie mentale ?

□ Le retour visuel seul (main virtuelle)
□ Le retour haptique seul (vibreur sur le poignet)
□ Le retour combiné visuel et haptique (main virtuelle et vibreur sur le poignet)
□ Aucun

40) Quelle condition vous a permis d'atteindre la meilleure illusion de mouvement ?

□ Le retour visuel seul (main virtuelle)
□ Le retour haptique seul (vibreur sur le poignet)
□ Le retour combiné visuel et haptique (main virtuelle animée plus vibreur sur le poignet)
□ Je n'ai jamais ressenti d'illusion de mouvement

Bibliography

Here are the references in citation order.

[1] Ranganatha Sitaram et al. 'Closed-loop brain training: the science of neurofeedback'. In: *Nature Reviews Neuroscience* 18.2 (Feb. 2017), pp. 86–100. DOI: 10.1038/nrn.2016.164 (cited on pages 1, 10, 23, 36).

[2] Camille Lecoffre et al. 'National Trends in Patients Hospitalized for Stroke and Stroke Mortality in France, 2008 to 2014'. eng. In: *Stroke* 48.11 (2017), pp. 2939–2945. DOI: 10.1161/STROKEAHA.117.017640 (cited on pages 1, 10, 69, 82).

[3] Nick Ward. 'Assessment of cortical reorganisation for hand function after stroke'. In: *The Journal of physiology* 589.23 (2011), pp. 5625–5632 (cited on pages 1, 10).

[4] Catharina Zich et al. 'Real-time EEG feedback during simultaneous EEG-fMRI identifies the cortical signature of motor imagery'. In: *NeuroImage* 114 (2015), pp. 438–447. DOI: 10.1016/j.neuroimage.2015.04.020 (cited on pages 1, 10, 31, 32).

[5] Tianlu Wang, Dante Mantini, and Celine R Gillebert. 'The potential of real-time fMRI neurofeedback for stroke rehabilitation: A systematic review'. In: *cortex* 107 (2018), pp. 148–165 (cited on pages 1, 10, 34, 110, 122).

[6] Nikos K Logothetis. 'What we can do and what we cannot do with fMRI'. In: *Nature* 453.7197 (2008), pp. 869–878 (cited on pages 2, 10, 19).

[7] JR Ives et al. 'Monitoring the patient's EEG during echo planar MRI'. In: *Electroencephalography and clinical neurophysiology* 87.6 (1993), pp. 417–420 (cited on pages 2, 11).

[8] Kenneth K Kwong et al. 'Dynamic magnetic resonance imaging of human brain activity during primary sensory stimulation.' In: *Proceedings of the National Academy of Sciences* 89.12 (1992), pp. 5675–5679 (cited on pages 2, 11).

[9] Stefan Debener et al. 'Trial-by-trial coupling of concurrent electroencephalogram and functional magnetic resonance imaging identifies the dynamics of performance monitoring'. In: *Journal of Neuroscience* 25.50 (2005), pp. 11730–11737 (cited on pages 2, 11, 23).

[10] Mahesh R Patel et al. 'Echo-planar functional MR imaging of epilepsy with concurrent EEG monitoring'. In: *American journal of neuroradiology* 20.10 (1999), pp. 1916–1919 (cited on pages 2, 11).

[11] Yehudit Meir-Hasson et al. 'An EEG Finger-Print of fMRI deep regional activation'. In: *Neuroimage* 102 (2014), pp. 128–141 (cited on pages 3, 11, 25, 29).

[12] Lorraine Perronnet et al. 'Learning 2-in-1: towards integrated EEG-fMRI-neurofeedback'. In: *BioRxiv* (2020), p. 397729 (cited on pages 3, 11, 30, 88, 112, 113, 116).

[13] Ruth Campbell et al. *Hearing by eye II: Advances in the psychology of speechreading and auditory-visual speech*. Vol. 2. Psychology Press, 1998 (cited on pages 3, 12).

[14] Aaron R Seitz and Hubert R Dinse. 'A common framework for perceptual learning'. In: *Current opinion in neurobiology* 17.2 (2007), pp. 148–153 (cited on pages 3, 12).

[15] Roland Sigrist et al. 'Augmented visual, auditory, haptic, and multimodal feedback in motor learning: A review'. In: *Psychonomic Bulletin & Review* 20.1 (Feb. 2013), pp. 21–53. DOI: 10.3758/s13423-012-0333-8 (cited on pages 3, 12, 55).

[16] Sharon Oviatt. 'Ten myths of multimodal interaction'. In: *Communications of the ACM* 42.11 (1999), pp. 74–81 (cited on pages 3, 12, 34).

[17] Christopher D Wickens. 'Multiple resources and mental workload'. In: *Human factors* 50.3 (2008), pp. 449–455 (cited on pages 3, 12).

[18] Ethan Buch et al. 'Think to move: a neuromagnetic brain-computer interface (BCI) system for chronic stroke.' In: *Stroke* 39.3 (Mar. 2008), pp. 910–7. DOI: 10.1161/STROKEAHA.107.505313 (cited on pages 3, 12, 45–47, 84).

[19] A.-M. Brouwer and J.B.F. van Erp. 'A tactile P300 brain-computer interface'. In: *Frontiers in Neuroscience* 4.MAY (2010). DOI: 10.3389/fnins.2010.00019 (cited on pages 3, 12, 36, 50, 55).

[20] G Pfurtscheller et al. 'Brain oscillations control hand orthosis in a tetraplegic'. In: *Neuroscience Letters* 292.3 (Oct. 2000), pp. 211–214. DOI: 10.1016/S0304-3940(00)01471-3 (cited on pages 4, 13, 44, 45, 47).

[21] Hans Berger. 'Über das elektroenkephalogramm des menschen'. In: *Archiv für psychiatrie und nervenkrankheiten* 87.1 (1929), pp. 527–570 (cited on page 19).

[22] Paul L Nunez and Richard B Silberstein. 'On the relationship of synaptic activity to macroscopic measurements: does co-registration of EEG with fMRI make sense?' In: *Brain topography* 13.2 (2000), pp. 79–96 (cited on pages 19–21, 34).

[23] Peter A Bandettini et al. 'Time course EPI of human brain function during task activation'. In: *Magnetic resonance in medicine* 25.2 (1992), pp. 390–397 (cited on page 19).

[24] Xu Lei, Pedro A Valdes-Sosa, and Dezhong Yao. 'EEG/fMRI fusion based on independent component analysis: integration of data-driven and model-driven methods'. In: *Journal of integrative neuroscience* 11.03 (2012), pp. 313–337 (cited on pages 20, 23).

[25] João Jorge, Wietske Van der Zwaag, and Patricia Figueiredo. 'EEG–fMRI integration for the study of human brain function'. In: *Neuroimage* 102 (2014), pp. 24–34 (cited on pages 20, 21).

[26] Li Dong et al. 'Neuroscience information toolbox: An open source toolbox for EEG–fMRI multimodal fusion analysis'. In: *Frontiers in Neuroinformatics* 12 (2018), p. 56 (cited on page 20).

[27] L.E. Stoeckel et al. 'Optimizing real time fMRI neurofeedback for therapeutic discovery and development'. In: *NeuroImage: Clinical* 5 (Jan. 2014), pp. 245–255. DOI: 10.1016/J.NICL.2014.07.002 (cited on pages 20, 23, 84).

[28] Felix Biessmann et al. 'Analysis of multimodal neuroimaging data'. In: *IEEE reviews in biomedical engineering* 4 (2011), pp. 26–58 (cited on pages 20, 23, 24).

[29] Vadim Zotev et al. 'Self-regulation of human brain activity using simultaneous real-time fMRI and EEG neurofeedback'. In: *Neuroimage* 85 (2014), pp. 985–995 (cited on pages 21, 28–32).

[30] György Buzsáki, Costas A Anastassiou, and Christof Koch. 'The origin of extracellular fields and currents—EEG, ECoG, LFP and spikes'. In: *Nature reviews neuroscience* 13.6 (2012), pp. 407–420 (cited on page 21).

[31] William O Tatum IV. *Handbook of EEG interpretation*. Demos Medical Publishing, 2014 (cited on page 21).

[32] John H Gruzelier. 'EEG-neurofeedback for optimising performance. I: a review of cognitive and affective outcome in healthy participants'. In: *Neuroscience & Biobehavioral Reviews* 44 (2014), pp. 124–141 (cited on page 22).

[33] Stephen M LaConte. 'Decoding fMRI brain states in real-time'. In: *Neuroimage* 56.2 (2011), pp. 440–454 (cited on page 22).

[34] Nikos K Logothetis et al. 'Neurophysiological investigation of the basis of the fMRI signal'. In: *nature* 412.6843 (2001), pp. 150–157 (cited on page 22).

[35] Owen J Arthurs and Simon Boniface. 'How well do we understand the neural origins of the fMRI BOLD signal?' In: *TRENDS in Neurosciences* 25.1 (2002), pp. 27–31 (cited on page 23).

[36] Roberto Lent et al. 'How many neurons do you have? Some dogmas of quantitative neuroscience under revision'. In: *European Journal of Neuroscience* 35.1 (2012), pp. 1–9 (cited on page 23).

[37] Sergio Ruiz et al. 'Real-time fMRI brain computer interfaces: self-regulation of single brain regions to networks'. In: *Biological psychology* 95 (2014), pp. 4–20 (cited on pages 23, 24, 128).

[38] Nikolaus Weiskopf. 'Real-time fMRI and its application to neurofeedback'. In: *Neuroimage* 62.2 (2012), pp. 682–692 (cited on page 23).

[39] Michal Ramot et al. 'Direct modulation of aberrant brain network connectivity through real-time NeuroFeedback'. In: *Elife* 6 (2017), e28974 (cited on page 23).

[40] Samantha J Fede et al. 'A guide to literature informed decisions in the design of real time fMRI neurofeedback studies: A systematic review.' In: *Frontiers in Human Neuroscience* (2020) (cited on pages 23, 30).

[41] Xu Lei. 'Simultaneous EEG-fMRI'. In: *EEG Signal Processing and Feature Extraction*. Springer, 2019, pp. 377–405 (cited on page 23).

[42] Xu Lei et al. 'fMRI functional networks for EEG source imaging'. In: *Human Brain Mapping* 32.7 (2011), pp. 1141–1160 (cited on pages 23, 34).

[43] NJ Trujillo-Barreto et al. 'A symmetrical Bayesian model for fMRI and EEG/MEG neuroimage fusion'. In: *Int. J. Bioelectromagn* 3.1 (2001), pp. 1998–2000 (cited on page 24).

[44] Pedro A Valdes-Sosa et al. 'Model driven EEG/fMRI fusion of brain oscillations'. In: *Human brain mapping* 30.9 (2009), pp. 2701–2721 (cited on page 24).

[45] Jean Daunizeau et al. 'Symmetrical event-related EEG/fMRI information fusion in a variational Bayesian framework'. In: *Neuroimage* 36.1 (2007), pp. 69–87 (cited on page 24).

[46] Jean Daunizeau, Helmut Laufs, and Karl J Friston. 'EEG–fMRI information fusion: Biophysics and data analysis'. In: *EEG-fMRI*. Springer, 2009, pp. 511–526 (cited on page 24).

[47] Dirk Ostwald, Camillo Porcaro, and Andrew P Bagshaw. 'Voxel-wise information theoretic EEG-fMRI feature integration'. In: *Neuroimage* 55.3 (2011), pp. 1270–1286 (cited on page 24).

[48] Sergio Ruiz et al. 'Brain network connectivity and behaviour enhancement: a fMRI-BCI study'. In: *17th Annual Meeting of the Organization for Human Brain Mapping*. 2011 (cited on pages 24, 128).

[49] Bharat Biswal et al. 'Functional connectivity in the motor cortex of resting human brain using echo-planar MRI'. In: *Magnetic resonance in medicine* 34.4 (1995), pp. 537–541 (cited on page 24).

[50] Vincent G van de Ven et al. 'Functional connectivity as revealed by spatial independent component analysis of fMRI measurements during rest'. In: *Human brain mapping* 22.3 (2004), pp. 165–178 (cited on pages 24, 25).

[51] KJ Friston et al. 'Functional connectivity: the principal-component analysis of large (PET) data sets'. In: *Journal of Cerebral Blood Flow & Metabolism* 13.1 (1993), pp. 5–14 (cited on page 24).

[52] Lorraine Perronnet. 'Combining EEG and FMRI for Neurofeedback'. PhD thesis. Sept. 2017 (cited on pages 25, 30, 35).

[53] Robert T Thibault et al. 'Neurofeedback with fMRI: A critical systematic review'. In: *Neuroimage* 172 (2018), pp. 786–807 (cited on pages 25, 88, 114).

[54] Tomas Ros et al. 'Mind over chatter: Plastic up-regulation of the fMRI salience network directly after EEG neurofeedback'. In: *NeuroImage* 65 (2013), pp. 324–335. DOI: 10.1016/j.neuroimage.2012.09.046 (cited on pages 25, 32).

[55] Claire Cury et al. 'A Sparse EEG-Informed fMRI Model for Hybrid EEG-fMRI Neurofeedback Prediction'. In: *Frontiers in Neuroscience* 13.January (2020), pp. 1–12. DOI: 10.3389/fnins.2019.01451 (cited on pages 25, 26, 32, 33).

[56] Marco Simoes et al. 'How much of the BOLD-fMRI signal can be approximated from simultaneous EEG data: Relevance for the transfer and dissemination of neurofeedback interventions'. In: *Journal of Neural Engineering* 17.4 (2020). DOI: 10.1088/1741-2552/ab9a98 (cited on pages 25, 32).

[57] Rodolfo Abreu, Alberto Leal, and Patricia Figueiredo. 'EEG-informed fMRI: a review of data analysis methods'. In: *Frontiers in human neuroscience* 12 (2018), p. 29 (cited on page 25).

[58] Teresa Murta et al. 'Electrophysiological correlates of the BOLD signal for EEG-informed fMRI'. In: *Human brain mapping* 36.1 (2015), pp. 391–414 (cited on page 25).

[59] Xia Wu et al. 'A real-time method to reduce ballistocardiogram artifacts from EEG during fMRI based on optimal basis sets (OBS)'. In: *Computer methods and programs in biomedicine* 127 (2016), pp. 114–125 (cited on pages 26, 123).

[60] Ahmad Mayeli et al. 'Real-time EEG artifact correction during fMRI using ICA'. In: *Journal of neuroscience methods* 274 (2016), pp. 27–37 (cited on page 26).

[61] Ilana Klovatch-Podlipsky et al. 'Dual array EEG-fMRI: an approach for motion artifact suppression in EEG recorded simultaneously with fMRI'. In: *Neuroimage* 142 (2016), pp. 674–686 (cited on page 26).

[62] Marsel Mano et al. 'How to build a hybrid neurofeedback platform combining EEG and fMRI'. In: *Frontiers in neuroscience* 11 (2017), p. 140 (cited on pages 26, 105, 112, 116).

[63] Patrick L Purdon et al. 'An open-source hardware and software system for acquisition and real-time processing of electrophysiology during high field MRI'. In: *Journal of neuroscience methods* 175.2 (2008), pp. 165–186 (cited on page 26).

[64] Giulia Lioi et al. 'Simultaneous EEG-fMRI during a neurofeedback task, a brain imaging dataset for multimodal data integration'. In: *Scientific Data* 7.1 (2020), pp. 1–15 (cited on page 27).

[65] Harald Kugel et al. 'Hazardous situation in the MR bore: induction in ECG leads causes fire'. In: *European radiology* 13.4 (2003), pp. 690–694 (cited on page 26).

[66] David Moher et al. 'Preferred reporting items for systematic reviews and meta-analyses: the PRISMA statement'. In: *PLoS med* 6.7 (2009), e1000097 (cited on page 28).

[67] Stephen J Johnston et al. 'Neurofeedback: a promising tool for the self-regulation of emotion networks'. In: *Neuroimage* 49.1 (2010), pp. 1066–1072 (cited on page 28).

[68] Elizabeth A Phelps et al. 'Activation of the left amygdala to a cognitive representation of fear'. In: *Nature neuroscience* 4.4 (2001), pp. 437–441 (cited on page 29).

[69] F Schneider et al. 'Differential amygdala activation in schizophrenia during sadness'. In: *Schizophrenia research* 34.3 (1998), pp. 133–142 (cited on page 29).

[70] Vadim Zotev et al. 'Self-regulation of amygdala activation using real-time fMRI neurofeedback'. In: *PloS one* 6.9 (2011), e24522 (cited on page 29).

[71] R Christopher DeCharms et al. 'Control over brain activation and pain learned by using real-time functional MRI'. In: *Proceedings of the National Academy of Sciences* 102.51 (2005), pp. 18626–18631 (cited on page 29).

[72] Karen J Hartwell et al. 'Individualized real-time fMRI neurofeedback to attenuate craving in nicotine-dependent smokers'. In: *Journal of psychiatry & neuroscience: JPN* 41.1 (2016), p. 48 (cited on page 29).

[73] Anna Zilverstand et al. 'fMRI neurofeedback facilitates anxiety regulation in females with spider phobia'. In: *Frontiers in behavioral neuroscience* 9 (2015), p. 148 (cited on page 29).

[74] Andrew A. Nicholson et al. 'Alpha oscillation neurofeedback modulates amygdala complex connectivity and arousal in posttraumatic stress disorder'. In: *NeuroImage: Clinical* 12 (2016), pp. 506–516. DOI: 10.1016/j.nicl.2016.07.006 (cited on pages 29, 32, 34).

[75] David EJ Linden et al. 'Real-time self-regulation of emotion networks in patients with depression'. In: *PloS one* 7.6 (2012), e38115 (cited on page 29).

[76] Richard J Davidson. 'Anterior cerebral asymmetry and the nature of emotion'. In: *Brain and cognition* 20.1 (1992), pp. 125–151 (cited on page 29).

[77] Ryan Thibodeau, Randall S Jorgensen, and Sangmoon Kim. 'Depression, anxiety, and resting frontal EEG asymmetry: a meta-analytic review.' In: *Journal of abnormal psychology* 115.4 (2006), p. 715 (cited on page 29).

[78] Vadim Zotev et al. 'Emotion self-regulation training in major depressive disorder using simultaneous real-time fMRI and EEG neurofeedback'. In: *NeuroImage: Clinical* 27 (2020), p. 102331 (cited on pages 29, 32, 34).

[79] Jackob N Keynan et al. 'Limbic activity modulation guided by functional magnetic resonance imaging–inspired electroencephalography improves implicit emotion regulation'. In: *Biological Psychiatry* 80.6 (2016), pp. 490–496 (cited on page 29).

[80] Jackob N. Keynan et al. 'Electrical fingerprint of the amygdala guides neurofeedback training for stress resilience'. In: *Nature Human Behaviour* 3.1 (2019), pp. 63–73. DOI: 10.1038/s41562-018-0484-3 (cited on pages 29, 32, 33).

[81] María A. Cervera et al. 'Brain-computer interfaces for post-stroke motor rehabilitation: a meta-analysis'. In: *Annals of Clinical and Translational Neurology* 5.5 (May 2018), pp. 651–663. DOI: 10.1002/acn3.544 (cited on pages 30, 34, 110).

[82] Douglas Owen Cheyne. 'MEG studies of sensorimotor rhythms: a review'. In: *Experimental neurology* 245 (2013), pp. 27–39 (cited on page 30).

[83] G. Pfurtscheller and C. Neuper. 'Motor imagery and direct brain-computer communication'. In: *Proceedings of the IEEE* 89.7 (July 2001), pp. 1123–1134. DOI: 10.1109/5.939829 (cited on pages 30, 44, 80).

[84] Brian D Berman et al. 'Self-modulation of primary motor cortex activity with motor and motor imagery tasks using real-time fMRI-based neurofeedback'. In: *Neuroimage* 59.2 (2012), pp. 917–925 (cited on pages 30, 110).

[85] David MA Mehler et al. 'The BOLD response in primary motor cortex and supplementary motor area during kinesthetic motor imagery based graded fMRI neurofeedback'. In: *NeuroImage* 184 (2019), pp. 36–44 (cited on pages 30, 84, 96, 110, 111).

[86] Lorraine Perronnet et al. 'Unimodal versus bimodal EEG-fMRI neurofeedback of a motor imagery task'. In: *Frontiers in Human Neuroscience* 11 (2017), p. 193 (cited on pages 32, 116, 123).

[87] Vadim Zotev et al. 'Correlation between amygdala BOLD activity and frontal EEG asymmetry during real-time fMRI neurofeedback training in patients with depression'. In: *NeuroImage: Clinical* 11 (2016), pp. 224–238 (cited on pages 32, 34).

[88] Vadim Zotev et al. 'Real-time fMRI neurofeedback training of the amygdala activity with simultaneous EEG in veterans with combat-related PTSD'. In: *NeuroImage: Clinical* 19 (2018), pp. 106–121 (cited on pages 32, 34).

[89] 'Feature analysis for correlation studies of simultaneous EEG-fMRI data: A proof of concept for neurofeedback approaches'. In: *Proceedings of the Annual International Conference of the IEEE Engineering in Medicine and Biology Society, EMBS* 2015-November (2015), pp. 4065–4068 (cited on page 32).

[90] Marco Simoes et al. 'Correlated alpha activity with the facial expression processing network in a simultaneous EEG-fMRI experiment'. In: *Proceedings of the Annual International Conference of the IEEE Engineering in Medicine and Biology Society, EMBS* (2017), pp. 2562–2565. DOI: 10.1109/EMBC.2017.8037380 (cited on page 32).

[91] Juan L. Terrasa et al. 'Self-Regulation of SMR Power Led to an Enhancement of Functional Connectivity of Somatomotor Cortices in Fibromyalgia Patients'. In: *Frontiers in Neuroscience* 14.March (2020), pp. 1–14. DOI: 10.3389/fnins.2020.00236 (cited on page 32).

[92] Sivan Kinreich et al. 'Neural dynamics necessary and sufficient for transition into pre-sleep induced by EEG NeuroFeedback'. In: *NeuroImage* 97 (2014), pp. 19–28. DOI: 10.1016/j.neuroimage.2014.04.044 (cited on page 32).

[93] Yehudit Meir-Hasson et al. 'One-class FMRI-inspired EEG model for self-regulation training'. In: *PLoS ONE* 11.5 (2016), pp. 1–17. DOI: 10.1371/journal.pone.0154968 (cited on page 32).

[94] Jackob N. Keynan et al. 'Limbic Activity Modulation Guided by Functional Magnetic Resonance Imaging–Inspired Electroencephalography Improves Implicit Emotion Regulation'. In: *Biological Psychiatry* 80.6 (2016), pp. 490–496. DOI: 10.1016/j.biopsych.2015.12.024 (cited on page 32).

[95] Simon H Kohl et al. 'The Potential of Functional Near-Infrared Spectroscopy-Based Neurofeedback—A Systematic Review and Recommendations for Best Practice'. In: *Frontiers in neuroscience* 14 (2020), p. 594 (cited on page 33).

[96] Javad Safaie et al. 'Toward a fully integrated wireless wearable EEG-NIRS bimodal acquisition system'. In: *Journal of neural engineering* 10.5 (2013), p. 056001 (cited on page 33).

[97] Ali Kassab et al. 'Multichannel wearable f NIRS-EEG system for long-term clinical monitoring'. In: *Human brain mapping* 39.1 (2018), pp. 7–23 (cited on page 33).

[98] Jake D Rieke et al. 'Development of a Combined, Sequential Real-Time fMRI and fNIRS Neurofeedback System Enhance Motor Learning After Stroke'. In: *Journal of Neuroscience Methods* (2020), p. 108719 (cited on page 33).

[99] Siamac Fazli et al. 'Learning from more than one data source: data fusion techniques for sensorimotor rhythm-based brain–computer interfaces'. In: *Proceedings of the IEEE* 103.6 (2015), pp. 891–906 (cited on page 33).

[100] Fabio Babiloni et al. 'Estimation of the cortical functional connectivity with the multimodal integration of high-resolution EEG and fMRI data by directed transfer function'. In: *Neuroimage* 24.1 (2005), pp. 118–131 (cited on page 34).

[101] Saman Noorzadeh et al. 'Multi-modal EEG and fMRI source estimation using sparse constraints'. In: *International Conference on Medical Image Computing and Computer-Assisted Intervention*. Springer. 2017, pp. 442–450 (cited on page 34).

[102] Edward Waltz, James Llinas, et al. *Multisensor data fusion*. Vol. 685. Artech house Boston, 1990 (cited on page 34).

[103] David L Hall and James Llinas. 'An introduction to multisensor data fusion'. In: *Proceedings of the IEEE* 85.1 (1997), pp. 6–23 (cited on page 34).

[104] Febo Cincotti et al. 'Vibrotactile feedback for brain-computer interface operation.' In: *Computational intelligence and neuroscience* 2007 (Sept. 2007), p. 48937. DOI: 10.1155/2007/48937 (cited on pages 35, 37, 45, 47, 55, 84).

[105] Floriana Pichiorri et al. 'Brain-computer interface boosts motor imagery practice during stroke recovery'. In: *Annals of Neurology* 77.5 (May 2015), pp. 851–865. DOI: 10.1002/ana.24390 (cited on pages 35, 47, 122).

[106] Thilo Hinterberger et al. 'A multimodal brain-based feedback and communication system'. In: *Experimental Brain Research* 154.4 (Feb. 2004), pp. 521–526. DOI: 10.1007/s00221-003-1690-3 (cited on pages 36, 84).

[107] T. Sollfrank et al. 'The effect of multimodal and enriched feedback on SMR-BCI performance'. In: *Clinical Neurophysiology* 127.1 (Jan. 2016), pp. 490–498. DOI: 10.1016/J.CLINPH.2015.06.004 (cited on pages 36, 55).

[108] Marieke E Thurlings et al. 'Does bimodal stimulus presentation increase ERP components usable in BCIs?' In: *Journal of Neural Engineering* 9.4 (Aug. 2012), p. 045005. DOI: 10.1088/1741-2560/9/4/045005 (cited on pages 36, 50, 84).

[109] Hayrettin Gürkök and Anton Nijholt. 'Brain–Computer Interfaces for Multimodal Interaction: A Survey and Principles'. In: *International Journal of Human-Computer Interaction* 28.5 (May 2012), pp. 292–307. DOI: 10.1080/10447318.2011.582022 (cited on page 36).

[110] Fabien Lotte, Florian Larrue, and Christian Mühl. 'Flaws in current human training protocols for spontaneous Brain-Computer interfaces: Lessons learned from instructional design'. In: *Frontiers in Human Neuroscience* 7.SEP (2013), pp. 1–11. DOI: 10.3389/fnhum.2013.00568 (cited on page 36).

[111] James Minogue and M Gail Jones. 'Haptics in education: Exploring an untapped sensory modality'. In: *Review of Educational Research* 76.3 (2006), pp. 317–348 (cited on page 36).

[112] M Gomez-Rodriguez et al. 'Closing the sensorimotor loop: haptic feedback facilitates decoding of motor imagery'. In: *Journal of Neural Engineering* 8.3 (June 2011), p. 036005. DOI: 10.1088/1741-2560/8/3/036005 (cited on pages 36, 45–47, 85).

[113] Andreas Herweg et al. 'Wheelchair control by elderly participants in a virtual environment with a brain-computer interface (BCI) and tactile stimulation.' In: *Biological psychology* 121.Pt A (Dec. 2016), pp. 117–124. DOI: 10.1016/j.biopsycho.2016.10.006 (cited on pages 36, 49, 50).

[114] Tobias Kaufmann, Elisa M Holz, and Andrea Kübler. 'Comparison of tactile, auditory, and visual modality for brain-computer interface use: a case study with a patient in the locked-in state.' In: *Frontiers in neuroscience* 7 (2013), p. 129. DOI: 10.3389/fnins.2013.00129 (cited on pages 36, 50).

[115] JP Roll et al. *Posture and Gait: Development, Adaptation and Modulation*. 1988 (cited on page 36).

[116] J.B.F. Van Erp and A.-M. Brouwer. 'Touch-based Brain Computer Interfaces: State of the art'. In: *IEEE Haptics Symposium, HAPTICS*. 2014, pp. 397–401. DOI: 10.1109/HAPTICS.2014.6775488 (cited on pages 36, 44).

[117] Aniruddha Chatterjee et al. 'A brain-computer interface with vibrotactile biofeedback for haptic information'. In: *Journal of NeuroEngineering and Rehabilitation* 4.1 (Oct. 2007), p. 40. DOI: 10.1186/1743-0003-4-40 (cited on pages 37, 45, 47, 53, 60, 80).

[118] Camille Jeunet et al. 'Using Recent BCI Literature to Deepen our Understanding of Clinical Neurofeedback: A Short Review'. In: *Neuroscience* (Mar. 2018). DOI: 10.1016/J.NEUROSCIENCE.2018.03.013 (cited on page 37).

[119] Léa Pillette. 'Redefining and Adapting Feedback for Mental-Imagery based Brain-Computer Interface User Training to the Learners' Traits and States'. PhD thesis. Université de Bordeaux, 2019 (cited on page 37).

[120] Seiji Aoyagi, Takaaki Tanaka, and Mamoru Minami. 'Recognition of contact state of four layers arrayed type tactile sensor by using neural network'. In: *Proceedings of IEEE ICIA 2006 - 2006 IEEE International Conference on Information Acquisition* (2006), pp. 393–397. DOI: 10.1109/ICIA.2006.305744 (cited on page 37).

[121] Håkan Olausson, Johan Wessberg, and Naoyuki Kakuda. 'Tactile directional sensibility: peripheral neural mechanisms in man'. In: *Brain research* 866.1-2 (2000), pp. 178–187 (cited on page 37).

[122] Kairu Li et al. 'Non-Invasive Stimulation-Based Tactile Sensation for Upper-Extremity Prosthesis: A Review'. In: *IEEE Sensors Journal* 17.9 (May 2017), pp. 2625–2635. DOI: 10.1109/JSEN.2017.2674965 (cited on page 37).

[123] Margherita Antona and Constantine Stephanidis. *Universal Access in Human-Computer Interaction. Access to the Human Environment and Culture: 9th International Conference, UAHCI 2015, Held as Part of HCI International 2015, Los Angeles, CA, USA, August 2-7, 2015, Proceedings*. Vol. 9178. Springer, 2015 (cited on page 38).

[124] Adolf Faller, Michael Schünke, and Gabriele Schünke. *Der Körper des Menschen: Einführung in Bau und Funktion*. Thieme Stuttgart, 2012 (cited on page 38).

[125] Claudio Pacchierotti et al. 'Wearable haptic systems for the fingertip and the hand: Taxonomy, review, and perspectives'. In: *IEEE Transactions on Haptics* 10.4 (2017), pp. 580–600. DOI: 10.1109/TOH.2017.2689006 (cited on page 38).

[126] Seahak Kim et al. *Haptic Interface with 7 DOF Using 8 Strings : SPIDAR-G*. 2000. URL: https://www.semanticscholar.org/paper/Haptic-Interface-with-7-DOF-Using-8-Strings-%7B%5C%%7D3A-Kim-Ishii/ea161352c53bb1339bc553c5ae8f259af03c6407 (cited on pages 38, 43).

[127] Thomas H Massie, J Kenneth Salisbury, et al. 'The phantom haptic interface: A device for probing virtual objects'. In: *Proceedings of the ASME winter annual meeting, symposium on haptic interfaces for virtual environment and teleoperator systems*. Vol. 55. 1. Citeseer. 1994, pp. 295–300 (cited on pages 38, 41).

[128] Claudio Pacchierotti et al. 'Wearable haptic systems for the fingertip and the hand: taxonomy, review, and perspectives'. In: *IEEE transactions on haptics* 10.4 (2017), pp. 580–600 (cited on pages 39, 42).

[129] Victor Rodrigo Mercado, Maud Marchal, and Anatole Lécuyer. 'ENTROPiA: Towards Infinite Surface Haptic Displays in Virtual Reality Using Encountered-Type Rotating Props'. In: *IEEE Transactions on Visualization and Computer Graphics* (2019) (cited on page 39).

[130] Lenny Lucas, Matthew DiCicco, and Yoky Matsuoka. 'An EMG-controlled hand exoskeleton for natural pinching'. In: *Journal of Robotics and Mechatronics* 16 (2004), pp. 482–488 (cited on page 39).

[131] Claudio Pacchierotti et al. 'The hRing: A wearable haptic device to avoid occlusions in hand tracking'. In: *2016 IEEE Haptics Symposium (HAPTICS)*. IEEE. 2016, pp. 134–139 (cited on page 39).

[132] James J Gibson. 'Psychological Review Observations on Active Touch ''. In: *Psychological Review* 69.6 (1962), pp. 477–491 (cited on page 39).

[133] A. Frisoli et al. 'A Fingertip Haptic Display for Improving Curvature Discrimination'. In: *Presence: Teleoperators and Virtual Environments* 17.6 (Dec. 2008), pp. 550–561. DOI: 10.1162/pres.17.6.550 (cited on pages 39, 40).

[134] Carlos Bermejo and Pan Hui. 'A survey on haptic technologies for mobile augmented reality'. In: (2017), pp. 1–24 (cited on page 39).

[135] Tom Carter et al. 'UltraHaptics: multi-point mid-air haptic feedback for touch surfaces'. In: *Proceedings of the 26th annual ACM symposium on User interface software and technology*. ACM. 2013, pp. 505–514 (cited on page 39).

[136] Susan J Lederman and I Introduction. 'Chapter 6 : Touch'. In: *Most* 4 (2002), pp. 147–176 (cited on page 40).

[137] Lynette A. Jones and Nadine B. Sarter. 'Tactile displays: Guidance for their design and application'. In: *Human Factors* 50.1 (2008), pp. 90–111. DOI: 10.1518/001872008X250638 (cited on pages 40, 41).

[138] BL Richardson and MA Symmons. 'Vibrotactile devices for the deaf: are they out of touch?' In: *The Annals of otology, rhinology & laryngology. Supplement* 166 (1995), pp. 458–461 (cited on page 40).

[139] Roger W Cholewiak and Amy A Collins. 'Vibrotactile localization on the arm: Effects of place, space, and age'. In: *Perception & psychophysics* 65.7 (2003), pp. 1058–1077 (cited on page 40).

[140] Massimiliano Gabardi et al. 'A new wearable fingertip haptic interface for the rendering of virtual shapes and surface features'. In: *2016 IEEE Haptics Symposium (HAPTICS)*. IEEE. 2016, pp. 140–146 (cited on page 40).

[141] Xavier de Tinguy et al. 'WeATaViX: WEarable Actuated TAngibles for VIrtual reality eXperiences'. In: *EUROHAPTICS 2020*. 2020 (cited on page 40).

[142] Mohamed Guiatni et al. 'A combined force and thermal feedback interface for minimally invasive procedures simulation'. In: *Ieee/Asme Transactions On Mechatronics* 18.3 (2012), pp. 1170–1181 (cited on pages 41, 43).

[143] Yoonju Cho et al. 'Wireless temperature sensing cosmesis for prosthesis'. In: *2007 IEEE 10th International Conference on Rehabilitation Robotics*. IEEE. 2007, pp. 672–677 (cited on page 41).

[144] Lynette A Jones and Hsin-Ni Ho. 'Warm or cool, large or small? The challenge of thermal displays'. In: *IEEE Transactions on Haptics* 1.1 (2008), pp. 53–70 (cited on page 41).

[145] Ian R Summers et al. 'Vibrotactile and electrotactile perception of time-varying pulse trains'. In: *The Journal of the Acoustical Society of America* 95.3 (1994), pp. 1548–1558 (cited on page 41).

[146] Kurt A Kaczmarek and Steven J Haase. 'Pattern identification as a function of stimulation on a fingertip-scanned electrotactile display'. In: *IEEE Transactions on neural systems and rehabilitation engineering* 11.3 (2003), pp. 269–275 (cited on page 41).

[147] Katrin Wolf and Timm Bäder. 'Illusion of surface changes induced by tactile and visual touch feedback'. In: *Proceedings of the 33rd Annual ACM Conference Extended Abstracts on Human Factors in Computing Systems*. 2015, pp. 1355–1360 (cited on page 41).

[148] Gary B Rollman. 'Electrocutaneous stimulation.' In: (1974) (cited on page 41).

[149] Max Pfeiffer and Michael Rohs. 'Haptic feedback for wearables and textiles based on electrical muscle stimulation'. In: *Smart textiles*. Springer, 2017, pp. 103–137 (cited on pages 41, 42).

[150] Febo Cincotti et al. 'Preliminary experimentation on vibrotactile feedback in the context of mu-rhythm based BCI.' In: *Conference proceedings : ... Annual International Conference of the IEEE Engineering in Medicine and Biology Society. IEEE Engineering in Medicine and Biology Society. Annual Conference* 2007 (2007), pp. 4739–42. DOI: 10.1109/IEMBS.2007.4353398 (cited on page 43).

[151] Francesco Chinello et al. 'A three DoFs wearable tactile display for exploration and manipulation of virtual objects'. In: *2012 IEEE Haptics Symposium (HAPTICS)*. IEEE, Mar. 2012, pp. 71–76. DOI: 10.1109/HAPTIC.2012.6183772 (cited on page 43).

[152] Adam J Wilson et al. 'Lingual electrotactile stimulation as an alternative sensory feedback pathway for brain – computer interface applications'. In: (2012). DOI: 10.1088/1741-2560/9/4/045007 (cited on pages 43, 45, 47).

[153] Ander Ramos-Murguialday et al. 'Proprioceptive Feedback and Brain Computer Interface (BCI) Based Neuroprostheses'. In: *PLoS ONE* 7.10 (Oct. 2012). Ed. by Michael Hendricks, e47048. DOI: 10.1371/journal.pone.0047048 (cited on pages 43, 45, 46, 84).

[154] Robert Leeb et al. 'BCI controlled neuromuscular electrical stimulation enables sustained motor recovery in chronic stroke victims'. In: *Proceedings of the 6th International Brain-Computer Interface Meeting*. CONF. 2016 (cited on pages 42, 43, 45).

[155] Eduardo López-Larraz et al. 'Brain-machine interfaces for rehabilitation in stroke: a review'. In: *NeuroRehabilitation* June (2018). DOI: 10.3233/NRE-172394 (cited on pages 41, 47).

[156] Makoto Sato. 'SPace Interface Device for Artificial Reality-SPIDAR. The Transactions of the Institute of Electronics'. In: *Information and Communication Engineers (D-II)* 74.7 (1991), pp. 887–894 (cited on page 42).

[157] Robert L Williams II. 'Cable-suspended haptic interface'. In: () (cited on page 42).

[158] Daniele Leonardis et al. 'An EMG-Controlled Robotic Hand Exoskeleton for Bilateral Rehabilitation'. In: *IEEE Transactions on Haptics* 8.2 (Apr. 2015), pp. 140–151. DOI: 10.1109/TOH.2015.2417570 (cited on page 42).

[159] Hugh Herr. 'Exoskeletons and orthoses: classification, design challenges and future directions'. In: *Journal of neuroengineering and rehabilitation* 6.1 (2009), p. 21 (cited on page 42).

[160] Gert Pfurtscheller et al. ''Thought'–control of functional electrical stimulation to restore hand grasp in a patient with tetraplegia'. In: *Neuroscience letters* 351.1 (2003), pp. 33–36 (cited on pages 42, 45, 47).

[161] Kairu Li et al. 'Non-Invasive Stimulation-Based Tactile Sensation for Upper-Extremity Prosthesis: A Review'. In: *IEEE Sensors Journal* 17.9 (May 2017), pp. 2625–2635. DOI: 10.1109/JSEN.2017.2674965 (cited on page 42).

[162] TaeHoon Kim, SeongSik Kim, and ByoungHee Lee. 'Effects of Action Observational Training Plus Brain-Computer Interface-Based Functional Electrical Stimulation on Paretic Arm Motor Recovery in Patient with Stroke: A Randomized Controlled Trial'. In: *Occupational Therapy International* 23.1 (Mar. 2016), pp. 39–47. DOI: 10.1002/oti.1403 (cited on page 42).

[163] Alexander A. Frolov et al. 'Post-stroke Rehabilitation Training with a Motor-Imagery-Based Brain-Computer Interface (BCI)-Controlled Hand Exoskeleton: A Randomized Controlled Multicenter Trial'. In: *Frontiers in Neuroscience* 11 (July 2017), p. 400. DOI: 10.3389/fnins.2017.00400 (cited on pages 42, 45–47).

[164] Natalie Mrachacz-Kersting et al. 'Efficient neuroplasticity induction in chronic stroke patients by an associative brain-computer interface'. In: *Journal of Neurophysiology* 115.3 (Mar. 2016), pp. 1410–1421. DOI: 10.1152/jn.00918.2015 (cited on page 42).

[165] Gert Pfurtscheller and Christa Neuper. 'Motor imagery activates primary sensorimotor area in humans'. In: *Neuroscience letters* 239.2-3 (1997), pp. 65–68 (cited on page 44).

[166] Stuart N Baker. 'Oscillatory interactions between sensorimotor cortex and the periphery'. In: *Current opinion in neurobiology* 17.6 (2007), pp. 649–655 (cited on page 44).

[167] Han Yuan and Bin He. 'Brain–computer interfaces using sensorimotor rhythms: current state and future perspectives'. In: *IEEE Transactions on Biomedical Engineering* 61.5 (2014), pp. 1425–1435 (cited on page 44).

[168] Laurent George et al. 'Combining Brain-Computer Interfaces and Haptics: Detecting Mental Workload to Adapt Haptic Assistance'. In: Springer, Berlin, Heidelberg, 2012, pp. 124–135. DOI: 10.1007/978-3-642-31401-8_12 (cited on page 44).

[169] Roberta L Klatzky and Susan J Lederman. 'Touch'. In: *Handbook of psychology* (2003), pp. 147–176 (cited on page 44).

[170] A Chowdhury et al. 'Active Physical Practice Followed by Mental Practice Using BCI-Driven Hand Exoskeleton: A Pilot Trial for Clinical Effectiveness and Usability'. In: *IEEE Journal of Biomedical and Health Informatics* (2018), pp. 1–1. DOI: 10.1109/JBHI.2018.2863212 (cited on pages 45–47).

[171] Sam Darvishi et al. 'Proprioceptive Feedback Facilitates Motor Imagery-Related Operant Learning of Sensorimotor β-Band Modulation'. In: *Frontiers in Neuroscience* 11 (Feb. 2017), p. 60. DOI: 10.3389/fnins.2017.00060 (cited on pages 45, 46).

[172] Ander Ramos-Murguialday et al. 'Brain–machine interface in chronic stroke rehabilitation: a controlled study'. In: *Annals of neurology* 74.1 (2013), pp. 100–108 (cited on pages 45, 47).

[173] Surjo R Soekadar et al. 'ERD-based online brain–machine interfaces (BMI) in the context of neurorehabilitation: optimizing BMI learning and performance'. In: *IEEE Transactions on Neural Systems and Rehabilitation Engineering* 19.5 (2011), pp. 542–549 (cited on pages 45–47).

[174] Surjo R Soekadar et al. 'Enhancing Hebbian learning to control brain oscillatory activity'. In: *Cerebral cortex* 25.9 (2015), pp. 2409–2415 (cited on page 45).

[175] Takashi Ono et al. 'Brain-computer interface with somatosensory feedback improves functional recovery from severe hemiplegia due to chronic stroke'. In: *Frontiers in Neuroengineering* 7 (Aug. 2014), p. 19. DOI: 10.3389/fneng.2014.00019 (cited on pages 45–47).

[176] David T. Bundy et al. 'Contralesional Brain–Computer Interface Control of a Powered Exoskeleton for Motor Recovery in Chronic Stroke Survivors'. In: *Stroke* 48.7 (July 2017), pp. 1908–1915. DOI: 10.1161/STROKEAHA.116.016304 (cited on pages 45–47).

[177] Chih-Wei Chen, Chou-Ching K Lin, Ming-Shaung Ju, et al. 'Hand orthosis controlled using brain-computer interface'. In: *Journal of Medical and Biological Engineering* 29.5 (2009), pp. 234–241 (cited on pages 45, 46).

[178] SR Soekadar et al. 'Hybrid EEG/EOG-based brain/neural hand exoskeleton restores fully independent daily living activities after quadriplegia'. In: *Science Robotics* 1.1 (2016), eaag3296–1 (cited on page 45).

[179] Kai Keng Ang et al. 'Clinical study of neurorehabilitation in stroke using EEG-based motor imagery brain-computer interface with robotic feedback'. In: *2010 Annual International Conference of the IEEE Engineering in Medicine and Biology*. IEEE, Aug. 2010, pp. 5549–5552. DOI: 10.1109/IEMBS.2010.5626782 (cited on pages 45–47).

[180] Kai Keng Ang et al. 'Brain-computer interface-based robotic end effector system for wrist and hand rehabilitation: results of a three-armed randomized controlled trial for chronic stroke'. In: *Frontiers in Neuroengineering* 7 (Aug. 2014), p. 30. DOI: 10.3389/fneng.2014.00030 (cited on pages 45, 46).

[181] Robert Leeb et al. 'Freeing the visual channel by exploiting vibrotactile BCI feedback'. In: *2013 35th Annual International Conference of the IEEE Engineering in Medicine and Biology Society (EMBC)*. IEEE, Aug. 2013, pp. 3093–3096. DOI: 10.1109/EMBC.2013.6610195 (cited on pages 45, 47, 53).

[182] S. P. Liburkina et al. 'A Motor Imagery-Based Brain–Computer Interface with Vibrotactile Stimuli'. In: *Neuroscience and Behavioral Physiology* 48.9 (2018). DOI: 10.1007/s11055-018-0669-2 (cited on pages 45, 47).

[183] Camille Jeunet et al. 'Continuous tactile feedback for motor-imagery based brain-computer interaction in a multitasking context'. In: *IFIP Conference on Human-Computer Interaction*. Springer. 2015, pp. 488–505 (cited on pages 45, 82).

[184] B. M. London et al. 'Designing stimulation patterns for an afferent BMI: Representation of kinetics in somatosensory cortex'. In: *2011 Annual International Conference of the IEEE Engineering in Medicine and Biology Society*. IEEE, Aug. 2011, pp. 7521–7524. DOI: 10.1109/IEMBS.2011.6091854 (cited on page 44).

[185] A.R. Murguialday et al. 'Transition from the locked in to the completely locked-in state: A physiological analysis'. In: *Clinical Neurophysiology* 122.5 (2011), pp. 925–933. DOI: 10.1016/j.clinph.2010.08.019 (cited on page 46).

[186] G Lioi et al. 'Bimodal EEG-fMRI neurofeedback for stroke rehabilitation: A case report'. In: *Annals of Physical and Rehabilitation Medicine* 61 (2018), e482–e483 (cited on pages 47, 84).

[187] Giulia Lioi et al. 'A Multi-Target Motor Imagery Training Using Bimodal EEG-fMRI Neurofeedback: A Pilot Study in Chronic Stroke Patients'. In: *Frontiers in Human Neuroscience* 14 (2020), p. 37 (cited on page 47).

[188] Ethan R. Buch et al. 'Parietofrontal integrity determines neural modulation associated with grasping imagery after stroke'. In: *Brain* 135.2 (Feb. 2012), pp. 596–614. DOI: 10.1093/brain/awr331 (cited on page 47).

[189] NS Ward et al. 'Neural correlates of motor recovery after stroke: a longitudinal fMRI study'. In: *Brain* 126.11 (2003), pp. 2476–2496 (cited on page 47).

[190] F Aloise et al. 'Multimodal stimulation for a P300-based BCI'. In: *Int. J. Bioelectromagn* 9.3 (2007), pp. 128–130 (cited on pages 48, 50).

[191] Zulay R. Lugo et al. 'A Vibrotactile P300-Based Brain–Computer Interface for Consciousness Detection and Communication'. In: *Clinical EEG and Neuroscience* 45.1 (Jan. 2014), pp. 14–21. DOI: 10.1177/1550059413505533 (cited on page 50).

[192] Z. Qiu et al. 'Comparisons of three BCIs which do not rely on the visual modality'. In: *2016 3rd International Conference on Systems and Informatics, ICSAI 2016*. 2017, pp. 82–86. DOI: 10.1109/ICSAI.2016.7810934 (cited on page 50).

[193] Christoph Guger et al. 'Complete Locked-in and Locked-in Patients: Command Following Assessment and Communication with Vibro-Tactile P300 and Motor Imagery Brain-Computer Interface Tools.' In: *Frontiers in neuroscience* 11 (May 2017), p. 251. DOI: 10.3389/fnins.2017.00251 (cited on pages 49, 50).

[194] M. Severens et al. 'Comparing tactile and visual gaze-independent brain-computer interfaces in patients with amyotrophic lateral sclerosis and healthy users'. In: *Clinical Neurophysiology* 125.11 (2014), pp. 2297–2304. DOI: 10.1016/j.clinph.2014.03.005 (cited on page 50).

[195] Marjolein van der Waal et al. 'Introducing the tactile speller: an ERP-based brain–computer interface for communication'. In: *Journal of Neural Engineering* 9.4 (2012), p. 045002 (cited on pages 49, 50).

[196] Katsuhiko Hamada et al. 'Airborne ultrasonic tactile display brain-computer interface paradigm'. In: *arXiv preprint arXiv:1404.4184* (2014) (cited on pages 48, 50).

[197] Kensuke Shimizu et al. 'Tactile pressure brain-computer interface using point matrix pattern paradigm'. In: *2014 Joint 7th International Conference on Soft Computing and Intelligent Systems (SCIS) and 15th International Symposium on Advanced Intelligent Systems (ISIS)*. IEEE. 2014, pp. 473–477 (cited on pages 48, 50).

[198] S. Kono et al. 'EEG signal processing and classification for the novel tactile-force brain-computer interface paradigm'. In: *Proceedings - 2013 International Conference on Signal-Image Technology and Internet-Based Systems, SITIS 2013*. 2013, pp. 812–817. DOI: 10.1109/SITIS.2013.132 (cited on pages 48, 50).

[199] Emanuel Donchin, Kevin M Spencer, and Ranjith Wijesinghe. 'The mental prosthesis: assessing the speed of a P300-based brain-computer interface'. In: *IEEE transactions on rehabilitation engineering* 8.2 (2000), pp. 174–179 (cited on page 48).

[200] Tomasz M Rutkowski and Hiromu Mori. 'Tactile and bone-conduction auditory brain computer interface for vision and hearing impaired users'. In: *Journal of Neuroscience Methods* 244 (2015), pp. 45–51 (cited on page 48).

[201] Hiromu Mori et al. 'Multi-command tactile and auditory brain computer interface based on head position stimulation'. In: *arXiv preprint arXiv:1301.6357* (2013) (cited on page 48).

[202] BZ Allison and C Neuper. *Could anyone use a BCI?(B+H) CI: Brain–Computer Interfaces (Human–Computer Interaction series)*. 2010 (cited on page 48).

[203] Joseph R. Duffy. *Motor speech disorders : substrates, differential diagnosis, and management*, p. 499 (cited on page 48).

[204] Ahmed A. Karim et al. 'Neural Internet: Web Surfing with Brain Potentials for the Completely Paralyzed'. In: *Neurorehabilitation and Neural Repair* 20.4 (Dec. 2006), pp. 508–515. DOI: 10.1177/1545968306290661 (cited on page 48).

[205] Jonathan R Wolpaw et al. 'Brain–computer interfaces for communication and control'. In: *Clinical Neurophysiology* 113.6 (June 2002), pp. 767–791. DOI: 10.1016/S1388-2457(02)00057-3 (cited on pages 1, 10, 48).

[206] T Kaufmann, A Herweg, and A Kübler. 'Tactually-evoked event-related potentials for bci-based wheelchair control in a virtual environment'. In: *Proceedings of the Fifth International Brain Computer Interface Meeting*. 2013 (cited on page 49).

[207] G.R. Müller-Putz et al. 'Steady-state somatosensory evoked potentials: Suitable brain signals for brain-computer interfaces?' In: *IEEE Transactions on Neural Systems and Rehabilitation Engineering* 14.1 (2006), pp. 30–37. DOI: 10.1109/TNSRE.2005.863842 (cited on pages 49, 51).

[208] C. Breitwieser et al. 'Somatosensory evoked potentials elicited by stimulating two fingers from one hand — Usable for BCI?' In: *2011 Annual International Conference of the IEEE Engineering in Medicine and Biology Society*. IEEE, Aug. 2011, pp. 6373–6376. DOI: 10.1109/IEMBS.2011.6091573 (cited on page 51).

[209] L. Yao et al. 'A BCI System Based on Somatosensory Attentional Orientation'. In: *IEEE Transactions on Neural Systems and Rehabilitation Engineering* 25.1 (2017), pp. 78–87. DOI: 10.1109/TNSRE.2016.2572226 (cited on page 51).

[210] Sangtae Ahn et al. 'Achieving a hybrid brain-computer interface with tactile selective attention and motor imagery.' In: *Journal of neural engineering* 11.6 (Dec. 2014), p. 066004. DOI: 10.1088/1741-2560/11/6/066004 (cited on page 51).

[211] K.-T. Kim and S.-W. Lee. 'Towards an EEG-based intelligent wheelchair driving system with vibro-tactile stimuli'. In: *2016 IEEE International Conference on Systems, Man, and Cybernetics, SMC 2016 - Conference Proceedings*. 2017, pp. 2382–2385. DOI: 10.1109/SMC.2016.7844595 (cited on pages 49, 51, 59).

[212] Christian Breitwieser et al. 'Stability and distribution of steady-state somatosensory evoked potentials elicited by vibro-tactile stimulation'. In: *Medical & biological engineering & computing* 50.4 (2012), pp. 347–357 (cited on page 49).

[213] Marianne Severens et al. 'A multi-signature brain – computer interface : use of transient and steady-state responses'. In: (2013). DOI: 10.1088/1741-2560/10/2/026005 (cited on page 49).

[214] Sangtae Ahn, Kiwoong Kim, and Sung Chan Jun. 'Steady-State Somatosensory Evoked Potential for Brain-Computer Interface—Present and Future'. In: *Frontiers in Human Neuroscience* 9 (Jan. 2016), p. 716. DOI: 10.3389/fnhum.2015.00716 (cited on page 49).

[215] Sangtae Ahn and Sung Chan Jun. 'Feasibility of hybrid BCI using ERD- and SSSEP-BCI'. In: *2012 12th International Conference on Control, Automation and Systems* (2012), pp. 2053–2056 (cited on page 49).

[216] Thomas T Hewett et al. *ACM SIGCHI curricula for human-computer interaction*. ACM, 1992 (cited on page 53).

[217] Xiaokang Shu et al. 'Enhanced Motor Imagery-Based BCI Performance via Tactile Stimulation on Unilateral Hand.' In: *Frontiers in human neuroscience* 11 (Dec. 2017), p. 585. DOI: 10.3389/fnhum.2017.00585 (cited on pages 53, 54).

[218] Ainhoa Insausti-Delgado et al. 'Influence of trans-spinal magnetic stimulation in electrophysiological recordings for closed-loop rehabilitative systems'. In: *Engineering in Medicine and Biology Society (EMBC), 2017 39th Annual International Conference of the IEEE*. IEEE. 2017, pp. 2518–2521 (cited on page 53).

[219] L Kauhanen et al. 'HAPTIC FEEDBACK COMPARED WITH VISUAL FEEDBACK FOR BCI'. In: (2006) (cited on page 53).

[220] Maximilian Hommelsen et al. 'Sensory Feedback Interferes with Mu Rhythm Based Detection of Motor Commands from Electroencephalographic Signals'. In: *Frontiers in Human Neuroscience* 11 (Nov. 2017), p. 523. DOI: 10.3389/fnhum.2017.00523 (cited on pages 53, 80).

[221] Hossein Bashashati et al. 'Comparing different classifiers in sensory motor brain computer interfaces'. In: *PloS one* 10.6 (2015), e0129435 (cited on page 54).

[222] Robert A Scheidt et al. 'Persistence of motor adaptation during constrained, multi-joint, arm movements'. In: *Journal of neurophysiology* 84.2 (2000), pp. 853–862 (cited on page 54).

[223] Chi-Ying Lin et al. 'Development of a novel haptic glove for improving finger dexterity in poststroke rehabilitation'. In: *Technology and Health Care* 24.s1 (2016), S97–S103 (cited on page 54).

[224] Andreas Wege and Günter Hommel. 'Development and control of a hand exoskeleton for rehabilitation of hand injuries'. In: *2005 IEEE/RSJ International Conference on Intelligent Robots and Systems*. IEEE. 2005, pp. 3046–3051 (cited on page 54).

[225] Sasha Blue Godfrey, Rahsaan J Holley, and Peter S Lum. 'Clinical effects of using HEXORR (Hand Exoskeleton Rehabilitation Robot) for movement therapy in stroke rehabilitation'. In: *American journal of physical medicine & rehabilitation* 92.11 (2013), pp. 947–958 (cited on page 54).

[226] HyunKi In et al. 'Jointless structure and under-actuation mechanism for compact hand exoskeleton'. In: *2011 IEEE International Conference on Rehabilitation Robotics*. IEEE, July 2011, pp. 1–6. DOI: 10.1109/ICORR.2011.5975394 (cited on page 54).

[227] M. V. Lukoyanov et al. 'The Efficiency of the Brain-Computer Interfaces Based on Motor Imagery with Tactile and Visual Feedback'. In: *Human Physiology* 44.3 (May 2018), pp. 280–288. DOI: 10.1134/S0362119718030088 (cited on pages 54, 55).

[228] Carmen Vidaurre and Benjamin Blankertz. 'Towards a Cure for BCI Illiteracy'. In: *Brain Topography* 23.2 (June 2010), pp. 194–198. DOI: 10.1007/s10548-009-0121-6 (cited on page 54).

[229] Benjamin Blankertz et al. 'Neurophysiological predictor of SMR-based BCI performance'. In: *NeuroImage* 51.4 (July 2010), pp. 1303–1309. DOI: 10.1016/J.NEUROIMAGE.2010.03.022 (cited on page 55).

[230] Kai Keng Ang and Cuntai Guan. 'Brain–Computer Interface for Neurorehabilitation of Upper Limb After Stroke'. In: *Proceedings of the IEEE* 103.6 (June 2015), pp. 944–953. DOI: 10.1109/JPROC.2015.2415800 (cited on page 55).

[231] Martijn Schreuder, Benjamin Blankertz, and Michael Tangermann. 'A New Auditory Multi-Class Brain-Computer Interface Paradigm: Spatial Hearing as an Informative Cue'. In: *PLoS ONE* 5.4 (Apr. 2010). Ed. by Jun Yan, e9813. DOI: 10.1371/journal.pone.0009813 (cited on page 55).

[232] Gaetano Gargiulo et al. 'Investigating the role of combined acoustic-visual feedback in one-dimensional synchronous brain computer interfaces, a preliminary study'. In: *Medical Devices: Evidence and Research* 5 (Sept. 2012), p. 81. DOI: 10.2147/MDER.S36691 (cited on page 55).

[233] Jörn Rittweger. 'Vibration as an exercise modality: how it may work, and what its potential might be'. eng. In: *European Journal of Applied Physiology* 108.5 (2010), pp. 877–904. DOI: 10.1007/s00421-009-1303-3 (cited on pages 58, 85).

[234] N. Murillo et al. 'Focal vibration in neurorehabilitation'. eng. In: *European Journal of Physical and Rehabilitation Medicine* 50.2 (2014), pp. 231–242 (cited on pages 58, 85).

[235] Na Jin Seo et al. 'Use of imperceptible wrist vibration to modulate sensorimotor cortical activity'. In: *Experimental brain research* 237.3 (2019), pp. 805–816 (cited on page 58).

[236] G. M. Goodwin, D. I. McCloskey, and P. B. Matthews. 'Proprioceptive illusions induced by muscle vibration: contribution by muscle spindles to perception?' eng. In: *Science (New York, N.Y.)* 175.4028 (1972), pp. 1382–1384 (cited on pages 58, 64, 68).

[237] Jeffrey M. Kenzie et al. 'Illusory limb movements activate different brain networks than imposed limb movements: an ALE meta-analysis'. eng. In: *Brain Imaging and Behavior* 12.4 (2018), pp. 919–930. DOI: 10.1007/s11682-017-9756-1 (cited on page 58).

[238] Eiichi Naito, Per E Roland, and H Henrik Ehrsson. 'I feel my hand moving: a new role of the primary motor cortex in somatic perception of limb movement'. In: *Neuron* 36.5 (2002), pp. 979–988 (cited on pages 58, 85).

[239] Eiichi Naito et al. 'Illusory Arm Movements Activate Cortical Motor Areas: A Positron Emission Tomography Study'. en. In: *Journal of Neuroscience* 19.14 (1999), pp. 6134–6144. DOI: 10.1523/JNEUROSCI.19-14-06134.1999. (Visited on 11/24/2018) (cited on pages 58, 68, 81).

[240] Patricia Romaiguère et al. 'Motor and parietal cortical areas both underlie kinaesthesia'. In: *Cognitive Brain Research* 16.1 (2003), pp. 74–82 (cited on pages 58, 80).

[241] Cosimo Costantino, Laura Galuppo, and Davide Romiti. 'Short-term effect of local muscle vibration treatment versus sham therapy on upper limb in chronic post-stroke patients: a randomized controlled trial'. eng. In: *European Journal of Physical and Rehabilitation Medicine* 53.1 (Feb. 2017), pp. 32–40. DOI: 10.23736/S1973-9087.16.04211-8 (cited on page 58).

[242] Kapka Mancheva et al. 'Vibration-Induced Kinesthetic Illusions and Corticospinal Excitability Changes'. eng. In: *Journal of Motor Behavior* 49.3 (2017), pp. 299–305. DOI: 10.1080/00222895.2016.1204263 (cited on page 58).

[243] Lior Botzer and Amir Karniel. 'Feedback and feedforward adaptation to visuomotor delay during reaching and slicing movements'. en. In: *European Journal of Neuroscience* 38.1 (2013), pp. 2108–2123. DOI: 10.1111/ejn.12211. (Visited on 05/24/2019) (cited on page 58).

[244] William Shelstad, Dustin C. Smith, and Barbara Chaparro. 'Gaming on the Rift: How Virtual Reality Affects Game User Satisfaction'. In: *Proceedings of the Human Factors and Ergonomics Society Annual Meeting* 61 (2017), pp. 2072–2076. DOI: 10.1177/1541931213602001 (cited on page 58).

[245] Mar Gonzalez-Franco and Christopher C. Berger. 'Avatar embodiment enhances haptic confidence on the out-of-body touch illusion'. eng. In: *IEEE transactions on haptics* (2019). DOI: 10.1109/TOH.2019.2925038 (cited on page 58).

[246] Daniel Perez-Marcos, Mel Slater, and Maria V. Sanchez-Vives. 'Inducing a virtual hand ownership illusion through a brain–computer interface:' en. In: *NeuroReport* 20.6 (2009), pp. 589–594. DOI: 10.1097/WNR.0b013e32832a0a2a. (Visited on 02/05/2019) (cited on page 59).

[247] Daniel Perez-Marcos. 'Virtual reality experiences, embodiment, videogames and their dimensions in neurorehabilitation'. eng. In: *Journal of Neuroengineering and Rehabilitation* 15.1 (2018), p. 113. DOI: 10.1186/s12984-018-0461-0 (cited on page 59).

[248] Nassima Ouramdane, Samir Otmane, and Malik Mallem. 'Interaction 3D en Réalité Virtuelle - Etat de l'art'. In: *Technique et Science Informatiques* 28.8 (2009), pp. 1017–1049. DOI: 10.3166/tsi.28.1017-1049. (Visited on 09/24/2019) (cited on page 59).

[249] Rebecca Fribourg et al. 'Avatar and Sense of Embodiment: Studying the Relative Preference Between Appearance, Control and Point of View'. In: *IEEE Transactions on Visualization and Computer Graphics* 26.5 (2020), pp. 2062–2072 (cited on page 59).

[250] Maria Pyasik, Gaetano Tieri, and Lorenzo Pia. 'Visual appearance of the virtual hand affects embodiment in the virtual hand illusion'. In: *Scientific reports* 10.1 (2020), pp. 1–11 (cited on page 59).

[251] So-Yeon Kim et al. 'Impact of Body Size Match to an Avatar on the Body Ownership Illusion and User's Subjective Experience'. In: *Cyberpsychology, Behavior, and Social Networking* 23.4 (2020), pp. 234–241 (cited on page 59).

[252] Mar Gonzalez-Franco and Jaron Lanier. 'Model of Illusions and Virtual Reality'. eng. In: *Frontiers in Psychology* 8 (2017), p. 1125. DOI: 10.3389/fpsyg.2017.01125 (cited on page 59).

[253] M. D. Rinderknecht et al. 'Combined tendon vibration and virtual reality for post-stroke hand rehabilitation'. In: *2013 World Haptics Conference (WHC)*. 2013, pp. 277–282. DOI: 10.1109/WHC.2013.6548421 (cited on pages 59, 60, 70).

[254] Maria V Sanchez-Vives et al. 'Virtual hand illusion induced by visuomotor correlations'. In: *PloS one* 5.4 (2010), e10381 (cited on page 59).

[255] Elena Kokkinara and Mel Slater. 'Measuring the effects through time of the influence of visuomotor and visuotactile synchronous stimulation on a virtual body ownership illusion'. In: *Perception* 43.1 (2014), pp. 43–58 (cited on page 59).

[256] Th Mulder. 'Motor imagery and action observation: cognitive tools for rehabilitation'. In: *Journal of neural transmission* 114.10 (2007), pp. 1265–1278 (cited on pages 59, 80).

[257] Tácia Cotinguiba Machado et al. 'Efficacy of motor imagery additional to motor-based therapy in the recovery of motor function of the upper limb in post-stroke individuals: a systematic review'. In: *Topics in Stroke Rehabilitation* 26.7 (2019), pp. 548–553 (cited on page 59).

[258] Jean Decety. 'The neurophysiological basis of motor imagery'. In: *Behavioural brain research* 77.1-2 (1996), pp. 45–52 (cited on page 59).

[259] Marina Kilintari et al. 'Brain activation profiles during kinesthetic and visual imagery: An fMRI study'. In: *Brain research* 1646 (2016), pp. 249–261 (cited on page 59).

[260] Parth Chholak et al. 'Visual and kinesthetic modes affect motor imagery classification in untrained subjects'. In: *Scientific reports* 9.1 (2019), pp. 1–12 (cited on pages 59, 96).

[261] Giovanni Buccino. 'Action observation treatment: a novel tool in neurorehabilitation'. In: *Philosophical Transactions of the Royal Society B: Biological Sciences* 369.1644 (2014), p. 20130185 (cited on page 59).

[262] Hirotaka Nagai and Toshihisa Tanaka. 'Action observation of own hand movement enhances event-related desynchronization'. In: *IEEE Transactions on Neural Systems and Rehabilitation Engineering* 27.7 (2019), pp. 1407–1415 (cited on pages 59, 82).

[263] Gert Pfurtscheller and FH Lopes Da Silva. 'Event-related EEG/MEG synchronization and desynchronization: basic principles'. In: *Clinical neurophysiology* 110.11 (1999), pp. 1842–1857 (cited on pages 60, 73, 113).

[264] Christa Neuper and Gert Pfurtscheller. 'Event-related dynamics of cortical rhythms: frequency-specific features and functional correlates'. In: *International journal of psychophysiology* 43.1 (2001), pp. 41–58 (cited on pages 60, 81).

[265] Fabien Lotte. 'A tutorial on EEG signal-processing techniques for mental-state recognition in brain–computer interfaces'. In: *Guide to Brain-Computer Music Interfacing*. Springer, 2014, pp. 133–161 (cited on page 60).

[266] Martin Lotze et al. 'Activation of cortical and cerebellar motor areas during executed and imagined hand movements: an fMRI study'. In: *Journal of cognitive neuroscience* 11.5 (1999), pp. 491–501 (cited on page 60).

[267] Chloé Thyrion and Jean-Pierre Roll. 'Perceptual integration of illusory and imagined kinesthetic images'. In: *Journal of Neuroscience* 29.26 (2009), pp. 8483–8492 (cited on page 60).

[268] Lin Yao et al. 'A novel calibration and task guidance framework for motor imagery BCI via a tendon vibration induced sensation with kinesthesia illusion'. In: *Journal of neural engineering* 12.1 (2014), p. 016005 (cited on pages 60, 80, 81).

[269] Michele Barsotti et al. 'Effects of Continuous Kinaesthetic Feedback Based on Tendon Vibration on Motor Imagery BCI Performance'. In: *IEEE Transactions on Neural Systems and Rehabilitation Engineering* 26.1 (2018), pp. 105–114. DOI: 10.1109/TNSRE.2017.2739244 (cited on pages 60, 70, 82).

[270] D. Leonardis et al. 'Illusory perception of arm movement induced by visuo-proprioceptive sensory stimulation and controlled by motor imagery'. In: *2012 IEEE Haptics Symposium (HAPTICS)*. 2012, pp. 421–424. DOI: 10.1109/HAPTIC.2012.6183825 (cited on pages 60, 64).

[271] Emmanuele Tidoni et al. 'Illusory movements induced by tendon vibration in right- and left-handed people'. eng. In: *Experimental Brain Research* 233.2 (Feb. 2015), pp. 375–383. DOI: 10.1007/s00221-014-4121-8 (cited on pages 60, 64, 68, 70, 81, 82).

[272] Gabriele Fusco et al. 'Illusion of arm movement evoked by tendon vibration in patients with spinal cord injury'. eng. In: *Restorative Neurology and Neuroscience* 34.5 (2016), pp. 815–826. DOI: 10.3233/RNN-160660 (cited on pages 60, 68).

[273] M. F. Tardy-Gervet, J. C. Gilhodes, and J. P. Roll. 'Interactions between visual and muscular information in illusions of limb movement'. eng. In: *Behavioural Brain Research* 20.2 (May 1986), pp. 161–174 (cited on page 60).

[274] M. Guerraz et al. 'Integration of visual and proprioceptive afferents in kinesthesia'. In: *Neuroscience* 223 (2012), pp. 258–268. DOI: 10.1016/j.neuroscience.2012.07.059. (Visited on 02/19/2019) (cited on page 60).

[275] Caroline Blanchard et al. 'Differential contributions of vision, touch and muscle proprioception to the coding of hand movements'. eng. In: *PloS One* 8.4 (2013), e62475. DOI: 10.1371/journal.pone.0062475 (cited on page 60).

[276] J. P. Roll, J. C. Gilhodes, and M. F. Tardy-Gervet. '[Effects of vision on tonic vibration response of a muscle or its antagonists in normal man (author's transl)]'. fre. In: *Experientia* 36.1 (1980), pp. 70–72 (cited on pages 60, 69).

[277] A. G. Feldman and M. L. Latash. 'Inversions of vibration-induced senso-motor events caused by supraspinal influences in man'. eng. In: *Neuroscience Letters* 31.2 (1982), pp. 147–151 (cited on pages 60, 68).

[278] James R. Lackner and Amy Beth Taublieb. 'Influence of vision on vibration-induced illusions of limb movement'. en. In: *Experimental Neurology* 85.1 (1984), pp. 97–106. DOI: 10.1016/0014-4886(84)90164-X. (Visited on 02/16/2019) (cited on pages 60, 68).

[279] Morgane Metral et al. 'Kinaesthetic mirror illusion and spatial congruence'. eng. In: *Experimental Brain Research* 233.5 (May 2015), pp. 1463–1470. DOI: 10.1007/s00221-015-4220-1 (cited on page 61).

[280] Barbara Caola et al. 'The Bodily Illusion in Adverse Conditions: Virtual Arm Ownership During Visuomotor Mismatch'. eng. In: *Perception* (2018), p. 301006618758211. DOI: 10.1177/0301006618758211 (cited on page 61).

[281] Nobuhiro Hagura et al. 'Activity in the Posterior Parietal Cortex Mediates Visual Dominance over Kinesthesia'. en. In: *Journal of Neuroscience* 27.26 (2007), pp. 7047–7053. DOI: 10.1523/JNEUROSCI.0970-07.2007. (Visited on 02/16/2019) (cited on page 68).

[282] Michele Barsotti et al. 'Effects of Continuous Kinaesthetic Feedback Based on Tendon Vibration on Motor Imagery BCI Performance'. eng. In: *IEEE transactions on neural systems and rehabilitation engineering: a publication of the IEEE Engineering in Medicine and Biology Society* 26.1 (2018), pp. 105–114. DOI: 10.1109/TNSRE.2017.2739244 (cited on pages 68, 80).

[283] K. S. Sunnerhagen, A. Opheim, and M. Alt Murphy. 'Onset, time course and prediction of spasticity after stroke or traumatic brain injury'. eng. In: *Annals of Physical and Rehabilitation Medicine* (May 2018). DOI: 10.1016/j.rehab.2018.04.004 (cited on page 68).

[284] G. Sheean. 'The pathophysiology of spasticity'. en. In: *European Journal of Neurology* 9 (May 2002), pp. 3–9. DOI: 10.1046/j.1468-1331.2002.0090s1003.x (cited on page 68).

[285] Preeti Raghavan. 'Upper Limb Motor Impairment Post Stroke'. In: *Physical medicine and rehabilitation clinics of North America* 26.4 (2015), pp. 599–610. DOI: 10.1016/j.pmr.2015.06.008. (Visited on 04/28/2019) (cited on page 68).

[286] M. Chancel et al. 'Hand movement illusions show changes in sensory reliance and preservation of multisensory integration with age for kinaesthesia'. eng. In: *Neuropsychologia* 119 (2018), pp. 45–58. DOI: 10.1016/j.neuropsychologia.2018.07.027 (cited on pages 69, 82).

[287] Lauren L Edwards et al. 'Putting the "Sensory" Into Sensorimotor Control: The Role of Sensorimotor Integration in Goal-Directed Hand Movements After Stroke'. In: *Frontiers in integrative neuroscience* 13 (2019), p. 16 (cited on pages 69, 96).

[288] Katlyn E Brown et al. 'Sensorimotor integration in chronic stroke: baseline differences and response to sensory training'. In: *Restorative neurology and neuroscience* 36.2 (2018), pp. 245–259 (cited on pages 69, 96).

[289] Eiichi Naito et al. 'Illusory arm movements activate cortical motor areas: a positron emission tomography study'. In: *Journal of Neuroscience* 19.14 (1999), pp. 6134–6144 (cited on pages 71, 89).

[290] Wolfgang Förstner and Boudewijn Moonen. 'A metric for covariance matrices'. In: *Geodesy-the Challenge of the 3rd Millennium*. Springer, 2003, pp. 299–309 (cited on pages 73, 115).

[291] Victoria L Ives-Deliperi and James Thomas Butler. 'Relationship between EEG electrode and functional cortex in the international 10 to 20 system'. In: *Journal of Clinical Neurophysiology* 35.6 (2018), pp. 504–509 (cited on page 80).

[292] Eriko Shibata, Fuminari Kaneko, and Masaki Katayose. 'Muscular responses appear to be associated with existence of kinesthetic perception during combination of tendon co-vibration and motor imagery'. In: *Experimental Brain Research* 235.11 (2017), pp. 3417–3425 (cited on page 80).

[293] R Kitada, E Naito, and M Matsumura. 'Perceptual changes in illusory wrist flexion angles resulting from motor imagery of the same wrist movements'. In: *Neuroscience* 109.4 (2002), pp. 701–707 (cited on page 80).

[294] Sébastien Rimbert et al. 'Median nerve stimulation based BCI: a new approach to detect intraoperative awareness during general anesthesia'. In: *Frontiers in neuroscience* 13 (2019), p. 622 (cited on page 80).

[295] Sébastien Rimbert et al. 'Modulation of beta power in EEG during discrete and continuous motor imageries'. In: *2017 8th International IEEE/EMBS Conference on Neural Engineering (NER)*. IEEE. 2017, pp. 333–336 (cited on page 81).

[296] Sébastien Rimbert, Oleksii Avilov, and Laurent Bougrain. 'Discrete motor imageries can be used to allow a faster detection'. In: 2017 (cited on page 81).

[297] Fernando Lopes da Silva. 'Neural mechanisms underlying brain waves: from neural membranes to networks'. In: *Electroencephalography and clinical neurophysiology* 79.2 (1991), pp. 81–93 (cited on page 81).

[298] Fabien Cignetti et al. 'Boosted activation of right inferior frontoparietal network: a basis for illusory movement awareness'. In: *Human brain mapping* 35.10 (2014), pp. 5166–5178 (cited on page 81).

[299] Michela Balconi, Davide Crivelli, and Marco Bove. ''Eppur si move': the association between electrophysiological and psychophysical signatures of perceived movement illusions'. In: *Journal of Motor Behavior* 50.1 (2018), pp. 37–50 (cited on page 81).

[300] Toshiyuki Kondo et al. 'Effect of instructive visual stimuli on neurofeedback training for motor imagery-based brain–computer interface'. In: *Human movement science* 43 (2015), pp. 239–249 (cited on page 82).

[301] Yumie Ono et al. 'Enhancement of motor-imagery ability via combined action observation and motor-imagery training with proprioceptive neurofeedback'. In: *Neuropsychologia* 114 (2018), pp. 134–142 (cited on page 82).

[302] Minkyu Ahn and Sung Chan Jun. 'Performance variation in motor imagery brain–computer interface: A brief review'. In: *Journal of Neuroscience Methods* 243 (Mar. 2015), pp. 103–110. DOI: 10.1016/J.JNEUMETH.2015.01.033 (cited on page 82).

[303] Silvia Marchesotti et al. 'Quantifying the role of motor imagery in brain-machine interfaces'. In: *Scientific reports* 6 (2016), p. 24076 (cited on page 82).

[304] Tomonori Kito et al. 'Sensory processing during kinesthetic aftereffect following illusory hand movement elicited by tendon vibration'. In: *Brain research* 1114.1 (2006), pp. 75–84 (cited on page 82).

[305] Alexander B Remsik et al. 'Ipsilesional Mu rhythm desynchronization and changes in motor behavior following post stroke BCI intervention for motor rehabilitation'. In: *Frontiers in neuroscience* 13 (2019), p. 53 (cited on page 82).

[306] Katlyn E. Brown et al. 'Sensorimotor integration in chronic stroke: Baseline differences and response to sensory training'. eng. In: *Restorative Neurology and Neuroscience* 36.2 (2018), pp. 245–259. DOI: 10.3233/RNN-170790 (cited on page 82).

[307] Lauren L. Edwards. *Putting the "Sensory" Into Sensorimotor Control: The Role of Sensorimotor Integration in Goal-Directed Hand Movements After Stroke*. 2019. (Visited on 09/02/2019) (cited on page 82).

[308] Mathis Fleury et al. 'A Survey on the Use of Haptic Feedback for Brain-Computer Interfaces and Neurofeedback'. In: *Frontiers in Neuroscience* 14 (2020), p. 528. DOI: 10.3389/fnins.2020.00528 (cited on pages 82, 85).

[309] Christian Paret et al. 'Current progress in real-time functional magnetic resonance-based neurofeedback: Methodological challenges and achievements'. In: *Neuroimage* 202 (2019), p. 116107 (cited on page 84).

[310] Hayrettin Gürkök and Anton Nijholt. 'Brain–computer interfaces for multimodal interaction: A survey and principles'. In: *International Journal of Human-Computer Interaction* 28.5 (2012), pp. 292–307 (cited on page 84).

[311] Fabien Lotte, Florian Larrue, and Christian Mühl. 'Flaws in current human training protocols for spontaneous brain-computer interfaces: lessons learned from instructional design'. In: *Frontiers in human neuroscience* 7 (2013), p. 568 (cited on page 84).

[312] Lior Botzer and Amir Karniel. 'Feedback and feedforward adaptation to visuomotor delay during reaching and slicing movements'. In: *European Journal of Neuroscience* 38.1 (2013), pp. 2108–2123 (cited on page 85).

[313] Steen Moeller et al. 'Multiband multislice GE-EPI at 7 tesla, with 16-fold acceleration using partial parallel imaging with application to high spatial and temporal whole-brain fMRI'. In: *Magnetic resonance in medicine* 63.5 (2010), pp. 1144–1153 (cited on page 86).

[314] A Donald Keedwell and József Dénes. *Latin squares and their applications*. Elsevier, 2015 (cited on page 86).

[315] Helena Pongrac. 'Vibrotactile perception: examining the coding of vibrations and the just noticeable difference under various conditions'. In: *Multimedia systems* 13.4 (2008), pp. 297–307 (cited on page 89).

[316] Matthew Brett et al. 'Region of interest analysis using an SPM toolbox'. In: *8th international conference on functional mapping of the human brain*. Vol. 16. 2. Sendai, Japan. 2002, p. 497 (cited on page 90).

[317] Isabelle Favre et al. 'Upper limb recovery after stroke is associated with ipsilesional primary motor cortical activity: a meta-analysis'. In: *Stroke* 45.4 (2014), pp. 1077–1083 (cited on pages 96, 110).

[318] Camille Lecoffre et al. 'L'accident vasculaire cérébral en France: patients hospitalisés pour AVC en 2014 et évolutions 2008-2014'. In: *Bulletin Epidémiologique Hebdomadaire-BEH* (2017) (cited on page 96).

[319] M Chancel et al. 'Hand movement illusions show changes in sensory reliance and preservation of multisensory integration with age for kinaesthesia'. In: *Neuropsychologia* 119 (2018), pp. 45–58 (cited on page 96).

[320] György Buzsáki, Costas A. Anastassiou, and Christof Koch. 'The origin of extracellular fields and currents — EEG, ECoG, LFP and spikes'. In: *Nature Reviews Neuroscience* 13.6 (June 2012), pp. 407–420. DOI: 10.1038/nrn3241 (cited on page 98).

[321] Shingo Murakami and Yoshio Okada. 'Contributions of principal neocortical neurons to magnetoencephalography and electroencephalography signals'. In: *The Journal of physiology* 575.3 (2006), pp. 925–936 (cited on page 98).

[322] H. Petsche, H. Pockberger, and P. Rappelsberger. 'On the search for the sources of the electroencephalogram'. In: *Neuroscience* 11.1 (Jan. 1984), pp. 1–27. DOI: 10.1016/0306-4522(84)90212-4 (cited on page 98).

[323] Alexander Strobel et al. 'Novelty and target processing during an auditory novelty oddball: A simultaneous event-related potential and functional magnetic resonance imaging study'. In: *NeuroImage* 40.2 (Apr. 2008), pp. 869–883. DOI: 10.1016/J.NEUROIMAGE.2007.10.065 (cited on page 98).

[324] Deepak Khosla, Manuel Don, and Betty Kwong. 'Spatial mislocalization of EEG electrodes–effects on accuracy of dipole estimation'. In: *Clinical neurophysiology* 110.2 (1999), pp. 261–271 (cited on page 98).

[325] Charles C Wood and Truett Allison. 'Interpretation of evoked potentials: A neurophysiological perspective.' In: *Canadian Journal of Psychology/Revue canadienne de psychologie* 35.2 (1981), p. 113 (cited on page 98).

[326] P Adjamian et al. 'Co-registration of magnetoencephalography with magnetic resonance imaging using bite-bar-based fiducials and surface-matching'. In: *Clinical Neurophysiology* 115.3 (Mar. 2004), pp. 691–698. DOI: 10.1016/J.CLINPH.2003.10.023 (cited on page 98).

[327] Christopher Whalen et al. 'Validation of a method for coregistering scalp recording locations with 3D structural MR images'. In: *Human Brain Mapping* 29.11 (Nov. 2008), pp. 1288–1301. DOI: 10.1002/hbm.20465 (cited on page 98).

[328] J Sijbers et al. 'Automatic localization of EEG electrode markers within 3D MR data'. In: *Magnetic resonance imaging* 18.4 (2000), pp. 485–488 (cited on page 98).

[329] L. Koessler et al. 'EEG–MRI Co-registration and Sensor Labeling Using a 3D Laser Scanner'. In: *Annals of Biomedical Engineering* 39.3 (Mar. 2011), pp. 983–995. DOI: 10.1007/s10439-010-0230-0 (cited on page 98).

[330] Timothy Bardouille et al. 'Improved localization accuracy in magnetic source imaging using a 3-D laser scanner'. In: *IEEE Transactions on Biomedical Engineering* 59.12 (2012), pp. 3491–3497 (cited on page 98).

[331] Jian Le et al. 'A rapid method for determining standard 10/10 electrode positions for high resolution EEG studies'. In: *Electroencephalography and clinical neurophysiology* 106.6 (1998), pp. 554–558 (cited on page 98).

[332] Jan C. de Munck et al. 'A semi-automatic method to determine electrode positions and labels from gel artifacts in EEG/fMRI-studies'. In: *NeuroImage* 59.1 (Jan. 2012), pp. 399–403. DOI: 10.1016/J.NEUROIMAGE.2011.07.021 (cited on pages 98, 103).

[333] Russell Butler et al. 'Application of polymer sensitive MRI sequence to localization of EEG electrodes'. In: *Journal of Neuroscience Methods* 278 (2017), pp. 36–45. DOI: https://doi.org/10.1016/j.jneumeth.2016.12.013 (cited on pages 98, 99, 103).

[334] Marco Marino et al. 'Automated detection and labeling of high-density EEG electrodes from structural MR images'. In: *Journal of neural engineering* 13.5 (2016), p. 056003 (cited on pages 98, 108).

[335] Joanne E. Holmes and Graeme M. Bydder. 'MR imaging with ultrashort TE (UTE) pulse sequences: Basic principles'. In: *Radiography* 11.3 (Aug. 2005), pp. 163–174. DOI: 10.1016/J.RADI.2004.07.007 (cited on page 99).

[336] Vincent Keereman et al. 'MRI-based attenuation correction for PET/MRI using ultrashort echo time sequences'. In: *Journal of nuclear medicine* 51.5 (2010), pp. 812–818 (cited on page 99).

[337] Fabian Springer et al. 'Three-dimensional ultrashort echo time imaging of solid polymers on a 3-Tesla whole-body MRI scanner'. In: *Investigative radiology* 43.11 (2008), pp. 802–808 (cited on page 99).

[338] V. Popescu et al. 'Optimizing parameter choice for FSL-Brain Extraction Tool (BET) on 3D T1 images in multiple sclerosis'. In: *NeuroImage* 61.4 (July 2012), pp. 1484–1494. DOI: 10.1016/j.neuroimage.2012.03.074 (cited on page 99).

[339] Luke Xie et al. 'Magnetic resonance histology of age-related nephropathy in the Sprague Dawley rat.' In: *Toxicologic pathology* 40.5 (July 2012), pp. 764–78. DOI: 10.1177/0192623312441408 (cited on page 99).

[340] Dorit Borrmann et al. 'The 3d hough transform for plane detection in point clouds: A review and a new accumulator design'. In: *3D Research* 2.2 (2011), p. 3 (cited on page 99).

[341] Paul J Besl, Neil D McKay, et al. 'A method for registration of 3-D shapes'. In: *IEEE Transactions on pattern analysis and machine intelligence* 14.2 (1992), pp. 239–256 (cited on page 101).

[342] Yang Chen and Gérard Medioni. 'Object modelling by registration of multiple range images'. In: *Image and vision computing* 10.3 (1992), pp. 145–155 (cited on page 101).

[343] Robert N Kavanagk et al. 'Evaluation of methods for three-dimensional localization of electrical sources in the human brain'. In: *IEEE Transactions on Biomedical Engineering* 5 (1978), pp. 421–429 (cited on page 103).

[344] Vernon L. Towle et al. 'The spatial location of EEG electrodes: locating the best-fitting sphere relative to cortical anatomy'. In: *Electroencephalography and Clinical Neurophysiology* 86.1 (Jan. 1993), pp. 1–6. DOI: 10.1016/0013-4694(93)90061-Y (cited on page 103).

[345] David Thornton et al. 'Sensorimotor activity measured via oscillations of EEG mu rhythms in speech and non-speech discrimination tasks with and without segmentation demands'. In: *Brain and Language* (Apr. 2017). DOI: 10.1016/J.BANDL.2017.03.011 (cited on page 103).

[346] David Jenson et al. 'Trait related sensorimotor deficits in people who stutter: An EEG investigation of μ rhythm dynamics during spontaneous fluency'. In: *NeuroImage: Clinical* 19 (Jan. 2018), pp. 690–702. DOI: 10.1016/J.NICL.2018.05.026 (cited on page 103).

[347] Sheng Ge et al. 'Temporal-Spatial Features of Intention Understanding Based on EEG-fNIRS Bimodal Measurement'. In: *IEEE Access* 5 (2017), pp. 14245–14258. DOI: 10.1109/ACCESS.2017.2723428 (cited on page 103).

[348] Sarang S. Dalal et al. 'Consequences of EEG electrode position error on ultimate beamformer source reconstruction performance'. In: *Frontiers in Neuroscience* 8 (Mar. 2014), p. 42. DOI: 10.3389/fnins.2014.00042 (cited on page 108).

[349] Moritz Grosse-Wentrup, Donatella Mattia, and Karim Oweiss. 'Using brain–computer interfaces to induce neural plasticity and restore function'. In: *Journal of neural engineering* 8.2 (2011), p. 025004 (cited on page 110).

[350] Nikhil Sharma, Valerie M Pomeroy, and Jean-Claude Baron. 'Motor imagery: a backdoor to the motor system after stroke?' In: *Stroke* 37.7 (2006), pp. 1941–1952 (cited on pages 110, 111).

[351] Mark Chiew, Stephen M LaConte, and Simon J Graham. 'Investigation of fMRI neurofeedback of differential primary motor cortex activity using kinesthetic motor imagery'. In: *Neuroimage* 61.1 (2012), pp. 21–31 (cited on pages 110, 111, 122).

[352] Maria L Blefari et al. 'Improvement in precision grip force control with self-modulation of primary motor cortex during motor imagery'. In: *Frontiers in behavioral neuroscience* 9 (2015), p. 18 (cited on pages 110, 111, 122).

[353] Ela B Plow et al. 'Rethinking stimulation of the brain in stroke rehabilitation: why higher motor areas might be better alternatives for patients with greater impairments'. In: *The Neuroscientist* 21.3 (2015), pp. 225–240 (cited on page 110).

[354] Giovanni Di Pino et al. 'Modulation of brain plasticity in stroke: a novel model for neurorehabilitation'. In: *Nature Reviews Neurology* 10.10 (2014), pp. 597–608 (cited on pages 110, 123).

[355] Sébastien Hétu et al. 'The neural network of motor imagery: an ALE meta-analysis'. In: *Neuroscience & Biobehavioral Reviews* 37.5 (2013), pp. 930–949 (cited on page 111).

[356] Philip J Allen, Oliver Josephs, and Robert Turner. 'A method for removing imaging artifact from continuous EEG recorded during functional MRI'. In: *Neuroimage* 12.2 (2000), pp. 230–239 (cited on page 112).

[357] Herbert Ramoser, Johannes Muller-Gerking, and Gert Pfurtscheller. 'Optimal spatial filtering of single trial EEG during imagined hand movement'. In: *IEEE transactions on rehabilitation engineering* 8.4 (2000), pp. 441–446 (cited on page 113).

[358] Axel R Fugl-Meyer et al. 'The post-stroke hemiplegic patient. 1. a method for evaluation of physical performance.' In: *Scandinavian journal of rehabilitation medicine* 7.1 (1975), p. 13 (cited on page 115).

[359] Michelle L Woodbury et al. 'Rasch analysis staging methodology to classify upper extremity movement impairment after stroke'. In: *Archives of physical medicine and rehabilitation* 94.8 (2013), pp. 1527–1533 (cited on page 115).

[360] Rensis Likert. 'A technique for the measurement of attitudes.' In: *Archives of psychology* (1932) (cited on page 115).

[361] Cathy M Stinear et al. 'Functional potential in chronic stroke patients depends on corticospinal tract integrity'. In: *Brain* 130.1 (2007), pp. 170–180 (cited on page 115).

[362] Jong Sea Lee et al. 'Fiber tracking by diffusion tensor imaging in corticospinal tract stroke: topographical correlation with clinical symptoms'. In: *Neuroimage* 26.3 (2005), pp. 771–776 (cited on page 115).

[363] Cathy M Stinear et al. 'The PREP algorithm predicts potential for upper limb recovery after stroke'. In: *Brain* 135.8 (2012), pp. 2527–2535 (cited on page 115).

[364] Stephen J Page, George D Fulk, and Pierce Boyne. 'Clinically important differences for the upper-extremity Fugl-Meyer Scale in people with minimal to moderate impairment due to chronic stroke'. In: *Physical therapy* 92.6 (2012), pp. 791–798 (cited on page 119).

[365] Sook-Lei Liew et al. 'Improving motor corticothalamic communication after stroke using real-time fMRI connectivity-based neurofeedback'. In: *Neurorehabilitation and neural repair* 30.7 (2016), pp. 671–675 (cited on page 122).

[366] M. Mihara et al. 'Near-infrared Spectroscopy-mediated Neurofeedback Enhances Efficacy of Motor Imagery-based Training in Poststroke Victims: A Pilot Study'. In: *Stroke* 44.4 (Apr. 2013), pp. 1091–1098. DOI: 10.1161/STROKEAHA.111.674507 (cited on page 122).

[367] Assia Jaillard et al. 'Vicarious function within the human primary motor cortex? A longitudinal fMRI stroke study'. In: *Brain* 128.5 (2005), pp. 1122–1138 (cited on page 123).

[368] Lynley V Bradnam, Cathy M Stinear, and Winston D Byblow. 'Ipsilateral motor pathways after stroke: implications for non-invasive brain stimulation'. In: *Frontiers in human neuroscience* 7 (2013), p. 184 (cited on page 123).

[369] Niels Birbaumer, Sergio Ruiz, and Ranganatha Sitaram. 'Learned regulation of brain metabolism'. In: *Trends in cognitive sciences* 17.6 (2013), pp. 295–302 (cited on page 123).

[370] Bettina Sorger et al. 'When the brain takes 'BOLD'steps: real-time fMRI neurofeedback can further enhance the ability to gradually self-regulate regional brain activation'. In: *Neuroscience* 378 (2018), pp. 71–88 (cited on page 124).

Titre : Neurofeedback Multimodal basée sur de l'imagerie EEG/IRMf et des feeedbacks Visuo-Haptique pour de la rééducation cérébrale

Mot clés : Neurofeedback (NF), Electroencéphalographie (EEG), Imagerie par Résonance Magnétique fonctionnel (IRMf), Feedback Visuo-Haptique, Rééducation post-AVC

Résumé :

Le Neurofeedback (NF) est une technique consistant à renvoyer à un individu des informations sur son activité cérébrale, lui permettant ainsi de la moduler. Le NF a ainsi été étudié comme outil de rééducation cérébrale dans un grand nombre de troubles neurologique et psychiatrique, notamment pour de la rééducation post-Accident Vasculaire Cérébrale (AVC). Dans cette thèse, nous avons proposé et étudié de nouveaux systèmes de NF multimodaux, tant au niveau de l'entrée, en combinant plusieurs modalités de neuroimageries - en particulier l'ElectroEncephaloGraphie (EEG) et l'Imagerie par Résonance Magnétique fonctionnelle (IRMf), qu'au niveau de la sortie, en proposant des feedbacks multimodaux combinant feedback visuel et haptique. Dans la première partie de cette thèse, nous avons étudié la possibilité de combiné feedback visuel et feedback haptique pour une tâche de NF. Dans un premier temps, nous avons ainsi montré que la combinaison d'un feedback visuel (main en 3D en mouvement), avec l'association de vibrations sur les poignets, produisaient des illusions de mouvement plus intense que l'utilisation d'une main statique ou sans feedback. Dans un second temps, nous avons montré que l'utilisation d'un feedback visuo-haptique (VH) associé à une tâche d'imagerie motrice (IM) produisait des activations plus importantes que lors de tâche d'IM seule. Enfin, nous avons étudié et implémenté ce feedback VH dans le contexte d'une étude MI-NF-IRMf, où ce feedback était confronté au même feedback mais visuel seul (V) et haptique seule (H). L'analyse des scores NF et des activations IRMf suggère que ce feedback VH a conduit à des activations dans le cortex motor plus intense que les feedback H et V seules et pourrait donc être potentiellement prometteur pour la rééducation post-AVC basée sur le fMRI-NF. Dans la sconde partie de cette thèse, nous avons implémenté un algorithme permettant de localiser la position des électrodes EEG lors d'expérience EEG-IRMf, cette information pourrait s'avérer utile à l'avenir pour des expériences EEG-fMRI-NF. Enfin, nous présentons une étude EEG-fMRI-NF multimodale, sur plusieurs séances, avec quatre patients victimes d'un AVC. Les résultats suggèrent que deux patients sur quatre ont bénéficié de l'entrainement NF et ont fait état d'un gain fonctionnel important, même s'ils étaient en phase chronique de l'AVC.

Title: Multimodal Neurofeedback based on EEG/fMRI Imaging Techniques and Visuo-Haptic feedback for brain rehabilitation

Keywords: Neurofeedback (NF), Electroencephalography (EEG), Functional Magnetic Resonance Imaging (fMRI), Feedback, Visuo-Haptic, Stroke rehabilitation

Abstract:

Neurofeedback (NF) is a technique that consists of sending back to an individual information on his brain activity, thus allowing him to modulate it. NF has thus been studied as a tool for brain rehabilitation in a large number of neurological and psychiatric disorders, and in particular for post-stroke rehabilitation. In this thesis, we have proposed and studied new multimodal NF systems, both at the input level, by combining multiple neuroimaging modalities - in particular Electroencephalography (EEG) and Functional Imaging Magnetic Resonance (fMRI), and at the output level, by proposing multimodal feedback combining visual and haptic feedback. In the first part of this thesis, we studied the possibility of combining visual and haptic feedback for a NF task. In a first step, we showed that the combination of visual feedback (3D moving hand), with the association of vibrations on the wrists, produced illusions of movement more intense than the use of a static hand or without feedback. In a second step, we showed that the use of visual-haptic (VH) feedback combined with a motor imaging (MI) task produced higher activations than with the MI task alone. Finally, we studied and implemented this VH feedback in the context of an MI-NF-IRMf study, where this feedback was confronted with the same feedback but visual alone (V) and haptic alone (H). Analysis of the NF scores and fMRI-fMRI activations suggests that this VH feedback led to more intense activations in the motor cortex than the H and V feedback alone and therefore may be potentially promising for stroke rehabilitation based on fMRI-NF. In the second part of this thesis, we have implemented an algorithm to locate the position of the EEG electrodes within EEG-fMRI experiments, which may prove useful in future EEG-fMRI-NF experiments. Finally, we present a multimodal, multi-session, EEG-fMRI-NF study with four stroke patients. Results suggest that two out of four patients benefited from NF training and reported significant functional gain, even though they were in the chronic phase of stroke.